69265

LCSAR – The World Bank

Climate Change and Agriculture in Latin America, 2020-2050

Projected Impacts and Response to Adaptation Strategies

Erick C.M. Fernandes, Ayat Soliman, Roberto Confalonieri, Marcello Donatelli, Francesco Tubiello,

Contents

Figures

Tables

Glossary of terms and abbreviations

Abbreviations and acronyms	Definition	Description (if needed)
Adaptation	Adjustment in natural or human systems—in response to actual or expected climatic stimuli or their effects—to moderate harm or exploit beneficial opportunities (IPCC 2007)	
Adaptive capacity	The ability of a system to adjust to climate change (including variability and extremes), to moderate potential damages, to take advantage of opportunities, or to cope with the consequences (IPCC 2007)	
AEZ	Agroecological zone	
AR4	Fourth Assessment Report of the Intergovernmental Panel on Climate Change	Published in 2007
AZS	Agroecological zone simulator	The agroecological zone simulator provides biophysical representations of crop growth as a function of agroclimatology and crop-field management.
BioMA	Biophysical model applications	
CGE	Computable general equilibrium model	
CH_4	Methane	A greenhouse gas
Climate change	Climate change refers to a change in the state of the climate that can be identified by changes in the mean or in the variability of its properties and that persists for an extended period—typically decades or longer	Climate change may be due to natural internal processes or external forcing, or to persistent anthropogenic changes in the composition of the atmosphere or in land use (IPCC 2007).
CO_2	Carbon dioxide	A greenhouse gas
CO_2-e	Carbon dioxide equivalent	A measure used to compare non-CO_2 gases with CO_2 based on their global warming potential (GWP—see below)
ECMWF	European Centre for Medium-Range Weather Forecasts	
ENSO	El Niño Southern Oscillation	
ENVISAGE	Environmental impacts and	See CGE

	sustainability applied general equilibrium model	
GCM	General circulation models	A general circulation model is a mathematical model of the general circulation of a planetary atmosphere or ocean and based on equations for a rotating sphere with thermodynamic terms for various energy sources (radiation, latent heat). These equations are the basis for simulating the atmosphere or ocean of the Earth. Atmospheric and Oceanic GCMs (AGCM and OGCM) are key components of global climate models along with sea ice and land-surface components. GCMs and global climate models are widely applied for weather forecasting, understanding the climate, and projecting climate change.
GHG	Greenhouse gas	Greenhouse gases are gaseous constituents of the atmosphere, both natural and anthropogenic, that absorb and emit radiation at specific wavelengths within the spectrum of thermal infrared radiation emitted by the Earth's surface, atmosphere, and clouds. This property causes the greenhouse effect (IPCC 2007).
GWP	Global warming potential	An estimate of the effectiveness of a gas in trapping heat in the atmosphere relative to CO_2 over a specific time horizon. As per IPCC, over 100 years, methane's GWP is 21 and nitrous oxide is 310.
IPCC	Intergovernmental Panel on Climate Change	
LUT	Land utilization types	
N_2O	Nitrous oxide	A greenhouse gas
NCAR	National Center for Atmospheric Research	
Probabilistic scenarios	The production of large ensembles of climate change scenarios enables the production of probability density functions to represent the range of projected change in a specific event	Specific probabilities may be assigned to individual events or climate change impacts by incorporating model uncertainties within a large model ensemble
R&D	Research and development	
RCMs	Regional climate models	
SFLAC	Spanish Fund for Latin America and the Caribbean	The Fund is meant to provide resources to enhance the impact of the Bank Group's development activities
SRES	Special Report on Emissions Scenarios	
UNFCCC	United Nations Framework Convention on Climate Change	The UN body charged with implementing climate change action globally

Acknowledgements

This study was made possible by the generous contribution of the Spanish Ministry of Economy and Finance, through the Spanish Fund for Latin America and the Caribbean (SFLAC).

The project was implemented by a Consortium led by the Consorzio Milano Ricerche, with the participation of the European Commission Joint Research Center (EC-JRC).

Consortium leader: Prof: Roberto Confalonieri ; Simone Bregaglio, Co-coordinator of the project "Development of an Adapter to run the APES Modelling Solutions into the BioMA Framework"

The project was made possible by accessing data and resources of the project EUROCLIMA, granted by DG AIDCO, under the action of the JRC's Institute of Environmental Sustainability (JRC-IES-MARS).

Scientific leader: Dr. Marcello Donatelli

Special thanks are also due to Dominique van der Mensbrugghe from the World Bank's Development Prospects Group (DECPG) for his inputs on coupling the climate-crop impact modeling outputs to the Bank's CGE model (ENVISAGE) and to John Nash, Lead Economist, in the Latin America and Caribbean Region.

Executive Summary

The impacts of climate change on agriculture are projected to be significant in coming decades, so response strategies and their likely costs should be evaluated now. Robust crop models are needed to estimate those impacts on agricultural productivity regionally, nationally, and even sub-nationally. But existing crop–climate change modeling platforms are not easily accessible to most stakeholders in developing countries. So there is less testing of those models than there might be, and there are fewer opportunities for further improvements based on local tests and emerging data.

That is why this study produced an open-access crop-climate-economic impact modeling platform for Latin America and the Caribbean that can be extended to other regions—and modified and improved by users as new crop, climate, and economic datasets become available. The new platform projects the likely impacts of agroclimatic factors on crop productivity on the basis of climate projections from two general circulation models and couples it with an economic model to derive and evaluate a range of climate-change scenarios and likely agricultural productivity and economic impacts over the next several decades.

The open-access modeling platform developed in this study, the agroecological zone simulator (AZS), provides biophysical representations of crop growth as a function of agroclimatology and crop-field management. It is based on the biophysical model applications (BioMA) approach used by the European Commission Joint Research Centre to investigate climate-change impacts in the EU. The AZS simulations used:

- The baseline climate (1989 to today) re-sampled to 0.25 degree grid cells (25 kilometers at the horizon).
- Two general circulation models—the U.K. Met Office's Hadley3 model and the National Center for Atmospheric Research (NCAR) model.
- Two special report on emissions scenarios (SRES), A1b and B1, to represent respectively a high scenario (business as usual) and low scenario (near carbon dioxide stabilization at 550 parts per million).
- Two time horizons for simulating risks to crop production, with little time for adaptation (2020) and with time for adaptation (2050).

The AZS biophysical results

The main results of the AZS simulations suggest that the prevailing and often expressed view that Latin America and the Caribbean will continue to be the breadbasket of the future—stepping in to supply grain to other regions affected by climate change—needs to be tempered and subjected to further rigorous testing. The AZS estimates confirm and extend previous findings indicating that the impacts of climate change on agriculture in the region could be significant even by 2020, with rising risks to maize, soybean, and wheat production in most producing countries by 2050. Encouragingly, however, adaptation interventions such as the targeted use of irrigation, the development and use of improved varieties, and the change of sowing dates could significantly reduce the projected negative impacts of plausible climate shocks. This finding emphasizes the urgency for adequate investments in adaptation strategies to ensure that the projected shocks to agricultural productivity can be reduced. In most cases, such investments may take several decades to begin having a positive impact.

It is important to note that the time windows in the study represent 30 year climate averages for the decade in question, so "2020" is the average climate change for the period 2005-2034. Moreover, the baseline for comparing climate regimes is not the 8 year period from 2012 to 2020, but rather the longer, 35 year interval from 1985 (the midpoint of the 1960-1990 baseline climatology used by the general circulation models) to 2020, the midpoint of the future time window. The projected climate impacts on the target crops account for the crop phonological sensitivities to temperature as well as the potentially large temperature-precipitation changes on rain fed crops. The projected impacts do not include assumptions regarding technological advances in the coming decades. To obtain more robust estimates of climate change impacts relative to today will require additional socio-economic information and modeling that is beyond the scope of this work.

Wheat

For wheat, yields could be significantly affected by climate change, regardless of the emission scenario or general circulation model. Percentage yield declines are projected to be deeper in Mexico, in the Caribbean region, and in the northeastern parts of the continent (Colombia and Brazil). The projected limited water productivity for 2020 and 2050 could be lower than the baseline, with southern and western countries less affected. Yield reductions due to the shortening of the crop cycle leave fewer days to fill grains. The projected yield declines due to disease in 2020 and 2050 could also be significant. Frost damage is expected to affect wheat yields less seriously in Chile, where shorter crop cycles could also reduce the crop exposure to pathogens, thus also reducing the pressure of wheat leaf rust. With few exceptions, insufficient water could affect wheat productivity more than other factors, highlighting the urgent need for developing drought-tolerant wheat varieties (such as deeper rooting).

With adaptation, the projected yield impacts are markedly less negative for all the production levels and scenarios considered, but low water availability still limits wheat productivity. Although the use of genotypes with longer crop cycles could partly compensate for the effect of climate change in reducing the grain-filling period, the longer crop cycle increases water demand because of increased transpiration. Except in Chile, disease pressure is expected to fall everywhere, even without adaptation strategies for leaf rust. Argentina could be most affected by disease pressure, whereas insufficient water availability appears to be the major wheat yield-reducing factor in Brazil and Chile.

Soybean

For soybean, yields could be reduced by climate change in 2020 and more so in 2050, though with different magnitudes throughout the region. Yield losses could be large in Brazil (more than 30% from the baseline) but less pronounced in Argentina, Bolivia, Colombia, and Uruguay. This can be explained by the greater impact of climate change in Brazil, where the crop cycle is projected to be shorter than in other parts of Latin America, markedly shortening the soybean grain-filling period. The impact of rust disease would not increase with warming, except in

Colombia, where the AZS shows an increase for all combinations of general circulation model (GCM) emission scenarios. This could be explained by the severity of the increase in temperature in an already warm environment, given Colombia's proximity to the equator, which in turn could lead to more favorable conditions for pathogens.

With adaptation—such as longer crop-cycle varieties, different sowing dates, and irrigation—the impacts across all scenarios and time windows could be reduced, especially in Ecuador and Uruguay. In Argentina the use of varieties with longer cycles could compensate for yield losses due to climate impacts that reduce the period for crop growth and maturity.

Maize

For maize, climate change could reduce yields throughout Latin America, regardless of the emission scenario or GCM. This is mainly due to the shorter grain-filling period not being compensated for by the higher daily biomass accumulation rates and the CO_2 fertilization effect. The countries most affected are likely to be Brazil, Ecuador, Mexico, and Caribbean countries, where maize is one of the main crops. The Hadley GCM produced the highest losses, except for Brazil and Ecuador (and for the latter, only for the B1 scenario). Because the yield impacts of climate change are highly heterogeneous across the region, national adaptation strategies will be critical in mitigating productivity declines.

Adaptation, especially in the 2020 timeframe, could dampen negative impacts of climate change on maize yields in most of the region, though yield declines could still be significant in major maize-producing countries, like Mexico. Higher percentage declines were simulated for the Hadley GCM than the NCAR, with the A1B emission scenario usually leading to the most severe declines. Adaptation strategies could limit but not completely offset the climate-change damage to maize production, even in countries where grey leaf spot disease appears as the most limiting factor.

Rice

For rice, the AZS estimates show that productivity could, on average, increase across the region. A major reason for this positive outlook appears to be related to the fact that rice is a wetland/irrigated crop. Except for Brazil, Mexico, and the Caribbean, the 2020 and 2050 projections are encouraging, with higher productivity projected in most cases. Rice has higher temperature growth requirements than other crops. Under the current climate (the baseline) production is slightly reduced by photosynthesis being limited by suboptimal temperatures. With warmer conditions the negative effect of the shorter grain-filling period would be counterbalanced by higher biomass accumulation rates because of more favorable conditions for photosynthesis.

The result of these two opposite effects is a general increase in productivity, except in countries already experiencing warm climates (where thermal conditions for photosynthesis are already close to optimal and the reduced grain-filling period leads to declines in final yields). In low-temperature areas (especially Uruguay) climate change could reduce the incidence of pre-flowering cold shocks inducing sterility. Except for Brazil and the Caribbean the blast disease pressure on the crop could ease, because of thermal and rainfall conditions less favorable for *Pyricularia grisea*, the blast disease pathogen.

With adaptation—including the use of different varieties and different sowing dates—future conditions could be decidedly favorable for rice across the region. Long-cycle genotypes allow long grain-filling periods and high daily biomass accumulation rates, because of negligible temperature limits to photosynthesis and the CO_2 fertilization effect, higher for the C3 species than for the C4 (such as maize).[1]

Economic impacts

The economic impacts of implementing the climate-induced agricultural productivity shocks in the four focus crops were investigated by coupling of AZS biophysical results to the ENVISAGE platform. (An example in chapter 4 shows the steps for implementing and potentially applying such a powerful coupling.) Results were limited by the focus on Latin America, assuming no impacts in the rest of the world. They thus are relevant to understanding first-order dynamics following a perturbation, but they would need to be updated with more consistent impact signals globally.

The aggregate impact of this partial shock could be as high as 1.7% of regional GDP in 2050 under the A1B emission scenario for the Hadley GCM, which produces the most severe yield shocks in the AZS projections. Although the impact signal is strong, this seems a fairly large decline in regional GDP, considering that the four affected crops would represent only about 1.3% of regional GDP in 2050 under the baseline scenario. Two reasons for such an outcome could be climate change affecting other sectors and agriculture having a big (multiplier) effect on other sectors. The projected impacts tend to accelerate between 2020 and 2050. They are larger for the Hadley model than the NCAR model, and they tend to be higher for the A1B emission scenario than the B1 emission scenario. The impacts on global output are negligible.

Most affected across all scenarios and GCMs are Argentina and Brazil, two of the region's largest agricultural producers. Uruguay would be the only country that would see gains in most of the scenarios—though under the more severe Hadley A1B scenario, even Uruguay could experience a 2.3% loss. Among those least affected are Chile, Ecuador, and Peru. Chile's agricultural sector, small as a share of the total economy in the base year, declines over time—particularly for the four focus crops. Ecuador and Peru have low production shares in the affected crops. Because this study focuses on four crops, the impacts for other crops—such as tropical fruits, coffee, and sugar, which are potentially important parts of GDP—are not included in the estimates.

[1] C3 photosynthesis is called C3 because the CO_2 is first incorporated into a 3-carbon compound. It is more efficient than C4 and CAM plants under cool and moist conditions and under normal light because requires fewer enzymes and no specialized anatomy. Most plants are C3. C4 photosynthesis is called C4 because the CO_2 is first incorporated into a 4-carbon compound. It photosynthesizes faster than C3 plants under high light intensity and high temperatures. Examples of C4 plants include maize, sugarcane, millet, and Brachiaria pasture grass.

The within-country distribution between agriculture and the rest of the economy would tend to worsen in all countries in the region. In Argentina agricultural value added could drop by 7% in 2020 in the best case and by 32% in 2050 in the worst. The loss in agricultural value added is significantly less in Brazil than in Argentina in 2050, even though the 2020 impacts are similar. Some countries (such as Uruguay) may see a rise in agricultural value added.

In a worst case scenario for the four focus crops in Latin America and the Caribbean, the loss in net export revenues could be $8–11 billion in 2020 and $30–52 billion in 2050. Brazil could bear the greatest absolute burden followed by Argentina and then Mexico.

Major findings and conclusions

The ability to test dynamic interactions between agroclimatic factors and field management is critical for policy makers assessing economically efficient investment options. This study produced a robust set of linked modeling tools and a coherent set of linked databases to facilitate the evaluation of dynamic interactions of high-resolution agroclimatic and field management factors affecting crop growth and development. It allowed interactions with a detailed general equilibrium model to include and test the constraints of realistic socioeconomic factors on production and welfare.

For Latin America and the Caribbean the projected yield shocks on wheat, maize, and soybean generated by the AZS platform could result in substantial negative economic impacts in the aggregate—particularly for Argentina and Brazil, which are heavily invested in the focus crops of this study.

The findings have several major policy implications.

1. The estimated negative impacts could be significantly larger than what has previously been predicted for Latin America and the Caribbean—and for precisely the two major agricultural producers (Brazil and Argentina) expected to play a major role in the global food supply chain. This should be a red flag for policy makers deciding on both mitigation and adaptation investments to combat global warming via greenhouse gas emissions reductions in the LCR countries and globally.
2. Despite the projected severity of climate change impacts for maize, soybean, and wheat, some findings were encouraging. For example, the study simulated the response to the use of simple adaptation strategies such as the use of improved varieties, change of sowing dates, and modest irrigation and found that although these strategies did not overcome the projected damages from climate change, they did reduce the yield shocks to a significant degree for some crops. Policy-relevant interventions related to adaptation strategies include:
    a. Allocating adequate research and development (R&D) resources to generate improved and adapted plant varieties—currently estimated to take at least a decade and to cost US$5–7 million for each new variety).
    b. Expanding high-efficiency irrigation to overcome moisture limitation during grain-filling, a major yield-limiting factor in the region for maize, soybean, and wheat. Less than 6% of Brazil‘s agriculture and less than 2% of Argentina‘s are irrigated yet these are the two countries projected to be hit most severely by climate change and moisture limitations for their major commodity crops.

3. One surprise from the study is the estimated positive impact of climate change on rice productivity in the region, which highlights to the potential for increasing rice production, especially since rice now feeds about 3 billion people worldwide, and global supplies expected to tighten significantly in coming years. The key policy-relevant issues for rice futures in LCR include:
    a. ***Raising the current low yield levels of irrigated rice in LCR***. Most of the region‘s rice is produced in the rainy season to ensure adequate supplies of water for most of the growing season. The yield plateau for rainy season rice is about 5 tons per hectare because sunlight is often reduced by clouds. If the rice could be produced during the dry season with adequate water capture and irrigation, the rice yield plateau could rise to between 8 and 12 tons per hectare.
    b. ***Ensuring adequate water supplies and water control in the landscape***. Most of the region‘s countries have plans to expand hydroenergy as a part of national low-carbon growth strategies. Ensuring that new hydroenergy programs also include irrigation would enhance the adaptation capacity for agriculture. Policies that promote multipurpose hydro would also permit relocating rice and other agriculture in coastal and low-lying areas to areas less vulnerable to major floods and rising sea levels—an adaptation-mitigation win-win.
    c. ***Reducing the environmental footprint of rice***. Because flooded rice is a major source of methane (a powerful greenhouse gas), adequate R&D funding and policy instruments will be needed to catalyze public-private partnerships to develop and extend rice field management strategies and the use of improved biological and new-generation "high efficiency-low emissions" synthetic fertilizers.
4. The study finding that moisture limitations are likely to strongly influence the reduction of future crop yields further emphasizes the importance of current discussions at the global level to include soil carbon sequestration in any post-2012 climate agreement. The available empirical evidence for a wide variety of soil and agroecosystem types confirms that an increase in soil carbon can also result in significant improvements in soil moisture holding capacity and thereby reduce the need for irrigation. Appropriate policy and market signals are urgently needed to encourage land-based carbon sequestration to facilitate better soil and water use and result in more resilient agroecosystems. Sequestration above and below ground could also increase rural income opportunities through more diverse ecosystem services.
5. The AZS estimates of climate impacts on agricultural productivity at relatively high spatial resolution could provide key information to reduce uncertainty for risk-reducing insurance and microfinance instruments. Insurance (risk-sharing) is likely to be important in future adaptation decisions, whether through traditional indemnity-based insurance or through other options that may be more suitable for climate-based insurance, such as index-based schemes, weather derivatives, and catastrophe bonds.
6. If a large share of world agriculture faces similar impacts to the AZS projections for the region and the four crops studied, initial economic simulations project higher food prices than the baseline. So, investments and grants are urgently needed to expand the current portfolio of crops in the AZS platform to include subsistence crops, biofuels crops, and horticultural crops beyond wheat, soybean, maize, and rice. This will allow more robust assessments of the intrasectoral impacts and economic implications in the region and across regions.

7. Policy makers in the region and elsewhere need more realistic assessments of their relative comparative advantages in agriculture and their priorities for investments in adaptive strategies. All regions should urgently conduct similar CC-agriculture impact assessments to allow a more robust cross-regional comparison of climate change's impacts on food security, trade, and GDP. To help facilitate participatory and robust analyses, the open-access AZS platform developed in this study is now available for further refinement, scaling up, and testing in the Latin American and Caribbean Region as well as for rapid deployment to and use by other regions.

Chapter 1. Introduction

Latin America and the Caribbean is a big region with varied climate, ecosystems, populations, and cultures. The Fourth Assessment Report of the Intergovernmental Panel on Climate Change (2007) notes that climate change in the region will affect different ecosystems and sectors over the coming decades, with specific impacts on agroecosystems. One is decreasing plant and animal species diversity. A second is shifts in ecosystems composition, biome boundaries, and area distributions. A third is reductions in the quantity and quality of irrigation water. A fourth is increasing aridity and desertification. And a fifth is the increasing incidence and impacts of crop pests and disease.

Agriculture in the region is likely to suffer larger and more direct impacts of climate change than industry or services. Total economic damage estimated for 2100 ranges from \$35 billion (Mendelsohn and Williams 2004) to more than \$100 billion (0.56% of GDP). Under pronounced warming scenarios the projected losses could already be substantial by 2050 (de la Torre and others 2009). For cropping systems Cline (2007), based on an average of four climate models, the projected significant yield losses in Latin America, aggregating declines as follows: –19% for higher income food-exporting countries; –13.5% for higher income food-importing countries, and –17% for middle and low income countries. The IPCC AR4 report indicated significant crop yield losses for Latin America and the Caribbean, including –30% for rainfed maize in Central America and –15% in Brazil.

Based on the projected yield impacts, Seo and Mendelsohn (2008) estimated average potential revenue losses to farming households from climate change of 12% for a mild climate-change scenario in 2100 to 50% for a more severe scenario, after adaptive action by farmers. Mendelsohn and others (2008) predicted changes in land values as a proxy for the decline in land productivity. In Mexico, expected to suffer severe effects, the predicted fall in values was greater than the value of the land itself for 30–85% of all farms, depending on the model and severity of warming.

Agronomic research indicates that the higher temperatures with climatic change will reduce the production of many crop and livestock groups. Where there is water stress, heat stress or a combination of the two, the world's cereal crops can be vulnerable to even minor changes in temperature. The agronomy of all crops will be affected by both temperature and precipitation changes and by the higher atmospheric concentration of carbon dioxide. Rice, for example, is predicted to experience increased yield due to carbon dioxide fertilization at higher concentrations (currently around 380 parts per million by volume). But the net yield increase turns negative as temperature increases by 3 or 4°C. But these projections often hold precipitation constant, and it is the seasonal availability of water that most heavily influences crop yield changes, perhaps affecting the largest grain-growing areas in the Asian subcontinent (see, for example IPCC and others 2007). So, the feedback impacts of climate change on the production of major crops, such as rice and wheat, are therefore highly uncertain.

The IPCC reports (Reilly and others 1996; Gitay and others 2001; Easterling and others 2007) review the results of available studies and find negative impacts on crop productivity and yields for the tropics, but competing evidence for beneficial effects for the high latitudes. At +2 to +3 degrees agricultural prices are expected to be affected, but the impact ranges from –10 to +20%, depending on the model. But at +3 to +5 degrees agricultural prices are expected to increase 10–40%, while cereal imports of developing countries are likely to increase 10–40% (Easterling and others 2007).

In addition to the impacts of climate change through changes in climatic variables, projected increases in the frequency and severity of extreme events pose serious threats to agricultural production. Rosenzweig and others (2002) found significant additional impacts of climate change on U.S. maize production, once effects of excessive soil moisture are included in simulations. Raddatz (2009) computed that climatic disasters reduce per capita GDP by 0.6% on average, and that drought and extreme temperatures are major drivers of such impacts (windstorms and hurricanes having significant effects in Central America and the Caribbean). These data suggest that agriculture is a major channel for transmitting the effects of climate change to the economy (de la Torre and others 2009). If the trends of the past four decades continue, climatic disasters could permanently reduce GDP 2% over a decade.

One study used the inputs of local stakeholders and local experts in diverse agroecological zones in Latin America to develop regional climate change action plans based on identifying and prioritizing improved adaptation strategies to climate change (Lee and others 2009). A key finding is the need for local communities to have access to information and decision support systems—such as early warning systems (for climate forecasts, extreme weather events, and pest and disease outbreaks), climate risk maps, and geographic information systems.

The long-term sustainability of agroecosystems and associated livelihoods is unattainable without sound adaptation strategies. These strategies will need to incorporate not only changes to existing cropping systems but also point to alternative production systems and environmental services—and production landscapes for enhanced environmental, social, and economic resilience. The following questions for decision makers will revolve around monitoring, planning, and implementation in the coming decades:

- What specific climate changes are expected over time, and what will be their regional distribution?
- Which land and water management adaptation practices can best minimize the expected impacts, and how can resources be mobilized regionally to implement them?
- What are the expected effects of the anticipated sectoral impacts on trade, employment, poverty, and inequality within and across countries?

To answer these questions and develop effective adaptation strategies requires robust and quantitative assessment tools that can estimate climate-change risks and vulnerabilities for land use systems, especially within a portfolio of development projects. Once developed, the tools can then identify and assess opportunities, risks, and vulnerabilities—and help prioritize and coordinate a range of adaptation actions.

The goal of this study is to enhance regional knowledge and capacity to simulate and assess the impact of climate change on agroecological zones and land use to 2050. The main objectives are:

- To develop a modeling platform for the impact of climate change on agricultural productivity (the agroecological zone simulator, or AZS) that is open-access and transparent for its data, components, and simulation capabilities.

- To test the platform and derive climate change–crop impact estimates for Latin America and the Caribbean for 2020 and 2050.

- To couple the crop impact estimates from the AZS platform with the World Bank's environmental impacts and sustainability applied general equilibrium model to estimate the possible economic impacts of climate change.

The modeling summarizes the impact of climate change on four major crops for Latin America and the Caribbean—corn, rice, soybean, and wheat—and assesses the economic policy implications.

Chapter 2. The Knowledge Base on Climate Change Projections and Assessments of Agricultural Impacts and Economic Implications

Climate change and agriculture

Based on a range of global climate models and development scenarios, it is estimated that the Earth could experience a global warming of 1.4 to 5.8 °C over the next 100 years. The increasing atmospheric concentration of carbon dioxide (CO_2) and other greenhouse gases is one driver of global warming. Agriculture both affects and is affected by global warming. Agricultural emissions of nitrous oxide from fertilizer and manure, of methane from ruminant livestock and flooded rice, and of CO_2 from associated land use and land cover change (deforestation) contribute about 30% of greenhouse gas emissions to the atmosphere. Such changes in atmospheric carbon dioxide concentration—and in temperature and rainfall—can influence crop productivity as follows:

- In general, and assuming no other limiting factors, higher levels of CO_2 should stimulate photosynthesis for the majority of crop species globally, particularly for wheat, rice, barley, cassava, and potato and especially in cooler and wetter habitats. Positive but smaller effects on yields should be observed for tropical crops as maize, sugar cane, sorghum, and millet, important for the food security of many developing countries and for pasture and forage grasses. This is commonly referred to as the "carbon fertilization effect." In reality, however, the negative impacts of the increased crop water requirements and increasing incidence of pests may negate any positive effects of CO_2 fertilization.

- Temperature influences crop production patterns directly and indirectly. For example, higher temperatures may benefit those crops periodically affected by freezes and chills but reduce yields of crops that need cool temperatures. Temperature indirectly affects crop growth and yields through its effect on crop water demand and on pest cycles and invasion dynamics. Of special concern is the expansion of pest ranges into new latitudes and altitudes, resulting in situations where farmers and crops would be face unfamiliar pests.

- Climate models estimate that both the frequency and intensity of rainfall events will change. Although some regions may become wetter, other drought-prone regions may suffer longer and more severe dry spells. As rainfall patterns change, there will be impacts on snow accumulation at high altitudes and latitudes and changes in surface rainfall runoff, with possible reductions of soil moisture and increases in soil erosion and land degradation.

Any shock that hits agriculture will also trigger a whole set of responses in the socioeconomic system—from farm to the global economy. These responses are essentially adaptation strategies to changing environment and economic conditions. They are of two major kinds: autonomous reactions, largely outcomes of existing self-regulatory processes, and planned policy interventions. Adaptation approaches from the farm to national and global scales include:

- Farmers switch to more pest-resistant or drought-tolerant varieties, install irrigation to overcome drought and irregular rainfall, and improve drainage to mitigate flooding.

- Countries substitute factors of production in response to changing prices as a function of scarcity of one or more of the resources.

- The agricultural sector in different countries is linked through the global economic system through flows of production, goods, and services factors. Climate-change shocks to agriculture are likely to differ across countries because of nation-specific environmental, socioeconomic, and institutional factors. These asymmetries translate into different price changes for domestic goods and factors, which in turn stimulate international trade flows that may benefit some countries and damage others, working both as buffers against or multipliers of the initial impact.

For each of the three adaptation levels, autonomous adaptive responses can be strengthened or modified through specific national policies, sectoral development strategies, and environmental laws. Given the complexity of the numerous drivers, responses, and interactions, most methodological approaches involve various types of modeling and simulation. For example, any reasonably comprehensive effort to investigate the effect of climate change on agriculture should in principle involve global climate models, environmental impact models, crop growth models, land use models, and economic models—and include the following considerations:

- Changes in climate variables: temperature increases and variability, increases in CO_2 concentration, and changes in precipitation patterns.

- Climate change–induced environmental consequences, such as changes in land quality, water availability, and the frequency and intensity of extreme events.

- Physiological effects on crop growth and production characteristics.

- Farm-level adaptation strategies, such as varietal changes, changes in sowing timing, and irrigation.

- Impacts of the main economic adjustment mechanisms, such as price effects and shifts in domestic and international supply and demand.

- Feedbacks of the changed socioeconomic and biophysical conditions to climate.

Chapter 3. An Open-Access Climate-Crop Impact Agroecological Zone Simulation Modeling Platform for Latin America and the Caribbean

A major output of this study is a robust agroecological zone simulator model platform that provides the framework for assembling relevant agroclimatology datasets. It includes equations for data manipulation by the user, calculations of generic crop suitability and water balances, and climate-crop mapping tools. It facilitates the evaluation of changes in cropping patterns and growing seasons as a function of projected changes in temperature, precipitation, and evaporative demands. And it permits investigations of adaptation potentials through simplified adaptive actions—such as improving drought and flood tolerant varieties, limiting irrigation, and altering cropping activities (such as sowing dates) in response to shifts in the start of the rainy season.

The agroecological zone simulator (AZS) platform fills a significant gap identified by the Fourth Assessment Report of the Intergovernmental Panel on Climate Change (2007) and various studies cited in the previous chapter, highlighting the urgent need for improved estimates of crop yields in coming decades as a function of interannual climate variability and extreme events and of the impacts of pest and disease. In addition, the IPCC AR4 also called for existing crop modeling platforms, including those coupling of biophysics and economics, to be more transparent and accessible to end users, so that their assumptions and applications could be tested more extensively and so that their use base could be enriched with contributions from researchers and users globally.

AZS conceptual framework

Because of the complex interactions between climate, agroecosystems and agromanagement at farm to regional levels, assessment studies for agriculture rely on a suite of crop models and land management decision tools (Tubiello and Ewert 2002). For example, assessments have used dynamic crop models such as the Decision Support System for Agrotechnology Transfer (Tsuji and others 1994), the Erosion-Productivity Impact Calculator (Williams 1995), and ecosystem models modified to include some agriculture details, such as TEM (Feltzer and others 2004). These models compute harvest yields, crop growth, and plant water dynamics as a function of specialized databases containing soil, climate, and management information.

Dynamic crop models are very detailed at the plant functional and agromanagement level, differentiating growth (phonological) stages of a crop, and are thus able to capture details affecting final yield, which are often missed by ecosystem models. The first set of crop models allows for simulation of more realistic field management activities such as water and fertilizer management and sowing and harvesting operations. For these reasons, dynamic crop models require many input data for calibration and validation. They perform best at local to national scales, if sufficiently detailed "representative sites" can be found to cover the area of study. By contrast, simplified ecosystem models use generalized crop algorithms. They thus are better suited to large-scale simulations, requiring less detailed input data. But they may be prone to larger errors and validation problems, due to the lack of both crop and management detail (Fischer and others 2005).

Additional efforts include statistical approaches, where historical production and yield databases are analyzed in detail against climate databases, to arrive at simple, often one-dimensional equations that relate regional or national climate regimes to production (Lobell and others 2008). These can be powerful, especially considering the paucity of data to validate more complicated models in key study areas in developing countries. But their ability to capture true climate-crop dynamics under climate regimes outside current experiences is limited.

Still other efforts include empirical approaches, where surface response functions are derived from more detailed dynamic crop models runs, and then used as a sort of look-up table when running more extended regional or global simulations. These too can be quite powerful, because they allow assessing large regional areas in detail while saving on the number of simulations and thus on the computer power necessary with the full models. But surface responses lack information on how interactions of key processes may change under different climate regimes. In the end both statistical and empirical approaches offer poor representations of the agroclimatic and biophysical processes of importance to crop yields.

By contrast, an agroecological zone (AEZ) modeling framework, synthesizes essential components of the dynamic crop and ecosystem models described above, offering ways to merge dynamic details with large-scale outlooks. It uses enough detailed agronomic-based knowledge to simulate land resource availability and use, farm-level management options, and crop production potentials. It also uses detailed spatial biophysical and socioeconomic datasets to distribute its computations at fine grid intervals over large areas, including in some efforts the entire globe (Fischer and others 2002a). This land-resource inventory is used to assess, for specified management conditions and levels of inputs, the suitability of crops in rainfed and irrigated conditions—and to quantify the expected attainable production of cropping activities relevant to specific agroecological contexts in the study area. The characterization of land resources includes climate, soils, landform, and present land cover. Crop modeling and environmental matching procedures identify crop-specific environmental limitations, under various input levels and management conditions (Fischer and others 2005).

In general, an AEZ framework is characterized by the following basic elements:

- Selecting agricultural production systems with defined input and management relationships, and crop-specific environmental requirements and adaptability characteristics. These are termed land utilization types (LUT).
- Combining geo-referenced climate, soil, and terrain data in a land-resource database.
- Accounting for spatial land use and land cover, including forests, protected areas, population distribution and density, and land for habitation and infrastructure.
- Calculating potential agronomically attainable yields and matching crop and LUT environmental requirements with the respective environmental characteristics in the land resource database, by land unit and grid cell.
- Assessing crop suitability and land productivity of cropping systems, leading to the AEZ simulations.

The best known of such efforts is the AEZ FAO/IIASA model, used in a variety of global and regional assessment studies over the past 20 years (Fischer and others 2002a; Tubiello and Fisher 2007). Coupled to a partial equilibrium economic model, it has been the foundation for many seminal papers on food security and climate change (Rosenzweig and Parry 1994; Parry and others 2004).

Although AEZ simulations can be validated in many places, its global outlook implies that validation cannot be carried out at every grid point considered. One way to overcome this validation and calibration bottleneck is to provide a transparent platform that could be accessed by users around the world to allow for continual enrichment of the underlying databases and validation checks. The AZS output presented here builds substantially on the FAO/IIASA effort while also making the new platform fully transparent and available for use and field validation by country and regional stakeholders.

Specifically, the user-friendly open-access AZS platform developed in this study provides for data and model sharing among all interested member countries in Latin America and the Caribbean. And it can be readily extended to other regions of the world. Extending the AEZ framework, the AZS facilitates the analysis of impacts and adaptation responses by:

- Selecting agricultural production systems with defined input and management relationships, and crop-specific environmental requirements and adaptability characteristics.
- Combining geo-referenced climate, soil, and terrain data in a land resource database.
- Calculating the potential agronomically attainable yield and matching crop environmental and management requirements with the respective environmental characteristics in the land resource database, by grid cell.
- Computing water-limited, biotic factor–limited, abiotic factor–limited, and actual crop yields, by grid cell.
- Assessing crop suitability and land productivity of cropping systems.

Figure 3.1 provides a conceptual framework of the various components and data flows of the AZS platform.

Figure 3.1. Flow of information (green=inputs; orange=outputs) linking agroclimatic datasets to assessments of yield categories depending on land utilization type through dynamic biophysical simulations

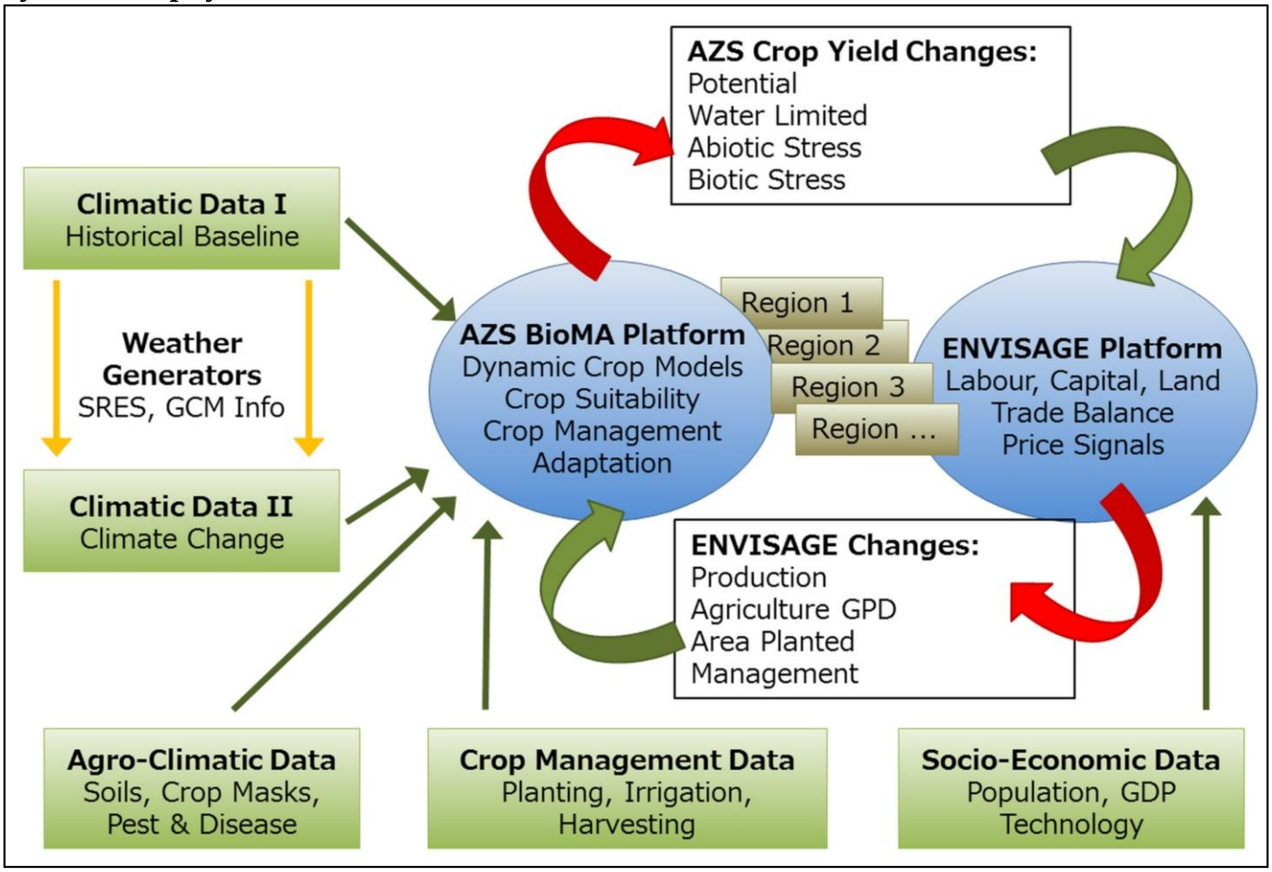

The AZS-BioMA and applications

The core output of this study, the modeling platform AZS-BioMA, provides the biophysical representation of crop development and growth, as a function of agroclimatology and management. The AZS is based on the BioMA (Biophysical Model Applications) platform, an extensible platform for running biophysical models on generic spatial units, based on discrete conceptual units codified in software components (both for simulation engines and for user interfaces). The guidelines followed in its development aimed at maximizing:

- Expansion and adaptation with new modeling solutions.
- Ease of customization in new environments.
- Ease of deployment (at national and local research and academic facilities).

This is the first time that such a coherent set of data and models are used to assess the impacts of climate change on Latin America crops across countries using the same consistent methodology. Simulations are carried out through modeling solutions, which are discrete simulation engines where different models are selected and integrated to carry out simulations for a specific goal, with each solution using extensible components. Third parties can extend BioMA independently by adding new modeling solutions, using components already in the application or using new ones.

The crop models compute development, growth, and productivity of selected crops (wheat, maize, soybean, rice) at each point over a 25 kilometers grid for Latin America, as a function of daily weather variables, including minimum and maximum temperature, precipitation, and solar radiation. Each of the grid level–results can be easily aggregated at any scale of interest.

The AZS-BioMA platform is briefly described here to provide a flavor of the kinds of data categories and the way data are harnessed for desired outputs. A detailed description of the AZS-BioMA platform is in annex I.

AZS-BioMA inputs

Climate data and weather generation

The climate database was developed in the following steps:

- Identifying a suitable and reliable historical climate database covering the study area.
- Selecting IPCC AR4 emission scenarios (A1B and B1) as inputs for two GCMs (Hadley and NCAR).
- Generating the baseline and of the climate change scenarios (using GCMs outputs) through a weather generator.

The historical climate data are those produced by the European Centre for Medium-Range Weather Forecasts (ECMWF), an intergovernmental organization supported by 32 countries. Among its main activities is the reanalysis of multidecade series of past observations.

Datain this project come from the ECMWF ERA-Interim, a global reanalysis of the data-rich period since 1989 (www.ecmwf.int/research/era/do/get/era-interim). The ERA-Interim reanalysis starts in January 1989 and provides meteorological data until today. The ERA-Interim data are, for our purposes, resampled to 0.25 degree grid cells (25 km x 25 km) to be consistent with other real time data, like outputs of the ECMWF global circulation model.

Variables available in the ECMWF ERA-Interim database are average surface air temperature, maximum and minimum surface air temperature, precipitation, evapotranspiration (over water, bare soil, and based on the Penman-Monteith method), global solar radiation, snow depth, average wind speed, and water vapor pressure. Other variables, including hourly values, are derived using the CLIMA libraries (Donatelli and others 2005, 2009; Bregaglio and others 2011).

A first phase involved the use of the weather generator to estimate parameters describing the features of the climate for each cell, such as monthly and annual trends, level of continentality, thermal excursion, and rainfall distribution. Once these parameters were estimated, they were used to generate the baseline climate. The baseline—a series of climate data with the same features as the historical ones—was regenerated to allow the most unbiased comparisons between the results of biophysical models based on generated baseline and climate change scenarios.

Two IPCC AR4 scenarios (A1B and B1; IPCC 2000) were selected as inputs for two general circulation models (GCMs): Hadley3 (Gordon and others 2000) and NCAR (Collins and others 2004). The GCMs are realizations of the emission scenario chosen. The Hadley3, maintained and run by the U.K. Meteorological Office, was chosen because it is a de facto standard. The NCAR model was chosen because it has been extensively evaluated in the Americas. The time span of the analysis is 2020 and 2050. The A1B scenario projects rapid economic growth, a global population peak in 2050 with a rapid introduction of new and more efficient technologies (that is, the A1 business as usual storyline) combined with a balanced input between fossil and nonfossil energy sources to support the technological changes envisaged (resulting in the A1B scenario). The B1 scenario is based on the same storyline as in the A1, but foresees rapid changes in economic structure that reduce material and carbon intensity by introducing clean and resource-efficient technologies.

Without being the most extreme, the two emission scenarios selected for this study represent most of the range of projected temperature increases over the coming decades. It is also worth noting that for a given emission scenario, the simulation outputs from more than 10 available GCMs overlap significantly with the two GCMs selected for this study. The emission scenarios differ at the end of the century, much less at 2050, and very little at 2020, the latter two being the time span for this study (figure 3.2).

Figure 3.2. Projected mean surface temperature change as a function of IPCC SRES scenario, indicating mean projected values (solid colors) from a range of GCM simulations corresponding to each family of greenhouse gas emission scenario (grey bars)

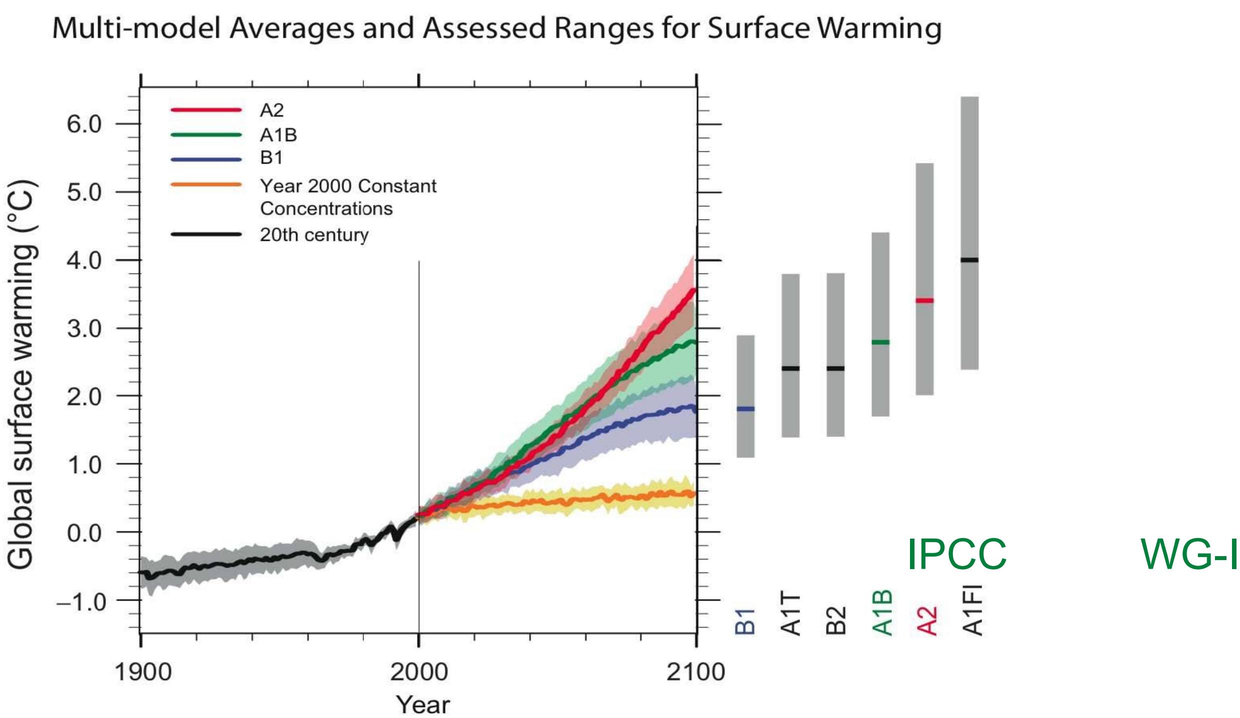

To generate spatially distributed weather data for the biophysical crop models, the Climak weather generator (Danuso 2002) was used, allowing the generation of synthetic, long-term daily weather data series through the statistical analysis of shorter term observed weather data at any location. At the same time, the statistical parameters extracted to characterize a given climate regime, such as the baseline climate, are easily modified to obtain new synthetic weather series representing future climate change regimes. This is done by using GCM-driven information, such as projected mean changes in temperature and precipitation for a given future time window, under a particular SRES scenario.

A first phase used the weather generator to estimate parameters describing the features of the climate for each cell, such as monthly and annual trends, level of continentality, thermal excursion, and rainfall distribution. These parameters, once estimated, generated the baseline climate (without applying any GCM-derived information to the parameters) and the climate scenarios (applying results from GCMs to specific parameters).

- The baseline—a series of climate data with the same feature of the historical ones was regenerated to allow the most unbiased comparisons of the results of biophysical models based on baseline and climate change scenarios (in both cases derived from a generation process).

- Regional climate models (RCMs) were not applied, as an intermediate step between the GCM outputs and the parameters of the weather generator, because we could not assess, in the time frame of the project, whether a homogenous set of models was available to cover the Central and Latin America. A heterogeneous set of RCMs, even assuming their ready availability, would likely have introduced a bias in the comparisons of different countries.

- The number of years generated is 10, not a larger number such as 50, due to the time and resource constraints of the project.

Figure 3.3 presents summer average daily thermal anomalies (°C; difference between climate change scenario and baseline data) for Hadley-A1B for the two time frames.

Figure 3.3. Summer (December, January, February) temperature anomalies obtained by generating A1B scenarios (2020 on the left, 2050 on the right) with the Hadley GCM

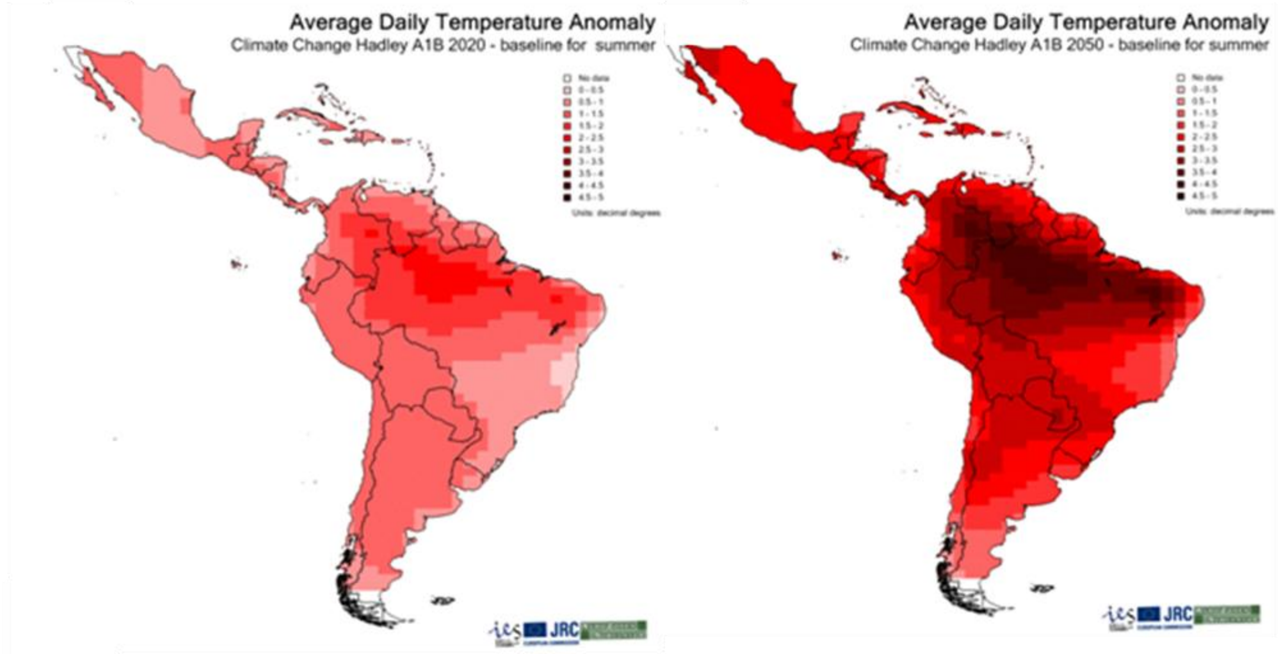

Soils

The soil dataset (Hoogenboom and others 2009) is derived from the updated version of the "World Inventory of Soil Emission Potentials" (WISE version 1.1, Batjes 2002). The WISE 1.1 database was created to provide a basic set of uniform soil data for a wide range of global and regional environmental studies (such as agroecological zoning and assessments of crop production). The profiles collected in the database came from five main sources:

- ISIS 4.0, the Soil Information System (van Waveren and Bos 1988) of the ISRIC (International Soil Reference and Information Centre).
- SDB, the FAO Soil Database System (FAO 1989).
- A digital soil dataset compiled by the Natural Resources Conservation Service of the United States of America (Soil Survey Staff 1996).
- International data gathering activity coordinated by WISE project staff, with national soil survey organizations asked to supply descriptions and analysis of profiles representative of the units of the Soil Map of the World (FAO-UNESCO 1974).
- Suitable profiles from a survey and stored in the ISRIC library.

Note that the simulations limited to soil water (not considering nitrogen) are sensitive to basic soil parameters derived from texture and soil depth, because they determine the hydraulic (water flow) characteristics. A more detailed database that better represented actual soil depths and presence in a given cell could improve the representativeness of simulations for that cell. But the differences in the output would not differ markedly except for extremely shallow soils. Figure 3.4 provides examples of soil water properties stored in the soil dataset.

Figure 3.4. Drainage rate (whole profile) and saturated hydraulic conductivity (top soil). Crops, distributions (masks), and calendars

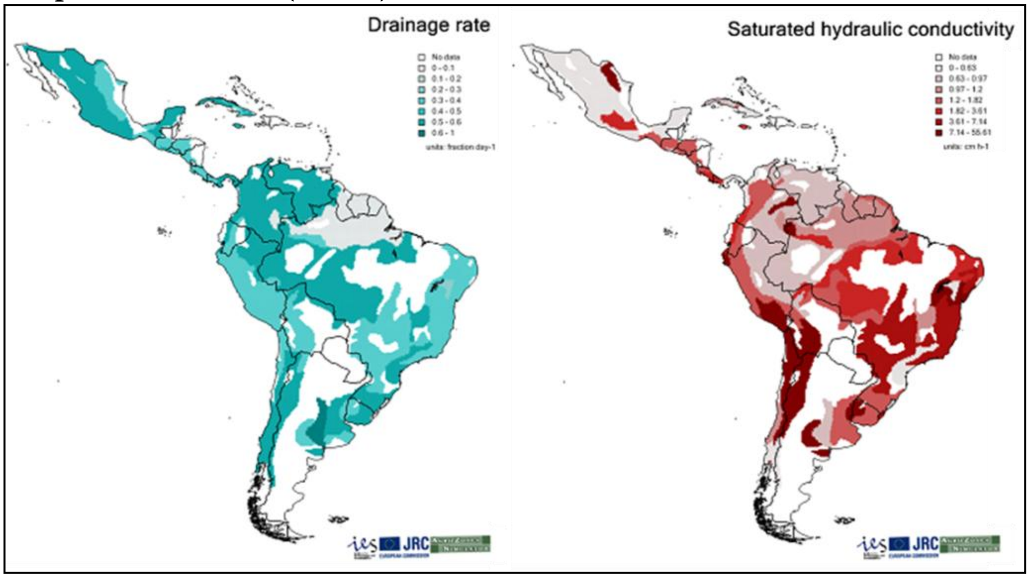

The crops considered in the study are wheat, soybean, maize, and rice, fundamental to both food security and economic trade for Latin America and globally. Indeed, the same set of crops was used in a recent analysis of current impacts of climate change on food security (Lobell and others 2011). According to 2008 FAO statistics (http://faostat.fao.org), the crop with the most tonnage in Latin America is sugarcane (table 3.1), even if it is second to soybean in economic production ($). The second crop in tonnage is soybean. Rice and maize rank third and fourth in economic production and fourth and third in tonnage. Wheat comes in at eighth in economic production and sixth in tonnage. Crop masks for wheat, soybean, maize, and rice were derived from the SAGE Center for Sustainability and the Global Environment—Nelson Institute of Environmental Studies, University of Wisconsin-Madison (SAGE www.sage.wisc.edu/index.html) (figure 3.5).

Figure 3.5. Crop masks (areas where crops are currently grown) used within the project

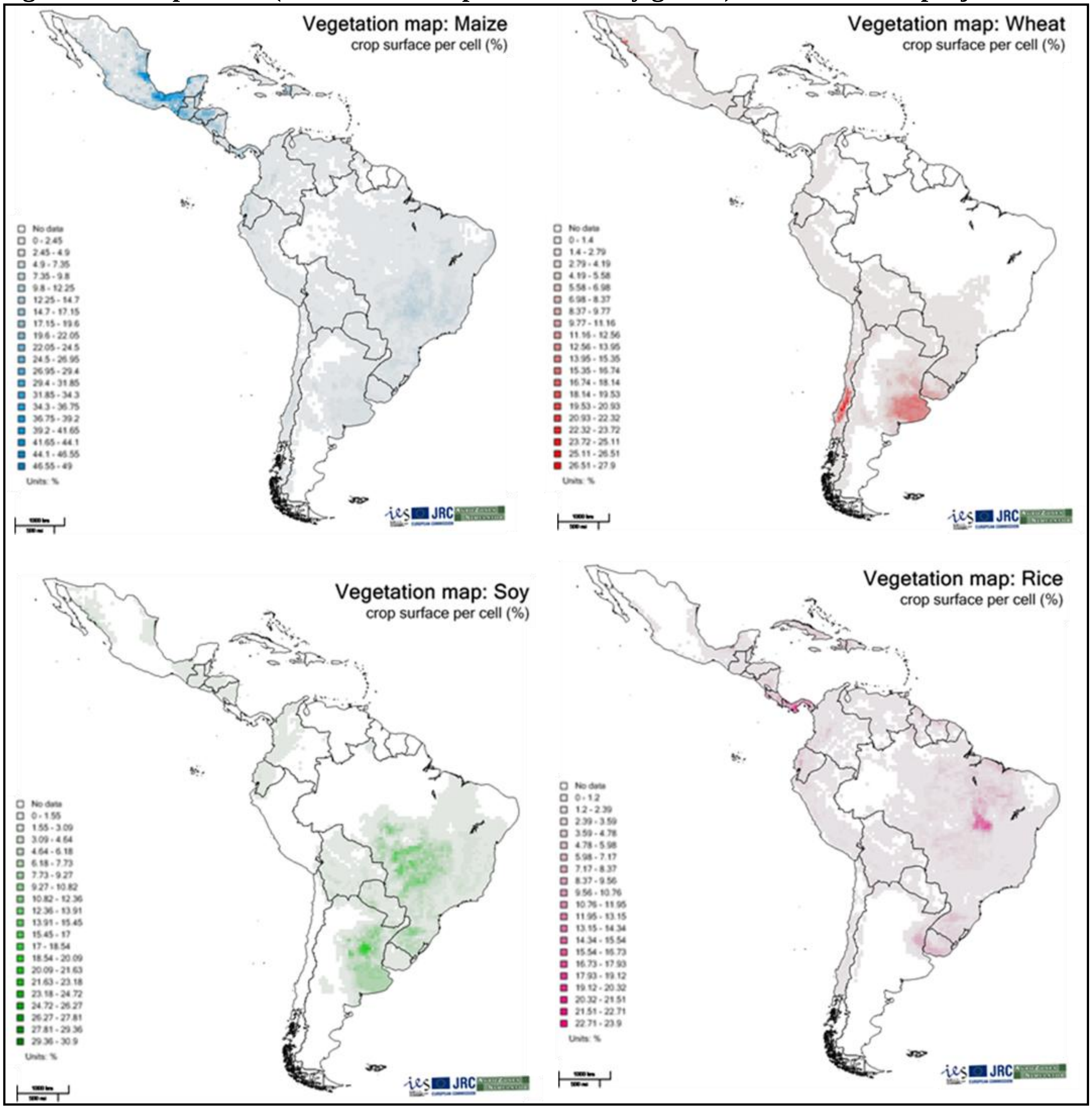

Source: Crop calendars for Latin America and the Caribbean were downloaded from the SAGE Center for Sustainability and the Global Environment database (www.sage.wisc.edu/download/sacks/crop_calendar.html).

Table 3.1. Tonnage and economic productivity for the four crops analysed in the project

	Crop production (Bt)				Economic production (M$)			
Country	Maize	Rice	Soybean	Wheat	Maize	Rice	Soybean	Wheat
Argentina	22,017	1,246	46,238	8,508	2,042	258	9,859	1,234
Bolivia	1,002	338	1,260	200	60	68	246	29
Brazil	58,933	12,061	59,242	6,027	1,925	2,523	12,361	877
Chile				1,238				163
Colombia		2,792				577		
Costa Rica		248				52		
Ecuador	804	1,442			26	299		
Guyana		507				105		
Guyana (Fr)		9				2		
Honduras	536	49			21	10		
Nicaragua	424	322			45	67		
Panama		301				63		
Paraguay	2,472	150	6,312	799	158	31	1,309	104
Peru		2,776				585		
Suriname		183				34		
Trinidad and Tobago		2						
Uruguay		1,330	880	1,288		278	180	187
Venezuela	2,996	1,361			187	189		
Total	89,184	25,117	113,932	18,060	4,464	5,143	23,954	2,595
Rank within Latin America and the Caribbean	**3**	**4**	**2**	**6**	**4**	**3**	**1**	**8**

The AZS-BioMA modeling platform

The modeling platform represents a paradigm shift in current modeling approaches—for three reasons:

- First, the concept of multiple options for simulation is made available and can be further extended, adding modeling approaches, such as the ones implemented in Decision Support System for Agrotechnology Transfer models.
- Second, because of the fine resolution used to implement models, users can implement variants of modeling approaches. In particular, given the goal of simulating crop growth under extreme weather conditions, a curvilinear response to hourly temperature of plant development phases and growth, with a decline beyond optimal temperature, is implemented (hourly temperatures are derived with good accuracy from daily maximum and minimum temperature data). This approach estimates suboptimal rates at high temperatures, reproducing biologically known patterns of responses to temperature, and leading to estimates of development and growth that are diversified with respect to the

known accumulation of growing degree days and the yield plateau response to temperature.

- Third, the software architecture allows users to easily simulate various production levels—such as potential water-limited, nitrogen-limited, and disease-limited productivity—thereby allowing deeper analysis of and insights from the production system simulated. In particular, biomass growth equations implemented in the current version of AZS-BioMA allow users to compute the impacts of elevated CO_2 on crop growth and yield.

BioMA is the platform currently used at the European Commission Joint Research Centre to investigate the impacts of climate change on crops in the EU-27, as well as in key production regions of the world, including Russia and the Commonwealth of Independent States, Latin America, China, India, and a few countries in Sub-Saharan Africa. Because BioMA is already a multiregional platform, it can be scaled up fairly easily to provide more intensive coverage of other regions.

Chapter 4. Estimates of Climate Change Impacts for Wheat, Soybean, Maize, and Rice in Latin America (2020 and 2050)

Crop simulations for each of the four crops and each of the eight climate-change scenarios were then performed and compared with the baseline results. Such simulation sets were made assuming no adaptation (the same cultivars and agromanagement used under current conditions) and with adaptation (allowing for modified plant and management conditions to minimize damage under future climate regimes). Clearly, the first set of simulation results is in practice rather unrealistic, given that farmers' responses to modified weather conditions are to be expected. Even so, the "no adaptation" set of results serves as a benchmark to measure the benefits of adaptation actions.

The adaptation solutions investigated here are quite simple, but it can be expected that farmers will need some time to develop enough experience and confidence for their large-scale application. And some solutions will require that infrastructure be in place at the time of need. For both reasons, the adaptation scenarios should be fairly plausible for 2050, but more limited for 2020.

The general definition of adaptation tested through simulation in this project is given by changes in agricultural management that farmers may implement to alleviate the negative impacts of the weather scenarios. Adaptation by farmers will occur, to some extent, regardless of any action to support or steer it from government or local authorities. So, although simulating impact assessment for "unchanged systems" is a prerequisite to getting insights about system behavior with the target of developing adaptation strategies, its results should not be considered as one of the possible "future scenarios for agriculture."

Adaptation tests are run considering three factors:

- Genotype—the duration of the crop cycle evaluated is medium for the analysis of the baseline, whereas early and late maturity genotypes are also evaluated in the simulation of weather scenarios.
- Planting time—explored by testing the anticipation of planting dates.
- Water supply—implemented using the same rule-based model as the baseline simulation, parameterized to provide a medium level of water availability, as detailed in annex I.

Water supply was always active in simulations for irrigated and potentially irrigated crops (maize and soybean in this study), while all combinations related to genotype and planting time were explored. Crops were simulated in cells where their relative occupancy was 1% or more of the agricultural area. The modeling capabilities of the platform allow simulating, for each crop, adaptation strategies, weather scenarios, and different abstractions of production systems identified as production levels:

- Potential production (P: crop growth solar radiation and temperature driven).
- Water–limited production (WL: all factors of P and water limitation).

- Abiotic stress–limited production (AL: P and effects due to temperature stresses of extreme events for crops).
- Disease–limited production (DL: P and impact from one crop-specific disease).
- Multiple factors–limited production (MFL: P, WL, AL, and DL).

The simulation of potential production is useful to test responses not constrained either by resources—as quantities—or by technology (or by both). So, estimating multiple factors–limited production allows estimating the technological gap (for example, we do not use a pivot system to irrigate weekly, so there are no more than four irrigation events per season by sprinkler) and water–limited production (for example, no more than 300 millimeters of water available per season). Notably, negative impacts of climate change on crop productivity can be minimized with simple adaptation measures—that is, either by planting different genotypes and changing the timing of sowing (same crop—we test both) or by changing crops (we provide only scenarios of land suitability for crops).

When water–limited production was simulated, a rule-based agromanagement model to supply water to crops was used. That is, adaptation for water use is included (adaptation is not constrained by water availability beyond setting rules and is not constrained by technology). The water–limited simulations estimate a possible technical adaptation, whereas context specific constraints (such as no more than 300 millimeters per irrigation season and no more than three irrigations) can be considered ex-post, evaluating the adaptation scenarios provided, or lead to another run of simulations.

The simulation of disease–limited production does not include agromanagement to alleviate the impact of possible increased pressure by plant pathogens due to climate change. These simulations can be of direct use if no chemical can be applied in a given context; otherwise simulation results would overestimate the impact of climate change neglecting possible adaptation. In the latter case, economists could use the quantitative estimates of disease–limited production in a semiqualitative fashion.

From the above, the assumption of water–limited production is that diseases, if affecting the crop, will be controlled either chemically or genetically.

The choice of production systems and adaptation focus on the basic food commodity–based production systems abstracted at the level of "crops." But the simulation of crop-disease impacts is innovative.

Limitations

Several assumptions were made while using data and selecting specific modeling solutions and designing the simulation experiments here. Such assumptions set the limits for using the results of this analysis. They should be carefully evaluated to avoid introducing conceptual errors in the final results of an integrated modeling chain, for which the crop biophysical simulations are an input. The assumptions follow.

Weather data

Weather data refer to the ERA-Interim interpolation. The time series representing each 25 km x 25 km grid cell refers to flat land at the predominant elevation above sea level. This makes the time series more representative of real systems, which are also more uniform in flat land areas. But the representativeness is more critical for areas where slopes change within cell. In these cases more detailed analysis using digital elevation models and a smaller spatial scale would articulate more system performance. But given the target of the study, Latin America and the Caribbean, the approximation can be considered acceptable.

Furthermore, general circulation models (GCMs) provide estimates primarily of mean temperature, rainfall, and solar radiation. Given model requirements as inputs, the pattern of variability of other variables (such as wind, and relative humidity) must also be used. It was kept unchanged in data layers of scenarios of climate change in these simulations. In addition, GCM outputs typically lack detailed and quantified indications of realistic changes in the frequency of extreme events. For this reason, climate variability—the shape of higher order moments—was kept at present values. The specific distributions—based on thresholds, such as the number of temperature or water-related stress events—were modified in our time series. But one could imagine developing climatic “subscenarios,” where the variability of specific climate variables could be changed in a sensitivity approach—using the features of the weather generator in the platform.

Model calibration

Model calibration, on literature resources, generally make available reference data for large areas. It needs to be refined by interacting with local experts and stakeholders, so that the right cultivars and cropping systems could be simulated as opposed to the idealized types simulated here. For this reason, although the general impact trends can be considered robust in terms of extensive regional signals across all four crop types, specific crop-country results need to be interpreted with caution, since they depend on the specific cultivars in this round of simulations. For weather data, analysis at a finer spatial scale using local expertise would yield better results for each target area.

Soils

As for weather data, soils were distributed on a flat surface—terrain. This may alter significantly the soil–water balance in areas with steep terrain. And in areas where soils are differentiated, ranging from high to low water-holding capacity, simulation results will represent only a limited portion of actual results, though they capture the predominant features of the system.

Effects of elevated carbon dioxide

The effects of elevated carbon dioxide (CO_2) on crop growth and yield included in the AZS-BioMA platform are consistent with current findings (Tubiello and others 2008). Even so, it is widely expected that CO_2 responses in farmers’ fields here will be lower than found experimentally, so that the functions in the simulations here are likely to overestimate actual field responses.

Production systems

Production systems were abstracted at the level of "crop," ignoring possible structure of cropping systems. If cropping systems were analyzed instead, crop performance in a given cell would result from its performance in different rotations and under different inputs of resources. And because of weather data resolution, model calibration, and soils, the simulation results are an abstraction of production systems for the area—and should thus be compared with actual point data, with caution. But the goal of the analysis is to estimate basic impact dynamics and adaptation strategies for the large areas considered.

Adaptation strategies

The adaptation strategies considered basic technical options likely available to farmers today. So, the alleviation of the impact of climate change was estimated on the basis of the same abstraction of production system evaluated in the baseline simulations (current conditions).

There was no consideration of agent-based feedback to building adaptation strategies—from neither agricultural models nor farm models—capable of identifying further options for production systems (such as new crops), and setting constraints due to technology limits, resource limits, or both. And given the time span of the analysis, no innovation (new genotypes) was tested. This hypothesis can be considered mostly adequate for 2020, but is probably quite conservative for 2050, when even the adapted systems tested would not be very effective at all sites in alleviating the consequences of climate change. For 2050 complete changes in the typology of production systems should be tested, rather than simple changes in agromanagement and resource use evaluated here. This section analyzes simulation results as percentage yield declines due to climate change—without and with adaptation strategies for 2020 and 2050.

Adaptation strategies for water management, tested in this report, were developed by considering current irrigation practices throughout the region—including maximum annual applications. But they do not consider future water availability in the region, either due to sector competition or hydrological changes from climate change. Sophisticated 2-D hydrological models coupled to socioeconomic projections, beyond the scope of this study, would be necessary to address this limitation. Thus the set of adaptation solutions we identified need to be evaluated case-by-case, on the basis of local expert knowledge and stakeholder involvement.

Results

Figures included in this section present the simulation results (percentage variations from the baseline) for water–limited and disease–limited yields. Results for the Hadley-A1B climate-change scenario were consistently more pronounced than for the National Center for Atmospheric Research (NCAR) projections. Full simulation results for both scenarios are in annex II. Figure 4.1 provides first an aggregated summary by country, indicating crop yield responses by crop with adaptations, including modifications to irrigation. This set of results was an input to an economic model to estimate damage to production, price effects including projections of agricultural value added (see box 4.1 on the environmental impacts and sustainability applied general equilibrium model).

Figure 4.1. Aggregate impacts on crop yields, with adaptation, computed by the AZS-BioMA platform under 2020 and 2050 NCAR GCM for the A1B scenario

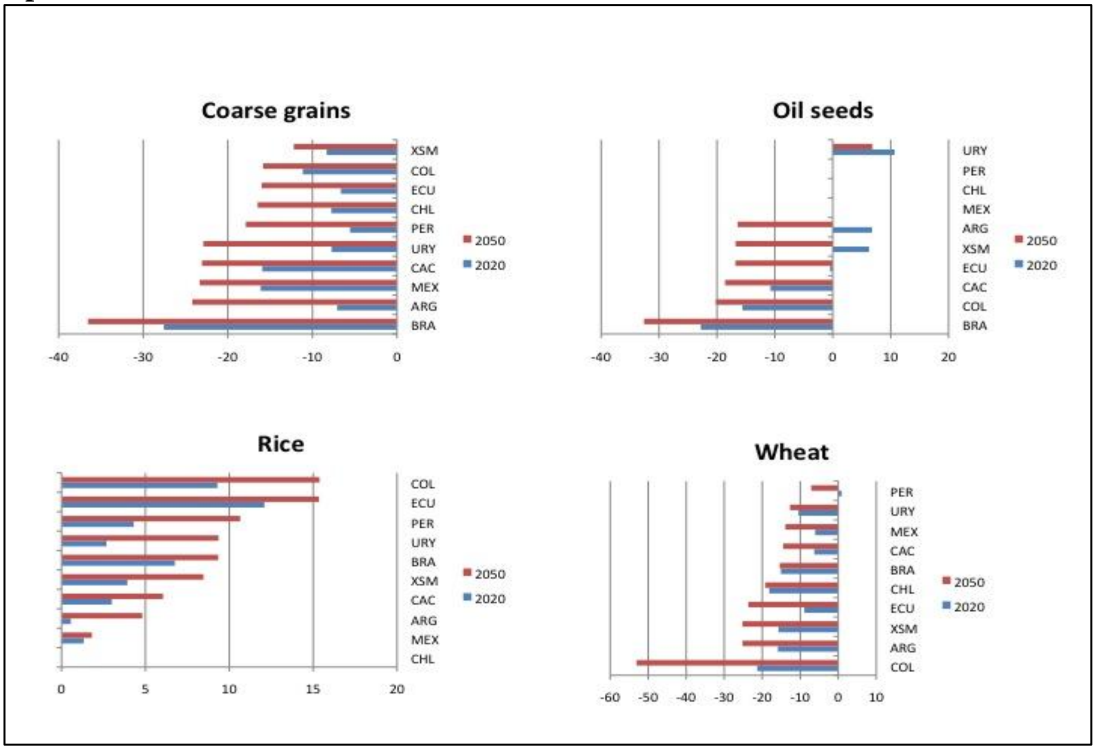

Wheat

Without adaptation, wheat yields could be significantly affected by climate change, regardless of the emission scenario or GCM (figures 4.2 and 4.3; annex II). Percentage yield declines were more pronounced in Mexico, in the Caribbean region, and in the northeastern parts of the continent (Colombia and Brazil). The projected water–limited production for 2020 and 2050 could be lower than in the baseline, with southern and western countries less affected. Yield reductions are due to the shortening of the crop cycle, due to higher thermal time accumulation, leaving fewer days available to fill grains. The projected yield declines due to disease in 2020 and 2050 could also significant. Frost damage is expected to affect wheat yields less seriously in Chile, where shorter cycles could reduce the crop exposure to pathogens, thus reducing also the pressure of wheat leaf rust. With few exceptions (such as Chile), insufficient water availability could affect wheat productivity more than other factors, suggesting the development of varieties with characteristics able to assure higher resistance to water shortages, such as more capability to deepen the soil portion explored by roots and more favorable leaf angle distribution.

Compared with the simulations carried out without the implementation of adaptation strategies, projected impacts were decidedly less pronounced for all the production levels and scenarios considered (figures 4.2 and 4.3; annex II). Impact on water limited yields was still significant however, with water availability playing a key role in limiting wheat productivity: the use of genotypes with longer cycles compensated for the climate change effect in reducing the grain filling period, but increased transpiration demands. Except in Chile, disease pressure decreased everywhere, though no adaptation strategies specific for leaf rust were applied. The highest indirect benefits of adaptation on disease–limited productions were simulated for Brazil and Uruguay and for Latin America and the Caribbean countries. Insufficient water availability played a major role in Brazil and Chile, whereas disease pressure affected productions especially in Argentina.

Figure 4.2. Wheat productivity shocks (Hadley A1B) to 2020

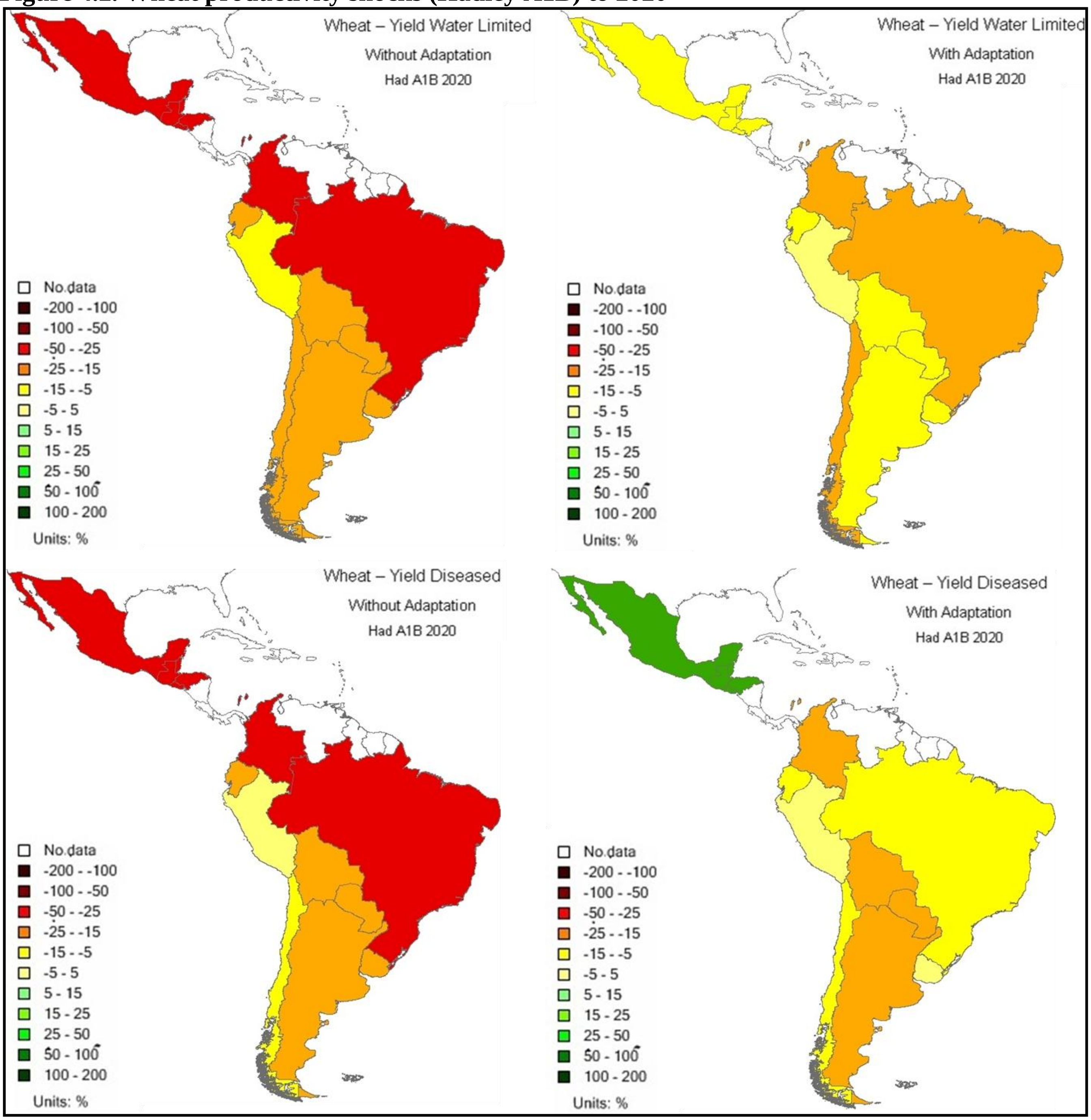

Figure 4.3. Wheat productivity shocks (Hadley A1B) to 2050

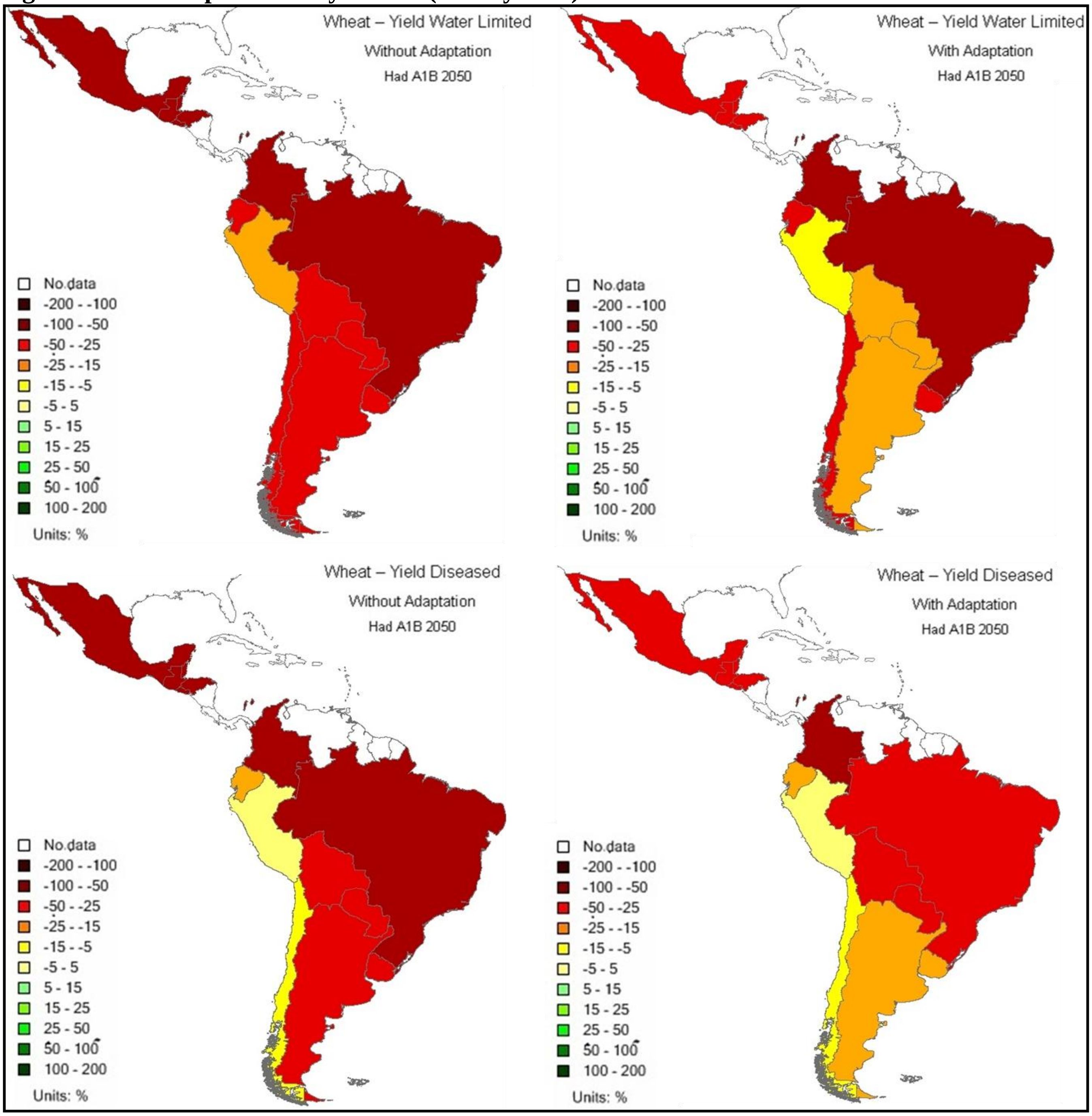

Soybean

Without adaptation strategies, soybean yields could be reduced by climate change in 2020 and more so in 2050, though with different magnitudes throughout Latin America (figures 4.4 and 4.5; annex II). Yield losses were larger in Brazil and in the northern part of the continent (more than -30% from the baseline), but less pronounced in Argentina, Bolivia, Colombia, and Uruguay.

By considering projected water–limited production level, yield losses were reduced in Argentina and Uruguay, whereas in Brazil, Central America and Caribbean regions they suffered reductions. This could be explained by the greater impact of climate change in Brazil (see D2 for further details), where the shorter crop cycle is more pronounced than in other parts of Latin America, markedly shortening the soybean grain-filling period. The impact of rust disease would not increase with warming, except for Colombia, where it increased for all combinations GCM × emission scenario. This can be explained by the severity of the increase in temperature regimes in a warm environment such as Colombia's, in turn leading to more favorable conditions for the pathogen.

Adaptation strategies (figures 4.4 and 4.5; annex II) reduced the magnitude of impacts across all scenarios and time windows considered. For example, considering the potential production level, there were situations with positive impacts of climate change with adaptation (Ecuador and Uruguay). The most affected country was Brazil, with a maximum percentage of yield losses still close to –25% (Hadley-A1B). In certain countries, percentage yield decreases were similar regardless of water management status (Brazil, Colombia, Uruguay, Latin America and the Caribbean). In others, the climate change impact was larger under water–limited conditions (Ecuador). In Argentina the use of varieties with longer cycle compensated the climate change negative effects tending to shorten crop cycles.

Figure 4.4. Soybean productivity shocks (Hadley A1B) to 2020

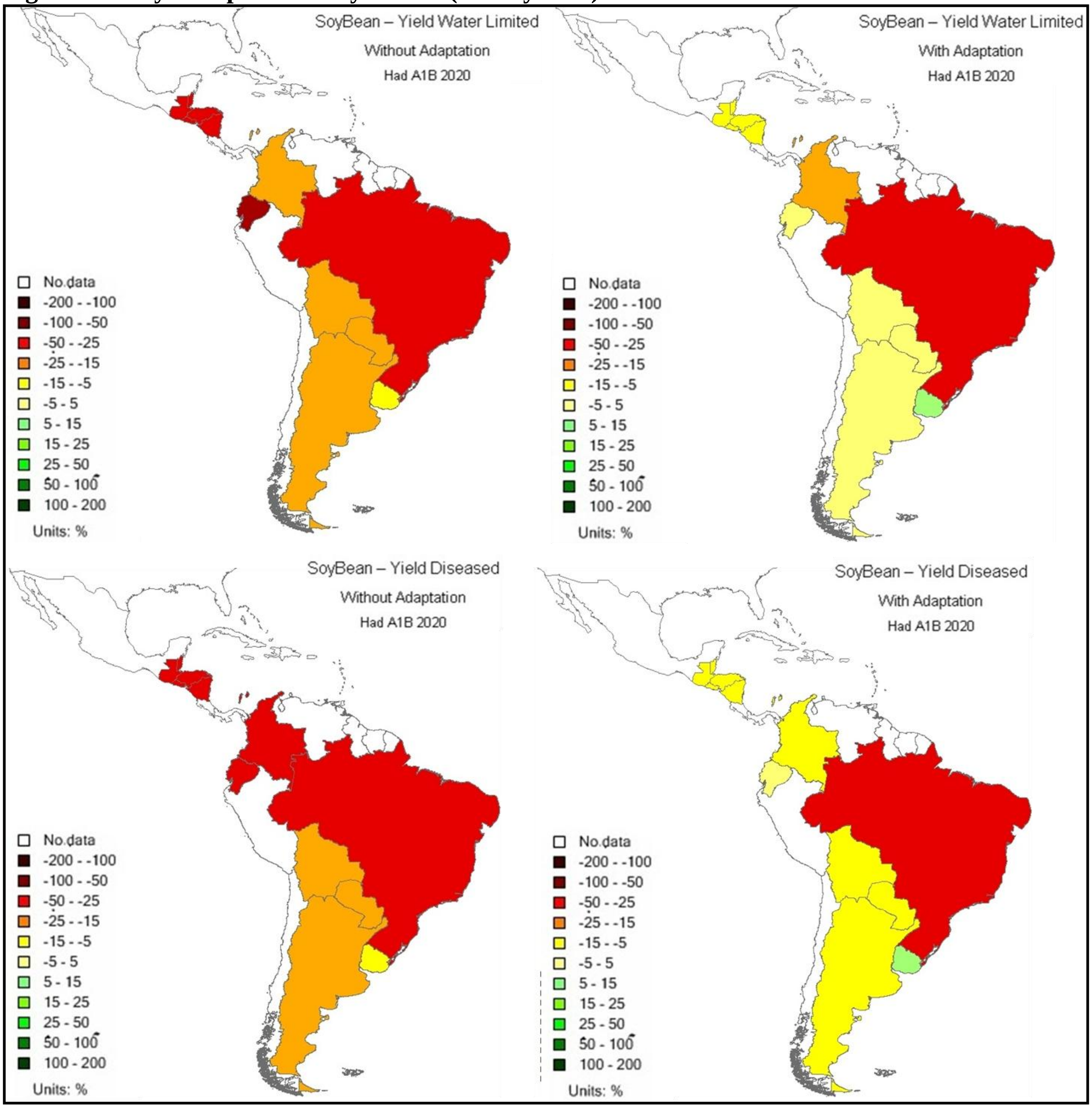

Figure 4.5. Soybean productivity shocks (Hadley A1B) to 2050

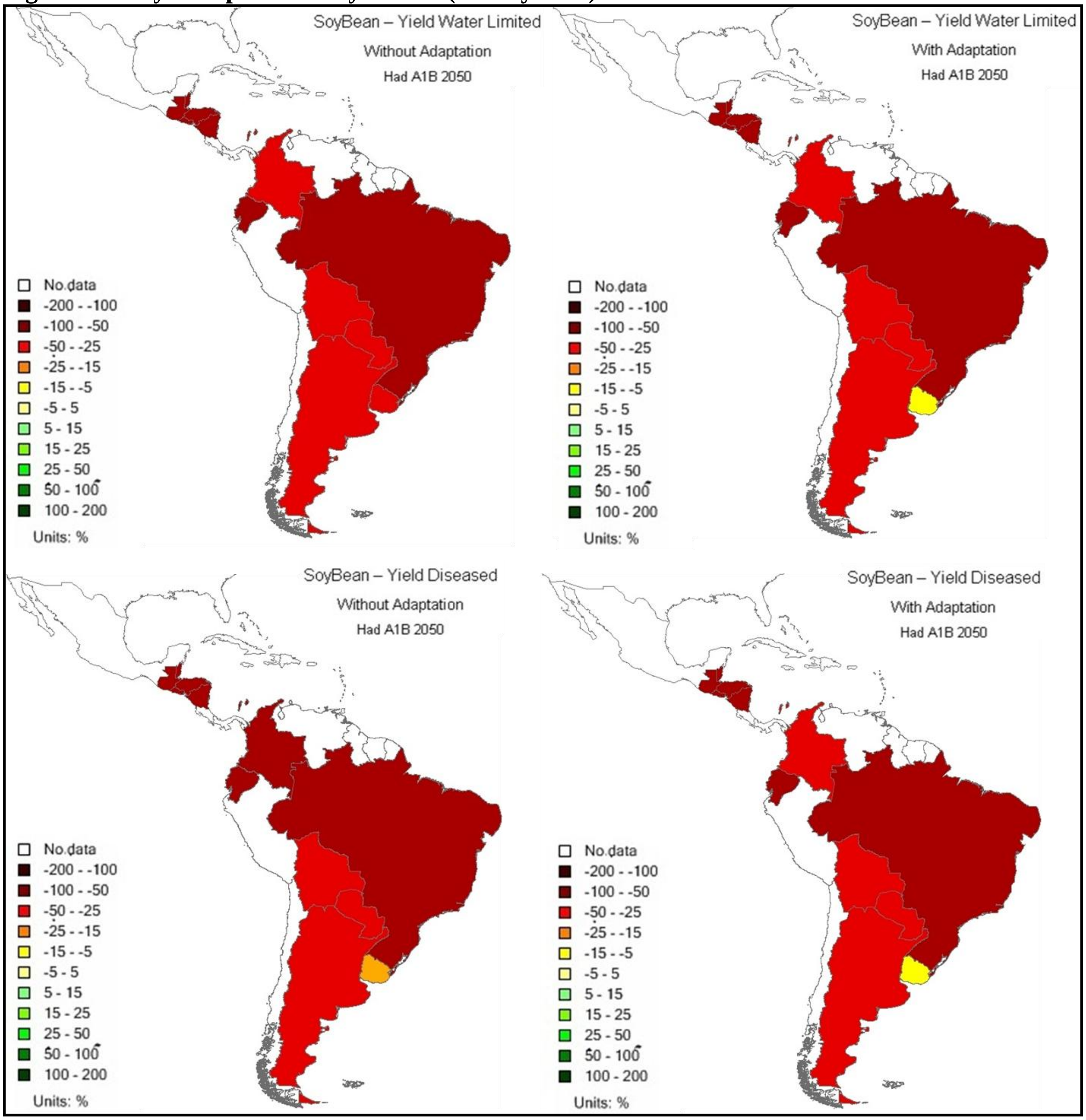

Maize

Climate change could reduce the yields throughout Latin America, regardless to the emission scenario or GCM (figures 4.6 and 4.7; annex II). This is mainly due to the shorter grain filling period under the higher thermal time accumulation rates, not being compensated for by the higher daily biomass accumulation rates and the CO_2 fertilization effect (lower in C4 species like maize).

The countries most affected were Brazil, Ecuador, Mexico, and Caribbean countries, where maize is one of the main crops. The Hadley GCM produced the highest losses, except for Brazil and Ecuador (for the latter, only for the B1 scenario). Abiotic factors did not significantly affected maize productions, with the only exceptions represented by a slight yield decrease in Mexico, Central America, and the Caribbean. Considering the heterogeneity of the responses in the area, the need for adaptations strategies developed at country level is evident.

For the 2020 timeframe, and to a much lower extent in 2050, adaptation strategies could dampen the negative climate change impacts on grain maize yields in most of the regions of interest (figures 4.6 and 4.7; annex II), though yield declines could still be relevant in major maize-producing countries, like Mexico.

Higher percentage decreases were simulated for the Hadley GCM compared with the NCAR one, with the A1B emission scenario usually leading to the most severe situations. Adaptation strategies positively concurred to limit climate-change damage to maize production, even in the countries where the grey leaf spot was the most limiting factor.

Figure 4.6. Maize productivity shocks (Hadley A1B) to 2020

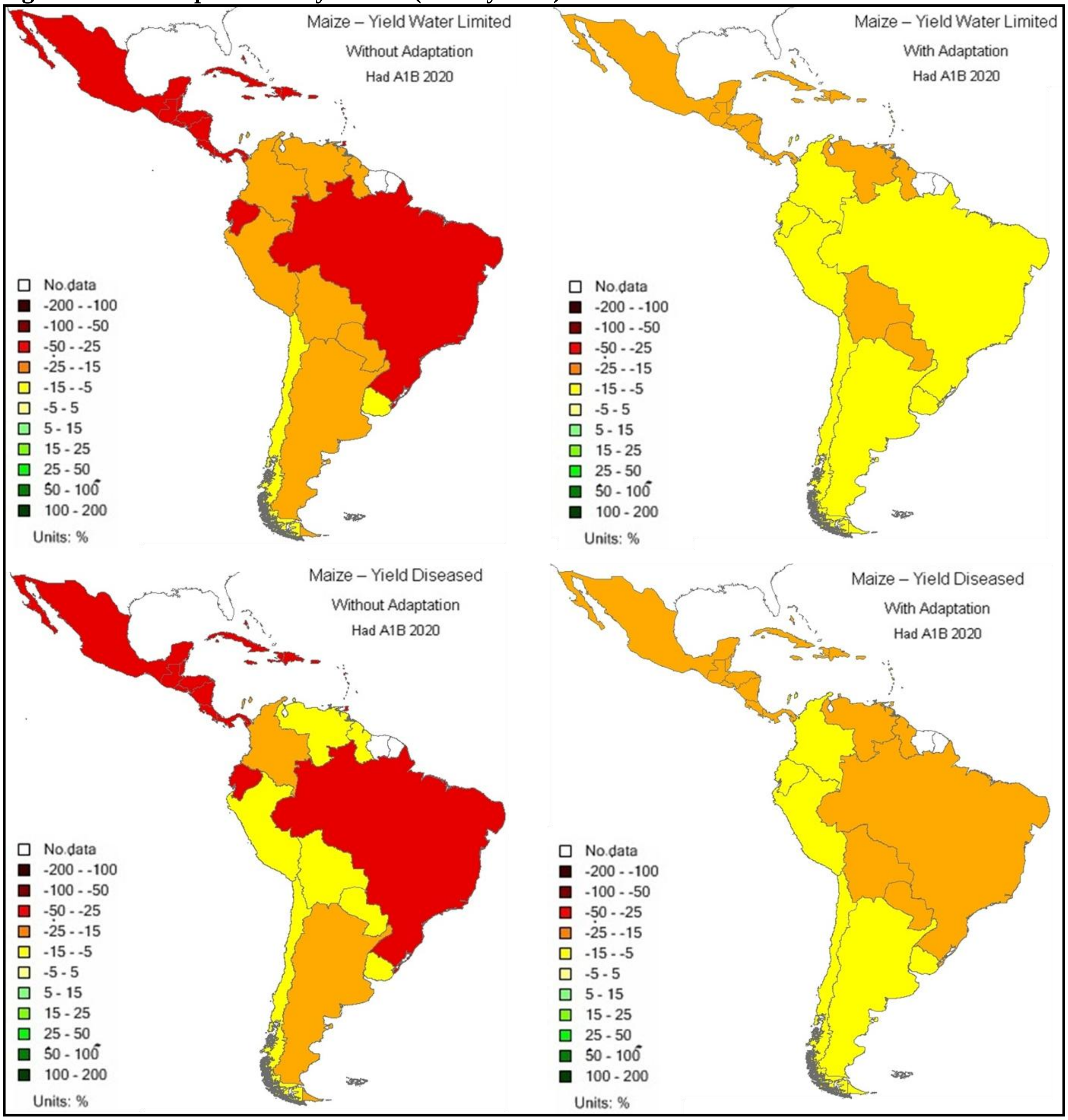

Figure 4.7. Maize productivity shocks (Hadley A1B) to 2050

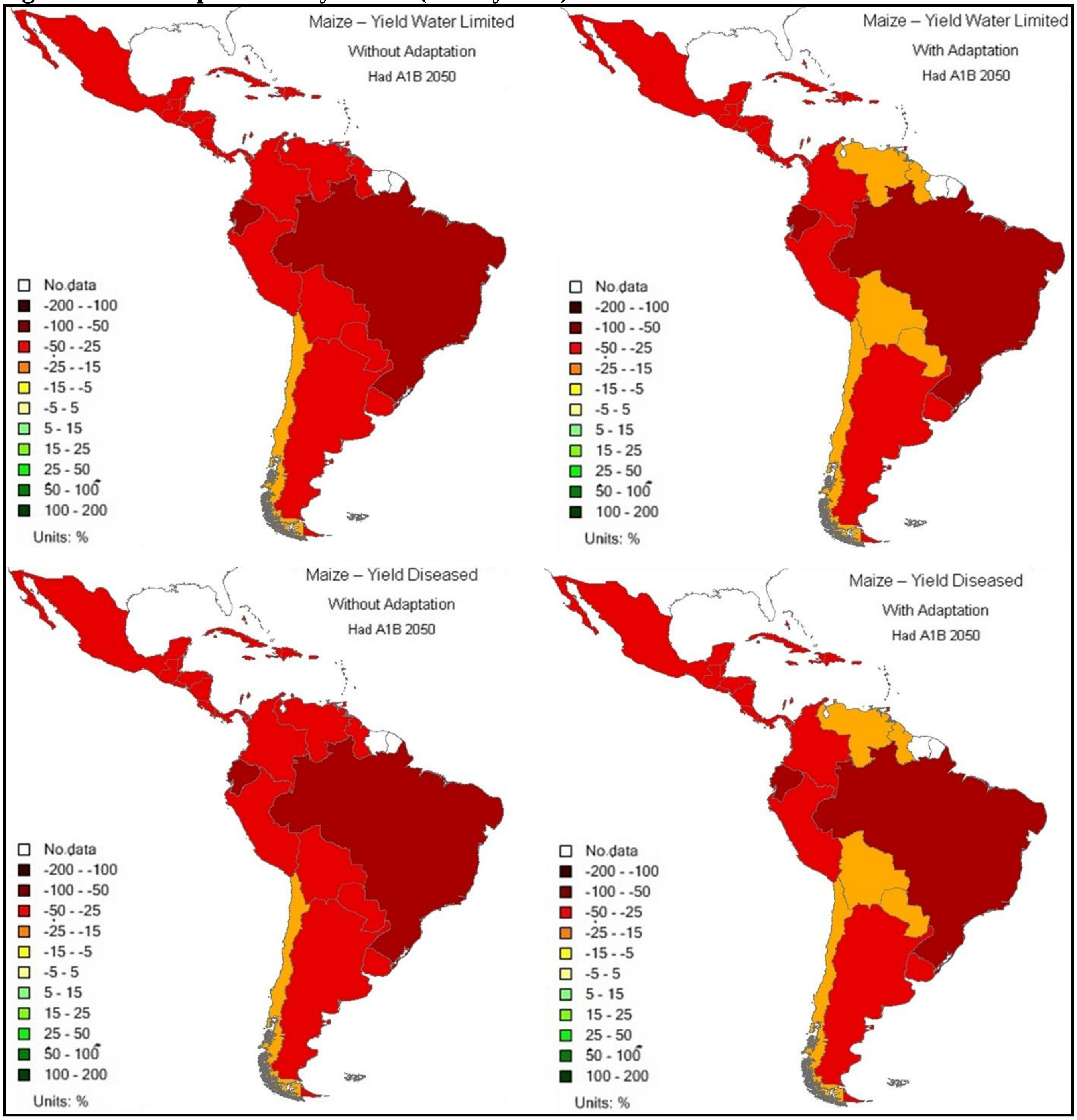

Rice

Except for Brazil, Mexico, and the Caribbean, the 2020 and 2050 projections are encouraging, with higher productivity projected in most of the cases (figures 4.8 and 4.9; annex II). Rice has higher thermal (temperature) requirements. Under current climate conditions (the baseline) production is slightly penalized by photosynthesis being limited by suboptimal temperatures.

With warmer conditions the negative effect of the shorter grain-filling period would be counterbalanced by higher biomass accumulation rates because of the most favorable conditions for photosynthesis.

The result of these two opposite effects is a general increase in productivity, except in countries already experiencing warm climates (where thermal conditions for photosynthesis are already close to optimal and the reduced grain-filling period leads to declines in final yields). In low-temperature areas (especially Uruguay) climate change could reduce the incidence of preflowering cold shocks inducing sterility. Except for Brazil and the Caribbean the blast disease pressure on the crop eases, because of thermal and rainfall conditions that are less favorable for the blast pathogen *Pyricularia grisea*.

Adaptation strategies—based on the use of different genotypes and of different sowing dates—were applied only for the countries where a decrease in production levels was observed (figures 4.8 and 4.9; annex II): Brazil, Ecuador, Mexico, and the Caribbean. The rationale behind the adaptation was mainly related to the use of genotypes with a longer cycle to compensate for the climate change effect in shortening the grain-filling period. Sowing dates were also changed. Results indicate that future conditions will be decidedly favorable for rice across the region. Long-cycle genotypes allow long grain-filling periods and high daily biomass accumulation rate, because of negligible thermal limits to photosynthesis and the CO_2 fertilization effect, higher for the C3 species than for the C4 (such as maize). As for wheat, the implementation of adaptation strategies targeting crop features mainly related to crop cycle length led to indirect benefits in pathogens pressure (figures 4.2 and 4.3). This could suggest a possible reduction of agrochemicals in the future in important rice producing countries like Brazil, and the reduced importance of investing efforts in developing blast-resistant varieties.

Figure 4.8. Rice productivity impacts (Hadley A1B) to 2020

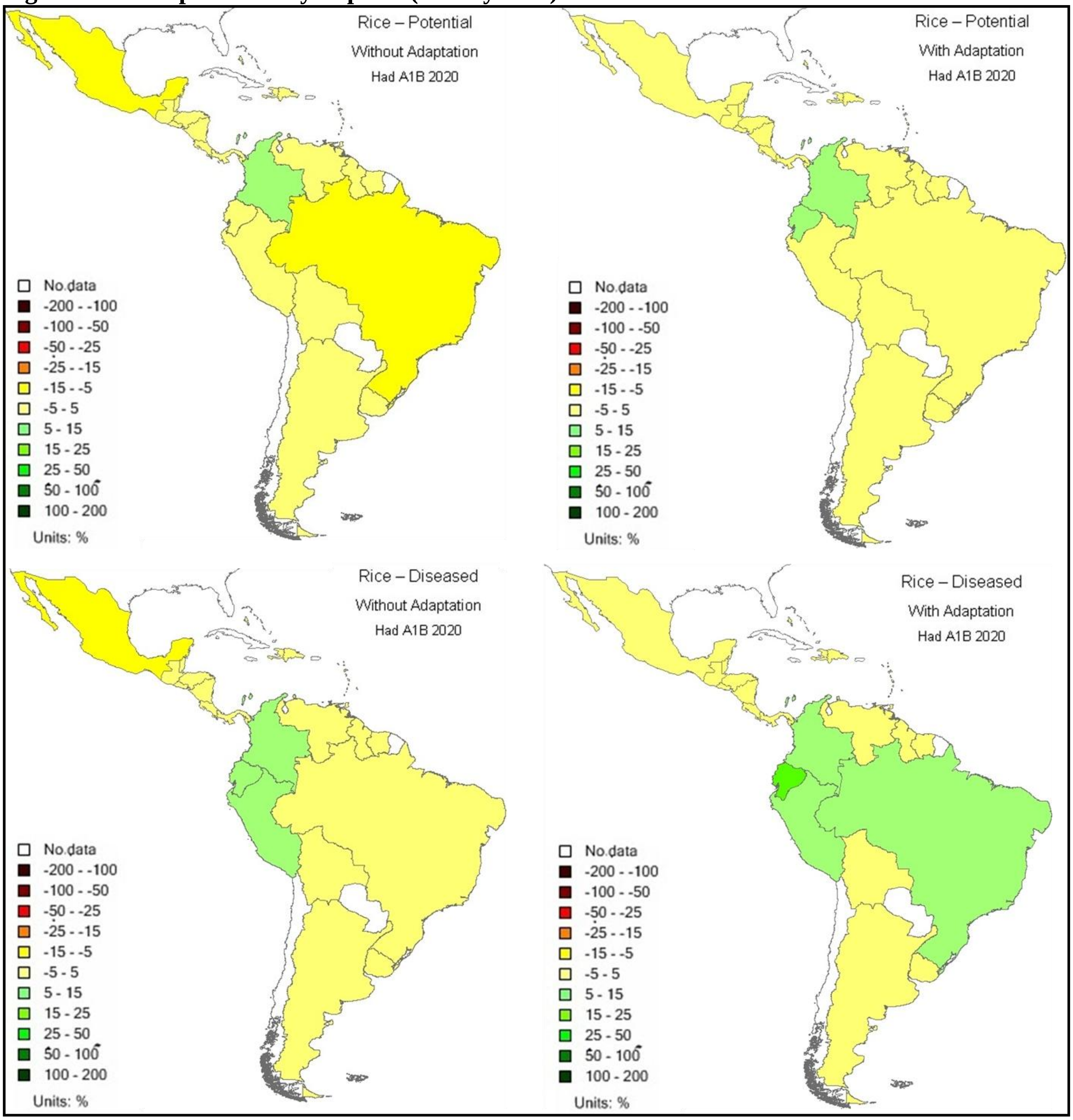

Figure 4.9. Rice productivity impacts (Hadley A1B) to 2050.

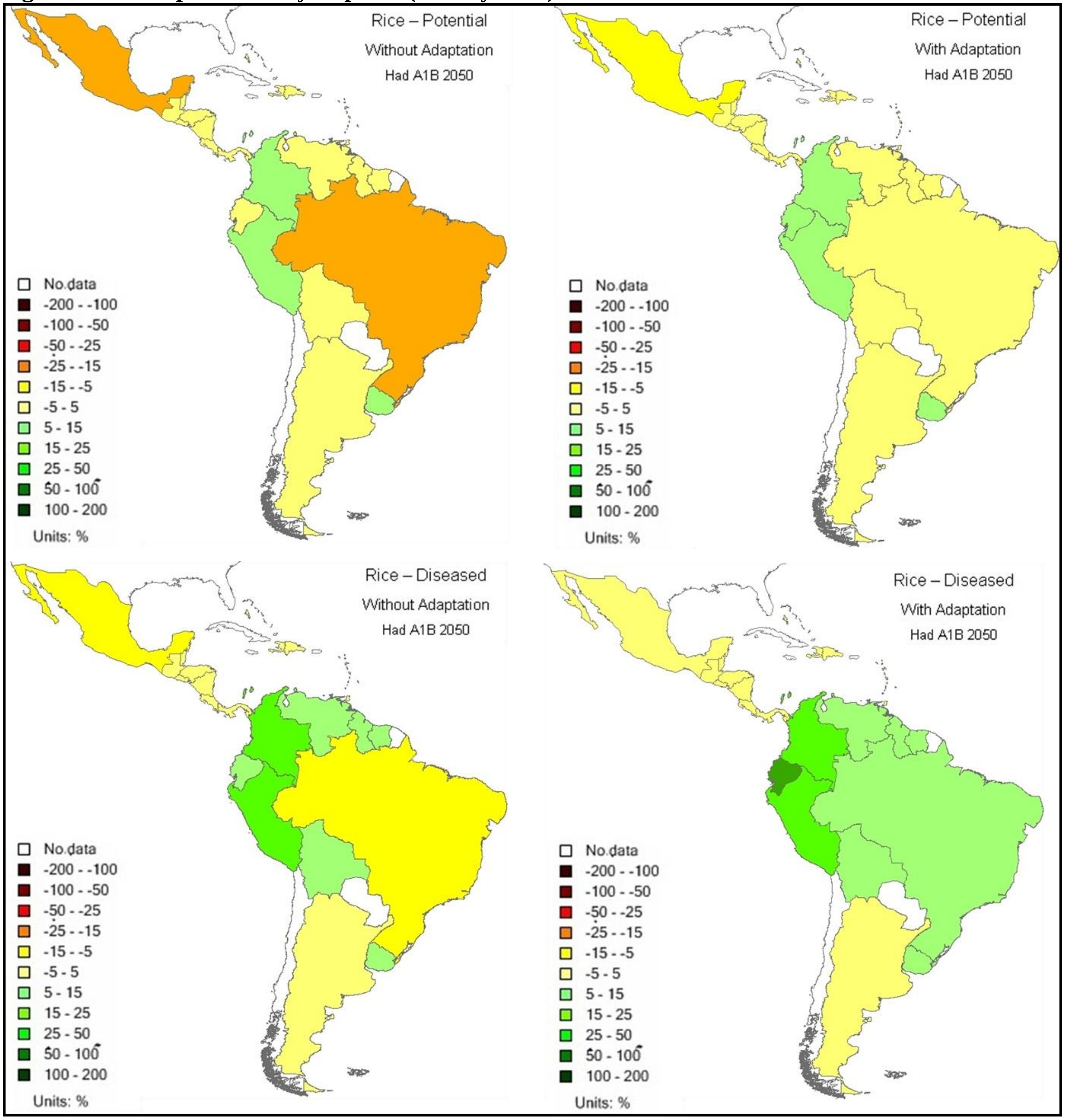

Agromanagement adaptation

At subnational scales, specific simulations and analyses were carried out to resolve irrigation solutions necessary to limit, at each simulated grid, the otherwise negative impacts under the no adaptation scenarios.

Region-specific reviews of irrigation information were carried out for the baseline climate, resulting in simulated irrigation where water was applied a limited number of times during a crop's growing period, and up to 300 millimeters depending on the region. Under the no adaptation scenarios, these baseline irrigation cases were repeated unchanged. With adaptation, the crop model was allowed to dynamically compute the need for irrigation, based on soil water status as determined by the new climate data and altered crop growing conditions. The realism of these adaptive simulations was maintained by setting the maximum annual irrigation amount to the same values found for current climate regimes (figures 4.10 and 4.11). Negative impacts of climate change are thus reduced by allowing more frequent irrigation with increased water demand.

Figure 4.10. Maize productivity impacts (Hadley A1B) 2020 and 2050

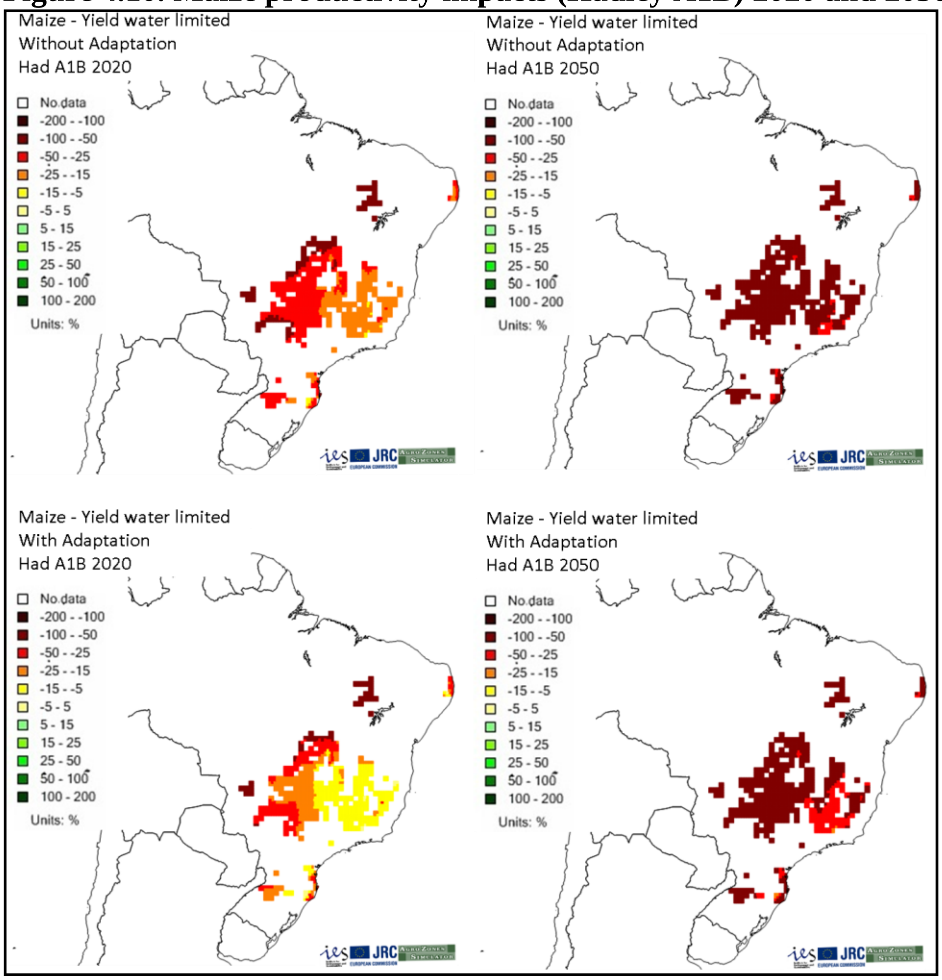

Figure 4.11. Soybean productivity impacts (Hadley A1B) 2020 and 2050

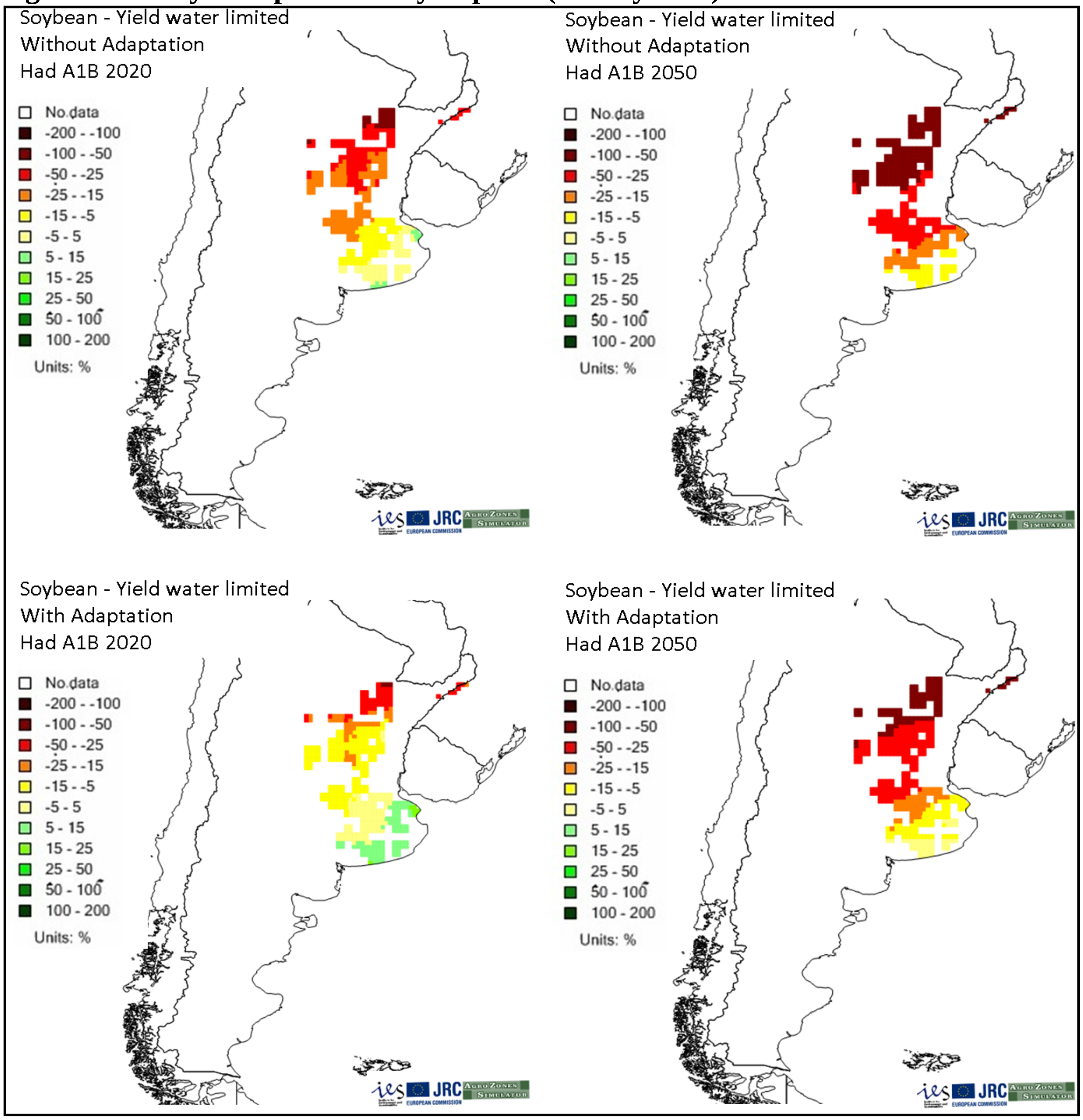

Box 4.1. Coupling AZS-BioMA to ENVISAGE for Economic Impact Assessments of climate change

Assessing the potential economic impacts of agricultural productivity shocks can be quantified by coupling biophysical crop models to partial or general equilibrium economic models. Such biophysics-economics coupling can be of great interest to policy analysts seeking to derive economic costs and benefits of specific response strategies, to compare them against a scenario of "no action."

We have developed such linkages between the AZS-BioMA platform and the environmental impacts and sustainability applied general equilibrium (ENVISAGE) model, a multisector multiregional, global computable general equilibrium (CGE) model (van der Mensbrugghe 2011). It is calibrated to the GTAP database with a 2004 base year. The model framework is dynamic, integrating assumptions for population and labor force growth, for savings and investment, and for sectoral productivity. With differences in comparative advantage and demand, the model also generates changes in trade patterns on a global scale.

Agricultural productivity in ENVISAGE is assumed to be neutral across all inputs. A change in agricultural productivity leads to a uniform expansion (or contraction) of the production possibility frontier:

$$X_{r,cr,t} = A_{r,cr,t} F\left(L, K, T, M, E, \ldots\right)$$

where X is production by region, crop, and time, A is a uniform productivity factor, F is the production function of labor, capital, land, material inputs (such as seeds and fertilizers), energy, and any other inputs. Note that ENVISAGE, like most CGE models, uses a production function approach to modeling agricultural output. Most partial equilibrium models use a supply function approach, where supply is a function of the market price of the good.

The parameter A grows at some rate influenced by historical experience and is then hit by climate change:

$$A_{r,cr,t} = A^{ND}_{r,cr,t} Dam_{r,cr,t} = (1+\gamma_{r,cr,t}) A^{ND}_{r,cr,t-1} Dam_{r,cr,t} = (1+\bar{\gamma}_{r,cr})^t A^{ND}_{r,cr,0} Dam_{r,cr,t}$$

where A^{ND} represents productivity in the absence of damage. A^{ND} grows at the rate γ a year, or an average of $\bar{\gamma}$ over the period 0 to t. The variable *Dam* is equal to 1 in the base year and is less than 1 if the climate impact is negative and greater than 1 if the climate impact is positive. Note that if A is 1 in the base year and grows at 2% a year, agricultural productivity will be 2.5 times higher in 2050 than in 2004—a 10% shock to agricultural productivity will lower yearly growth to 1.8% a year, resulting by 2050, with climate change, in yields that are still 2.3 times higher than present. The impact could be much greater in later decades when climate change is assumed to accelerate and if using a non-linear damage function.

The current coupling passes crop yield shock information (delta changes corresponding to a given climate change SRES scenario against a baseline without climate change) from AZS-BioMA to ENVISAGE, so that the latter model can compute costs of such impacts and derive changes in commodity prices and agricultural value added. For this study, we take the damage estimates from the AZS framework of the two time periods—2020 and 2050—and interpolate linearly between years (between 2004 and 2020, and again between 2020 and 2050).

For simplicity, we limited this exercise to climate change–yield shocks in Latin America and the Caribbean, while assuming a no climate change–impact scenario in the rest of the world. This is equivalent to investigating the zero-th order implications of a Latin America–only climate perturbation. It is therefore not an assessment of the full impacts of climate change on Latin American economies. The shocks would be equivalent to impacts on yields in the absence of any price-induced change in production structure. But in a general equilibrium framework, the climate-induced productivity shocks will induce changes in relative prices—particularly of land—and thus substitution across inputs. The impacts on yields will therefore reflect the exogenous component as well as an endogenous component reflecting a different mix of land and other inputs.

ENVISAGE results

The economic impacts of implementing the climate-induced agricultural productivity shocks in the four focus crops are generally negative—consistent with the shocks. At the aggregate level, the magnitude of the shock will reflect the overall level of the crop-specific shock, the relative importance of the crop in total production, and the general equilibrium feedback effects—both domestic and global. For example, a loss in export revenues typically leads to a real depreciation as exports of other goods must rise to compensate for the change in the trade balance—assumed to be fixed across scenarios.

The aggregate impact of this limited shock on Latin America and the Caribbean GDP could be as high as 1.7% in 2050 under the A1B emission scenario and using the results of the Hadley general circulation model (GCM). Even considering the strong climate signal, this seems a fairly large decline in regional GDP, considering that the four affected crops would only represent about 1.3% of total regional GDP in 2050 under the baseline scenario. From this, it can be inferred that the general equilibrium and multiplier effects are significant. The countries hit most across all scenarios and GCMs are Argentina and Brazil, two of the largest agricultural producers. Uruguay would be the only country that would see gains in most of the scenarios—though even under the A1B scenario of the Hadley model, Uruguay would lose and by a relatively significant 2.3%. Among the least hit are Chile, Ecuador, and Peru. Chile's agricultural sector as a share of the total economy is small in the base year and declines over time—particularly for the four affected crops. Ecuador and Peru have relatively low production shares in the affected crops. (It is useful to restate that the other sectors of the economy are not affected by climate change in this scenario—so such crops as coffee, sugar, and tropical fruits are not affected directly).

The negative impacts tend to accelerate between 2020 and 2050. They are larger for the Hadley model than the NCAR model, and they tend to be higher for the A1B emission scenario than the B1 emission scenario. Some of these findings are illustrated in box figure 1, which reflects the loss in agricultural value added in 2050 for the modeled regions and across the four combinations of GCM and emission scenario.

Changes in the region's ability to produce will affect global agricultural prices. The crops most affected are oil seeds, whose prices would rise between 11 and 17% in 2050—relative to a scenario where the four focus crops are not affected—depending on emission scenario and GCM, with HADA1B producing the highest rise. Other grains (essentially maize) would see the next largest impact—at around 5%, with little variation across scenarios and GCMs. Wheat prices would rise only by about 2%, again with little variation. Rice is an exception. Because its average productivity would rise, prices would drop (slightly)—as much as 0.7% in the more optimistic climate scenario (NCAR B1). These price changes would be larger if other regions in the world exhibit similar productivity shocks.

Box figure 1. Change in agricultural value added in 2050 from climate change damage for the four focus crops

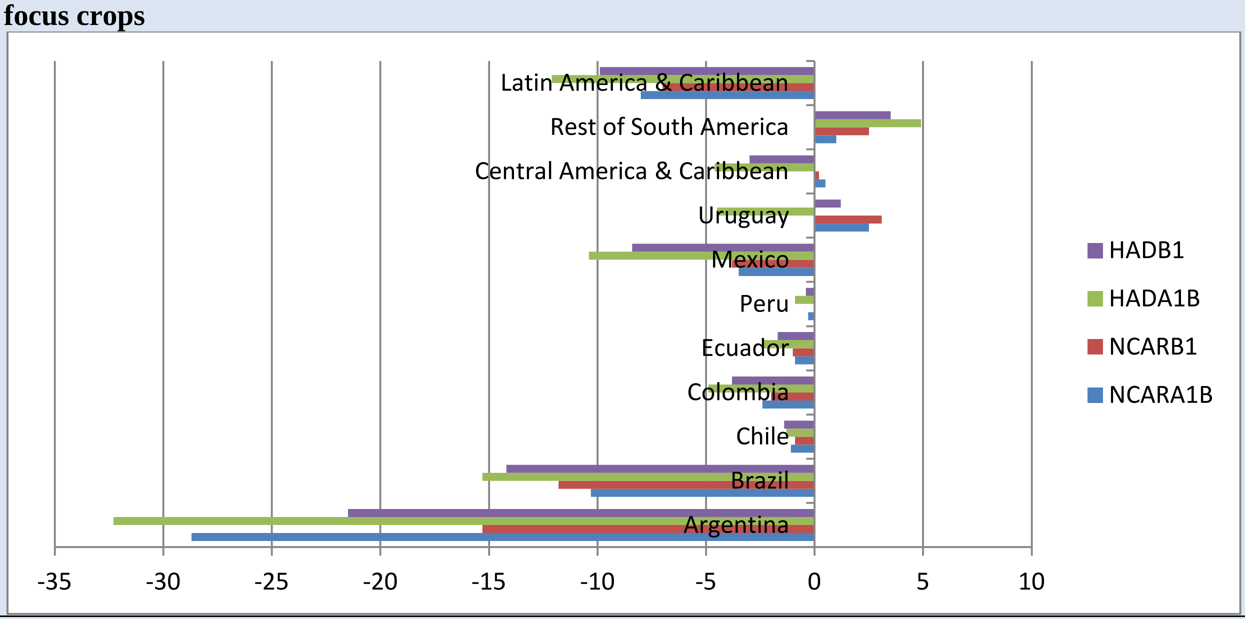

Climate change–induced damage in the four focus crops would generate a large drop in agricultural exports from Latin America and the Caribbean albeit relative to a situation where the rest of the world is unaffected by climate change. In aggregate, agricultural exports would decline between 25 and 33% in 2050 compared with a situation where the four focus crops are not hit. Argentina would suffer the largest percentage loss—between 46 and 67% in 2050. The export decline in Brazil, though significant, would be much lower than that in Argentina. For most of the other countries regions, the impacts on exports are mildly positive and potentially even significantly positive for Mexico. Agricultural exports from Uruguay could be volatile, with a decline of nearly 50% in 2050 in the worst scenario, and a sharp rise of 60% in 2050 in the more optimistic scenario. In value terms the loss in net export revenues for the four crops considered would be $8–11 billion in 2020, but much higher in 2050 and with a greater range—$30–52 billion. Brazil would take the greatest burden in absolute terms, followed by Argentina and then Mexico.

Main findings of the economic analysis for climate impacts on the four focus crops in LCR were:

- The new shocks generated by the AZS framework could have substantial economic impacts at the aggregate level—particularly for Argentina and Brazil, heavily invested in three of the four focus crops. If these shocks are representative for a broader set of sectors—such as coffee, fruits and livestock—the economic impacts could be amplified and affect a broader set of countries in Latin America and the Caribbean.
- A large swathe of the world's urban poor could be hurt by higher food prices, which could be even higher if a large share of world agriculture confronts impacts similar to those generated by the AZS framework.
- A complete and consistent global impact analysis using the AZS framework may eventually reveal Latin America's enhanced relative comparative advantage in agriculture. But if the comparison is with a no climate impact scenario, there is little doubt that Latin American agriculture has much at stake and should mitigate the worst consequences of climate change.

Future applications

The results here provide a first example of the kind of analyses that can be performed by using the coupled AZS-ENVISAGE tools. Future work will need to consider global distributions of climate change shocks, consistent with those run under the AZS BioMA platform, to better investigate the multiple interactions of changing productivity potentials, perturbations to supply curves, and price dynamics, both regionally and internationally. Such coupled platforms are needed to quantify the implications of specific actions in the agricultural sector, including synergies or offsets arising from the interactions of adaptation and mitigation needs in the region. With such a coherent framework, the region's stakeholders and policy makers could then analyze a range of scenarios of national to regional interest.

It would be of great interest to run simulations with and without adaptation of crops and crop management, to quantify the costs and benefits of selected adaptation strategies. It would be also important to enhance two-way communications between the biophysical and economic models, so that the former could run realistic adaptation strategies based on socio-economic drivers informed by the latter.

Note:
1. The GTAP database divides world economic activity into 112 regions (of which 94 are individual countries), and 57 sectors (8 of which are crop production, 4 livestock production, and 8 down-stream processed foods). For modeling purposes, the database has been aggregated to 19 regions—including 8 countries in Latin America and the Caribbean and two aggregate regions—and 28 sectors with an emphasis on agriculture and food.

Chapter 5. Conclusions and Policy Implications

Although several such platforms exist, the current work helps open several bottlenecks, following recommendations in Fourth Assessment Report of the Intergovernmental Panel on Climate Change (2007):

- The basic datasets and biophysical models are fully transparent, both in their validation and their availability, including remote access for interested users. Stakeholders around the world can now access the platform, evaluate it, test it, and where possible improve it by adding or refining datasets, or even by modifying or substituting component code, as appropriate for specific areas of study or local agricultural issues.
- The platform, extensible to any world region, is independent of spatial scale, which users can modify as more refined datasets for specific regions become available.
- The model allows for explicit, albeit simplified, adaptation of agromanagement, including a crop suitability assessment module—to test and evaluate adaptation strategies limiting risk under climate change scenarios.
- Explicit links between the biophysical and economic models allow, in principle, two-way interactions, with the ability to evaluate economic impacts of specific agromanagement solutions identified by the crop models. For future studies, the computable general equilibrium (CGE) economic model outputs can test and rank alternative adaptation options for updated agroecological zone simulator (AZS) outputs.

Helping policy makers assess the best options

The ability to test dynamic interactions between agroclimatic factors and field management is important for policy makers to assess economically efficient investment options. For example, the major findings of this study show:

For Latin America and the Caribbean the projected yield shocks on wheat, soybean, maize, and rice generated by the AZS platform could result in substantial negative economic impacts at the aggregate level—particularly for Argentina and Brazil, both heavily invested in three of the four crops under focus in this study. This finding is a red flag for policy makers in the region and elsewhere that are concerned about global food security and the role of global trade in mitigating food insecurity and the possible economic and political insecurity. If these shocks to the focus crops also hit a broader set of crops, the economic impacts could be amplified and hit a much broader set of countries in the region. Investments are thus needed to:

- Upgrade the AZS platform to include at least the crops important in current trade (such as coffee, fruits, and pastures for livestock).
- Expand the use of the AZS platform across countries to provide greater coherence in climate, crop, and economic models and assessment methods.

Even simple but realistic adaptation strategies tested with the AZS platform can mitigate (but not overcome!) the projected negative yield shocks. Policy-relevant interventions related to those strategies include:

- Allocating adequate research and development (R&D) resources to generate improved and adapted plant varieties—currently estimated to take at least a decade and to cost US$5–7 million for each new variety).
- Expanding high-efficiency irrigation to overcome moisture limitation during grain-filling, a major yield-limiting factor in the region for maize, soybean, and wheat. Less than 6% of Brazil's agriculture and less than 2% of Argentina's are irrigated yet these are the two countries projected to be hit most severely by climate change and moisture limitations for their major commodity crops.

The estimated gains in rice productivity in Latin America and the Caribbean show the potential for increasing future production (rice currently feeds more than 3 billion people worldwide, and future supplies are expected to be tight). Three policy-relevant issues:

- Most of the region's rice is produced in the rainy season to ensure adequate supplies of water for most of the growing season. The yield plateau for rainy season rice is about four tons per hectare because sunlight is often reduced by clouds. If the rice could be produced during the dry season with adequate water capture and irrigation, the rice yield plateau could rise to between 8 and 12 tons per hectare.
- Most of the region's countries have plans to expand hydroenergy as a part of national low-carbon growth strategies. Ensuring that new hydroenergy programs also include irrigation would enhance the adaptation capacity for agriculture. Policies that promote multipurpose hydro would also permit relocating rice and other agriculture in coastal and low-lying areas to areas less vulnerable to major floods and rising sea levels—an adaptation-mitigation win-win.
- Because flooded rice is a major source of methane (a powerful greenhouse gas), adequate R&D funding and policy instruments will be needed to catalyze public-private partnerships to develop and extend rice field management strategies and the use of improved biological and new-generation 'high efficiency-low emissions' synthetic fertilizers.

Next steps for World Bank and other donor agency investments, operations, and research

This study highlights the importance of undertaking robust assessments of the likely impacts on agriculture and the key steps to guide policy makers in the design of a rational economic response to climate change.

- The most obvious need is to identify and understand the impacts of climate change and their associated costs. An economic picture indicates the value at risk and thus the basis for an economically efficient adaptation response. Such an assessment clearly requires some mapping of down-scaled climate projections and their effect on vulnerable economic sectors, such as agriculture.

- Once the impacts have been identified and their magnitudes and economic impacts determined, it will be necessary to consider the range of adaptation responses, their associated costs, and whether they fall within public or private responsibility. The latter includes a range of less tangible interventions, such as information to facilitate private adaptation.
- The agriculture and land use sector offers significant mitigation potential at low cost. Countries should develop a sector emissions budget by concentrating on synergistic adaptation-mitigation win-wins, which are more likely to be low cost. Once this budget is determined, a range of voluntary and market-based approaches can provide incentives for their deployment.

The World Bank and other development agencies can facilitate the rapid development of robust and synergistic adaptation and mitigation approaches. They can support extending the development and testing of the AZS platform to a larger suite of traded and subsistence crops and to other regions. They can also support international and national agricultural research and development agencies to further refine the AZS platform with local data and to enable local agencies through appropriate capacity enhancement to use the AZS platform routinely for national and subnational climate impact assessments for ranking investments.

- The International Center for Tropical Agriculture, based in Cali, Colombia, has expressed an interest in hosting the AZS platform for Latin America and the Caribbean with a view to further improving the platform and enabling national programs to set up and use their own versions. Linking World Bank funded operations to such a regional capacity-enhancing agreement would greatly advance the current capacity at most national agricultural research agencies.
- The finding that moisture limitations during grain-filling periods for maize, soybean, and wheat could limit future yields highlights a major adaptation-mitigation synergy (soil carbon sequestration) that could significantly reduce yield losses. Enhancing soil carbon not only reduces emissions (mitigation) but can also result in significantly better water and nutrient holding capacity of the soils (Fernandes and Motavalli 1997). Such benefits are relevant both for commercial farmers and for poor smallholders. But to realize will require overcoming governance issues, low technical capacity, high transaction costs, and a lack of appropriate baseline and monitoring methodologies. There is a significant opportunity to create enabling conditions for further work on mitigation in agriculture in the post-2012 climate agreement.
- The quantitative AZS estimates of climate impacts on agricultural productivity at high spatial resolution provided by this study could provide key information and reduce some uncertainty for insurance and microfinance instruments. Insurance is likely to be key in future adaptation decisions, whether through traditional indemnity-based insurance or through other options that may be more suitable for climate-based insurance, such as index-based schemes, weather derivatives, and catastrophe bonds (Fankhauser and others 2008).

The AZS platform is available for rapid deployment to other regions. For future research, one of the outcomes that could be generated from the AZS framework is an ensemble of parametric agricultural-damage functions that could easily be coupled with CGE models and specific temperature profiles.

- Ideally, the damage function would have the following form:

$$Dam_{r,c} = \alpha^0_{r,c} + \alpha^1_{r,c}\left(T - T_0\right) + \alpha^2_{r,c}\left(T - T_0\right)^{\varepsilon}$$

  where *Dam* is specific to a country/region (*r*) and crop (*c*), as well as the α parameters, but the parameter estimated would also be tied to a specific combination of GCM and crop models. The functional form is nonlinear where the non-linear component, ε, could either be estimated or imposed. The variable *T* represents global mean temperature. The coefficients could capture the regional temperature change, assuming a stable relationship between global and regional temperature changes.
- The AZS framework is generating a huge dataset that could be used to econometrically estimate these parameters. In the context of this study, it would produce two families of damage estimates—one each for the NCAR and Hadley GCMs. This is another reason to extend the overall methodology to encompass all regions and crops.
- Another future research area is to more fully integrate the CGE models with the crop models. The CGE models generate results—such as changes in land use and input use—that could be reinserted into the crop models to ensure greater consistency. Experience with other model couplings shows rapid convergence in most cases.

Bibliography

Aaheim, A., F. Berkhout, D. McEvoy, R. Mechler, H. Neufeldt, A. Patt, P. Watkiss, A. Wreford, Z. Kundzewicz, C. Lavalle, and C. Egenhofer. 2008. "Adaptation to Climate Change: Why Is It Needed and How Can It Be Implemented?" CEPS Policy Brief 161. Center for European Policy Studies, Brussels.

Abildtrup, J., E. M. Audsley, C. Fekete-Farkas, M. Giupponi, P. Gylling, P. Rosato, and M. Rounsevell. 2006. "Socio-Economic Scenario Development for the Assessment of Climate Change Impacts on Agricultural Land Use: A Pairwise Comparison Approach." *Environmental Science and Policy* 9: 101–15.

Acock, B., and M. Acock. 1991. "Potential for Using Long-Term Field Research Data to Develop and Validate Crop Simulators." *Agronomy Journal* 83: 56–61.

Adams, R. M., C. C. Chen, B. A. McCarl, and D. E. Schimmelpfenning. 2000. "Climate Variability and Climate change: Implications for Agriculture." In *Advances in the Economics of Environmental Resources*, vol 3, ed. D. Hall and R. Howarth. New York: Elsevier Science Publisher.

Adams, R. M., R. A. Fleming, C. C. Change, B. A. McCarl, and C. Rosenzweig. 1995. "A Reassessment of the Economic Effects of Global Climate Change in US Agriculture." *Climatic Change* 30 (2): 147–67.

Adams, R. M., B. A. McCarl, K. Segerson, C. Rosenzweig, K. J. Bryant, B. L. Dixon, R. Conner, R. E. Evenson, and D. Ojima. 1999. "The Economic Effects of Climate Change on US Agriculture." In *The Economic Impact of Climate Change on the Economy of the United States*, ed. R. Mendelsohn and J.E. Neumann. Cambridge, UK: Cambridge University Press.

Adger, W. N., D. Pettenella, and M. Whitby, eds. 1997. *Climate Change Mitigation and European Land Use Policies*. Wallingford, UK: CAB International.

Adger, W. N., J. Paavola, S. Huq, and M.J. Mace, eds. 2006. *Fairness in Adaptation to Climate Change*. Cambridge, MA: MIT Press.

Adger, W. N. and K. Brown. 1994. *Land Use and the Causes of Global Warming*. Chichester, UK: Wiley.

Adger, W. N., and K. Vincent. 2005. "Uncertainty in Adaptive Capacity." *CR Geoscience* 337: 399–410.

AEA Energy and Environment. 2007. *Adaptation to Climate Change in the Agricultural Sector*. Didcot, UK: AEA Energy and Environment.

Agrawal, A. 2008. "The Role of Local Institutions in Livelihoods Adaptation to Climate Change." Presented at the World Bank Social Dimensions of Climate Change Workshop, Washington, DC, March 5–6.

Agrawala, S., and S. Fankhauser, eds. 2008. *Economic Aspects of Adaptation to Climate Change*. Paris: Organisation for Economic Co-operation and Development.

Ainsworth, E. A. and S. P. Long. 2005. "What Have We Learned from 15 Years of Free-Air CO_2 Enrichment (FACE)? A Meta-Analysis of the Responses of Photosynthesis, Canopy Properties and Plant Production to Rising CO_2." *New Phytologist* 165 (2): 351–71.

Alcamo, J., P. Döll, T. Heinrichs, F. Kaspar, B. Lehner, T. Rösch, and S. Siebert. 2003. "Global Estimates of Water Withdrawals and Availability under Current and Future Business-as-Usual Conditions." *Hydrological Sciences Journal* 48 (3): 339–48.

Allanson, P., and L. Hubbard. 1999. “On the Comparative Evaluation of Agricultural Income Distributions in the European Union.” *European Review of Agricultural Economics* 26 (1): 1–17.

Alley, R. B., J. Marotzke, W. D. Nordhaus, J. T. Overpeck4, D. M. Peteet, R. A. Pielke Jr., R. T. Pierrehumbert, P. B. Rhines, T. F. Stocker, L. D. Talley, and J. M. Wallace. 2003. “Abrupt Climate Change.” *Science* 299 (5615): 2005–10.

Antle, J. M., S. M. Capalbo, E. T. Elliott, and K. H. Paustian. 2004. “Adaptation, Spatial Heterogeneity, and the Vulnerability of Agricultural Systems to Climate Change and CO_2 Fertilization: An Integrated Assessment Approach.” Climate Change 64 (3): 289–315.

Arnell, N. W. 2003. “Effects of IPCC SRES Emissions Scenarios on River Runoff: A Global Perspective.” *Hydrology and Earth System Science* 7 (5): 619–41.

Arnell, N. W. 2004. “Climate Change and Global Water Resources: SRES Emissions and Socio-Economic Scenarios.” *Global Environmental Change* 14: 31–52.

Arnell, N. W., and E. K. Delaney. 2006. “Adapting to Climate Change: Public Water Supply in England and Wales.” *Climatic Change* 78 (2–4): 227–55.

Asseng, S. P., D. Jamieson, B. Kimball, P. Pinter, K. Sayre, J. W. Bowden, and S. M. Howden. 2004. “Simulated Wheat Growth Affected by Rising Temperature, Increased Water Deficit and Elevated Atmospheric CO_2.” Field Crops Research 85 (2–3): 85–102.

Audsley, E., K. R. Pearn, C. Simota, G. Cojocaru, E. Koutsidou, M. D. A. Rounsevell, M. Trnka, and V. Alexandrov. 2006. “What Can Scenario Modelling Tell Us about Future European Scale Agricultural Land Use, and What Not?” *Environmental Science and Policy* 9 (2): 148–64.

Azar, C. 1998. “Are Optimal CO_2 Emissions Really Optimal? Four Critical Issues for Economists in the Greenhouse.” *Environmental and Resource Economics* 11 (3–4): 301–15.

Baer, P. 2006. “Adaptation: Who Pays Whom?” In *Fairness in Adaptation to Climate Change*, ed. W. N. Adger, J. Paavola, S. Huq, and M. J. Mace. Cambridge, MA: MIT Press.

Baker, J. T. 2004. “Yield Responses of Southern US Rice Cultivars to CO2 and Temperature.” *Agricultural and Forest Meteorology* 122: 129–37.

Barnett, B. J., and O. Mahul. 2007. “Weather Index Insurance for Agriculture and Rural Areas in Lower Income Countries.” *American Journal of Agricultural Economics* 89 (5): 1241–7.

Batjes, N. H. 2002. “A homogenized soil profile data set for global and regional environmental research” (WISE, version 1.1). Report 2002/01. International Soil Reference and Information Centre, Wageningen, the Netherlands.

Berkhout, F., J. Hertin, and A. Jordan. 2002. “Socio-Economic Futures in Climate Change Impact Assessment: Using Scenarios as Learning Machines.” *Global Environmental Change* 12 (2): 83–95.

Berkhout, F. 2005. “Rationales for Adaptation in EU Climate Change Policies.” *Climate Policy* 5 (3): 377–91.

Berry, P. M., M. D. A. Rounsevell, P. A. Harrison, and E. Audsley. 2006. “Assessing the Vulnerability of Agricultural Land Use and Species to Climate Change and the Role of Policy in Facilitating Adaptation.” *Environmental Science and Policy* 9: 189–204.

Betts, R. A., P. M. Cox, M. Collings, P. P. Harris, C. Huntingford, and C. D. Jones. 2004. “The Role of Ecosystem-Atmosphere Interactions in Simulated Amazonian Precipitation Decrease and Forest Dieback under Global Climate Warming.” *Theoretical and Applied Climatology* 78 (1–3): 157–75.

Betts, R. A. 2000. “Offset of the Potential Carbon Sink from Boreal Forestation by Decreases in Surface Albedo.” *Nature* 408 (6809): 187–90.

Bohle, H. G., T. E. Downing, and M. Watts. 1994. “Climate Change and Social Vulnerability: Toward a Sociology and Geography of Food Insecurity.” *Global Environmental Change* 4 (1): 37–48.

Boogaard, H. L., C. A. van Diepen, R. P. Rötter, J. C. M. A. Cabrera, and H. H. van Laar. 1998. “WOFOST 7.1 User guide for the WOFOST 7.1 crop growth simulation model and WOFOST Control Center 5.1.” Technical Document 52. Alterra, WUR, Wageningen, The Netherlands.

Booker, F. L., S. A. Prior, H. A. Torbert, E. L. Fiscus, W. A. Pursley, and S. Hu. 2005. “Decomposition of Soybean Grown under Elevated Concentrations of CO_2 and O_3.” Global Change Biology 11 (4): 685–98.

Bosello, F., and J. Jhang. 2005 “Assessing Climate Change Impacts: Agriculture.” CIP—Climate Impacts and Policy Division Working Paper 02.2007. Fondazione Eni Enrico Mattei Castello, Venezia, Italy.

Bregaglio, S., M. Donatelli, R. Confalonieri, M. Acutis, and S. Orlandini. 2011. “Multi Metric Evaluation of Leaf Wetness Models for Large-Area Application of Plant Disease Models.” *Agricultural and Forest Meteorology* 151 (9): 1163–72.

Cline, W. R. 2007. *Global Warming and Agriculture: Impact Estimates by Country*. Washington, DC: Center for Global Development and Peterson Institute for International Economics.

Cohen, S., D. Nielsen, and R. Welbourn. 2004. “Expanding the Dialogue on Climate Change and Water Management in the Okanagan basin, British Columbia.” Environment Canada, Vancouver, Canada.

Collins, W. D., P. J. Rasch, B. A. Boville, J. J. Hack, J. R. McCaa, D. L. Williamson, J. T. Kiehl, B. Briegleb, C. Bitz, S.-J. Lin, M. Zhang, and Y. Dai. 2004. “Description of the NCAR Community Atmosphere Model (CAM3.0).” Technical Note TN-464+STR. National Center for Atmospheric Research, Boulder, CO.

Confalonieri, R., S. Bregaglio, and M. Acutis. 2010. “A Proposal of an Indicator for Quantifying Model Robustness Based on the Relationship between Variability of Errors and of Explored Conditions.” *Ecological Modelling* 221: 960–4.

Confalonieri, R., M. Acutis, G. Bellocchi, and M. Donatelli. 2009a. Multi-Metric Evaluation of the Models WARM, CropSyst, and WOFOST for Rice. *Ecological Modelling* 220 (11): 1395–410.

Confalonieri, R., A. S. Rosenmund, and B. Baruth. 2009b. “An Improved Model to Simulate Rice Yield.” *Agronomy for Sustainable Development* 29: 463–74.

Danuso, F. 2002. “CLIMAK: A Stochastic Model for Weather Data Generation.” *Italian Journal of Agronomy* 6: 57–71.

Darwin, R. F. 1999. “A Farmer’s View of the Ricardian Approach to Measuring Agricultural Effects of Climatic Change.” *Climatic Change* 41 (3–4): 371–411.

De la Torre, A., P. Fajnzylber, and J. Nash. 2009. *Low Carbon, High Growth: Latin America Responses to Climate Change*. World Bank Latin America and the Caribbean Studies, Report 47604. Washington, DC: World Bank.

Donatelli, M., G. Bellocchi, E. Habyarimana, R. Confalonieri, and F. Micale. 2009. “An Extensible Model Library for Generating Wind Speed Data.” *Computers and Electronics in Agriculture* 69: 165–70.

Donatelli, M., and A.E. Rizzoli. 2008. "A Design for Framework-Independent Model Components of Biophysical Systems." Proceedings of the International Congress on Environmental Modelling and Software, Barcelona, Spain, July 7–10.

Easterling, W. E., P. K. Aggarwal, P. Batima, K. M. Brander, L. Erda, S. M. Howden, A. Kirilenko, J. Morton, J.-F. Soussana, J. Schmidhuber, and F. N. Tubiello. 2007. "Food, Fibre and Forest Products." In *Climate Change 2007: Impacts, Adaptation and Vulnerability, Contribution of Working Group II to the Fourth Assessment Report of the Intergovernmental Panel on Climate Change*, ed. M. L. Parry O. F. Canziani, J. P. Palutikof, P. J. van der Linden, and C.E. Hanson. Cambridge, UK: Cambridge University Press.

Eliasson, A., R. J. A. Jones, F. Nachtergaele, D. G. Rossiter, J. M. Terres, J. Van Orshoven, H. Van Velthuizen, K. Bottcher, P. Haastrup, and C. Le Bas. 2010. "Common Criteria for the Redifinition of Intermediate Less Favoured Areas in the European Union." *Environmental Science and Policy* 13: 766–77.

FAO (Food and Agriculture Organization of the United Nations). 1989. *FAO-ISRIC Soil Database*. SDB. World Soil Resources Report 60. Rome: FAO.

FAO-UNESCO (Food and Agriculture Organization of the United Nations–United Nations Educational, Scientific and Cultural Organization). 1974. *Soil Map of the World, 1:5000000. Vol. 1 to 10*. Paris: UNESCO.

Fernandes, E. C. M., P. Motavalli, C. Castilla, and L. Mukurumbira. 1997. "Management Control of Soil Organic Matter Dynamics in Tropical Land-Use Systems." *Geoderma* 79: 49–67.

Fischer, G., K. Frohberg, M. L. Parry, and C. Rosenzweig. 1993. "Climate Change and World Food Supply, Demand and Trade." In *Costs, Impacts, and Benefits of CO_2 Mitigation*, ed. Y. Kaya, N. Nakicenovic, W. D. Nordhaus, and F.L. Toth. Laxenburg, Austria: International Institute for Applied Systems Analysis.

Gitay, H., S. Brown, W. Easterling, and B. Jallow. 2001. "Ecosystems and Their Goods and Services." In *Climate Change 2001: Impacts, Adaptation and Vulnerability*, ed. J.J. McCarthy, O. F. Canziani, N. A. Leary, D. J. Dokken, and K. S. White. Cambridge, UK: Cambridge University Press.

Gordon, C., C. Cooper, C.A. Senior, H. Banks, and others. 2000. "The Simulation of SST, Sea Ice Extents and Ocean Heat Transports in a Version of the Hadley Centre Coupled Model without Flux Adjustments." *Climate Dynamics* 16: 147–68.

Hoogenboom, G., C. C. Romero, A. J. Gijsman, J. Koo, and S. Wood. 2009. "Strengthening soil quality databases for application to agricultural production and resource management policy." University of Georgia, Griffin, GA.

Hoogenboom, G., J. W. Jones, P. W. Wilkens, C. H. Porter, W. D. Batchelor, L. A. Hunt, K. J. Boote, U. Singh, O. Uryasev, W. T. Bowen, A. J. Gijsman, A. du Toit, J. W. White, and G. Y. Tsuji. 2004. "Decision Support System for Agrotechnology Transfer Version 4.0 [CD-ROM]." University of Hawaii, Honolulu, HI.

Ingram, J. S. I., and E. C. M. Fernandes. 2001. "Managing Carbon Sequestration in Soils: Concepts and Terminology." *Agriculture, Ecosystems and Environment* 87: 111–17.

IPCC (Intergovernmental Panel on Climate Change). 2000. *IPCC Special Report: Emission Scenarios*. Geneva: IPCC.

———. 2007. "Food, fibre and forest products." In *Climate Change 2007: Impacts, Adaptation and Vulnerability. Contribution of WG II to the Fourth Assessment Report of the IPCC*, ed. M. L. Parry, O. F. Canziani, J. P. Palutikof, P. J. van der Linden, and C. E. Hanson. Cambridge, UK: Cambridge University Press.

Jarvis, N. J. 1994. "The MACRO Model (Version 3.1). Technical Description and Sample Simulations." Reports and Dissertation 19. Department of Soil Science, Swedish University of Agricultural Sciences, Uppsala, Sweden.

Jones, J. W., and J. T. Ritchie. 1990. "Crop Growth Models." In *Management of Farm Irrigation Systems*, ed. G. J. Hoffman, T. A. Howell, and K. H. Solomon. ASAE, St. Joseph, MI.

Kane, S., J. M. Reilly, and J. Tobey. 1992. "An Empirical Study of the Economic Effects of Climate Change on World Agriculture." *Climatic Change* 21: 17–35.

Lee, D. R., S. Edmeades, E. De Nys, A. McDonald, and W. Janssen. 2009. *Building Response Strategies to Climate Change in Agricultural Systems in Latin America*. Washington, DC: World Bank, Latin America and the Caribbean Region, Agriculture and Rural Development.

Lee, H. L. 2004. "Incorporating Agroecologically Zoned Land Use Data into the GTAP Framework." Presented at the 7th Annual GTAP Conference on Trade, Poverty and the Environment, Washington, DC, June 17–19.

Lobell, D. B., W. Schlenker, and J. Costa-Roberts. 2011. "Climate Trends and Global Crop Production since 1980." *Science*, doi: 10.1126/science.1204531.

Lobell, D. B., M. B. Burkel, C. Tebaldi, M. D. Mastrandea, W. P. Falconi, and R. L. Naylor. 2008. "Prioritizing Climate Change Adaptation Needs for Food Security in 2030." *Science* 319: 607–10

Mendelsohn, R., T. Sterner, M. Persson, and J. P. Weyant. 2008. "Comments on Simon Dietz and Nicholas Stern's 'Why Economic Analysis Supports Strong Action on Climate Change: A Response to the Stern Review's Critics.'" *Review of Environmental Economics and Policy* 2 (2): 309–13.

Mendelsohn, R., and L. Williams. 2004. "Comparing Forecasts of the Global Impacts of Climate Change." *Mitigation and Adaptation Strategies for Global Change* 9: 315–33.

Mendelsohn, R. O., W. D. Nordhaus, and D. Shaw. 1994. "The Impact of Global Warming on Agriculture: A Ricardian Analysis." *American Economic Review* 84 (4): 753–71.

———. 1996. "Climate Impacts on Aggregate Farm Value: Accounting for Adaptation." *Agricultural and Forest Meteorology* 80: 55–66.

———. 1999. "The Impact of Climate Variation on U.S. Agriculture." In *The Impact of Climate Change on the United States Economy*, ed. R. O. Mendelsohn and J. E. Neumann. Cambridge, UK: Cambridge University Press.

Mooney, S., and L. Arthur. 1990. "The Impacts of Climate Change on Agriculture in Manitoba." *Canadian Journal of Agricultural Economics* 38: 685–94.

Neitsch, S. L., J. G. Arnold, J. R. Kiniry, R. Srinivasan, and J. R. Williams. 2002. *Soil and Water Assessment Tool. User's Manual*. College Station, TX: Texas Water Resources Institute.

Raddatz, C. 2009. "The Wrath of God: Macroeconomic Costs of Natural Disasters." Policy Research Working Paper 5039. World Bank, Washington, DC.

Reilly, J. M., and D. Schimmelpfennig. 1999. "Agricultural Impact Assessment, Vulnerability, and the Scope for Adaptation." *Climatic Change* 43: 745–88.

Richards, L. A. 1931. "Capillary Conduction of Liquids through Porous Mediums." *Physics* 1: 318–33.

Rosenzweig, C., F. N. Tubiello, R. A. Goldberg, E. Mills, and J. Bloomfield. 2002. “Increased Crop Damage in the U.S. from Excess Precipitation under Climate Change.” *Global Environmental Change* 12: 197–202.

Rosenzweig, C., and M. L. Parry. 1994. “Potential Impact of Climate Change on World Food Supply.” *Nature* 367: 133–38.

Rosenzweig, M. R., and H. P. Binswanger. 1993. “Wealth, Weather Risk and the Composition and Profitability of Agricultural Investments.” *Economic Journal* 103: 56–78.

Schimmelpfennig, D., J. Lewandrowski, J. M. Reilly, M. Tsigas, and I. W. H. Parry. 1996. *Agricultural Adaptation to Climate Change—Issues of Long-run Sustainability*. Washington, DC: U.S. Department of Agriculture.

Seo, S. N., and R. Mendelsohn. 2008. “Measuring Impacts and Adaptations to Climate Change: A Structural Ricardian Model of African Livestock Management.” *Agricultural Economics* 38 (2):151–65.

Soil Survey Staff. 1996. *Soil survey laboratory method manual. Soil survey Investigations Report 42* (ver. 3). Lincoln, NE: U.S. Department of Agriculture, Natural Resources Conservation Service.

Stöckle, C. O., J. R. Williams, C. A. Rosenberg, and C. A. Jones. 1992. “A Method for Estimating Direct and Climatic Effects of Rising Atmospheric Carbon Dioxide on Growth and Yield Crops.” *Agricultural Systems* 38: 225–38.

Stöckle, C. O., M. Donatelli, and R. Nelson. 2003. CropSyst, a Cropping Systems Simulation Model. *European Journal of Agronomy* 18: 289–307.

Tsigas, M. E., G. B. Frisvold, and B. Kuhn. 1997. “Global Climate Change in Agriculture.” In *Global Trade Analysis: Modeling and Applications*, ed. T. W. Hertel. Cambridge, UK: Cambridge University Press.

Tubiello, F. N., A. Rahman, W. Mann, J. Schmidhuber, M. Koleva, and A. Müller. 2009. “Carbon Financial Mechanisms for Agriculture and Rural Development: Challenges and Opportunities along the Bali Roadmap.” *Climatic Change*, doi: 10.1007/s10584-009-9611-5.

Tubiello, F. N., and G. Fischer. 2007. “Reducing Climate Change Impacts on Agriculture: Global and Regional Effects of Mitigation, 1990–2080.” *Technical Forecasting and Social Change* 74: 1030–56.

Tubiello, F. N., and F. Ewert. 2002. “Modeling the Effects of Elevated CO_2 on Crop Growth and Yield: A Review.” *European Journal of Agronomy* 18 (1–2): 57–74.

Van Dam, J. C., J. Huygen, J. G. Wesseling, R. A. Feddes, P. Kabat, P. E. V. van Walsum, P. Groenendijk, and C. A. van Diepen. 1997. *Theory of SWAP version 2.0. Simulation of Water Flow, Solute Transport and Plant Growth in the Soil-Water-Atmosphere-Plant Environment*. Technical Document 45. Wageningen, the Netherlands: Wageningen Agricultural University and DLO Winand Staring Centre.

van der Mensbrugghe, D. 2011. “The Environmental Impact and Sustainability Applied General Equilibrium (ENVISAGE) Model: Version 7.1.” World Bank, Washington, DC.

van Keulen, H., and J. Wolf. 1986. “Modelling of Agricultural Production: Weather Soils and Crops.” Simulation Monographs. Pudoc, Wageningen, the Netherlands.

van Waveren, E. J., and A. B. Bos. 1988. “ISRIC Soil Information System—User manual and technical manual.” Technical Paper 15. ISRIC, Wageningen, the Netherlands.

Annex I. The Agroecological Zone Simulator and Applications

The agroecological zone simulator (AZS) is a realization based on the Biophysical Model Applications (BioMA) platform, an extensible platform for running biophysical models on generic spatial units. AZS-BioMA is based on discrete conceptual units codified in software components (both for simulation engines and user interface). The guidelines followed during its development aim at maximizing:

- Expansion and adaptation with new modeling solutions.
- Ease of customization in new environments.
- Ease of deployment (at national and local research and academic facilities).

Simulations are carried out through modeling solutions, discrete simulation engines where different models are selected and integrated to carry out simulations for a specific goal. Each modeling solution uses extensible components. Third parties can autonomously extend BioMA by adding new modeling solutions, using components that are already part of the application, or using new components.

The current version of BioMA includes heterogeneous modeling solutions:

- CropSyst-Water Limited.
- WARM-BlastDisease-Sterility.WOFOST-Water Limited.
- Agricultural Production and Externalities Simulator.
- PotentialDiseaseInfection.
- Diseases (linked to crops).
- ClimIndices.

Crop development and growth

The modeling platform designed for this study to assess the impact of climate change on agricultural productivity uses three approaches to model crop development and growth, all established platforms that follow the hierarchical distinction between potential and limited production. Crop growth is computed through light interception and carbon dioxide assimilation. Growth-driving processes depend on and are driven by crop phenological development stages, mainly through degree-day accumulation.

For example, the approaches currently being implemented are:

- *CropML-CropSyst* (Stöckle and others 1992, 2003) is a cropping system model with a generic crop simulator that allows for both determined and perennial species to be simulated. This component implements the plant-related part of the original CropSyst model, version 3.02.23.
- *CropML-WARM* (Water Accounting Rice Model, Confalonieri and others 2009a, 2009b) is a daily time-step model for simulating growth and development of paddy

rice crops. The model accounts for all the main processes that characterize this peculiar system.

- *CropML-WOFOST* (Van Keulen and Wolf 1986; Boogaard and others 1998) is part of the family of crop growth models developed in Wageningen by the school of C.T. de Wit.

During the project, CropSyst was used for maize, wheat, and soybean modeling, and WARM was used for rice modeling. The two models were selected because of their accuracy and robustness (Confalonieri and others 2010).

Soil water

SoilW is a software component implementing a wide range of alternative methods to simulate water dynamics into the soil profile, covering all those already in use in major crop modeling platforms worldwide. The component allows the following processes to be simulated:

- Water redistribution among soil layers.
- Effective plant transpiration (several options available).
- Soil evaporation (several options available).
- Drained water if pipe drains are present (under development).
- Effects of soil tillage and subsequent settling of hydrological properties of the soil (field capacity, wilting point, retention functions, conductivity functions, bulk density).

For each process, several approaches are implemented, allowing SoilW to reproduce the behavior of all the most diffused cropping systems models. For example, three approaches are implemented for water redistribution. The first is based on a numerical solution of the Richards' equation (Richards 1931), based on the physical concept that water flux between two points is driven by the pressure gradient between the points themselves and is a function of hydraulic conductivity. In this approach, water retention curves and hydraulic conductivity as a function of soil water content and water pressure are needed. This approach is used in several well-known models, such as CropSyst, SWAP (Van Dam and others 1997) and MACRO (Jarvis 1994). The second approach—cascading, or tipping bucket—is less demanding in terms of data needs and assumes that water can move only downward through the soil profile, filling up the layers until field capacity is reached, with the water exceeding this threshold moving to the deeper layer (Jones and Ritchie 1990). This approach is used in most of the Decision Support System for Agrotechnology Transfer models. The third approach is a modification of the cascading one, in which water movements are reduced by soil hydraulic conductivity, thus allowing water contents to be higher than field capacity. This approach is used in various simulation models such as SWAT (Neitsch and others 2002) and WARM (Confalonieri and others 2009a).

Rainfall and irrigation water actually infiltrating the soil (after possible runoff and plant and mulch interception) is simulated with a library of models implemented in the SoilRE component. A variety of approaches are also available for subprocess, involved in runoff volume, water interception by vegetation and mulch, actually infiltrating water. As an example, for runoff, approaches implementing the curve number and the kinematic wave methods are available.

Management events (see section on crop management below) involved with soil dynamics, such as irrigation, are processed by the SoilRE component. During the project, the cascading approach for simulating soil water redistribution was used because of lack of detail in the available data, which had to be homogeneous for the whole area considered.

Diseases and abiotic factors affecting productions

In almost all the climate change impact studies, cropping systems modelers have been used to consider only temperature, radiation, rainfall, atmospheric carbon dioxide concentration, and—in some cases—irrigation as forces driving crops productivity. Biotic (such as diseases) and abiotic (such as ozone concentration and frost events) factors were traditionally considered as having a constant impact on the crops under a changing climate. This assumption is false, because weather variables have a crucial effect—through, for example, modulating plant-pathogens interactions—that leads climate to alter the magnitude of the gaps in crops productivity due to diseases. This consideration is also valid for damages caused by abiotic factors (such as frost), which in most cases are driven by extreme weather events and are in some cases forecasted to increase by global climate models.

This project considered the impact of diseases (disease component) and abiotic damages induced by extreme temperatures (abiotic damage) on crop productions. The disease component simulates the progress of the epidemics of fungal pathogens by explicitly considering infection, incubation, latency, infectiousness, sporulation, and spore dispersal, all driven by weather conditions and by interactions with the host plant. The impact on the host is simulated mainly through lesions to the photosynthetic tissues. Host resistance (different varieties can greatly differ in terms of susceptibility to a specific disease) is accounted for in the component and based on a generic classification of resistance levels. Figure I1 shows the distribution of the pathogens simulated during the project (the most relevant ones for each of the considered crops) across Latin America.

Figure I1. Geographical distribution of (a) maize Gray leaf spots (*Cercospora zeae-maydis*), (b) wheat leaf rust (*Puccinia recondita*), (c) soybean rust (*Phakopsora pachyrizi*), and (d) rice blast disease (*Pyricularia oryzae*) across Latin America

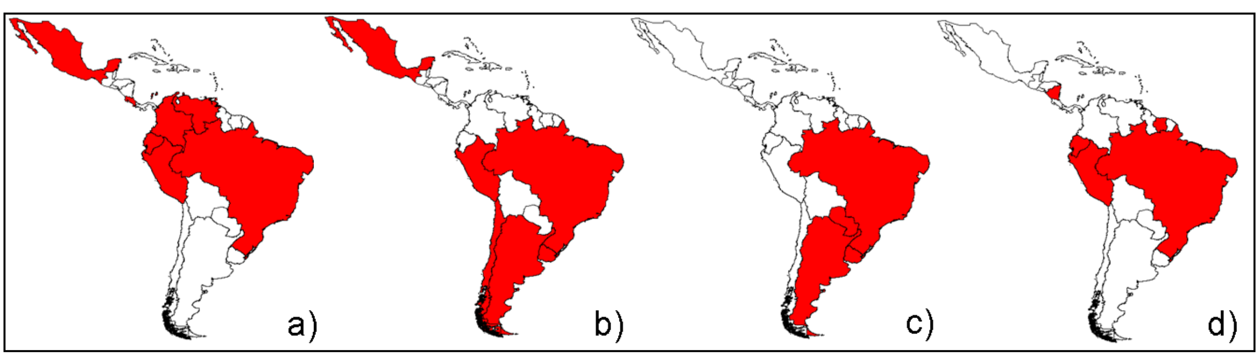

Damages due to extreme temperature events, such as frost and cold shock–induced sterility, were simulated using the abiotic damage component, implementing approaches for a variety of abiotic damages affecting crops, over and above those in use in most other crop modeling platforms. The models implemented belong to six categories: lodging, frost, cold-induced spikelet sterility, heat-induced spikelet sterility, ozone, and salinity.

Crop management

Dates of irrigation events and the amount of water needed by the crop under current or future climate conditions were simulated using rule-based models. This is based on the state of the system, mimicking farmers' behavior with respect to management decisions related to resources availability and on the physical characteristics of the system. A proper set of rules were implemented in the AgroManagement component.

Maize and soybean were simulated under irrigation conditions, and wheat was simulated under rainfed conditions. Water limited production was not simulated for rice, since it is grown in the study region under paddy conditions.

Irrigation events were simulated for both maize and soybean when soil water content fell below 50% of the plant available water, by limiting the total amount of irrigation water in a season to a maximum of 300 millimeters, and by setting the maximum amount of water to 40 millimeters for each event. This parameterization of irrigation rule allowed a standard typology of irrigation practices to be produced, leading to a medium satisfaction of crop water requirements during a season.

Crop suitability

Crop suitability is an important component of assessment studies, including changes to crops geographic distribution under climate change in coming decades. On the one hand, it is well known that crops will respond to specific changes in temperature and precipitation at the locations where they are currently grown; on the other, it is expected that not all crops and cultivars will remain suitable within their current geographical ranges, with tendencies to migrate toward higher latitudes and out of areas already at the margin of production. Yet most crop modeling platforms present fixed grid simulations of crops—that is, they do not allow for dynamical movements of ideal crop ranges and thus tend to underestimate likely adaptation responses by farmers. They will doubtlessly attempt to switch where possible to cultivars and crops better adapted to changing conditions. By the same token, those model platforms that have excelled in computing suitability have much less crop modeling detail than does the proposed platform.

The suitability component included in AZS-BioMA implements a variety of approaches for suitability estimation based on single-cell (that is, threshold-based approaches) or multicell (that is, multiple regression–based) computations. Among the approaches implemented, some are retrieved from the literature and based on soil or weather inputs—for example, FAO EcoCrop (http://ecocrop.fao.org) and Less Favorable Areas (Eliasson and others 2010). Others, developed during the project, derive a suitability index from simulated variables, such as yields, completion of crop cycle, and yield gaps due to biotic and abiotic factors affecting productions.

Implementing all the methods allows the methods to be selected in their original configuration or with categories of variables or parameters excluded from the computation. Another criterion implemented during the project (district criterion) assumes that crop choices by farmers tend to aggregate in production districts. This approach cannot be used alone, and the suitability component allows it to be coupled to all the other methods implemented.

The user can run the AZS-BioMA suitability component by deciding exactly which method to use or by leaving the component to selecting the most appropriate method in light of the actual data availability or the exercise that needs to be run.

BioMA is developed at JRC (project leader: M. Donatelli) in close cooperation with the University of Milan and the Italian Agricultural Research Council. Additional collaboration is being established with the INRA, France.

AZS use at different scales

This is a key feature of the platform that allows building configurations which access data-layer at different spatial resolution. The current setting use a grid 25 km x 25 km, but, say 1 km x 1 km DB can be used allowing detailed analysis for instance of a region in a country. The added value is that the same tools and methodology can be used to create figures from a region or a country based on less abstract production systems and technical adaptation strategies. This also sets a concrete and consistent basis for effective and transparent communication between regional offices and runners of large area analysis.

Data access as input to analysis external to the AZS platform

Read-only data will be accessible through dedicated web services (cross platform) to authorized users. This allows applications or utilities to be built that will be able to query data and use them in local applications. A target use of biophysical simulation output is the link to agroeconomic models. Figure I2 shows the linking and workflow to develop adaptation strategies. The workflow may include either agricultural sector models (as in the current project) or farm models. If the economic model is a farm model, technological and resource-driven constraints can be accounted for, allowing more context-specific detailed analysis of production systems. The dashed line connector suggests possible iterations between a bioeconomic farm model and biophysical models to further improve the definition of adaptation scenarios.

In this project, scenarios are not set to interact with economic models, and the adaptation strategies, as described in section 1.1, represent basic technical options. The study of further options could be driven by agricultural sector models needed to investigate, for instance, a specific crop, or specific constraints in resources.

Figure I2. Possible use of environmental outputs for selecting specific production systems

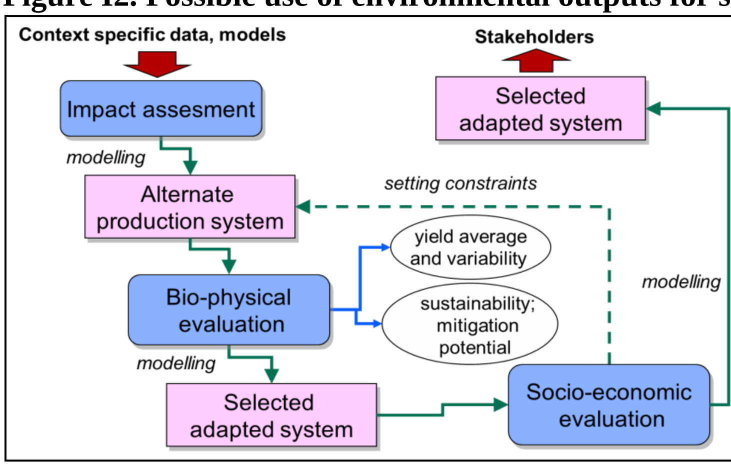

In more general terms, the outputs of biophysical analysis (which includes static indicators based on climate) could be used to build integrated indices to estimate, for instance, land use changes based on biophysical indicators, using the outputs as proxies for semiqualitative estimates of climate change impact. The figure highlights a possible use of outputs of environmental interest for selecting among possible alternate production systems.

Calibration and model evaluation

Calibration and model evaluation must be considered separately for current weather conditions and for conditions of climate change, as in the following paragraphs.

Process-based, deterministic models like the ones used for simulation in this project are evaluated against referenced data. This activity, often referred as model "validation," is done by simulating the same conditions where the reference data were collected (weather, soil, agricultural management) and comparing simulation results to data collected from the real system (such as biomass produced, yield, soil water content). Prior to actually performing model evaluation the model is calibrated, whereby the value of some model parameters are adjusted to minimize the difference between simulated and reference data. This is a very delicate process when performed with process-based models, where parameters have a biophysical meaning; in no case should calibration lead to parameter values that are out of the range known for the process they refer to. Once model parameters are calibrated, model evaluation is run as described above against an independent dataset.

In all cases, model evaluation is run against articulated dataset, in which the context is described in detail to allow simulating it and the measurements on the state of system regard different variables and time series. Yield, often the variable of major interest, is the final result of the simulation of several processes. As such (datasets always being limited in number because they are very costly), a calibration based only on yield often has multiple solutions, resulting in unpredictable model performance under changing biophysical contexts. Model outputs such as crop progression through different development stages (phenology) are typically driven by fewer factors than yield is.

Models are simplified representations of the real system and must include the essential processes (as sources of variability of responses) with respect to the goal of the planned analysis. Some processes can be omitted, in this case adding to the assumptions made for the simulation exercise. Although acceptable, this has implications for the data that can be used for model calibration and evaluation: for instance, if a model not simulating water limitation is used, reference data based on systems where water limitation occurs cannot properly be used either for calibration or evaluation.

The implications of which dataset can be used for evaluating a crop or cropping system model are important. Although models tend to simulate crop development and growth as limited by few factors, actual agricultural production systems, especially in developing countries, show a wide range of production constraints that can affect production nonlinearly. Unfortunately, yield statistics are presented as values, rather than ranges; when ranges are available, the upper limit could be used for calibration and model evaluation, allowing cases that cannot be represented by models because they include processes or technical mismanagement that increase the yield gap to be deleted from the reference. Furthermore, the technological gap of a production system can vary across regions and countries; when combined with environmental factors, it may lead to a different resiliency with respect to adverse weather. The impact is again on the usability of yield statistics to calibrate and evaluate process-based models, because it introduces a further bias as result of the year-by-year variability.

The models used in this project are well known and peer reviewed, which implies that they have been evaluated across a broad range of environmental conditions. The analyses carried out in this project are thus based on such evaluation, relying on data from the scientific literature for model calibration. This study uses crop production as a level of abstraction for production system, aiming at representing yield changes (at various production levels) in response to scenarios via a 25 km x 25 km grid. Even if yields are considered at the various production levels mentioned above, yield estimates represent potential and can have different realizations in different production systems if analyzed within more specific context constraints. This suggests that this type of analysis, using the very same tools that allow for different spatial resolutions, could benefit from a more detailed calibration in specific countries or regions. Yet this level of detail in the analysis was beyond this project's goals and resources; future applications involving local knowledge and expertise will be necessary to refine simulation results.

A different aspect of model evaluation relates to model use in scenarios of climate change. This refers to unexplored conditions where there are no site-specific data to represent production system performance. Because relationships among biophysical processes in the real system are nonlinear, system performance cannot be estimated using trends and statistical models. Likewise, empirical parameters whose empiricism is at the same level as the estimate cannot be relied on. The relationships used in process-based models also have some empiricism, but that empiricism will be one or more levels below the level of the prediction (figure I3).

Figure I3. Level of prediction and level of empiricism in process-based models (redrawn from Acock and Acock 1991)

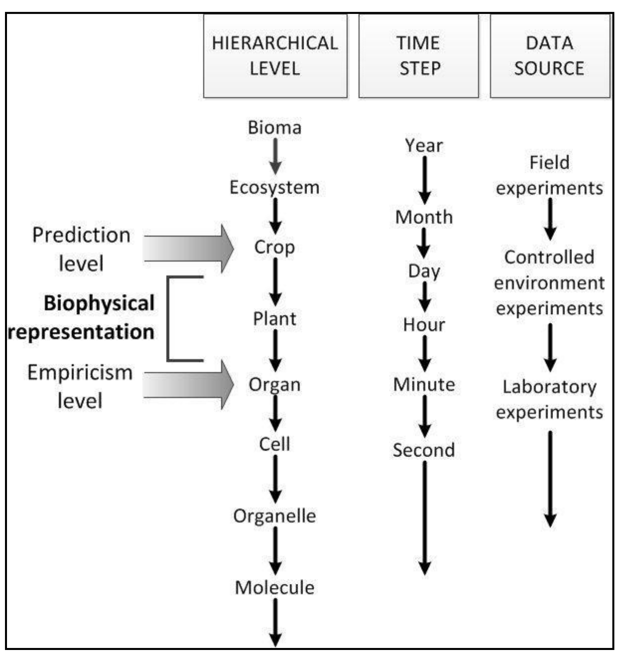

The goal in defining new models is using relationships that are known from physics or chemistry and parameters that have either a biological or a physical meaning. A process-based model can, in principle, extrapolate to conditions outside the ones used to develop it. By contrast, a fully empirical model, as any statistical model, can be used only for the context that originated the data used to build it.

Given that no evaluation against data can be done for scenarios of climate change impacting on crop development and growth, to accept their use in such condition a system analysis must be done confirming model adequacy under the new conditions. This has been done for the models used in this project, leading to changes in curves of response to temperature. The original models had a plateau of response to daily maximum air temperature, perfectly adequate in conditions such as the one of temperate climates, in which temperature rarely reaches levels above the optimum. Hence, making the plateau approximation is acceptable. However, it is known that rates of development and growth start decreasing above optimum temperature. For instance, a plateau model will estimate an overall increase of temperature-driven rates in the linear part of the response, and same response in the plateau region, when temperature increases as in climate change scenarios. By contrast, a curvilinear model will estimate a decrease of rates of development and growth at higher temperatures. The latter is the case in scenarios of climate change where the steep rise in temperature does not allow for accepting the hypothesis of good adaptation of crops to environmental conditions, as built in decades of agriculture under variable weather, but under no steep trend toward higher temperature. This is why the models used include curvilinear responses to temperature, which do not show any difference of estimates compared with the original ones under current weather, but start estimating differences at higher temperatures.

If the assumption of crop adaptation cannot be accepted, another aspect of model structure adequacy is the response to extreme meteorological events. Extreme events for a crop can be the values of environmental variables that are beyond the capability of providing a physiological response by the crop and that may lead to permanent damage or death of the crop. Referring to air temperature as discussed above, a crop will respond with a given rate to temperature, but if temperature goes above maximum temperature or below minimum temperature for growth, permanent damage occurs. These aspects were generally ignored in commonly used modeling solutions and are now implemented representing one of the simulated production levels.

To summarize, developing and implementing the identified temperature responses and the models of impact of extreme events allow models originally developed for temperate climates to be used in scenarios of climate change assuming good crop adaptation.

AZS-BioMA modeling solutions

Two modeling solutions were developed within the current project for the simulation of the four crops included in the land resources database (wheat, maize, soybean, and rice). They are customizations of the APES-BioMA solution for maize, soybean, and wheat and of the WARM-BioMA solution for rice (figure I4). Each solution implements a crop growth and development simulation model, a soil water hydrological model, a soil temperature model, a model for soil temperature across the profile, a model for assessing abiotic yield losses, and a model for simulating biotic yield losses.

Figure I4. The biophysical models implemented in the APES-BioMA and in the WARM-BioMA modeling solutions

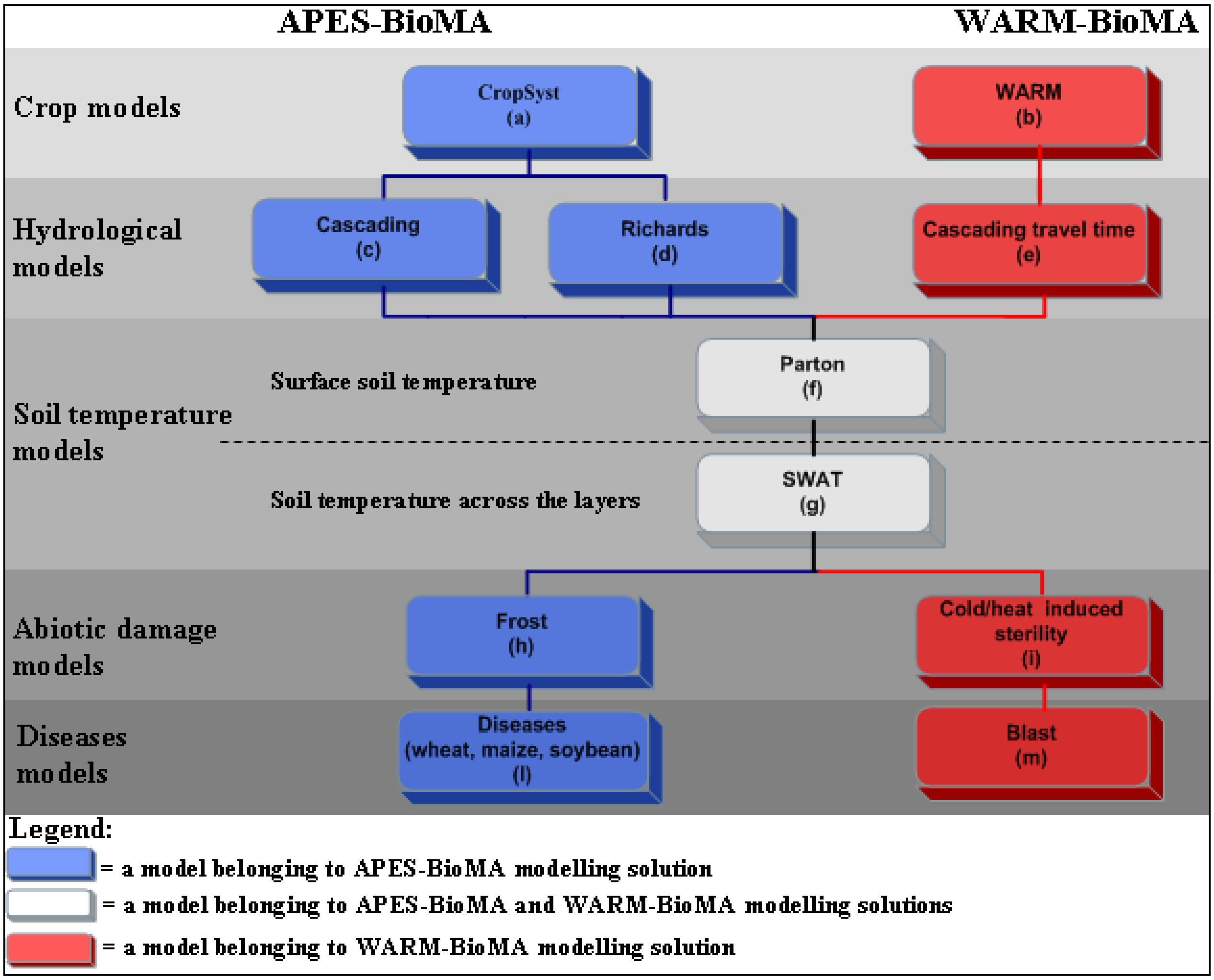

Source: (a) Stockle and others 2003; (b) Confalonieri and others 2009a; (c) Jones and Ritchie 1990; (d) Richards 1931; (e) adopted by SWAT, Neitsch and others 2002 and ANSWERS-2000, Bouraoui and Dillah 1996; (f) Parton 1984; (g) adopted by SWAT; (h) Ritchie 1991; (i) Confalonieri and others 2004 and Challinor and others 2005; (l) Salinari and others 2009; (m) Biloni and others 2007.

Sample point simulations

This section presents the results of sample simulations for AZS-BioMA, carried out for a single season in Brazil for wheat (medium-cycle varieties), for maize (long-cycle varieties), soybean (short-cycle varieties), and rice (short-cycle varieties). The grid cells chosen are a random sample within the area where crops are grown, without targeting a representativeness of the conditions chosen; data are shown purely as examples to illustrate the type of results. For each crop, the AZS-BioMA parameter editor—showing how the proper parameterization was set—is shown (figures I5, I8, I11, and I14), followed by simulation results for leaf area index (figures I6, I9, I10, I12, and I15) and aboveground biomass (figures I7, I10, I13, and I16). For both the simulated variables, the two screen shot of the AZS-BioMA data viewer show the results for the following conditions:

- Potential growth (temperature and radiation are the only factors limiting crop growth and development);
- Water limited growth (water limitations through soil availability and evaporative demand);
- Abiotic factor limited (frost damage to wheat, maize and soybean, and cold shock-induced spikelet sterility for rice);
- Biotic, or Diseases limited (impact of the following diseases on crop production: wheat rust [*Puccinia recondita*], maize gray leaf spot [*Cercospora zea-maydis*], soybean rust [*Phakopsora pachirizi*], rice blast [*Pyricularia oryzae*]); Actual (Water stress, abiotic and biotic factors).

Figure I5. Model parameter editor interface showing the CropSyst parameters for Wheat_SouthAmerica_3 crop key (variety with medium crop cycle length)

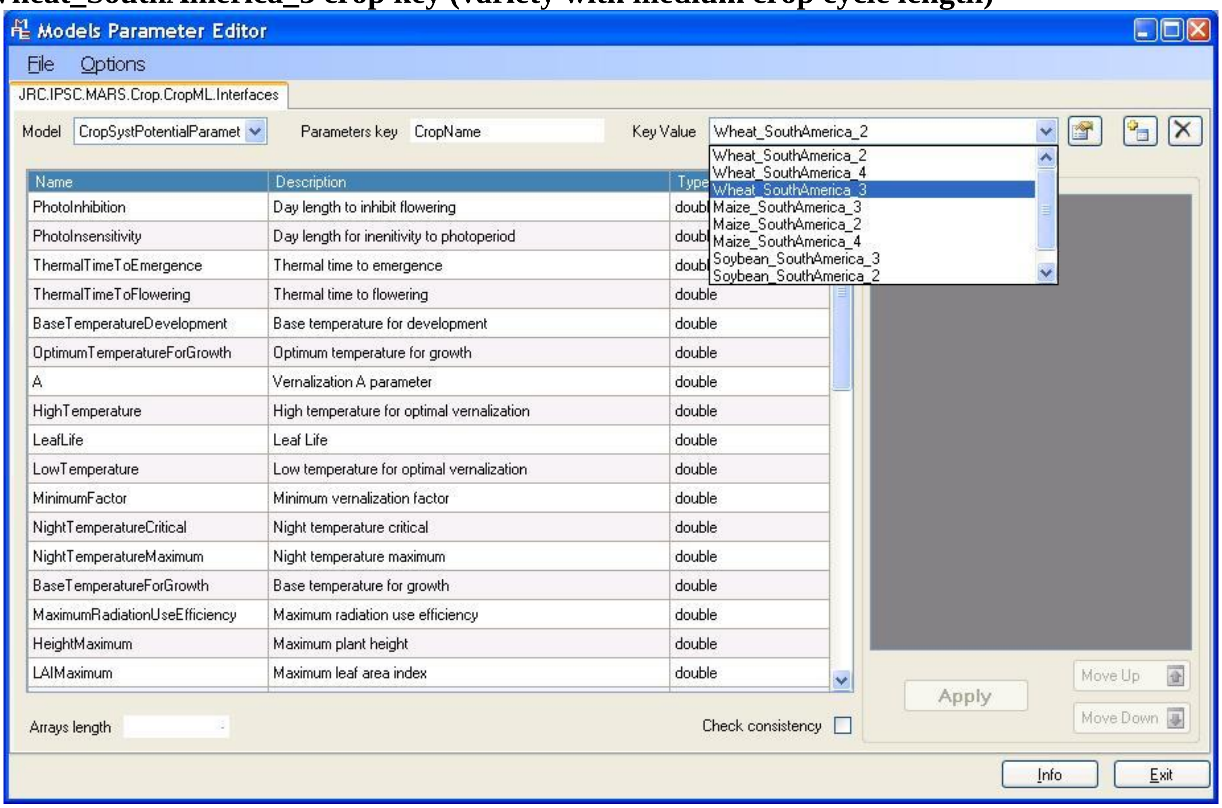

Figure I6. Graphic data display interface showing leaf area index (m2 m-2) of wheat (potential, disease limited, water limited, frost limited, and with all limitations) simulated in a sample cell of Brazil with the APES-BioMA modeling solution

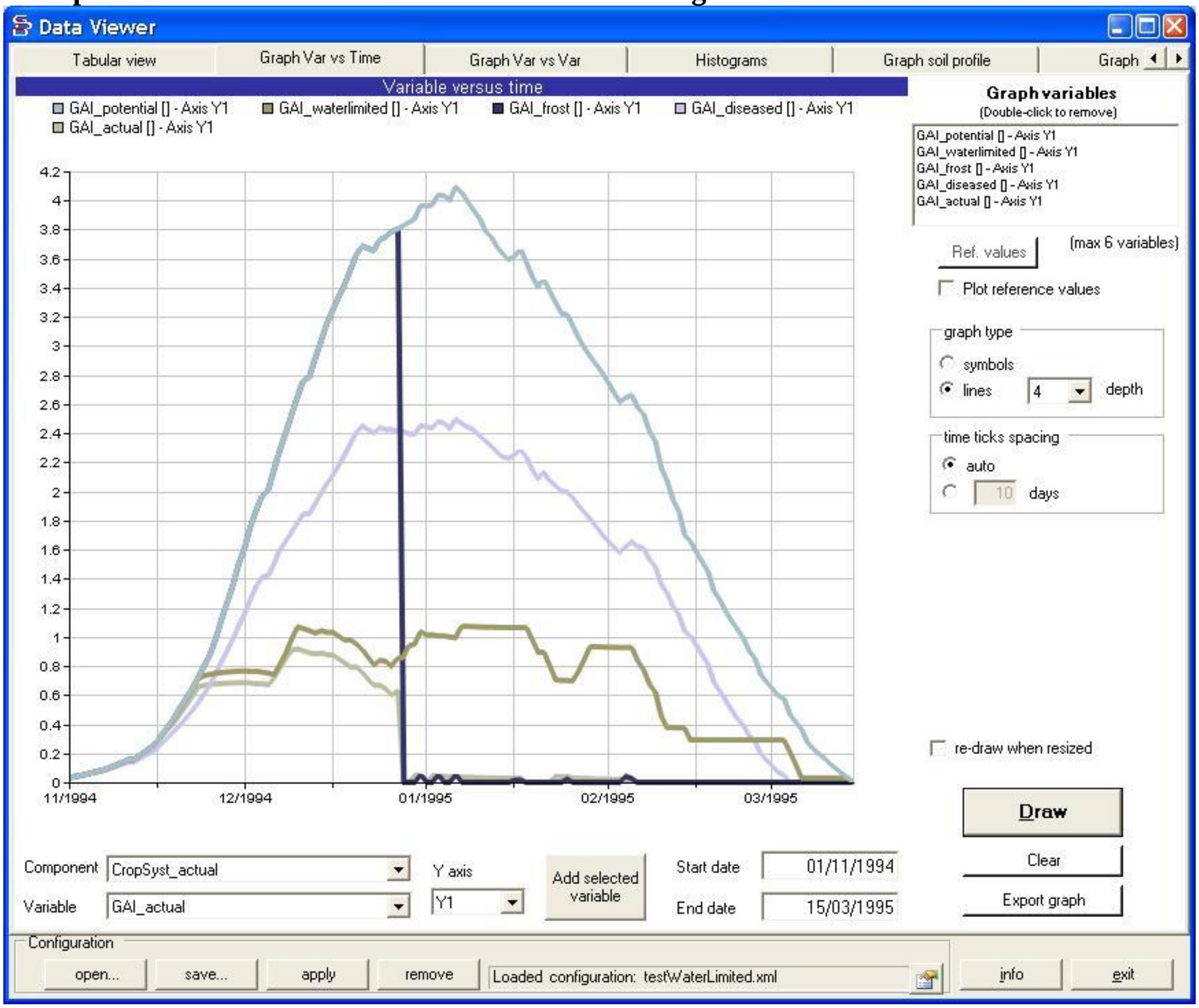

Figure I7. Graphic data display interface showing aboveground biomass (kg ha^{-1}) of wheat (potential, disease limited, water limited, frost limited, and with all limitations) simulated in a sample cell of Brazil with the APES-BioMA modeling solution

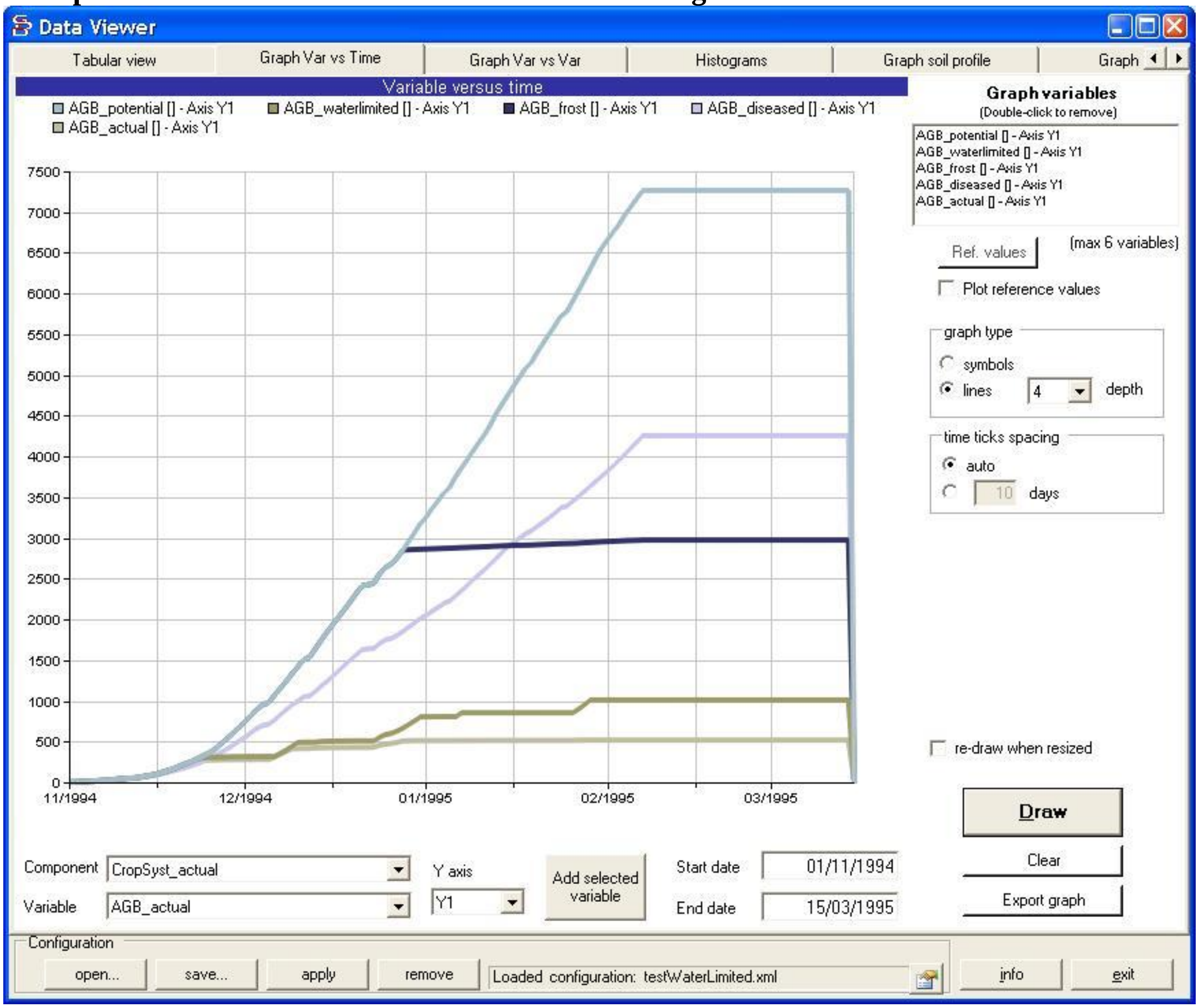

Figure I8. Model parameter editor interface showing the CropSyst parameters for Maize_SouthAmerica_4 crop key (variety with long crop cycle)

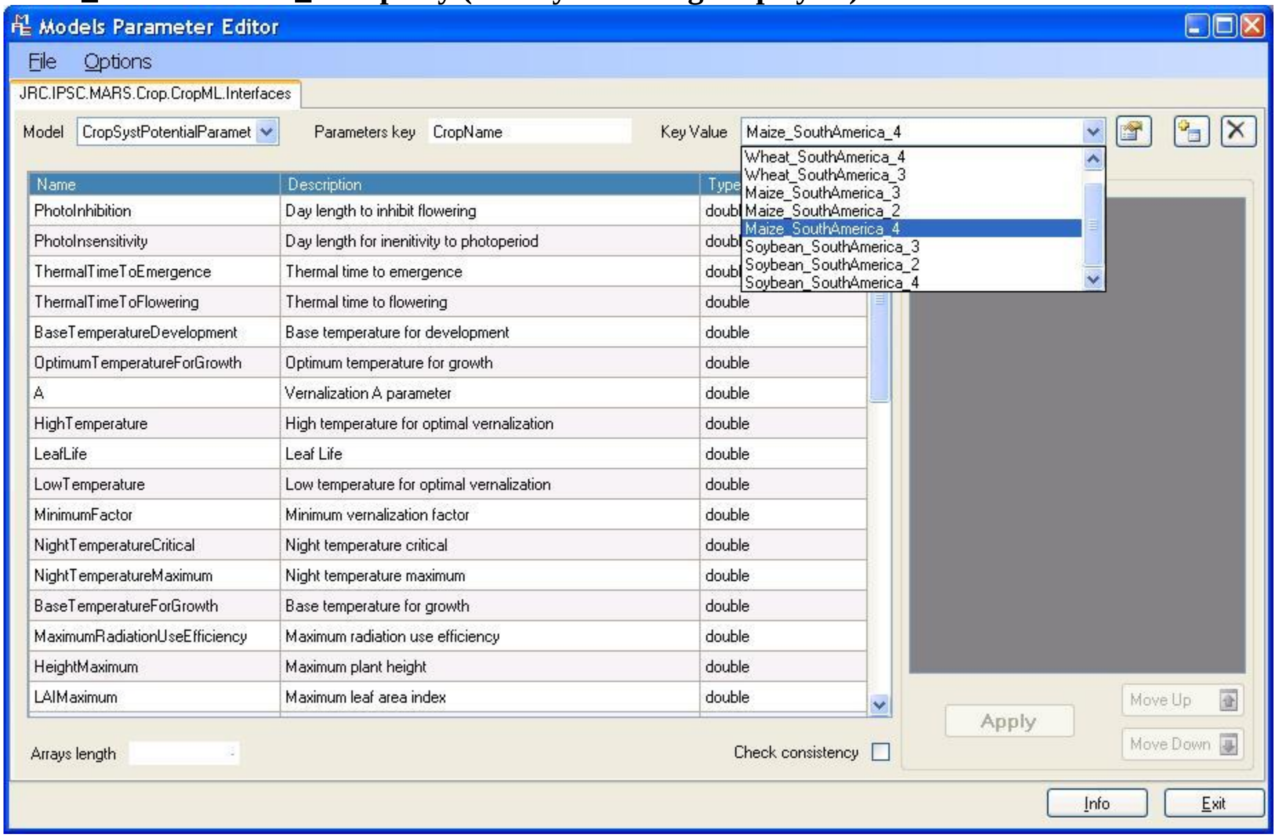

Figure I9. Graphic data display interface showing leaf area index (m2 m-2) curves of maize (potential, disease limited, water limited, frost limited, and with all limitations) simulated in a sample cell of Brazil with the APES-BioMA modeling solution

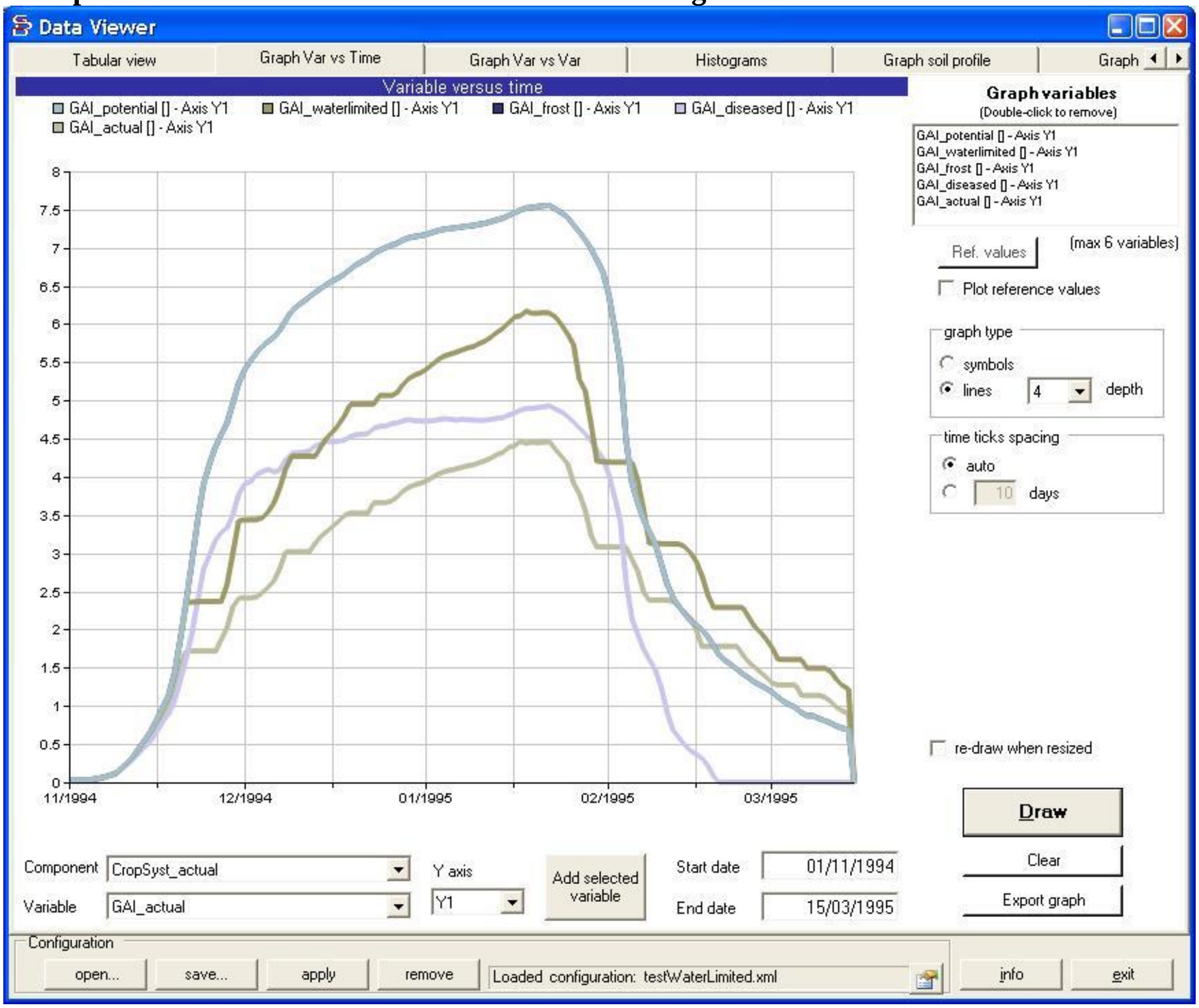

Note: Frost damages do not affect crop productivity in this simulation.

Figure I10. Graphic data display interface showing aboveground biomass (kg ha-1) curves of maize (potential, disease limited, water limited, frost limited, and with all limitations) simulated in a sample cell of Brazil with the APES-BioMA modeling solution

Note: Frost damages do not affect crop productivity in this simulation.

Figure I11. Model parameter editor interface showing the CropSyst parameters for Soybean_SouthAmerica_2 crop key (variety with short crop cycle)

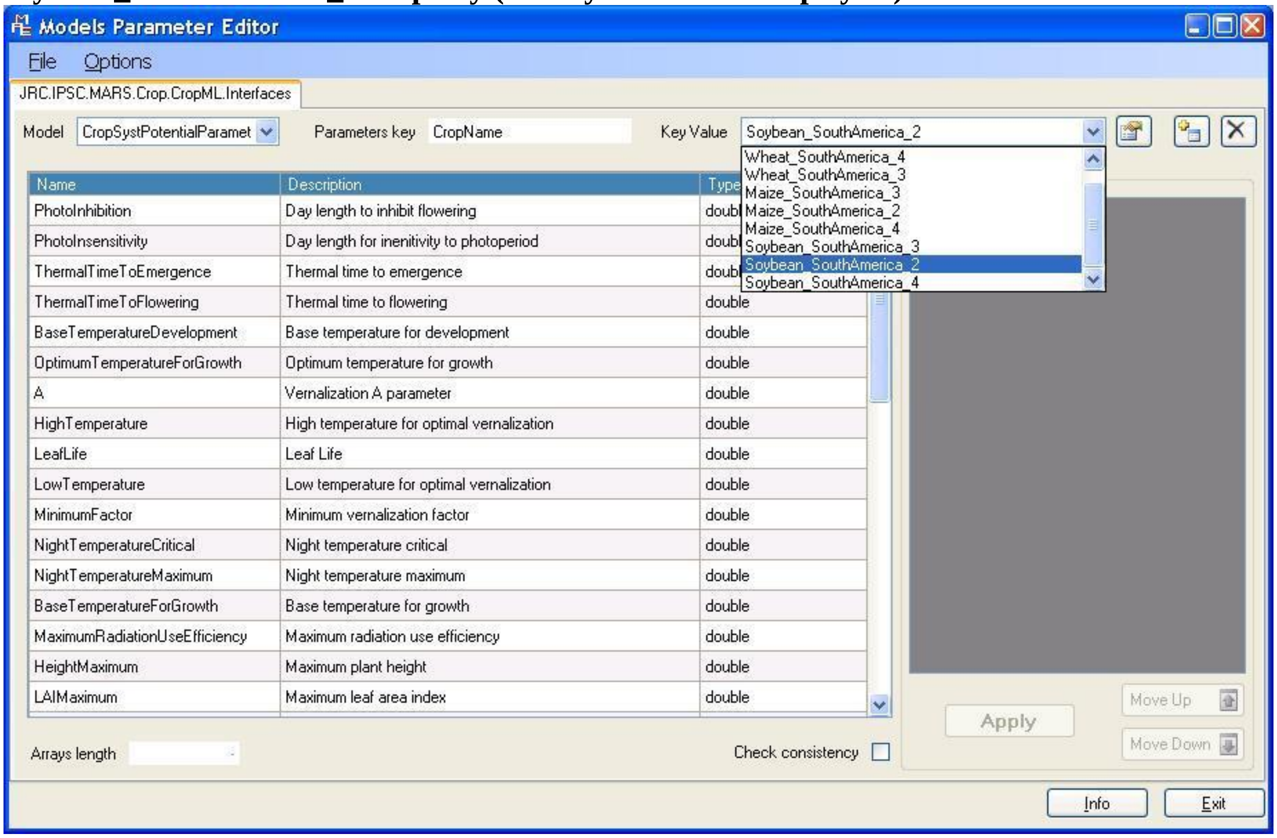

Figure I12. Graphic data display interface showing leaf area index (m2 m-2) curves of soybean (potential, disease limited, water limited, frost limited and with all limitations) simulated in a sample cell of Brazil with the APES-BioMA modeling solution. Frost damages do not affect productivity in this simulation.

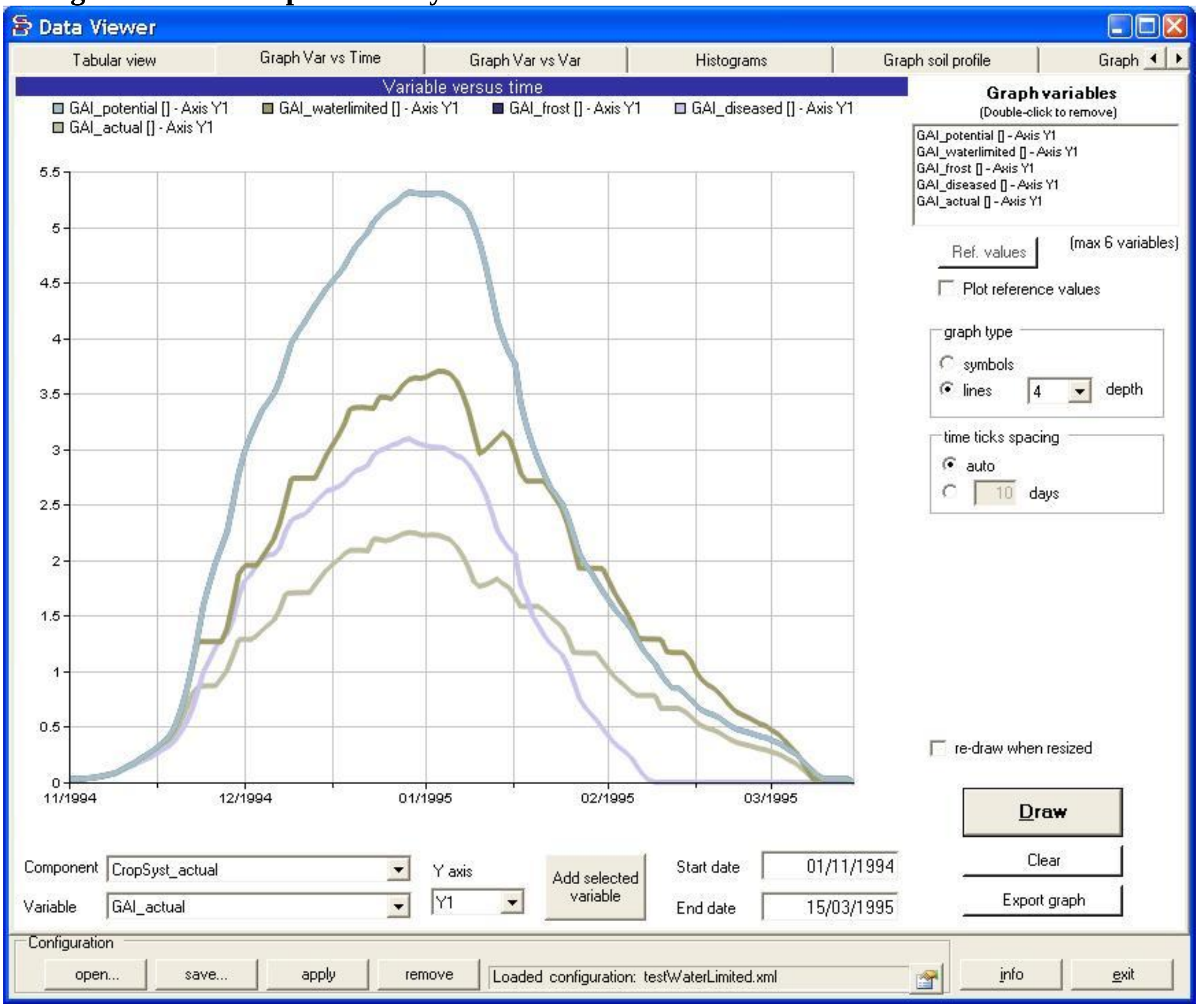

Note: Frost damages do not affect crop productivity in this simulation.

Figure I13. Graphic data display interface showing aboveground biomass (kg ha-1) curves of soybean (potential, disease limited, water limited, frost limited, and with all limitations) simulated in a sample cell of Brazil with the APES-BioMA modeling solution

Note: Frost damages do not affect crop productivity in this simulation.

Figure I14. Model parameter editor interface showing the WARM parameters for Rice_SouthAmerica_2 crop key (variety with short crop cycle)

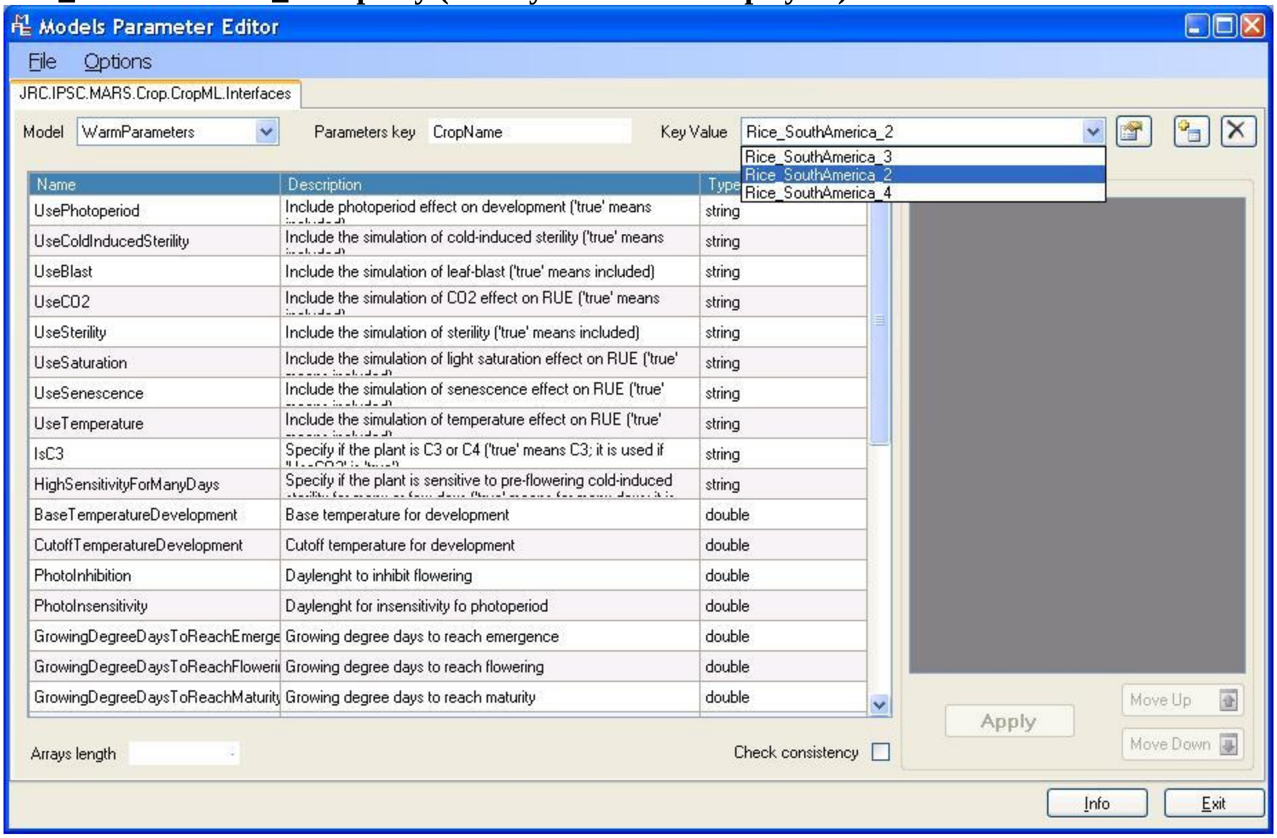

Figure I15. Graphic data display interface showing leaf area index (m2 m-2) curves of rice (potential, disease limited, water limited, and with all limitations) simulated in a sample cell of Argentina with the WARM-BioMA modeling solution

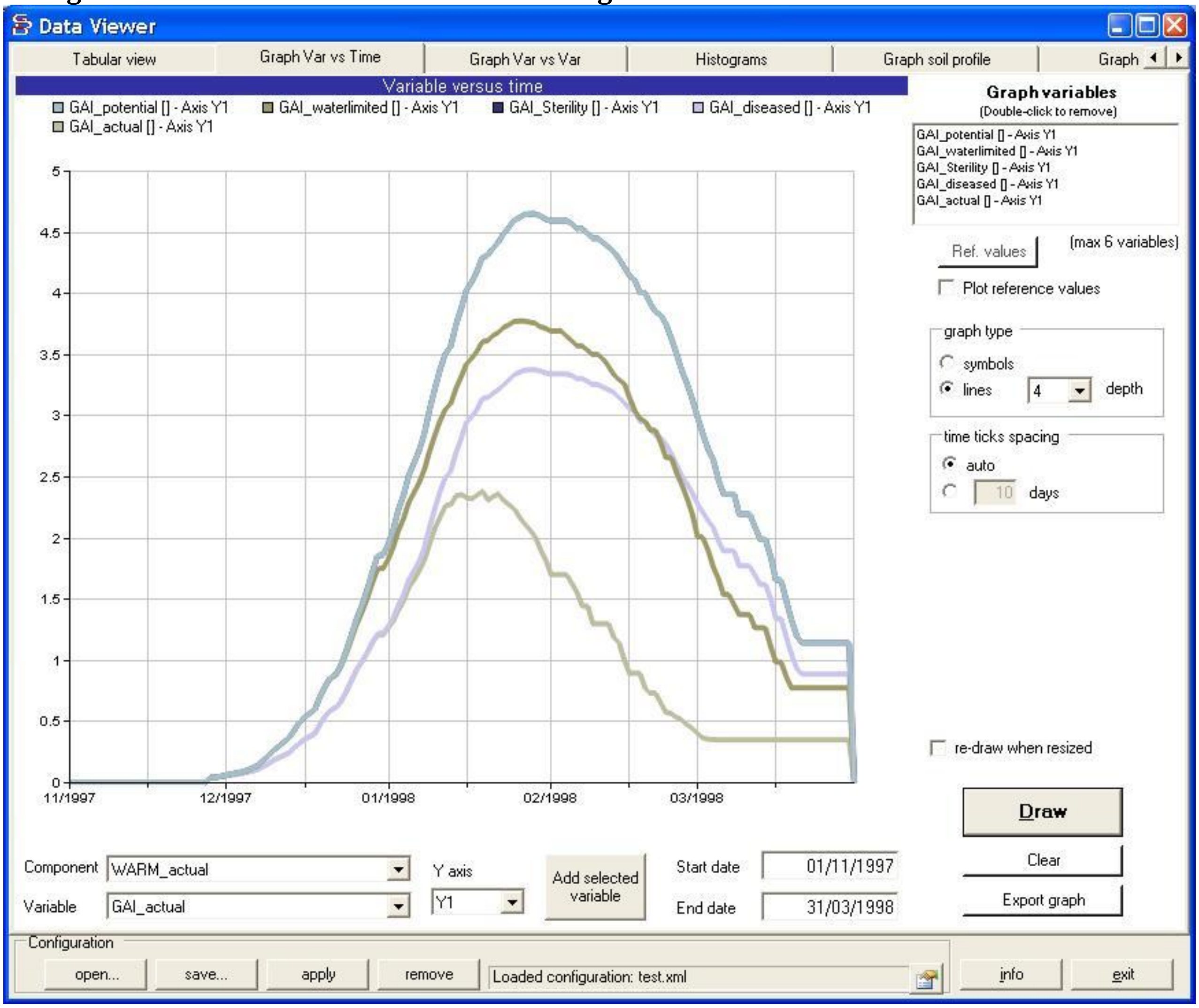

Figure I16. Graphic data display interface showing storage organs (kg ha-1) curves of rice (potential, disease limited, water limited, sterility cold limited, and with all limitations) simulated in a sample cell of Brazil with the APES-BioMA modeling solution

Note: Sterility cold damages do not affect productivity in this simulation.

The following section presents AZS-BioMA data viewer screen shots as sample point outputs related to simulated soil variables—that is, soil water content (figure I17) and temperature along the soil profile (figure I18).

Figure I17. Graphic data display interface showing soil water content simulated in a sample cell of Brazil with the APES-BioMA modeling solution

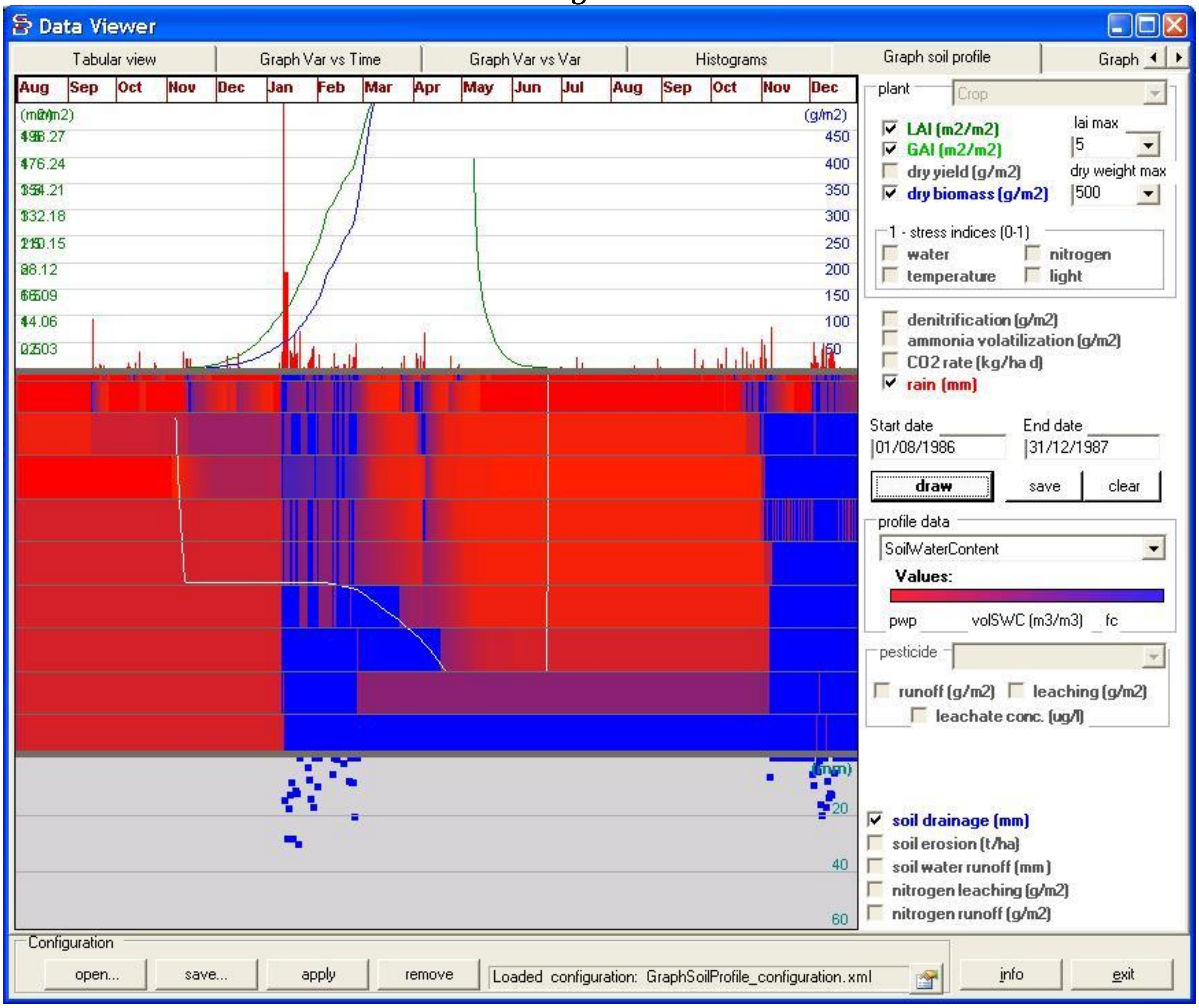

Figure I18. Graphic data display interface showing soil temperature simulated in a sample cell of Brazil with the APES-BioMA modeling solution

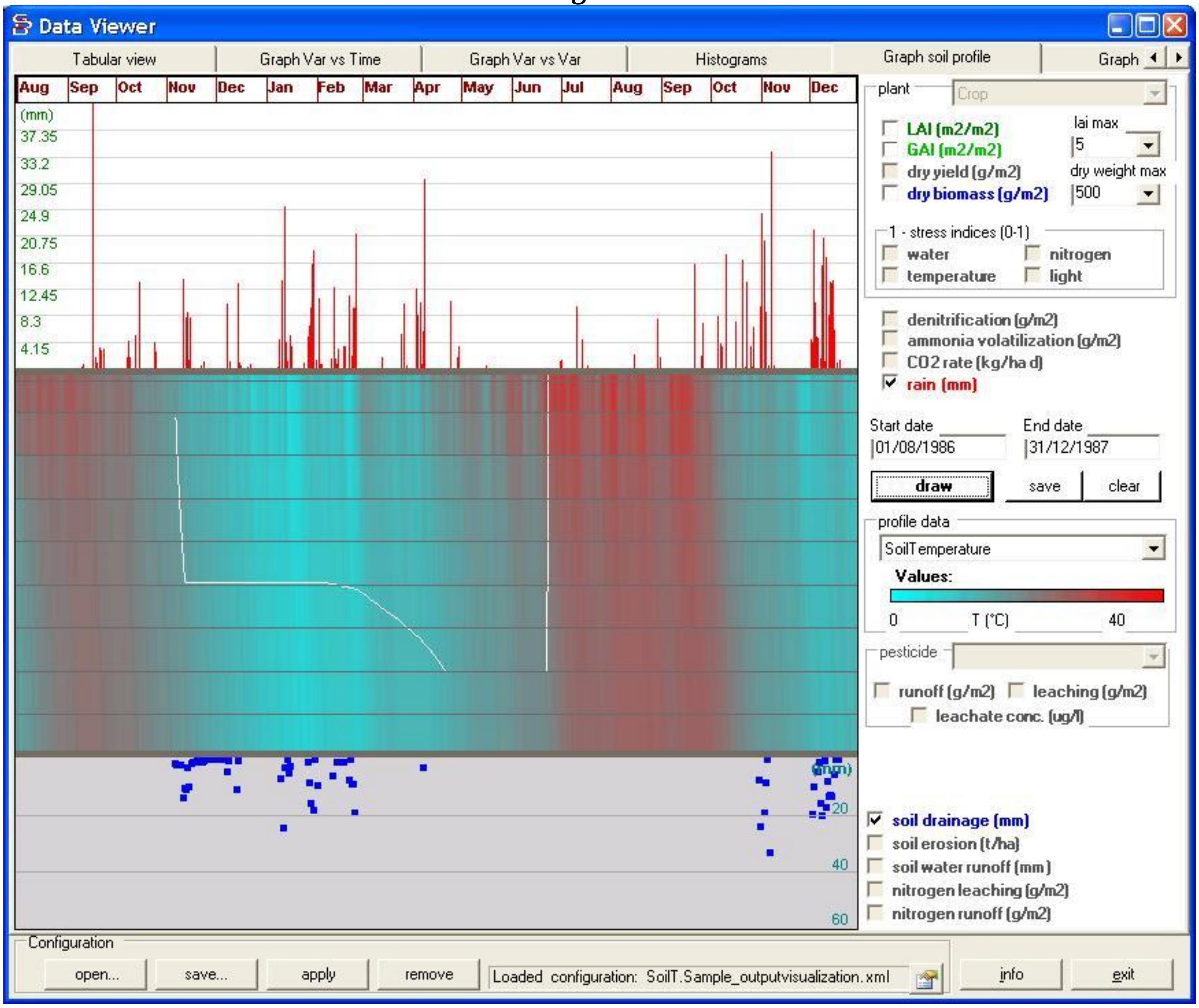

Figure I19 shows how the AZS-BioMA model can be parameterized for simulating the different pathogens within the APES-BioMA modeling solution.

Figure I19. Model parameter editor interface showing the options for simulating the three pathogens: *Cercospora Zeae-maydis* (maize), *Phakospora pachirizi* (soybean), and *Puccinia recondita* (wheat) accounted for by the APES-BioMA modeling solution in this study

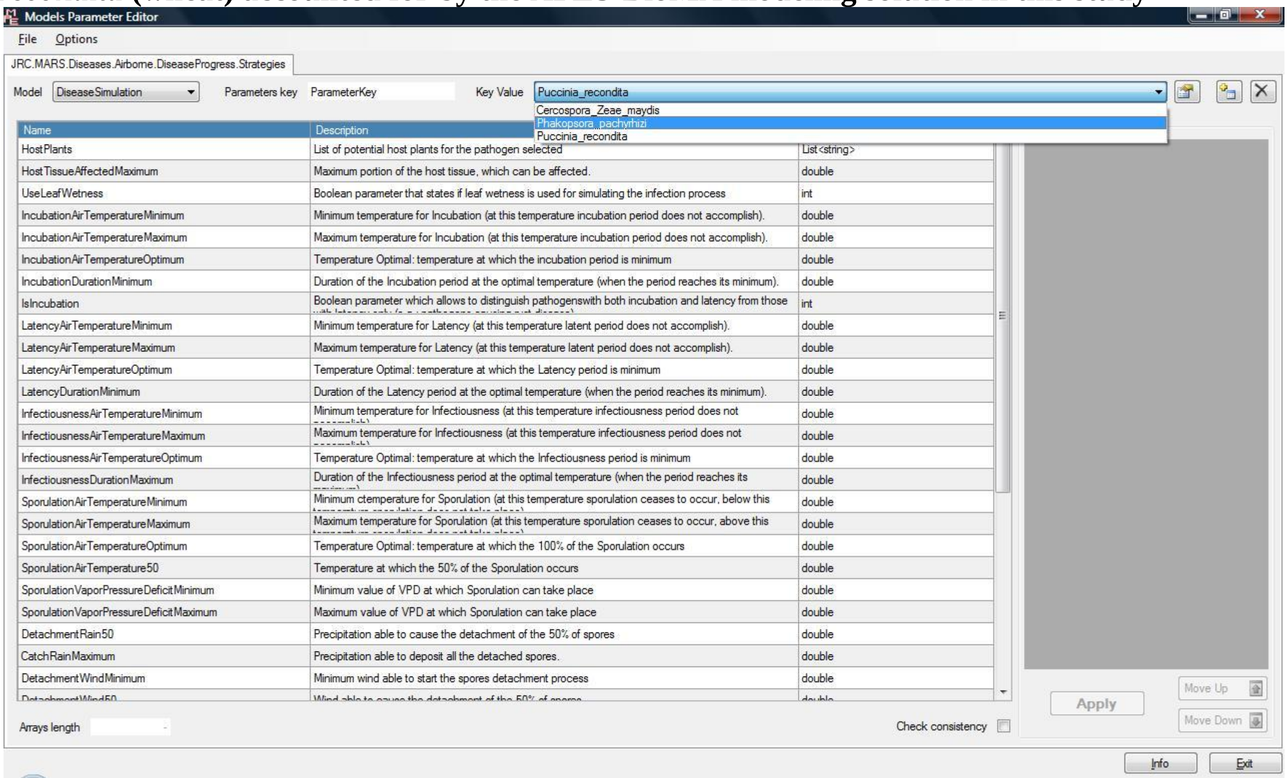

Note: Pyricularia oryzae (rice) is not included in this figure because it is simulated with the second AZS-BioMA modeling solution (WARM-BioMA).

AZS-BioMA: crop suitability and adaptation capabilities

Suitability

Crop suitability is an important component of assessment studies, including changes to geographic distribution under climate change in coming decades. If it is well known that crops will respond to specific changes in temperature and precipitation at the locations where they are currently grown, it can also be expcted that not all crops and cultivars will remain suitable within their current geographical ranges, with tendencies to migrate toward higher latitides from areas already at the margin of known temperature and water limitations. However, most crop modeling platforms present fixed grid simulations of crops—that is, they do not allow for dynamic movement of ideal crop ranges—and thus tend to underestimate likely adaptation responses by farmers, who will doubtlessly attempt to switch to cultivars and crops better adapted to changing conditions. By the same token, those model platforms that have excelled in computing suitability have much less crop modeling detail than available under the proposed platform.

Before designing the suitability component, a bibliographic review was conduced to determine which approaches are commonly adopted for suitability assessments, especially in climate change impact studies. Most of the available approaches are based on the definition of thresholds for specific environmental parameters. Examples of this typology of approaches are the FAO

EcoCrop criterion (http://ecocrop.fao.org) and the less favourable areas criterion developed at the European Commission Joint Research Centre (Eliasson and others 2010). Another approach recently proposed is based on a multiple regression to relate the percentage of crop presence in an area to climatic indicators (used as regressors) (Moriondo and others 2010). In this case, the regressors used were related to temperature, rainfall, heat stress and frost events.

The AZS-BioMA suitability component was developed implementing both these typologies of approaches: threshold- and multiple regression–based, with the latter developed by extending the concepts and criteria used in the first typology of methods. Our implementation of all the methods allow the user to select the methods in their original configuration and with categiories of variables or parameters excluded from the computation.

We also developed and implemented a district criterion, based on the assumption that crop choices by farmers tend to aggregate in production districts. This approach cannot be used alone; the UNIMIsSuitability component allows the user to couple it to all the other methods implemented. The component can be used in two modalities: single-cell and multicell. The latter is needed when multiple regression–based methods are selected.

All the approaches implemented will be evaluated and compared using current crop masks (see deliverable D2; Ref. 4) to provide AZS-BioMA with a default approach.

The user can run the AZS-BioMA suitability component by deciding exactly which method to use or by leaving the component to selecting the most appropriate method in light of the actual data availability or the particular exercise that needs to be run (figure I20). This feature was achieved with a suitable implementation of the strategy design pattern (figure I21). The user can access methods directly (light and intermediate blue in figure I20) or by selecting context strategies (dark blue in figure I21) that automatically perform the method selection.

Figure I20. Flow chart of the logic behind the UNIMI.Suitability feature for automatically selecting the most suitable approach according to the availability of data under specific conditions

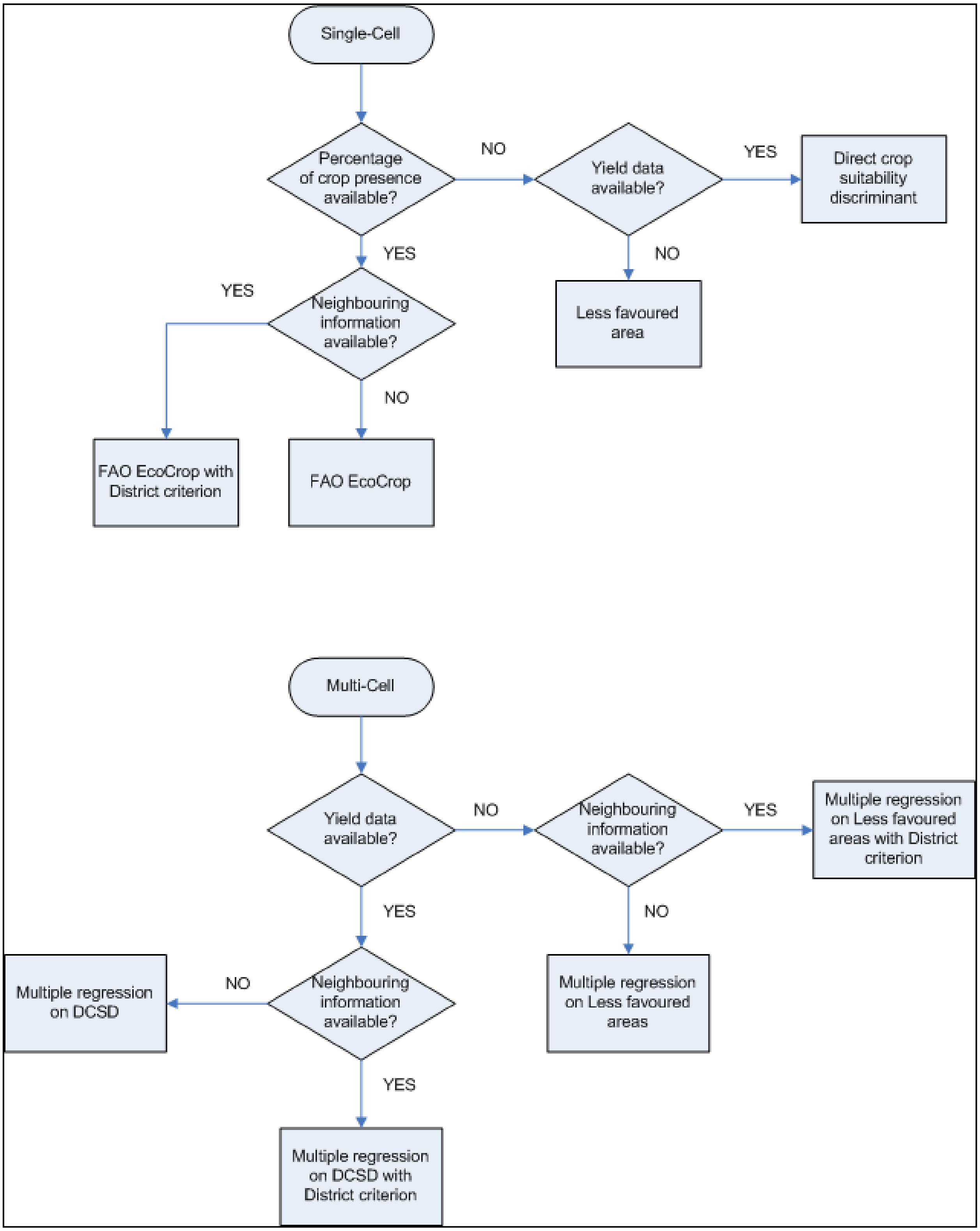

Figure I21. Strategy diagram of the AZS-BioMA UNIMI.Suitability component

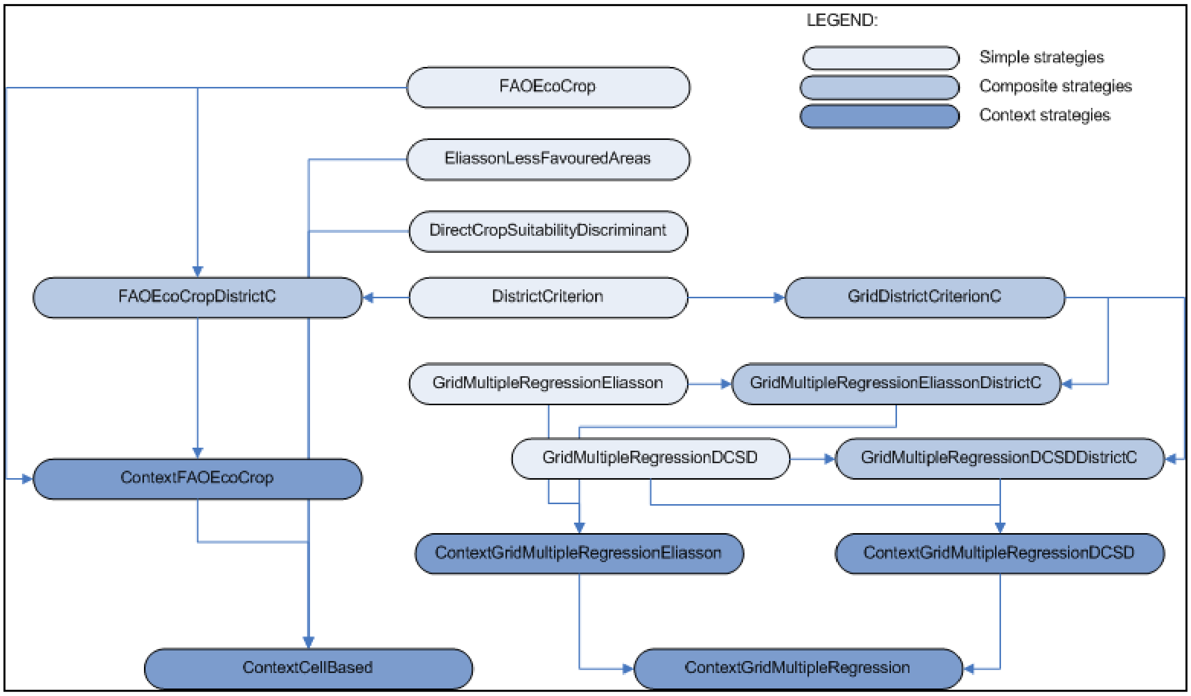

FAO EcoCrop criterion

The FAO EcoCrop approach is based on two response functions (figures I22 and I23) calculated by relating climatic data (temperature and rainfall considered during the crops cycles) to crop-specific parameters (figure I24). The values of these parameters were derived from interviews with experts and are available at http://ecocrop.fao.org/ecocrop/srv/en/home. After computing the two response functions, the lowest between temperature and rainfall sauitabilities is selected.

Figure I22. FAO EcoCrop response function for temperature suitability, using parameter values for maize

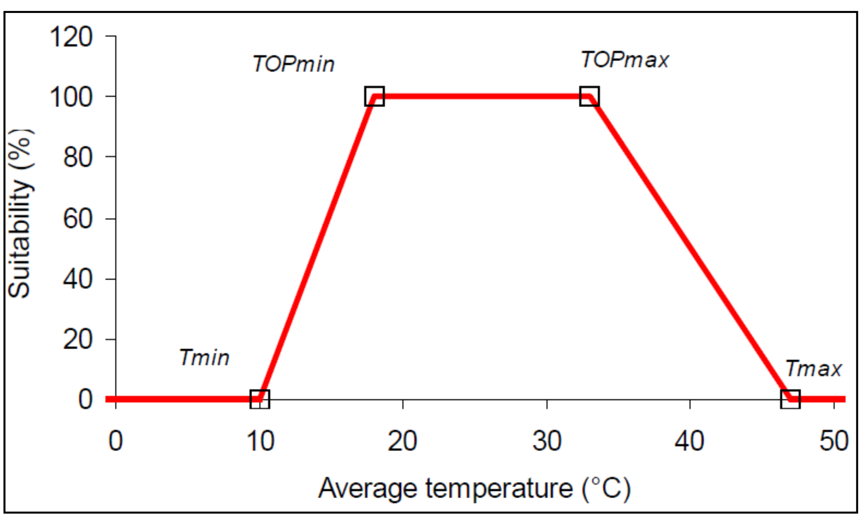

Figure I23. FAO EcoCrop response function for rainfall suitability using parameter values for maize

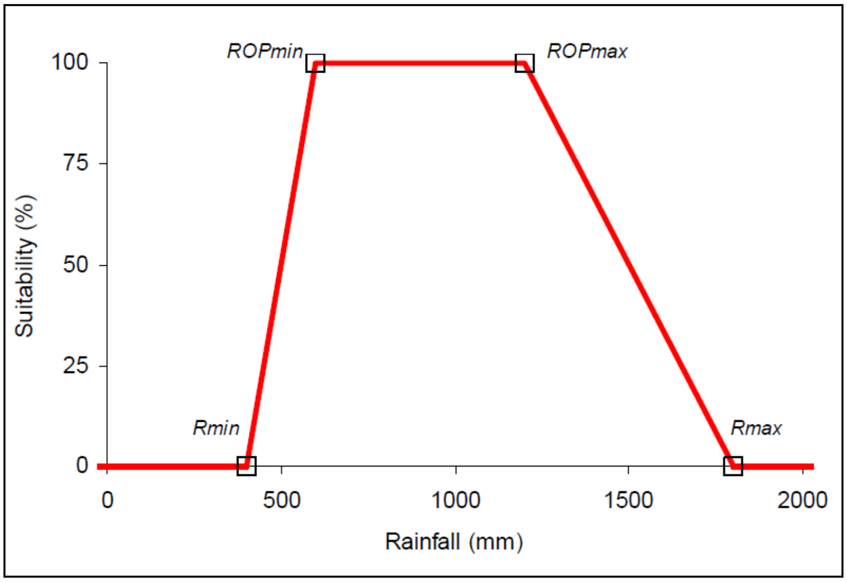

Figure I24. Flow chart of the FAO EcoCrop suitability criterion

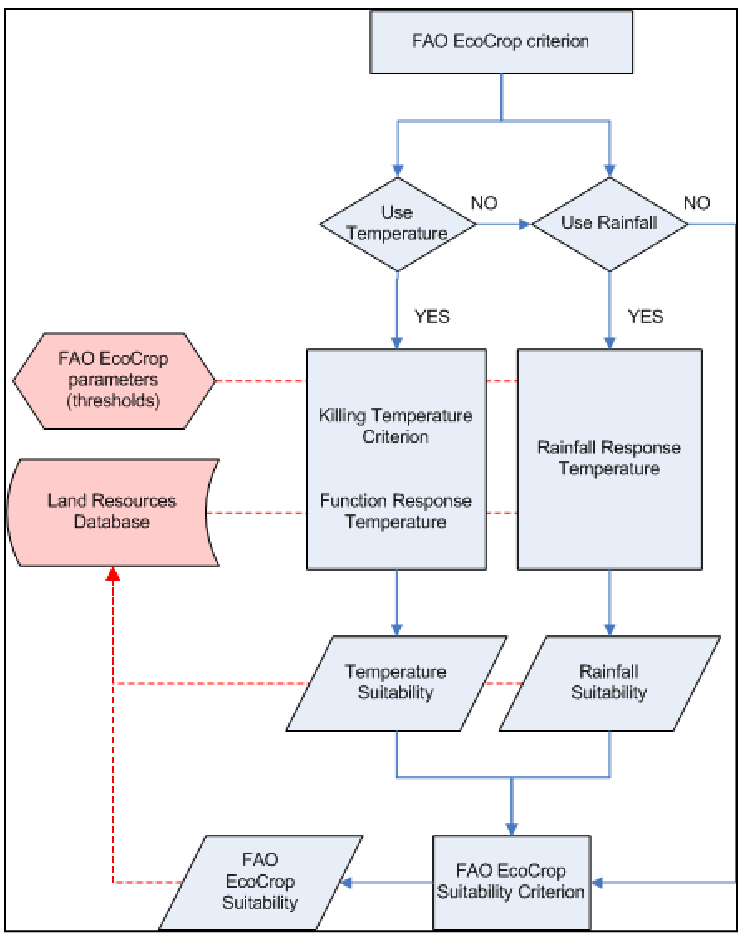

Less favored areas

The less favored areas approach derives from the work of Eliasson and others (2010), aimed at evaluating the suitability of generic agriculture areas according to natural constraints. The guidelines that led to the development of the original version of this approach are scientifically clear and understandable methodology; key soil, climate, and terrain characteristics–based criteria; classification related to areas that have natural handicaps to agriculture and not to how the land is used neither to the payment mechanisms such as eligibility rules, and level of payments; agricultural areas that include permanent grasslands, permanent crops, and arable land (forest is not included); and no crop specificity.

Our implementation includes options for using different typologies of information and can be parameterized for the different crops considered for this project (figure I25). Table I1 lists the eight criteria adapted from Eliasson and others (2010), together with their description and default thresholds. Two classes were developed for each criterion, based on relative thresholds: not limiting and severely or very severely limiting conditions. Criteria are assessed according to the agronomic law of the minimum (Liebig’s law). Once one of the considered criteria is rated severely limiting, the corresponding land is judged to present severe limitations for agricultural activities in general or for a specific crop (depending on the parameterization adopted). The criteria are not weighted or given a relative importance. To account for between-year variability of the length of the growing season, temperature accumulation, heat stress, and soil moisture balance, these characteristics are classified as severely limiting in a probabilistic approach. A characteristic is classified as being severely limiting if the probability of exceeding the severe limit is more than 20% (that is, the constraint occurs in at least 7 years out of 30). The criteria are applied to single cell points, and the mapping should ensure that the scales of the soil and climate data are compatible with the scale at which the area is classified.

The need to adapt the criteria selected by Eliasson to the project land resources database (see deliverable D2; Ref. 4) and to fulfill the possibility of handling them by the user led us to implement the approach (“Eliasson criterion” hereafter) in figure I25. In particular, we clustered the criteria in categories (climate, soil physics, soil chemistry, and water balance), thus enabling the choice to process the assessment tests also separately (obtaining criteria for partial suitability), according to user information and aims.

Figure I25. Flow chart of the less favored areas suitability criterion (Eliasson criterion)

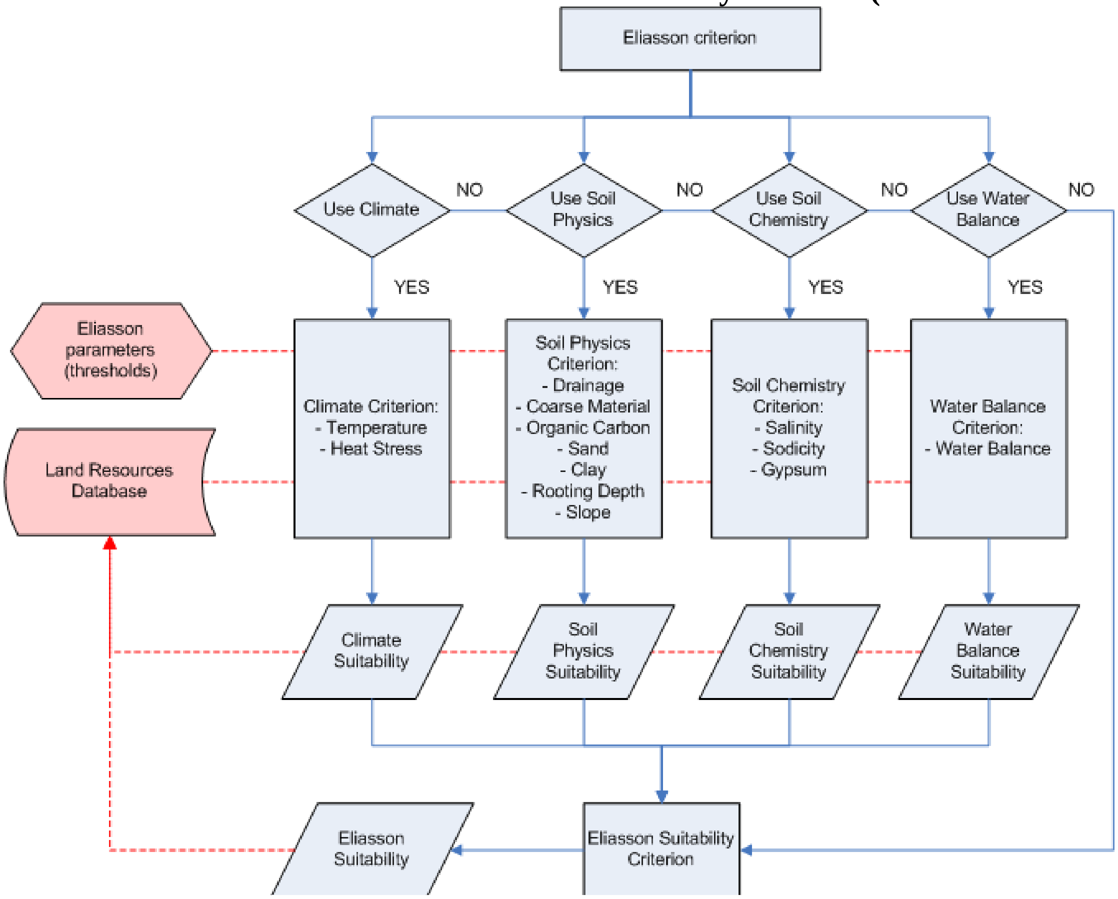

Table I1. Soil and climate criteria for classifying land according to its suitability for generic agricultural activity

Criterion	**Description**	**Threshold (default)**
Climate		
Temperature	Length of growing period defined as the number of days with daily temperature higher than a user-specified threshold (days) OR Growing degree days accumulated above a user-specified threshold (°C)	≤ 180 days with threshold temperature of 5°C ≤ 1,500 °C with threshold temperature of 5°C
Heat stress	Number of periods of consecutive days with temperature higher than a user-specified threshold (-)	At least one period of 10 consecutive days with daily temperature threshold of 35°C

Soil physics		
Drainage	Daily drainage (mm day^{-1})	≤ 0.5 mm day^{-1}
Texture	Sand (weight %) Clay (weight %) Organic matter (weight %) Coarse material (volume %)	> 70% > 60% > 30% > 15%
Rooting depth	Maximum rooting depth (cm)	< 30 cm
Slope	Change of elevation with respect to the planimetric distance	> 15%
Soil chemistry		
Chemical properties	Salinity (electric conductivity dS m^{-1}) Sodicity (exchangeable sodium percentage) Gypsum (%)	> 4 dS m^{-1} > 6% > 15%
Water balance		
Non dry day	Number of days within growing period with amount of rainfall and soil moisture exceeding half of potential evapotranspiration (days)	≤ 90 days

Note: Threshold values distinguish nonlimiting from severely limiting conditions (adapted from Eliasson and others 2010). Climate-related criteria are yearly time scale–based. In our implementation crop-specific thresholds can be used to extend the criterion to evaluate the suitability for different crops.

Direct crop suitability discriminant

The aim of the second approach implemented in the suitability component—direct crop suitability disccriminant criterion (DCSD)—is to propose a crop-specific criterion based on the outputs of cropping systems models. Criteria and related thresholds are presented in table I2. Criteria were selected according to:

- Actual yield and development stage of the considered crop at the end of the season (that is, yield and maximum development stage code criteria).
- Impact of abiotic factors and diseases on potential yield (that is, yield gap for frost, diseases, sterility, and water stress criteria).
- Abiotic factors and diseases in terms of events occurrence (that is, stem lodging and potential infection events criteria).

We applied the same suitability assessment methodology of the Eliasson criterion (that is, thresholds processed according to the Liebig's law of the minimum) with the possibility of processing separately different categories of criteria (yield, crop success, abiotic factors, diseases, and water stress). Compared with the Eliasson criterion, this approach allows for a more direct evaluation of crop suitability, since all the criteria involved are direct outputs of a cropping system model. Figure I26 presents the flowchart of the DCSD criterion for crop suitability.

Figure I26. Flow chart of the direct crop suitability discriminant criterion

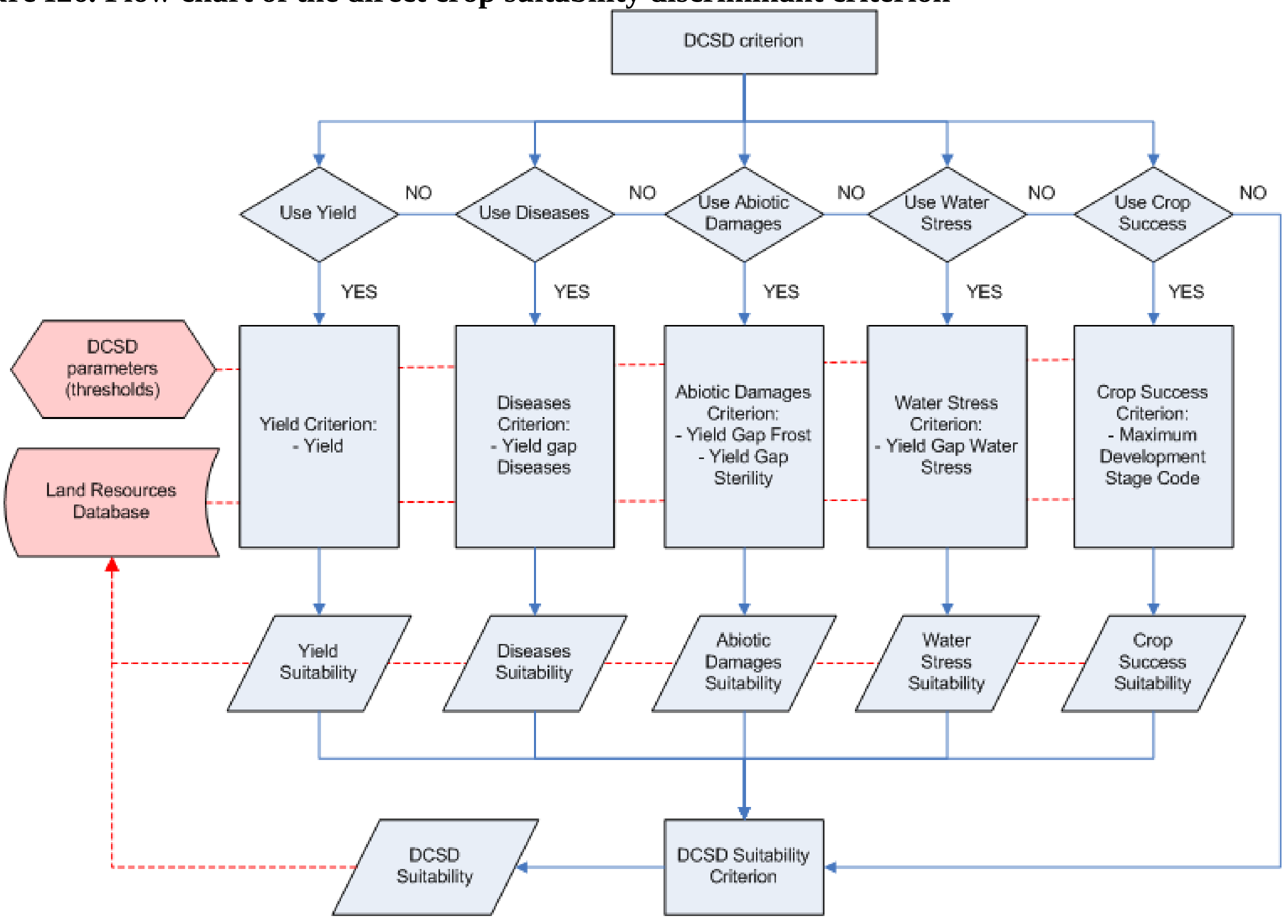

Table I2. Direct crop suitability discriminant for classifying an area according to its suitability for a particular crop

Criterion	Description	Threshold parameters
Yield suitability		
Yield	Yield of the crop (tha^{-1})	ThresholdYield
Crop success		
Maximum development stage code	Maximum development stage code for the crop (0: sowing; 1: emergence; 2: flowering; 3: maturity)	ThresholdMaxDevelopmentStageCode

Abiotic suitability		
Yield gap frost	Percentage yield gap due to frost conditions (%)	ThresholdYieldGapFrost
Yield gap sterility	Percentage yield gap due to temperature sterility conditions (%)	ThresholdYieldGapSterility
Stem lodging	Stem lodging affect the crop, which still survive (boolean)	ThresholdStemLodging
Diseases suitability		
Yield gap diseases	Percentage yield gap due to diseases presence (%)	ThresholdYieldGapDiseases
Potential infection events	Number of potential infection events (-)	ThresholdPotInfectionEvents
Water stress suitability		
Yield gap water stress	Percentage yield gap due to conditions of limited water (%)	ThresholdYieldGapWaterStress

Note: Threshold values separate nonlimiting from severely limiting conditions.

Multiple regression based on the Eliasson criterion

The Eliasson criterion has been extended herein and implemented within a multiple regressive model. In practice, the same variables considered by Eliasson and others (2010) are used as regressors and related to the crop percentage for a certain area, which therefore represent the dependent variable. The regression coefficients are then used to predict the percentage of crop presence for the same area under different conditions for the regressors (such as number of heat waves) because of climate change or perturbative events.

Multiple regressions for land suitability have been proposed in recent studies, also for evaluating the impact of climate change (see, for example, Moriondo and others 2010). Based on user needs, regressors belonging to different categories (climate, soil physics, and the like) could be selected, as with the standard Eliasson method.

Multiple regression based on the direct crop suitability discriminant criterion

A multiple regression suitability method has been developed also for the DCSD criterion. Based on user needs, regressors belonging to different categories can be used also for this approach.

District criterion

An accessory criterion, one that accounts for the fact that farmers tend to aggregate crops within the same production district, has also been developed. Based on the user needs, this district criterion can be coupled to all the others.

The criterion (figure I27) is based on the following rules (computation on the cell α):

- If the percentage of neighboring cells where the same crop is present is higher than a user-specified threshold, increase the crop presence percentage of the cell α by a user-specified relative value.
- If the percentage of neighboring cells where the same crop is present is lower than a user-specified threshold, then decrease the crop presence percentage of the cell α by a user-specified relative value.
- Otherwise, do not modify the crop presence percentage for the cell α.

Figure I27. Flow chart of the district criterion (to be coupled with one of the other methods)

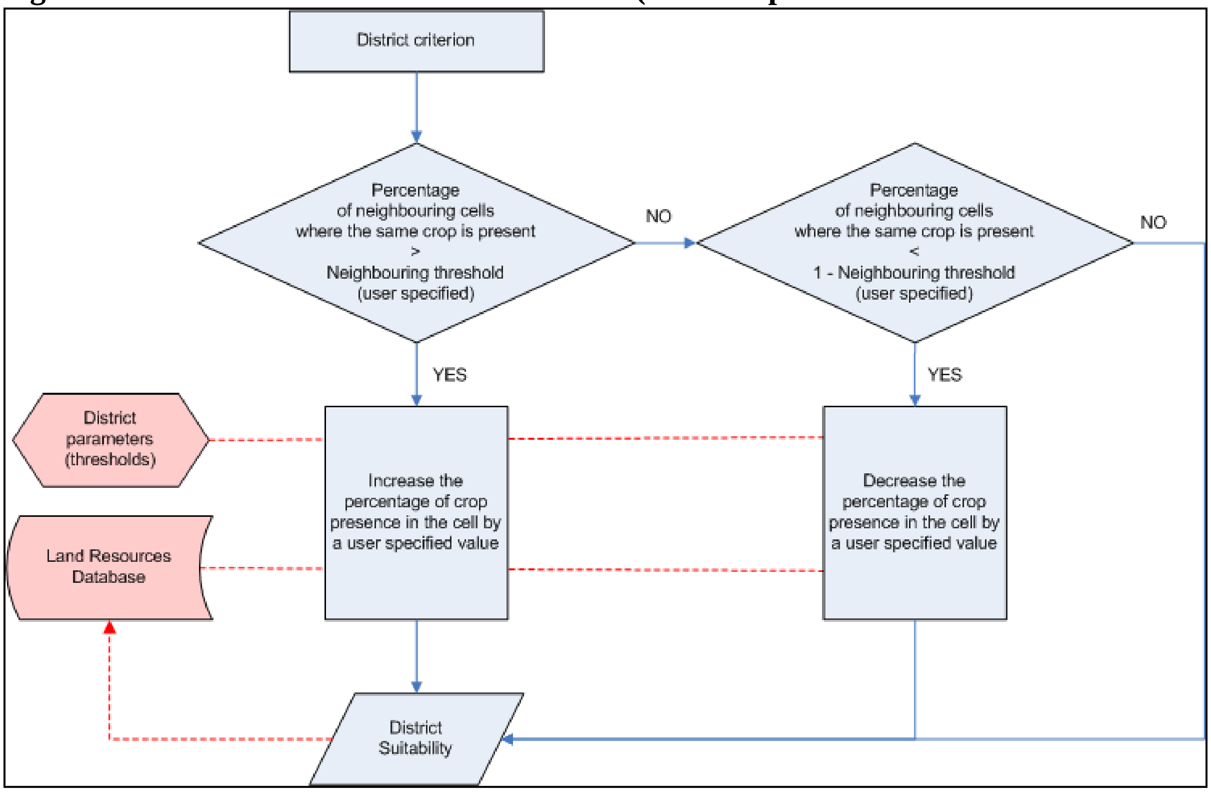

Sample tests on the component as implemented in the AZS-BioMA Model

All the suitability methods implemented in the component were extensively tested using inputs explicitly chosen to explore the highest variability of conditions. The following figures present sample tests carried out using the multiple regression method based on the Eliasson and others (2010) variables. Four situations are shown: all categories of regressors (climate, soil physics, soil chemistry, water balance) used; water balance information not used; soil physical and chemical information not used; only water balance information used. For each situation, how the AZS-BioMA Model is parameterized (figures I28–I31) and the corresponding results calculated for 15 sample cells (figure I32) are shown.

Figure I28. Screen-shot of the model parameter editor showing a configuration where all the Boolean parameters are set to true

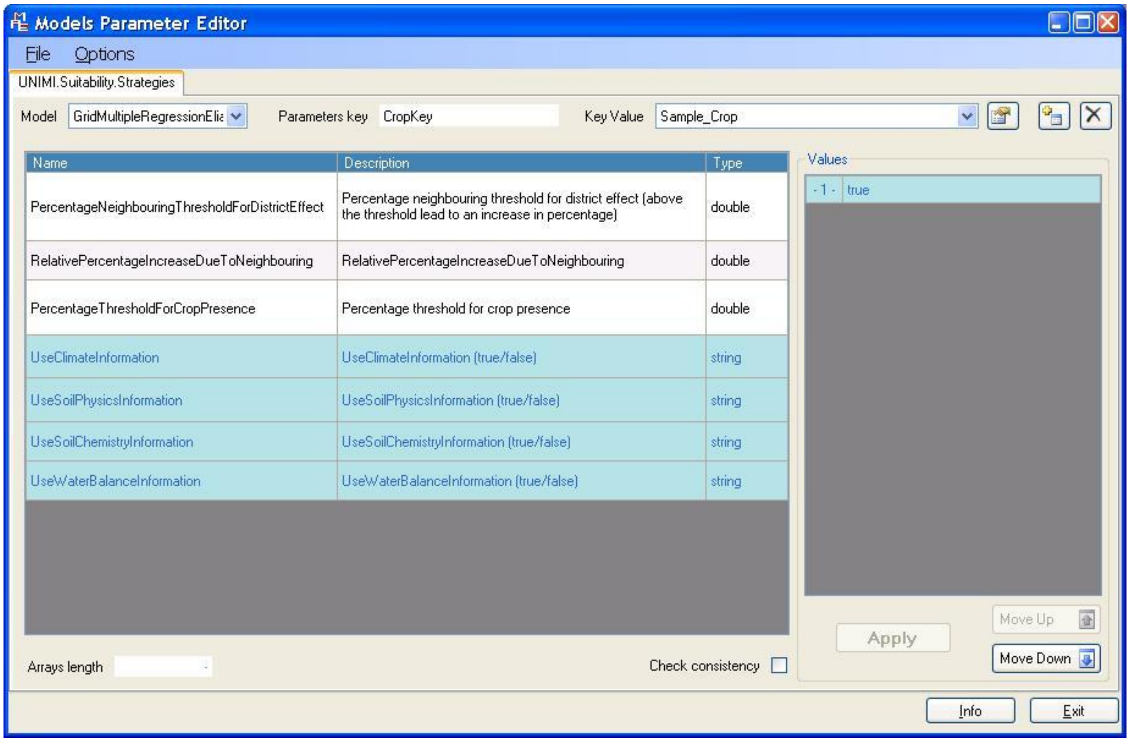

Figure I29. Screenshot of the model parameter editor showing a configuration where Use Water Balance Information is set to false

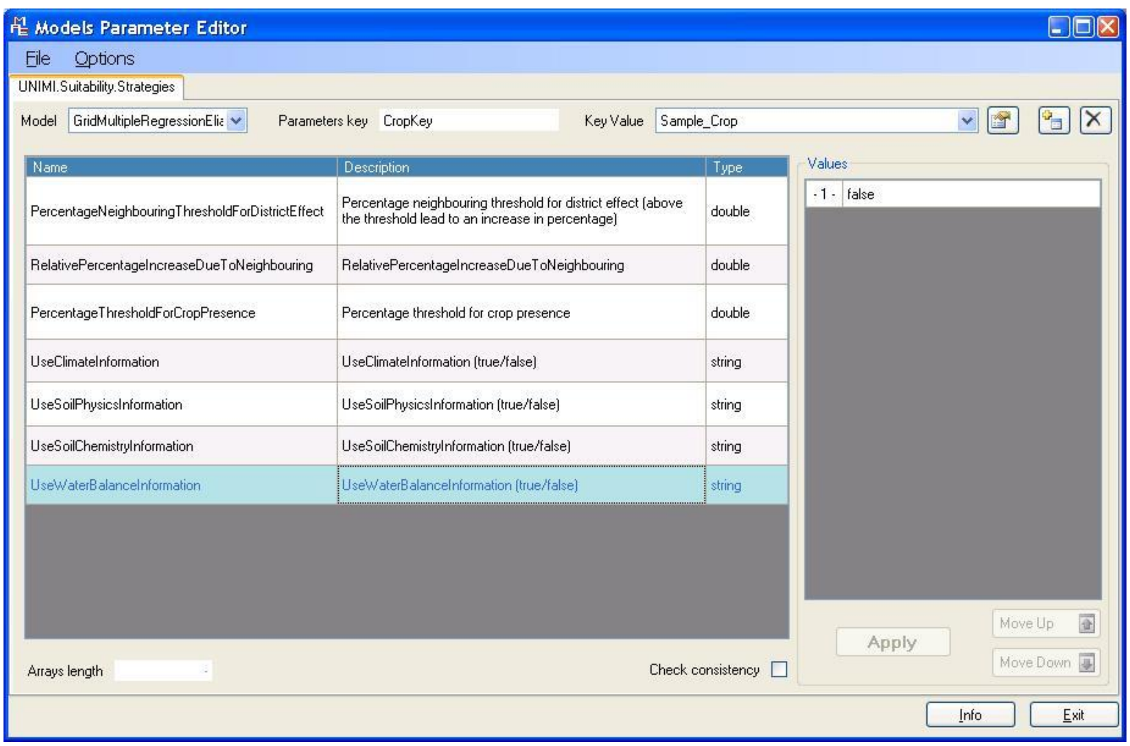

Figure I30. Screen-shot of the model parameter editor showing a configuration where Use Soil Physics Information and Use Soil ChemistryInformation are set to "false"

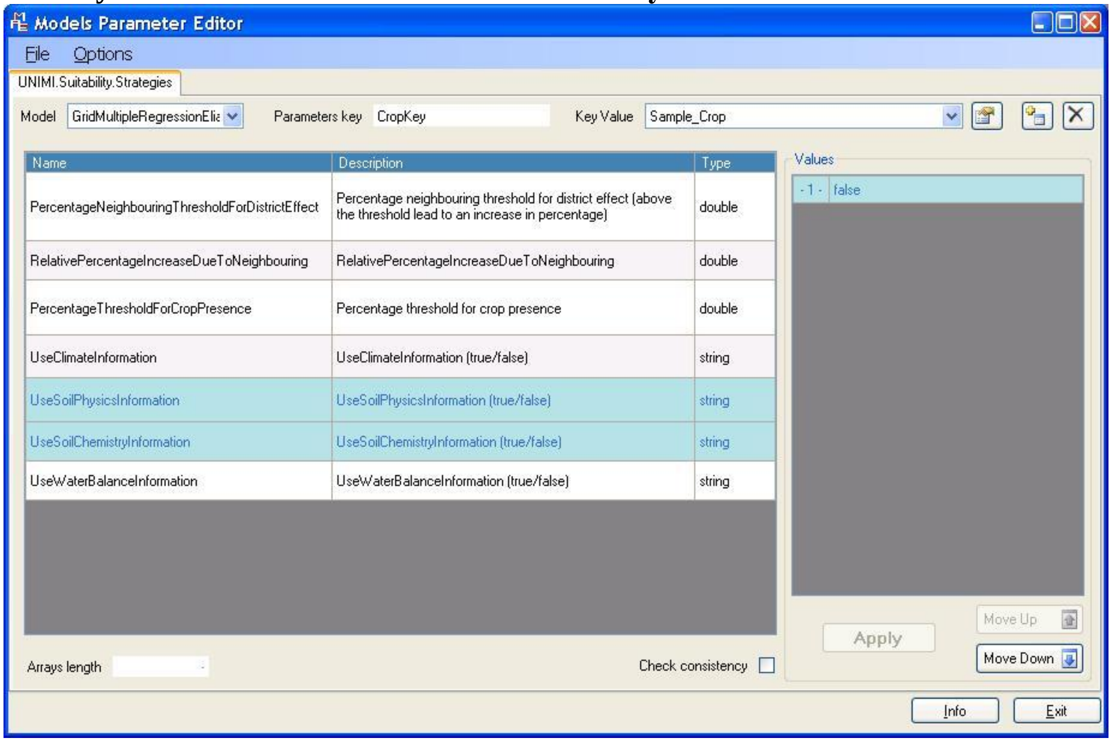

Figure I31. Screenshot of the model parameter editor showing a configuration where Use Climate Information, Use Soil Physics Information and Use Soil Chemistry Information are set to "false"

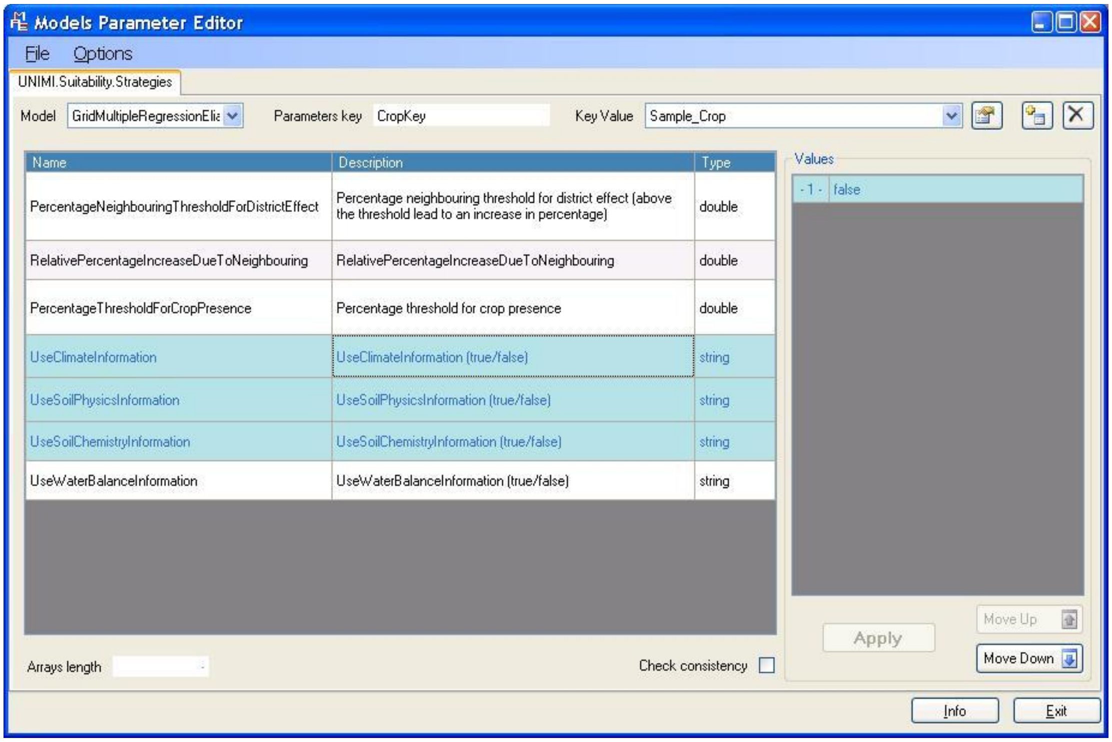

Figure I32. Test results of the application of the multiple regression approach based on the Eliasson and others (2010) regressors, mapping percentage of crop presence: (A) all categories of regressors (climate, soil physics, soil chemistry, water balance) used; (B) water balance regressor not used; (C) soil physical and chemical information not used; (D) only water balance regressor used

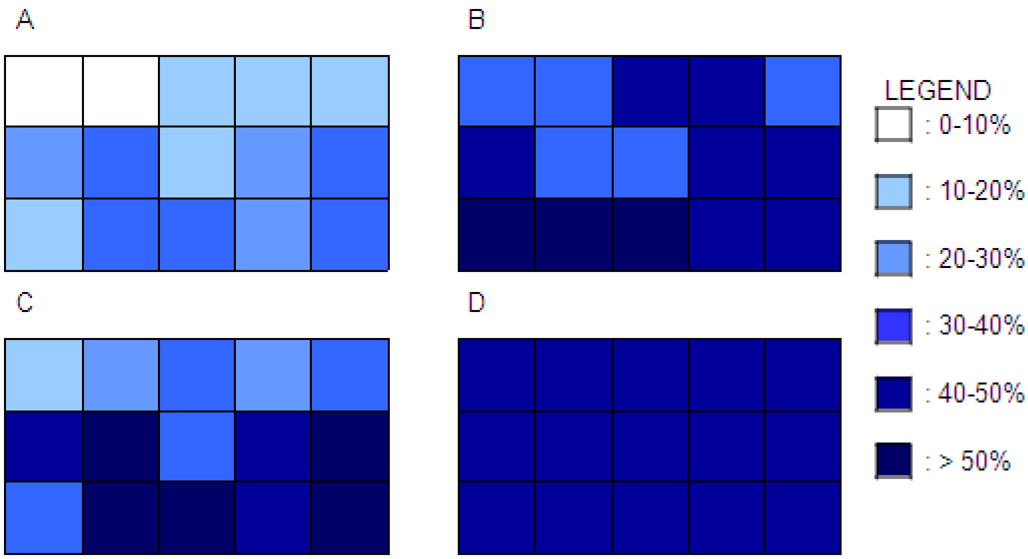

Figures I33–I34 show how the percentage of crop percentage changes when the district criterion is applied.

Figure I33. Screenshot of the model parameter editor showing a configuration where PercentageNeighbouringThresholdForDistrictEffect parameter is set to 75% and RelativePercentageIncreaseDueToNeighbouring is set to 10% and the district criterion is activated

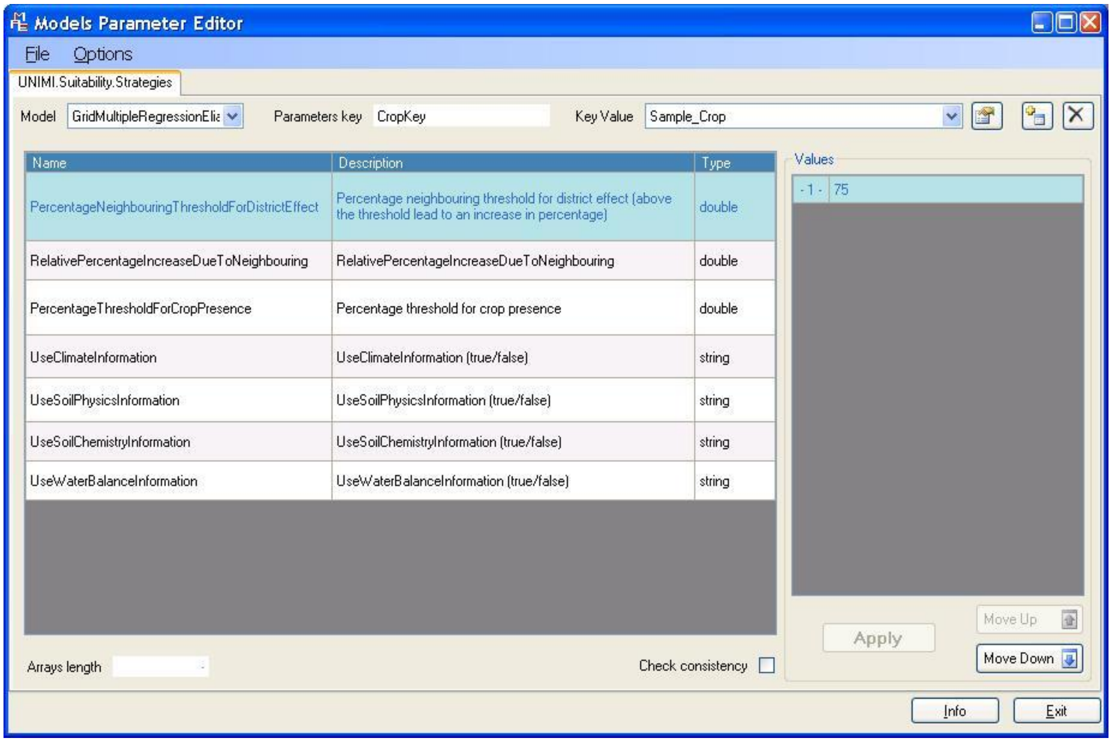

Figure I34. Test results of the application of the multiple regression approach based on the Eliasson and others (2010) regressors, mapping percentage of crop presence

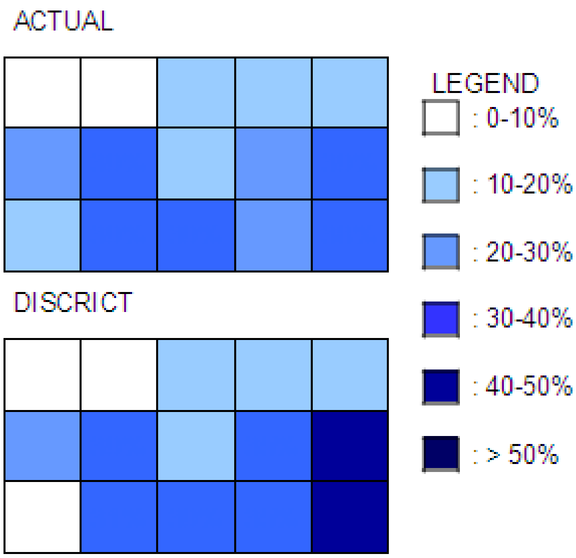

Note: For actual, all categories of regressor are used; for district, all categories of regressors are used and the district criterion is applied.

The district criterion increased the percentages of crop presence in the cells surrounded by others where the same crop is present above a threshold.

Adaptation strategies

Crop assessment studies must take into account adaptation potential and quantify the degree to which negative impacts can be minimized through management in order to be credible. Adaptation strategies can be subdivided into two groups: autonomous/short-term adaptations and planned/long-term adaptations (Tubiello and others 2009; Bates and others 2008; Olesen and Bindi 2002). Responses implemented by farmers, rural communities, or farmer organizations, taking into account real or perceived climate change, to optimize production without major system changes, pertain to the former group; while structural changes guided by interventions at the regional, national, or international levels, which involves other sectors (such as policy and research), are planned/long-term adaptations (Carpani and others 2011; Biesbroek and others 2010). We focused on building agromanagement rules for semiautomatic adaptation programs, and specifically on three main autonomous adaptation strategies: shifting the sowing period of the four simulated crops, changing the irrigation water volumes, and testing the performance of three varieties with different crop cycle length.

Sowing

According to Tubiello and others (2000) and Torriani and others (2007), early sowing for summer crops has positive effects on yield levels. However, Ouda and others (2009) demonstrated that an early sowing for maize increased season crop length, thus enhancing the irrigation crop requirements, which reduced water use efficiency under the tested climate change scenarios. The rules currently implemented in the CRA.AgroManagement component for setting a sowing event are described below:

RuleAirTemp

Trigger event based on a relative dates window, a rotation year, or a day counter based on daily average air temperature. If the rule is not triggered during the time window and the parameter DoItAnyWay is set to true, trigger the rule the last day of the window (figure I35).

Figure I35. RuleAirTemp object model diagram showing the parameters needed by this rule

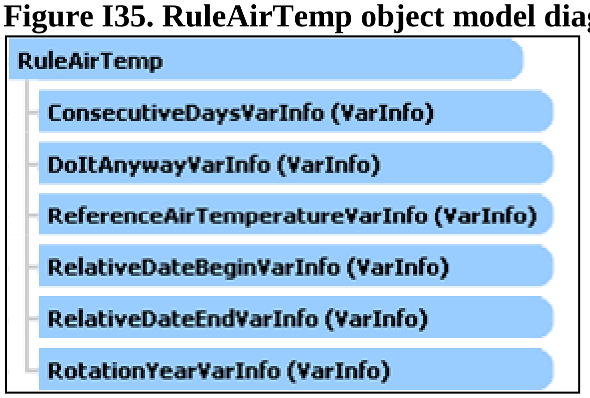

RuleDate

Triggers an event when a relative date and rotation year is reached (figure I36).

Figure I36. RuleDate object model diagram showing the parameters needed by this rule

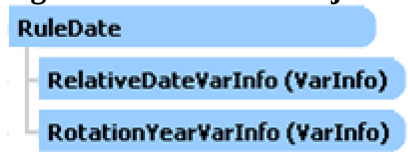

RuleDatesWindow

Triggers an event based on a relative dates window, a rotation year, or a day counter between events. The day counter restarts each time the rule is met (figure I37).

Figure I37. RuleDatesWindow object model diagram showing the parameters needed by this rule

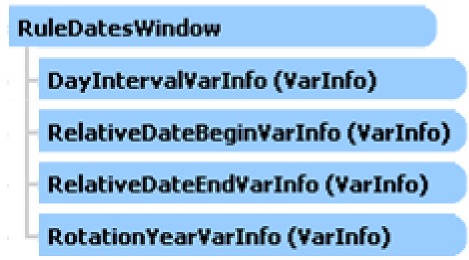

RuleDatesWindowNoRain

Triggers an event based on a relative dates window, a rotation year, a day counter between events, or a counter for no rainfall. The day counter restarts each time the rule is met, and the rain counter restarts when there is a rainfall event (figure I38).

Figure I38. RuleDatesWindowNoRain object model diagram showing the parameters needed by this rule

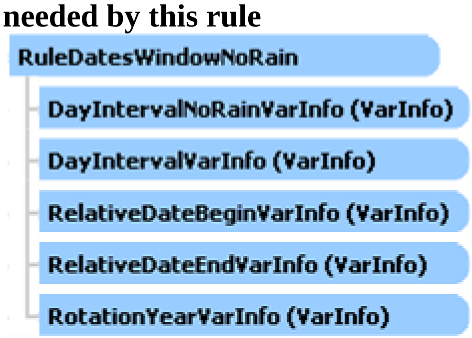

RuleSoilTempLayer

Rule based on a window date and upper layer soil temperature (figure I39).

Figure I39. RuleSoilTempLayer object model diagram showing the parameters needed by this rule

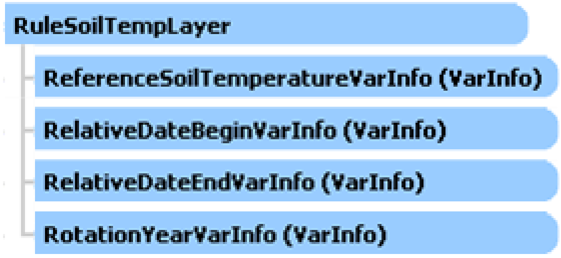

The impact associated with these rules for sowing is CropPlanting, which requires the name of the crop and the planting depth (figure I40).

Figure I40. CropPlanting object model diagram showing the parameters needed by this impact

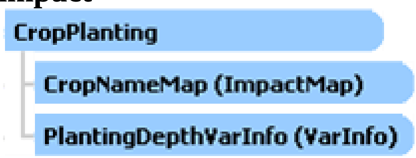

Irrigation

For the second adaptation strategy, Ouda and others (2009) noted that irrigation schedule could reduce yield losses and increase water use efficiency without adding irrigation water. This finding emphasizes the critical need to use improved irrigation management practices. These practices could reduce irrigation water losses, enhance plants growth potentialities, and increase final yield, especially under climate change conditions.

The rules currently implemented in the CRA.AgroManagement component for setting an irrigation event are described below.

RuleIrrigatePAW

Trigger irrigation within a time window, for a maximum number of times, if plant available water gets below a given threshold in a soil layer of chosen depth on a specific rotation year (figure I41).

Figure I41. RuleIrrigatePAW object model diagram showing the parameters needed by this rule.

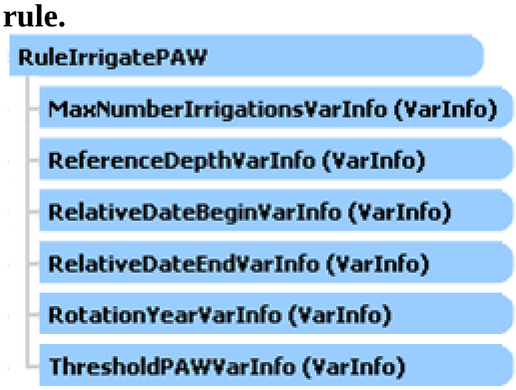

RulePAWOnce

Trigger irrigation within a range of date, once, if plant available water gets below the upper threshold and above the lower threshold in a soil layer of chosen depth, on a specific rotation year. If rule is not triggered during the time window and parameter DoItAnyWay set to true, trigger the rule the last day of the window (figure I42).

Figure I42. RuleIrrigatePAWOnce object model diagram showing the parameters needed by this rule

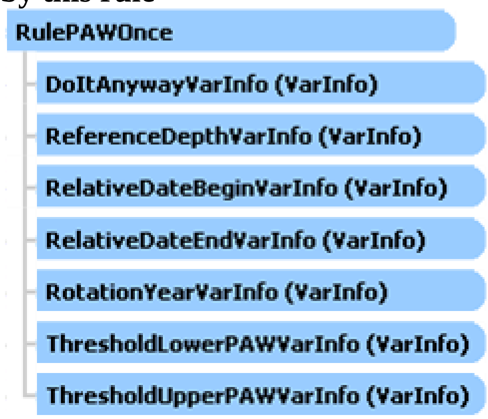

The impact associated to these rule for sowing is IrrigationSimple, which requires the irrigation type and the irrigation volume (figures I43).

Figure I43. IrrigationSimple object model diagram showing the parameters needed by this impact

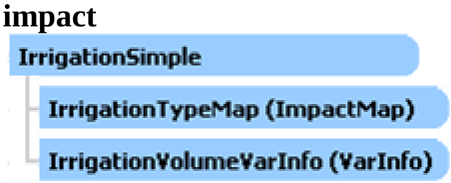

Crop cycle length

Technological advances in production, including crop improvements through breeding (Sinclair and Muchow 2001; Duvick 2005) or planting varieties with higher water use efficiency could reduce yield losses to minimal.

This study focused on crop cycle length by developing parameter sets for three varieties for each crop, with short, medium, and long crop cycles.

After the parameterization of the intermediate variety for each crop (see also section v of this report), we have built other two varieties in which the growing degree-days needed to reach each phenological phase are changed by ±20%. After this setting, these new varieties were tested under the same conditions in which the intermediate one was calibrated in order to verify their capability to reach the maturity stage under current climate scenario.

Figures I44–I48 show how to use the CRA.AgroManagement component implemented in the AZS-BioMA model for evaluating the impact of alternative management scenarios to define adaptation strategies.

Figure I44. Agro Management configuration generator interface showing how to set an agro management rule (a rule based on a relative date in this example)

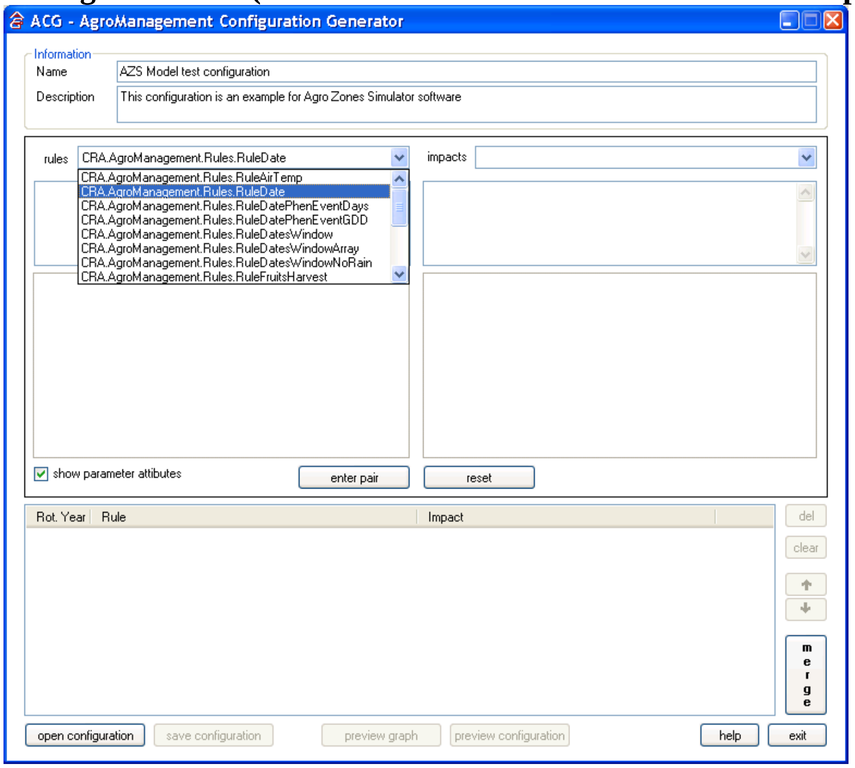

Figure I45. Agro Management configuration generator interface showing how to set an agro management impact (crop planting in this example)

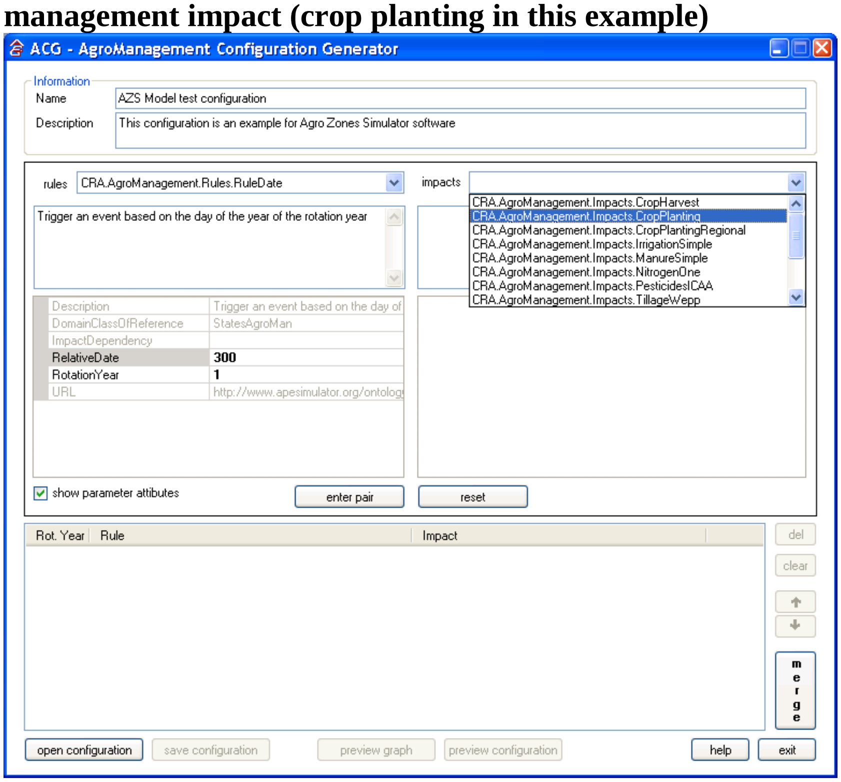

Figure I46. Agro Management configuration generator interface showing how to plan an irrigation set of rules based on soil water content

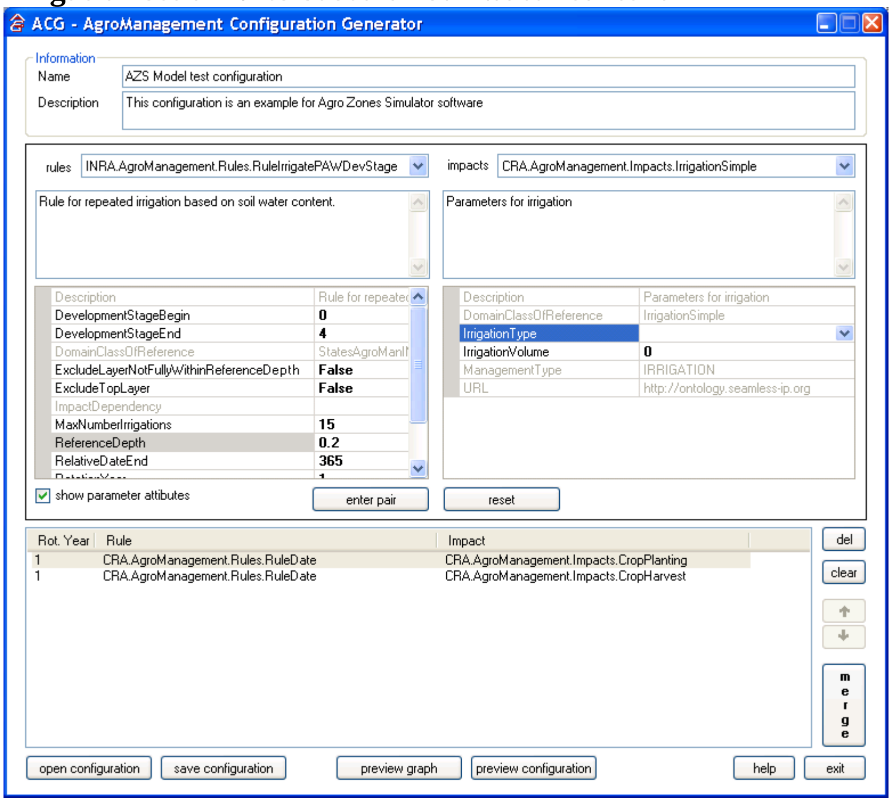

Figure I47. Available options for setting an irrigation event

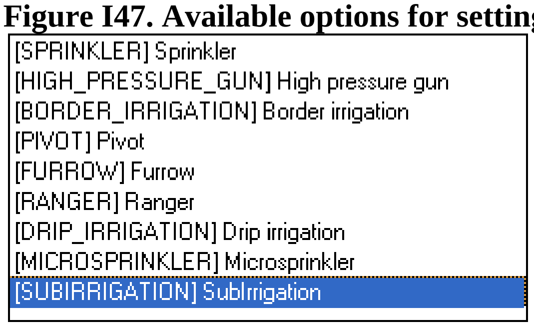

Figure I48. Agro Management configuration generator interface showing the diagram of the sample configuration built

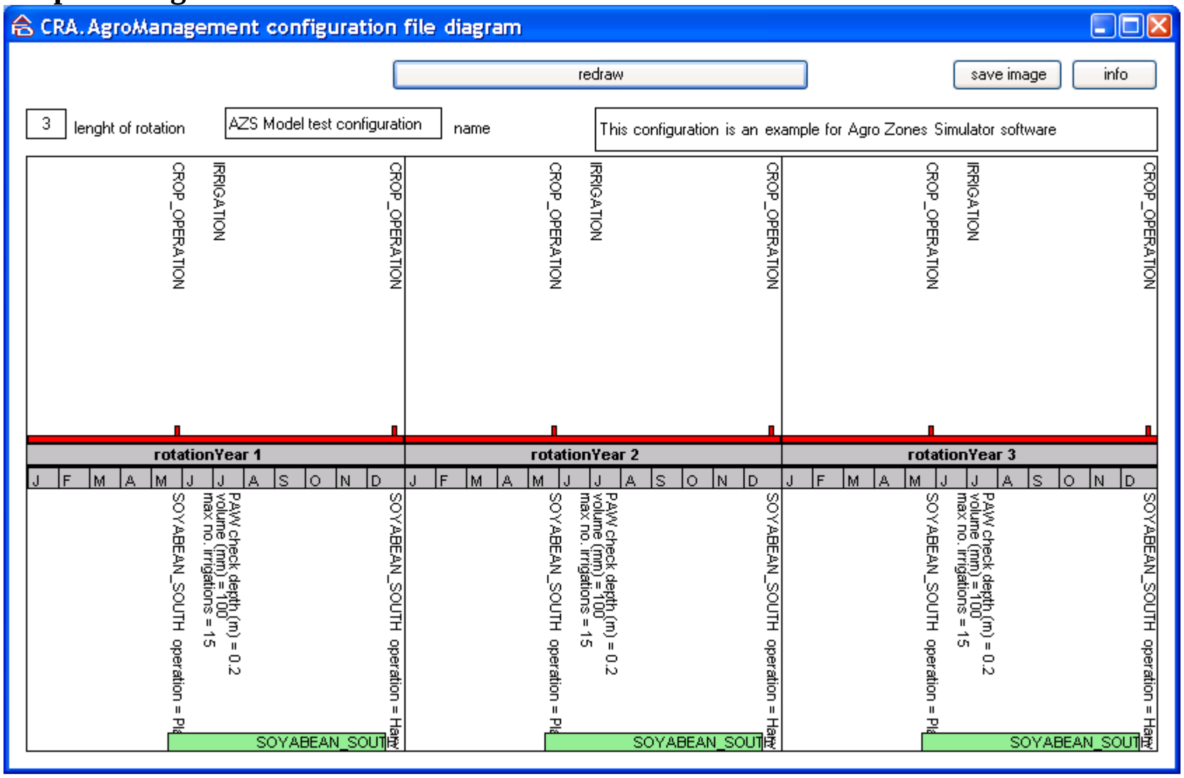

AZS-BioMA: System set-up

Calibration and validation, reference data

The modeling solutions within AZS-Bioma were calibrated for the four simulated crops (wheat, maize, soybean, and rice) before introducing them into the BioMA simulation platform, in order to test their behavior at diverse South American sites. For each crop, different areas were chosen to simulate crop development and growth in the grid cells where the fraction of crop coverage is maximum (source Interim Report – Vegetation Data Set – Crop masks; Ref. 4) and to maximize the spatial heterogeneity in terms of latitude and climatic conditions. The selected areas for the four crops are circled in figure I49.

Figure I49. Crop distribution of the four simulated crops, with circles indicating areas selected for the calibration of AZS-Bioma modeling solutions

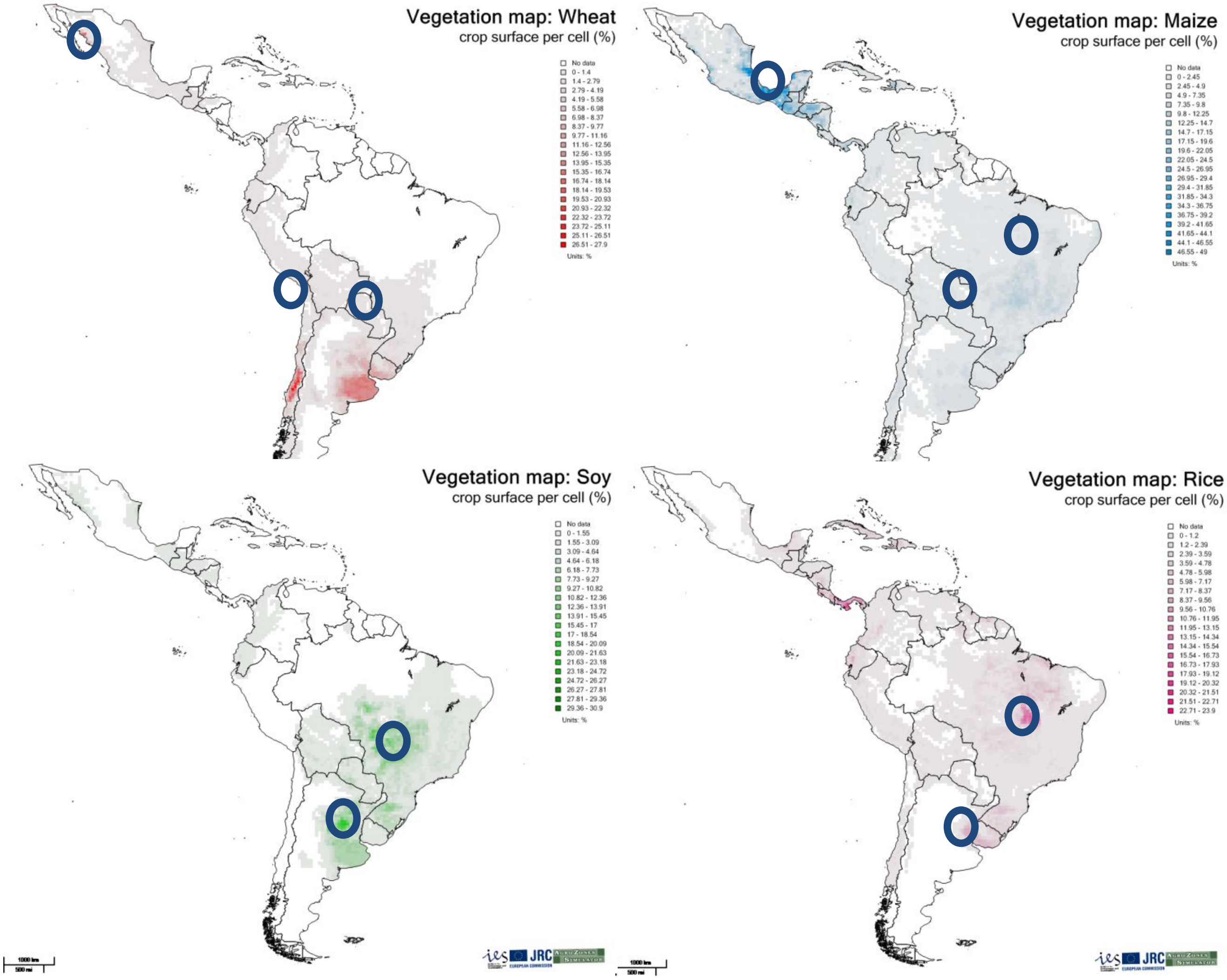

For each area, six grid cells were extracted from the climate database with weather series of 10 years (1990–99). Before running the modeling solutions, the meteorological files were analyzed to obtain information about the inner climatic variability of the sample cells. The results are shown in the subsequent sections, one for each simulated crop.

Then, an extensive literature review was undertaken to understand the agricultural management practices in the selected areas and to learn the mean values of yield, leaf area index, and sowing and harvest dates for each simulated crop (table I3).

Table I3. Reference data used for the calibration of crop models parameters describing morphological and physiological features of three groups of varieties for each crop

Crop	State	Latitude	Sowing	Harvest	Leaf area index	Yield (t/ha)	References
Wheat	Argentina	37°S	June 27	December 8			Scian and others 2005
					4–6.7		Golberg and others 1991
					5–6.5		Brisson and others 2001
			June 12			6	Mendez and others 2007
	Chile	33–37°S	June 17; June 22			5–6	Campillo and others 2010
					5		Acevedo and others 2006
				December–January		5.2–6.7	Acevedo and others 2009
			August 20; September 1				Lizana and others 2009
	Mexico	27°N	November 14; December 17	April–May	5		Rodriguez and others 2007
						8	Lobell and others 2008
Maize	Argentina	37°S				15	Otegui and others 1996
			September; early October				Otegui and others 1996
			September 24; October 6–8	Physiological maturity: March	6–8.8		Luque and others 2006
	Brazil	16°S			5.8		Franca, 1997
			October–December: for example, October 5–10	February 10–March 7			Bergamaschi and others 2007
						10	Andrioli and others 2009
	Mexico	17°N	June 28–30; July 11				Tinoco Alfaro and others 2008
			March 20; April 20; May 1–15			9–12	Avila Perches and others 2009
			April 1; May 8			11.8	Mendoza-Elos and others 2006
					7.4		Rodríguez and others 2007
			May 15	November 4			Amado Alvarez and others 1998
Soybean	Argentina	31°S			7		Canfalone and others 2002
					7		Bodrero, 2003
						5	Calviño and others 1999.
			October 1; January 10	March 12–June 2		5	Mercau and others 2007
						5.5	Maehler and others 2003.
	Brazil	16°S				4.4	Sinclair and others 2003
			November 11; November 22	March 21–27			Oya and others 2004
			October 15; October 30 November 15; November 30				Avila and others 2003
			November 20				Martorano and others 2004
				101–123 days after sowing			Borrmann and others 2009
			February 7; February 23	June 6–21	6.5		Souza and others 2009
Rice	Argentina	31°S	September;		6		Brizuela 2009

		November				
		October 10; October 28	March 7–30		11.5	Quintero 2009
					8.9	Torres 2009
Brazil	12°S			4–8		Guimaraes and others 2003
		November 1–6; December 5			5	Guimaraes 2008
		November 20				Pinheiro and others 1990
		October 1–15				Buzetti and others 2006
			February–May			Bragagnolo, 2006

Parameterization

The parameters of the CropSyst and WARM models (potential production) were calibrated, starting from the reference values included in the InterimReport (CropDataSet; Ref. 4) in order to obtain yield and leaf area index values comparable to those found in the literature for the actual climatic conditions. Table I4 lists the acronyms used for CropSyst model parameters, and table I5 lists the acronyms used for WARM model parameters.

Table I4. CropSyst parameters used to describe crop morphological and physiological features

Parameter	Unit	Acronym
Above ground biomass-transpiration coefficient	kPa kg m^{-3}	BTR
Light to above ground biomass conversion	g MJ^{-1}	LtBC
Optimum mean daily temperature for growth	°C	T_{opt}
Maximum water uptake	mm day^{-1}	$W_{up,max}$
Leaf water potential at the onset of stomatal closure	J kg^{-1}	W_{cr}
Specific leaf area	m^2 kg^{-1}	SLA
Stem/leaf partition coefficient	unitless	SLP
Leaf duration	°C-days	L_{dur}
Extinction coefficient for solar radiation	unitless	k_c
Evapotranspiration crop coefficient at full canopy	unitless	Et_{full}
Degree-days emergence	°C-days	GDD_{em}
Degree-days peak	°C-days	GDD_{peak}
Degree-days begin flowering	°C-days	GDD_{flo}
Degree-days begin grain filling	°C-days	GDD_{grain}
Degree days physiological maturity	°C-days	GDD_{mat}
Base temperature	°C	T_b
Cut-off temperature	°C	T_{cutoff}
Unstressed harvest index	unitless	UHI

Table I5. WARM parameters describing rice morphological and physiological features

Parameter	Unit	Acronym
Degree days from sowing to emergence	°C-days	GDD_{em}
Base temperature for development	°C	$T_{b,dev}$
Maximum temperature for development	°C	$T_{max,dev}$
Degree days from emergence to flowering	°C-days	GDD_{flo}
Degree days from flowering to maturity	°C-days	GDD_{mat}

Degree days from maturity to harvest	°C-days	GDD_{harv}
Radiation-use efficiency	g MJ^{-1}	RUE_{max}
Extinction coefficient for solar radiation	unitless	k_c
Base temperature for growth	°C	$T_{b,gro}$
Optimum T for growth	°C	$T_{opt,gro}$
Maximum T for growth	°C	$T_{max,gro}$
Specific leaf area at emergence	$m^2\ kg^{-1}$	SLA_{ini}
Specific leaf area end tillering	$m^2\ kg^{-1}$	SLA_{till}
Aboveground biomass partition to leaves at emergence	unitless	Rip*L*0
Leaf duration	°C-days	L_{dur}
Maximum panicle height	cm	$PanHeight_{max}$

The parameters listed in tables I4–I5 are those adjusted consistently with the results of the calibrations performed. Below, the results obtained for each simulated crop are presented. The figures show that the 12 sets of parameters proposed (three groups of varieties × four crops) allow the modeling solutions to simulate leaf area index and biomass data within the range of values found in the literature for the same conditions.

Wheat

The sample simulations for wheat were carried out in three areas: Mexico, Argentina and Chile. Figure I50 summarizes the climatic conditions (mean air temperature and global solar radiation data) for the six grid cells selected for testing the modeling solution. The test aims to reproduce the reference data on the wheat crop cycle, leaf area index, and yield (figure I51).

Figure I50. Representation of meteorological data for 1990–99 for Mexico, Argentina, and Chile for wheat calibration

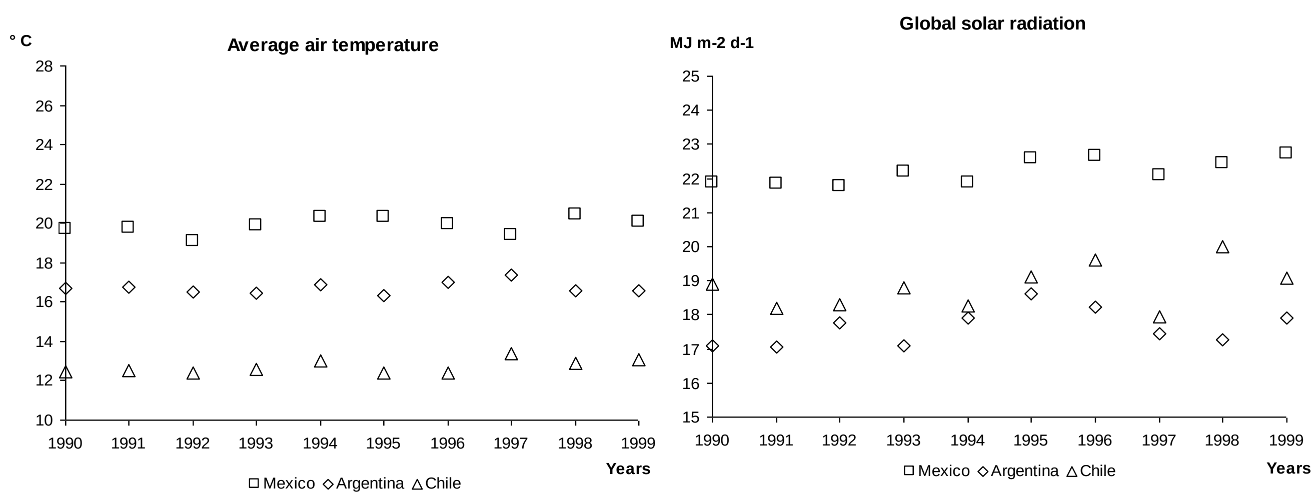

Table I5. Parameterizations adopted for wheat

Process	Parameter	Average cycle length	Short cycle length	Long cycle length
Thermal time accumulation	T_b	–1	–1	–1
	T_{cutoff}	20	20	20
Phenology	GDD_{em}	100	85	120
	GDD_{peak}	700	560	840
	GDD_{flo}	900	720	1,080
	GDD_{grain}	980	780	1,176
	GDD_{mat}	2,000	1,600	2,400
Growth	BTR	5	5	5
	LtBC	3	3	3
	SLA	25	25	25
	SLP	2.5	2.5	2.5
	T_{opt}	19	19	19
Transpiration	ET_{full}	1.05	1.05	1.05
	K_c	0.478	0.478	0.478
	$W_{up, max}$	9	9	9
Senescence	L_{dur}	600	600	600
Harvest	UHI	0.5	0.5	0.5

Figure I51. Reproducing the reference data about the wheat crop cycle, leaf area index, and yield for Mexico, Argentina, and Chile for wheat calibration

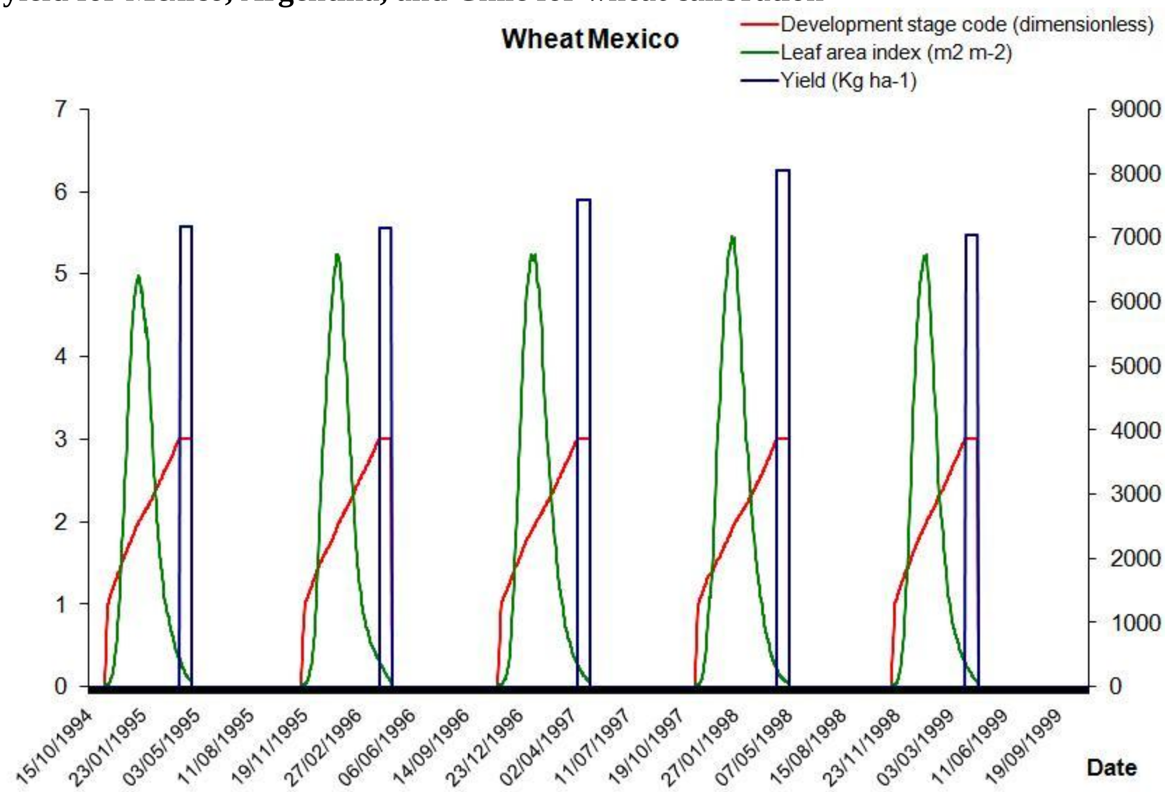

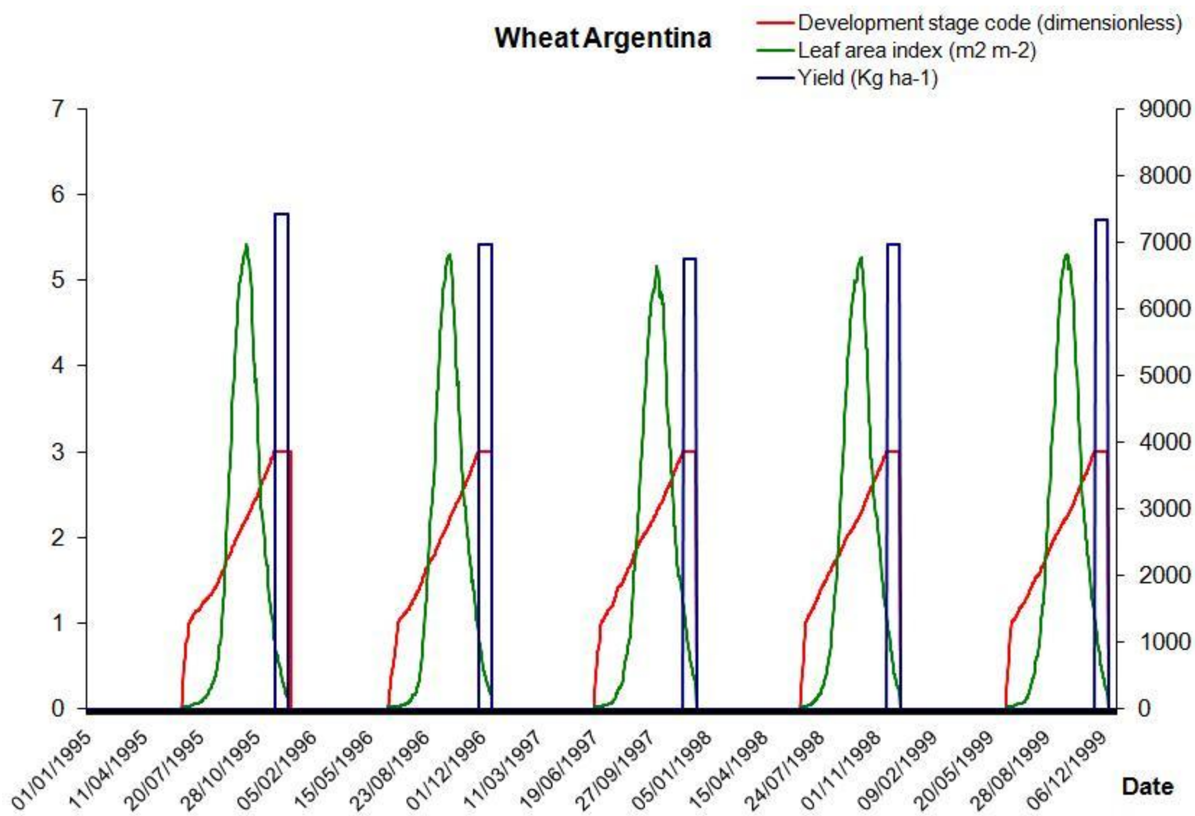
Wheat Argentina
Development stage code (dimensionless)
Leaf area index (m2 m-2)
Yield (Kg ha-1)
Date

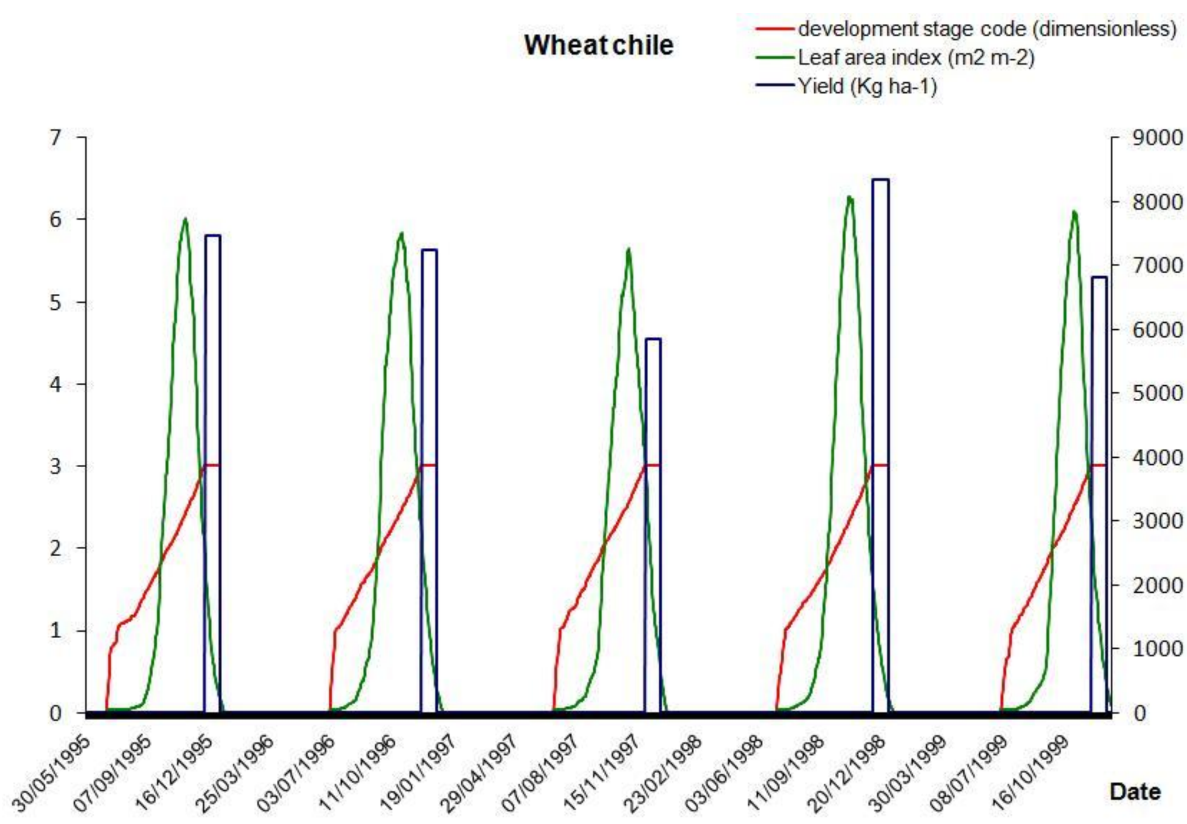
Wheat chile
development stage code (dimensionless)
Leaf area index (m2 m-2)
Yield (Kg ha-1)
Date

Maize

The sample simulations for maize were carried out in three areas: Argentina, Brazil, and Mexico. Table I6 and figure I52 summarize the climatic conditions (mean air temperature and global solar radiation data) for the six grid cells selected for testing the modeling solution. The test aims to reproduce the reference data on the maize crop cycle, leaf area index, and yield (figure I53).

Figure I52. Representation of meteorological data for 1990–99 for Argentina, Brazil, and Mexico for maize calibration

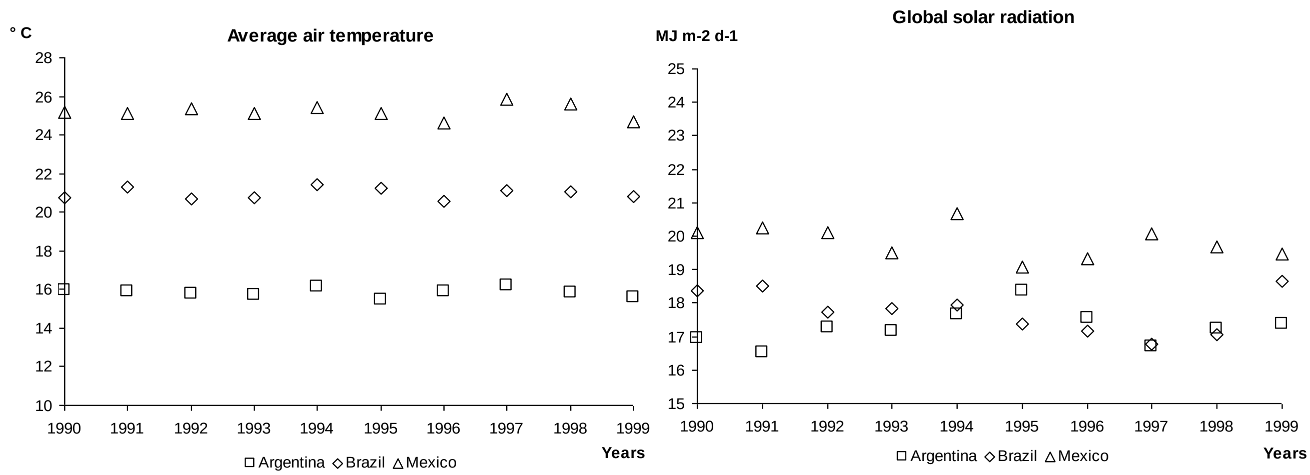

Table I6. Parameterizations adopted for maize

Process	Parameter	Average cycle length	Short cycle length	Long cycle length
Thermal time accumulation	T_b	8	8	8
	T_{cutoff}	34	34	34
Phenology	GDD_{em}	150	120	180
	GDD_{peak}	1020	816	1,140
	GDD_{flo}	950	760	1,224
	GDD_{grain}	1,124	900	1,348
	GDD_{mat}	1,900	1,520	2,280
Growth	BTR	8	8	8
	LtBC	4	4	4
	SLA	28	28	28
	SLP	3	3	3
	T_{opt}	22	22	22
Transpiration	ET_{full}	1	1	1
	K_c	0.47	0.47	0.47
	$W_{up, max}$	12	12	12
Senescence	L_{dur}	1,200	1,200	1,200
Harvest	UHI	0.43	0.43	0.43

Figure I53. Reproducing the reference data about the maize crop cycle, leaf area index, and yield for Mexico, Argentina, and Brazil for maize calibration

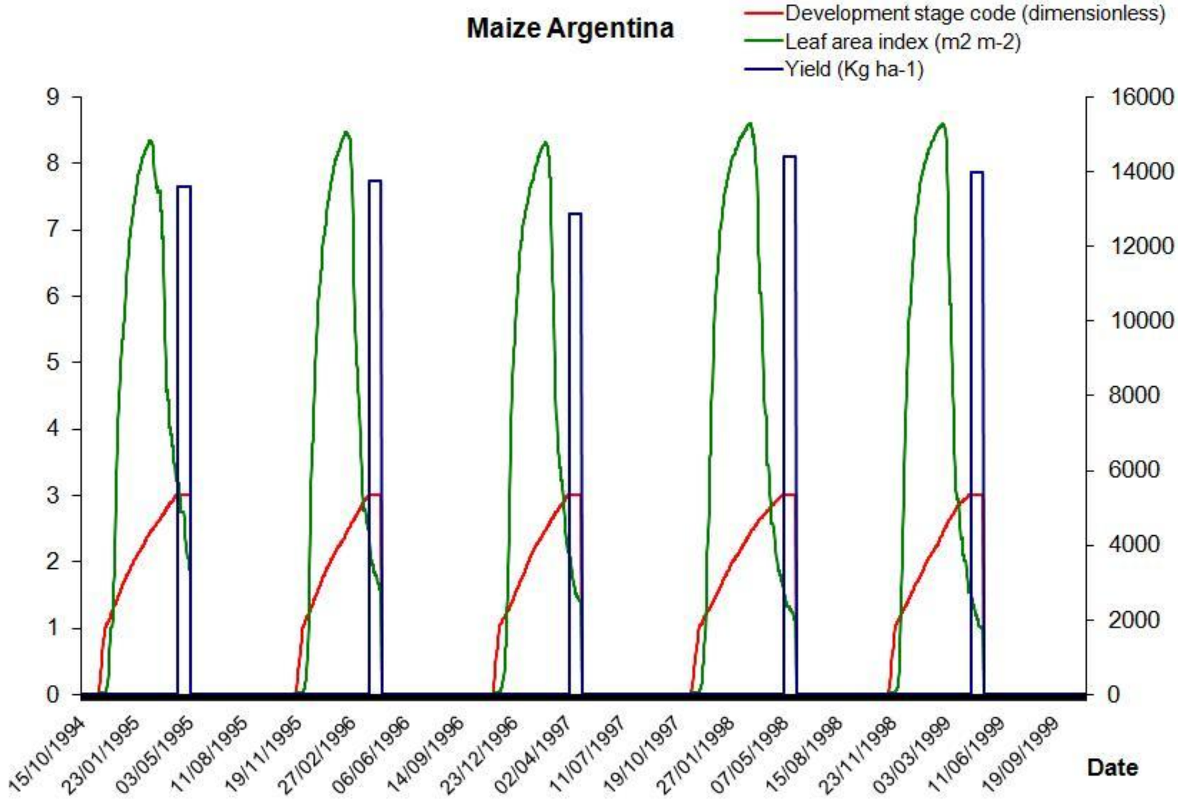

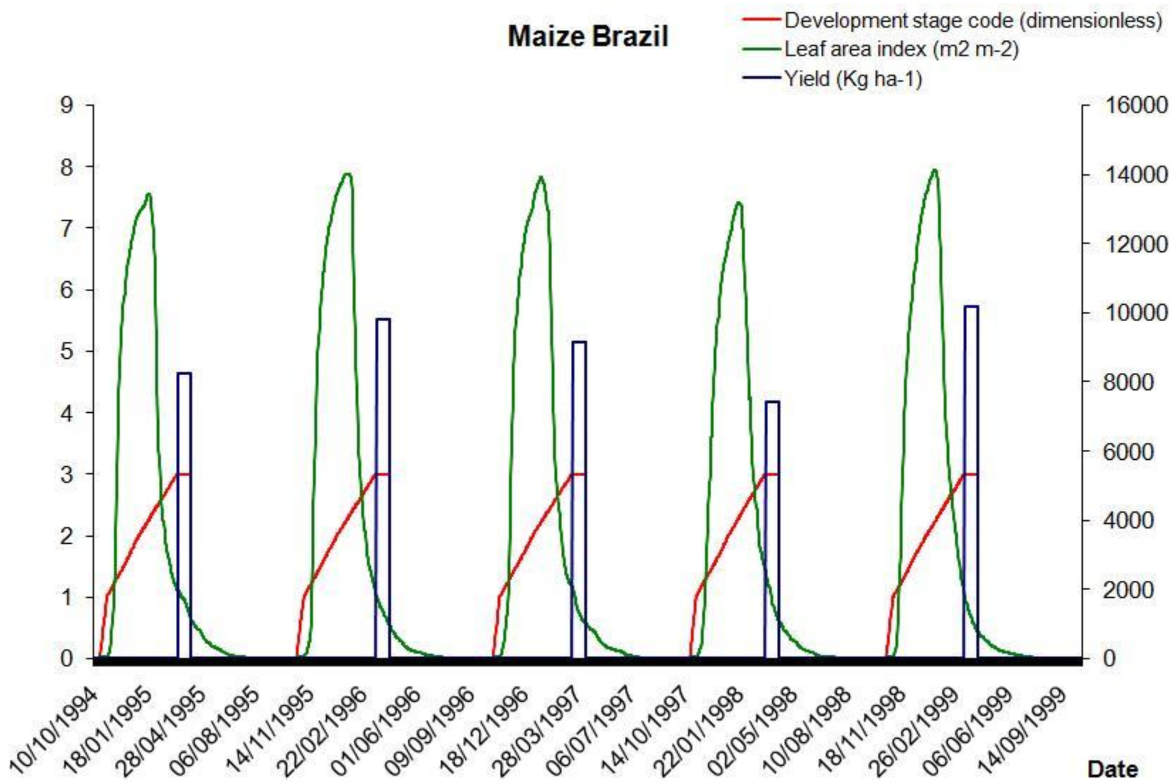

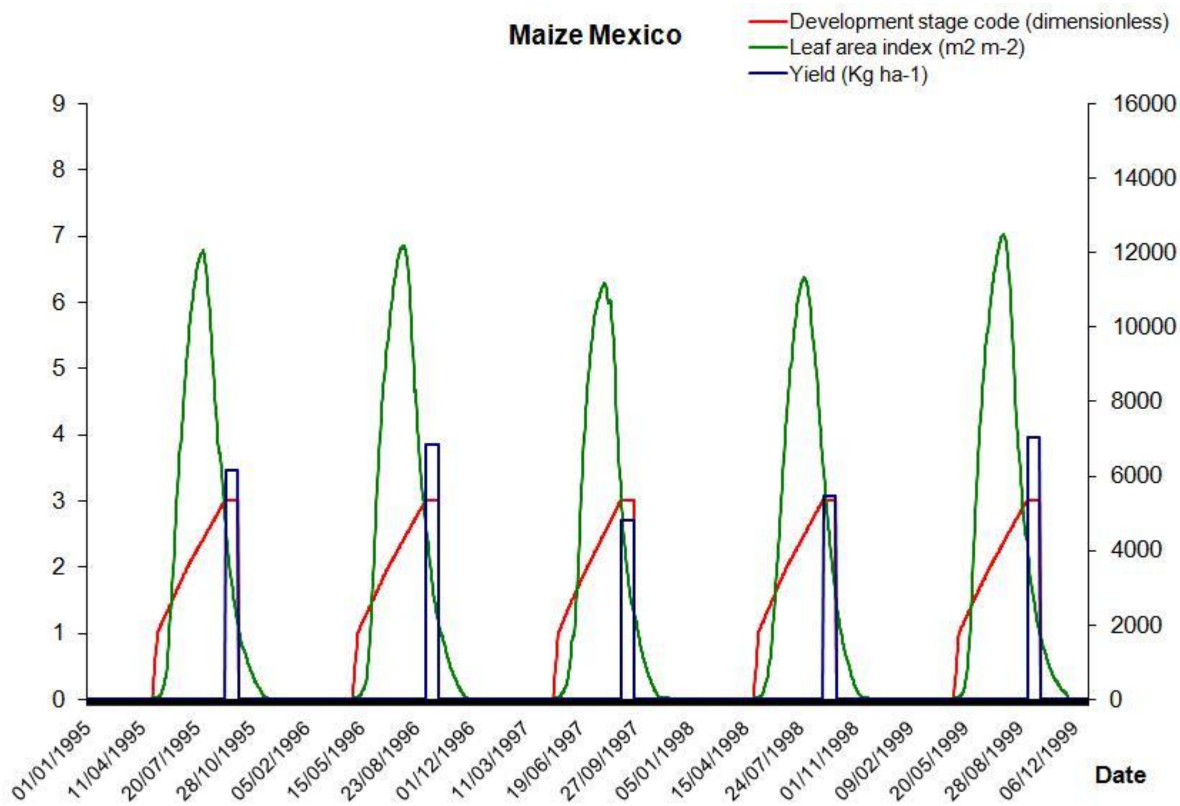

Soybean

The soybean sample simulations were carried out in two areas: Argentina and Brazil. Table I7 and figure I54 summarize the climatic conditions (mean air temperature and global solar radiation data) for the six grid cells selected for testing the modeling solution. The test aims to reproduce the reference data on the soybean crop cycle, leaf area, and yield (figure I55).

Figure I54. Representation of meteorological data for 1990–99 for Argentina and Brazil for soybean calibration

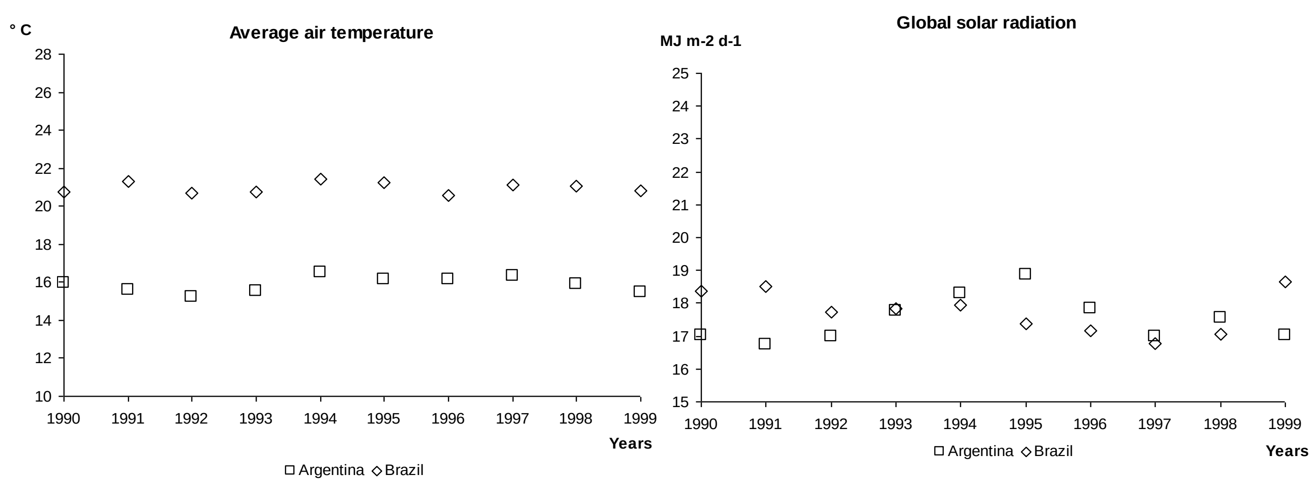

Table I7. Parameterizations adopted for soybean

Process	Parameter	Average cycle length	Short cycle length	Long cycle length
Thermal time accumulation	T_b	6	6	6
	T_{cutoff}	25	25	25
Phenology	GDD_{em}	150	120	180
	GDD_{peak}	1040	832	1,248
	GDD_{flo}	850	680	1,020
	GDD_{grain}	930	744	1,116
	GDD_{mat}	1,860	1488	2,232
Growth	BTR	5	5	5
	LtBC	2.5	2.5	2.5
	SLA	28	28	28
	SLP	3	3	3
	T_{opt}	22	22	22
Transpiration	ET_{full}	1	1	1
	K_c	0.45	0.45	0.45
	$W_{up, max}$	10	10	10
Senescence	L_{dur}	900	900	900
Harvest	UHI	0.43	0.43	0.43

Figure I55. Reproducing the reference data about the soybean crop cycle, leaf area index, and yield for Argentina and Brazil for soybean calibration

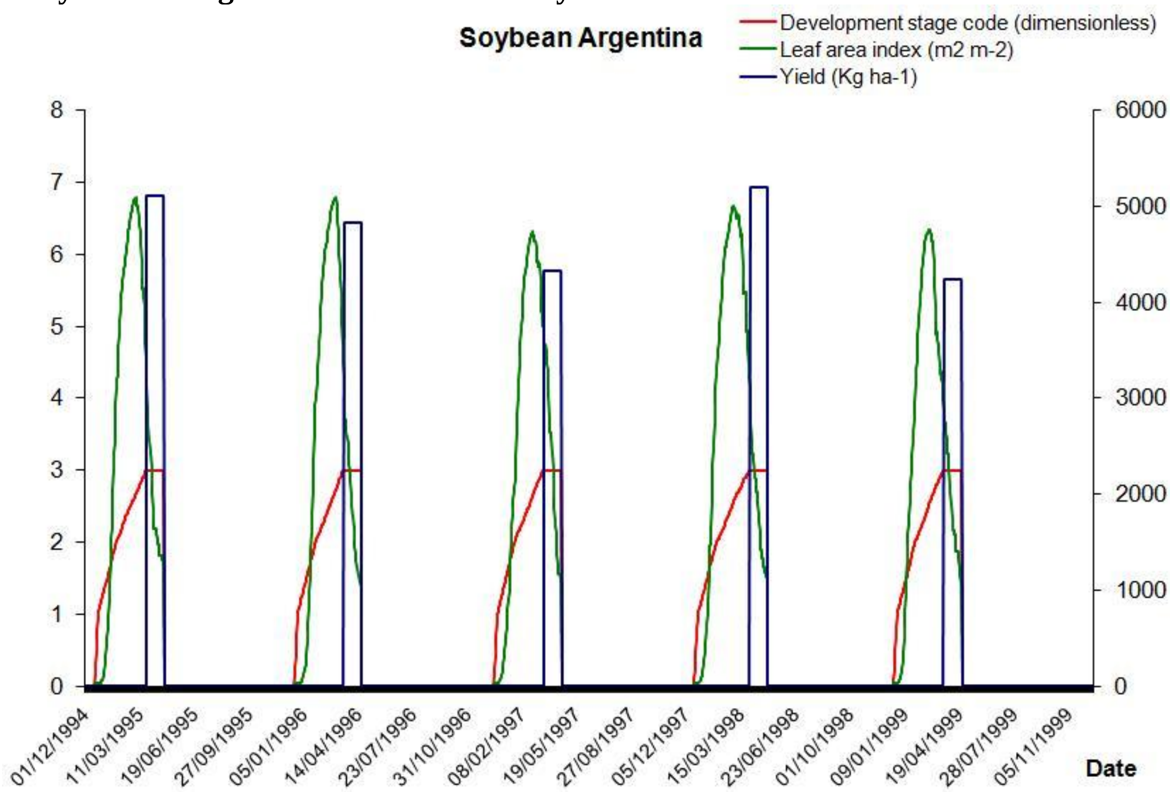

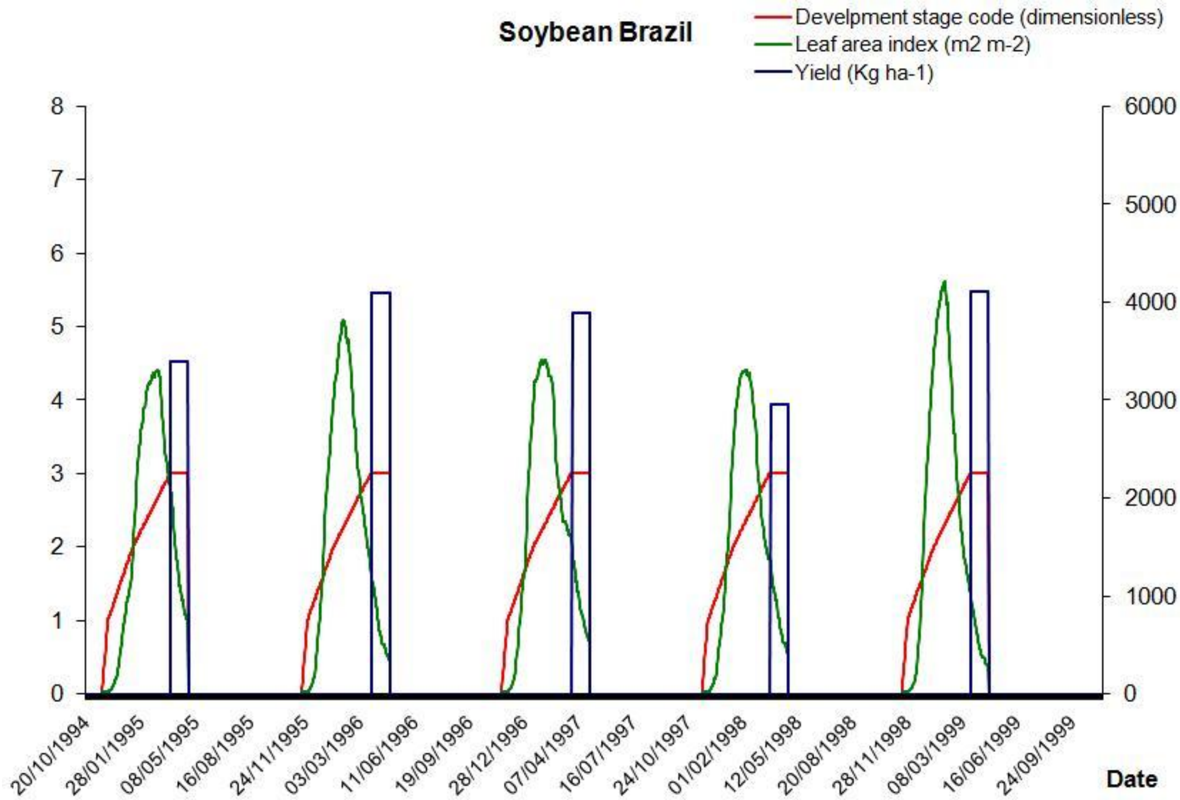

Rice

The results of the sample simulations carried out for reproducing the reference data about rice crop cycle, leaf area index, and yield are reported in the following figures. Figure I56 and table I8 summarize the climate conditions (mean air temperature and global solar radiation data) for the six grid cells chosen for testing the modeling solution (figure I57).

Figure I56. Representation of meteorological data for 1990–99 for Argentina and Brazil for rice calibration

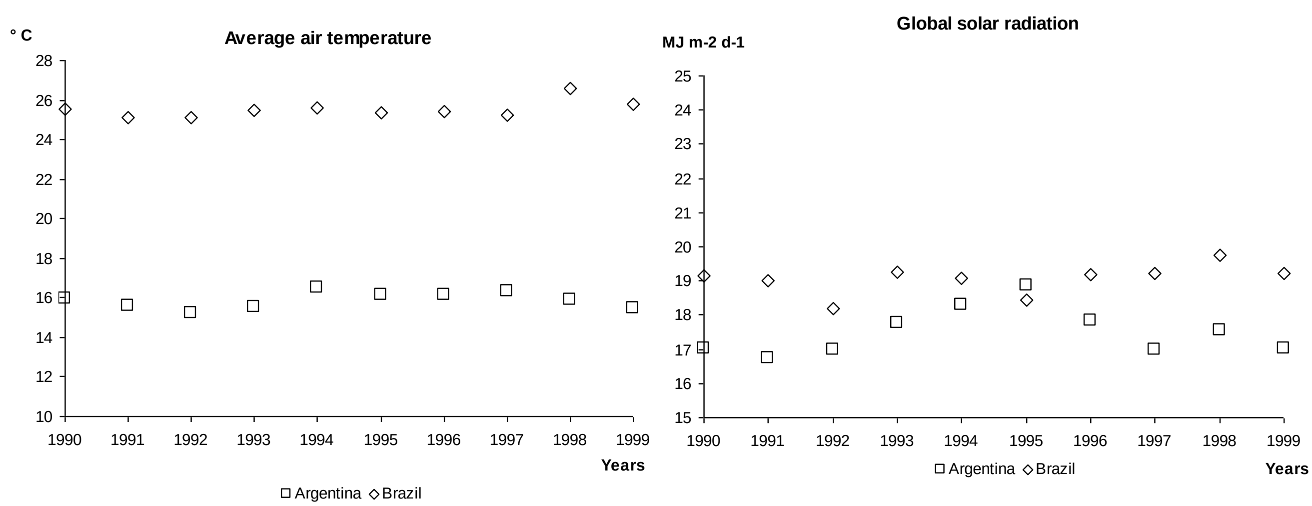

Table I8. Parameterizations adopted for rice

Process	Parameter	Average cycle length	Short cycle length	Long cycle length
Thermal time accumulation	$T_{b,dev}$	12	12	12
	$T_{max,dev}$	42	42	42
Phenology	GDD_{em}	70	56	84
	GDD_{flo}	800	640	960
	GDD_{mat}	430	344	516
	GDD_{harv}	80	64	96
Growth	RUE_{max}	2.8	2.8	2.8
	SLA_{ini}	27	27	27
	SLA_{till}	18	18	18
	Rip*L*0	0.6	0.6	0.6
	$T_{b,gro}$	42	42	42
	$T_{max,gro}$	11	11	11
	$T_{opt,gro}$	27	27	27
	$PanHeight_{max}$	100	100	100
Transpiration	K_c	0.5	0.5	0.5
Senescence	L_{dur}	600	600	600

Figure I57. Reproducing the reference data about the rice crop cycle, leaf area index, and yield for Argentina and Brazil for rice calibration

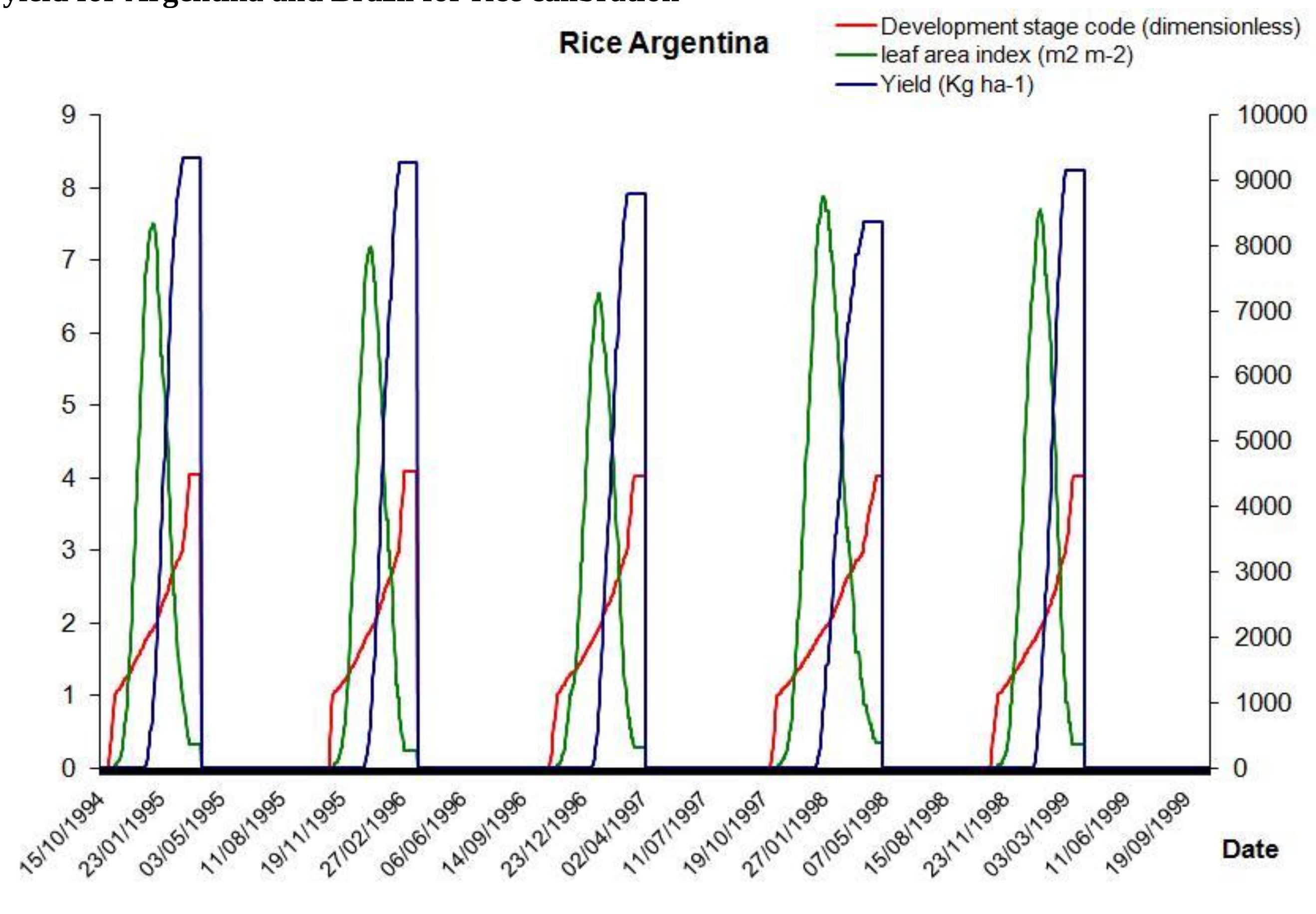

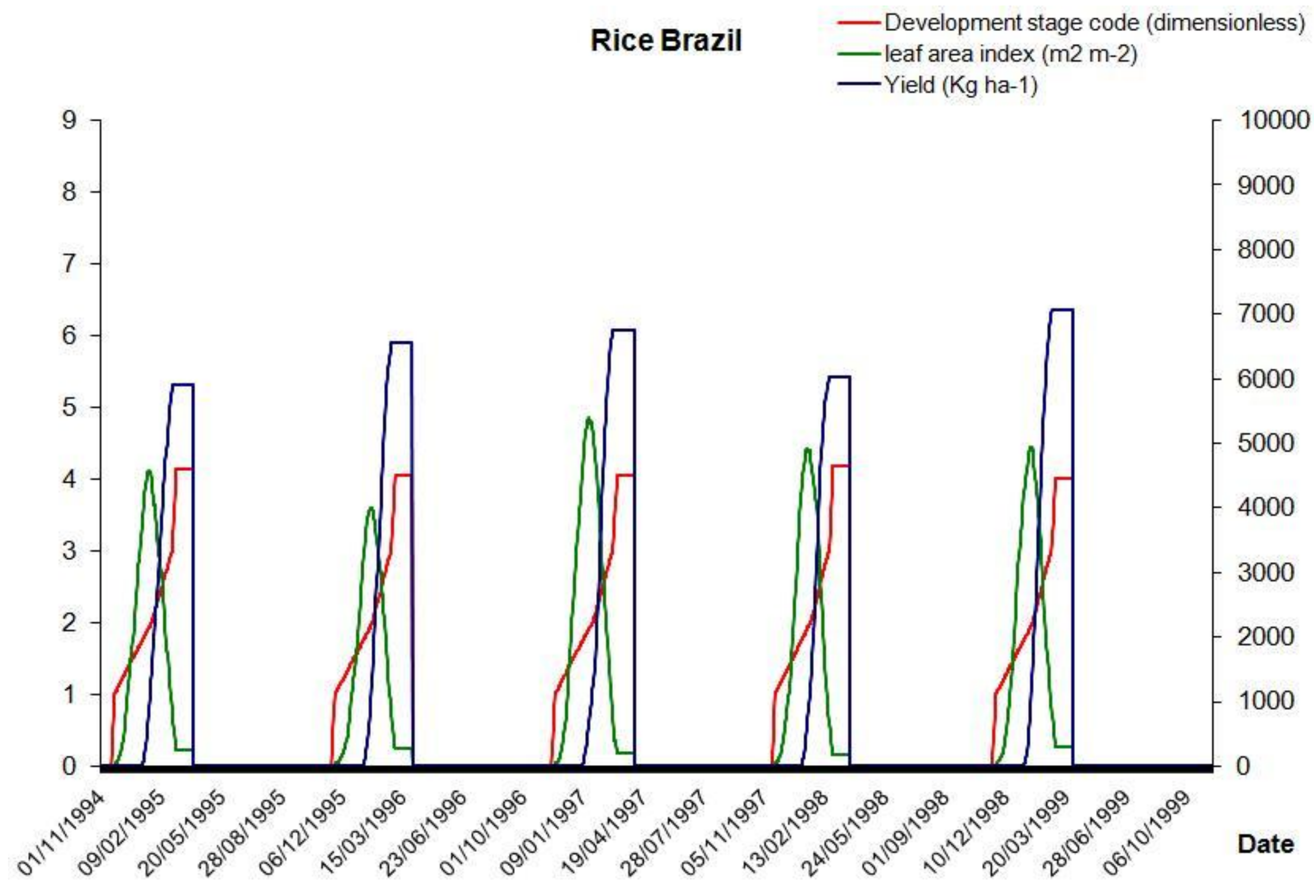

Pathogens

Cercospora zeae-maydis (**gray leaf spots)**

Symptoms: Rectangular, tan-colored lesions that are contained within leaf margins. As lesions mature they assume a graying cast due to sporulation of the fungi. Under severe disease pressure, entire leaves can be blighted and lesions can develop on cob sheaths (Carson 1999).

Epidemiology: *Cercospora zeae-maydis* is an airborne polycyclic fungus. The windborne spores, named conidia, provide primary inoculum to infect susceptible hybrids of maize, when the environmental conditions are favorable. The disease can develop when the optimum air temperature ranges from 22°C to 30°C (Latteral and others 1983) and when relative humidity is greater than 90%, while the conidia need at least six hours of continuous leaf wetness at temperatures between 18°C and 25°C for germination (Rupe and others 1982). The pathogen can penetrate the host leaf stomata through the development of an infection hook. After infection, flecks can appear within nine days, while the mature lesions become visible and necrotic in 14 or 21 days, marking the beginning of the intensive phase of sporulation. At this stage, high relative humidity can promote a secondary cycle of infection (Ward and others 1998). This foliar disease, if not treated, can result in a premature senescence and loss in photosynthetic leaf area, causing severe yield losses, that can range from 0% to 60% in countries where the disease is endemic (Ward and others 1996).

Geographic distribution: Figure I58 shows the geographic distribution of *Cercospora zeae-maydis.*

Figure I58. South American countries in which *Cercospora zeae-maydis* is present

Parameters:

Parameter	Unit	Value	Source
Maximum air temperature for infection (T_{max}inf)	°C	36	2; 4
Minimum air temperature for infection (T_{min}inf)	°C	10	5
Optimum air temperature for infection (T_{opt}inf)	°C	20–30; 22–30; 25–30; 24.8	2; 3; 4; 7; 8
Minimum wetness duration for infection (WDmin)	hours	6	3; 5
Maximum wetness duration for infection (WDmax)	hours	9	3; 5
Maximum air temperature for incubation (T_{max}inc)	°C	35	5
Minimum air temperature for incubation (T_{min}inc)	°C	10	5
Optimum air temperature for incubation (T_{opt}inc)	°C	18–25	5
Minimum incubation duration (MID)	days	9	3
Maximum air temperature for latency (T_{max}lat)	°C	35°	5
Minimum air temperature for latency (T_{min}lat)	°C	10	5
Optimum air temperature for latency (T_{opt}lat)	°C	18–25	5
Minimum latency duration (MLD)	days	14 (susceptible hybrids); 16 (moderately resistant hybrids)	2; 3; 9
Maximum air temperature for infectiousness (T_{max}ness)	°C	35; 32	2;
Minimum air temperature for infectiousness (T_{min}ness)	°C	20	2
Optimum air temperature for infectiousness (T_{opt}ness)	°C	27.2	2
Maximum infectiousness duration (MSD)	days	9	6
Maximum air temperature for sporulation (T_{max}spor)	°C	35; 32	2;
Minimum air temperature for sporulation (T_{min}spor)	°C	20	2
Optimum air temperature for sporulation (T_{opt}spor)	°C	27.2; 25	2;
Minimum rel. humidity for sporulation (RH_{min}spor)	percent	58; 65	1; 3
Rain for 50% detachment (Rain50)	mm day^{-1}	2.5	10
Maximum catch rain ($Rain_{max}$)	mm day^{-1}	6	10

Minimum wind for detachment (W_{min})	m s^{-1}	1.3 (dehydrated spores)	1
Wind for 50% detachment (W50)	m s^{-1}	2.4	1
Spores at Maximum wind for detachment (W_{max}spor)	percent	0.8	10
Maximum wind for detachment (W_{max})	m s^{-1}	4.7 (hydrated spores)	1
Wetness duration D50 (WD50)	hours	5	10

1: Lepaire and others 2003.
2: Paul and others 2005.
3: Ward and others 1998.
4: Beckman and others 1983.
5: Rupe and others 1982.
6: Castor and others 1977.
7: Li and others 2007.
8: Latteral and others 1983.
9: Ringer and others 1995.
10: Model default.

Phakopsora pachyrizi (soybean rust)

Symptoms: Infection begins on the lower first leaves of plants and appears as chlorotic or mosaic-like areas. The lesions, because of the sporulation, merge forming larger pustules characterized by a tan or red-brown color. With the progress of maturation, the lesions may become black, due to the formation of layers of teliospore in the pustules (Rupe and others 2008).

Epidemiology: Soybean rust is an airborne polycyclic fungus. Urediniospores of *Phakopsora pachyrizi* are transported readily by air currents and can be carried hundreds of miles in a few days. The conditions for the development of infection depend on the host vulnerability and on environmental suitability. Rust spores are able to penetrate the plant cells directly rather than through natural openings or through wounds in the leaf tissue. Generally, infection occurs when leaves are wet, the relative humidity is 75–80%, and temperatures are 12–27°C (Jarvie 2009), with an optimum of 23°C (Magarey and others 2005). At this temperature, some infection occurs in 6 hours of leaf wetness, but 12 hours are optimal (Rupe and others 2008). After infection, lesions can appear within 9 days, and the spores are produced in 10–21 days (Kawuki and others 2003). Soybean rust pathogen will go through many cycles of spore production, spore release, and new infections in a growing season, causing severe yield losses and complete plant defoliation.

Geographic distribution: Figure I59 shows the geographic distribution of *Phakopsora phachyrizi*.

Figure I59. South American countries in which *Phakopsora phachyrizi* is present

Parameters:

Parameter	Unit	Values	Source[a]
Maximum air temperature for infection (T_{max}inf)	°C	28; 28.5	1; 2; 3
Minimum air temperature for infection (T_{min}inf)	°C	8; 10	1; 2; 3
Optimum air temperature for infection (T_{opt}inf)	°C	16–28; 15–25; 18–26; 23	1; 2; 3; 13
Minimum wetness duration for infection (WDmin)	hours	6	1; 2; 9
Maximum wetness duration for infection (WDmax)	hours	12;10	1; 2
Maximum air temperature for incubation (T_{max}inc)	°C	30; 29	9; 12
Minimum air temperature for incubation (T_{min}inc)	°C	15; 12	9; 12
Optimum air temperature for incubation (T_{opt}inc)	°C	24	12
Minimum incubation duration (MID)	days	7–8; 5; 6	1; 4; 10
Maximum air temperature for latency (T_{max}lat)	°C	42	5; 6; 9
Minimum air temperature for latency (T_{min}lat)	°C	5	5; 6; 9
Optimum air temperature for latency (T_{opt}lat)	°C	26	5; 6; 9
Minimum latency duration (MLD)	days	6; 9	4; 6; 11
Maximum air temperature for infectiousness (T_{max}ness)	°C	28	6
Minimum air temperature for infectiousness (T_{min}ness)	°C	10	2; 3
Optimum air temperature for infectiousness (T_{opt}ness)	°C	16	6
Maximum infectiousness duration (MSD)	days	21; 28	4; 6
Maximum air temperature for sporulation (T_{max}spor)	°C	27	9
Minimum air temperature for sporulation (T_{min}spor)	°C	10	2; 3
Optimum air temperature for sporulation (T_{opt}spor)	°C	20	6
Minimum rel. humidity for sporulation (RH_{min}spor)	percent	75–80	8
Rain for 50% detachment (Rain50)	mm day^{-1}	2.5	14
Maximum catch rain ($Rain_{max}$)	mm day^{-1}	6	14
Minimum wind for detachment (W_{min})	m s^{-1}	1	7
Wind for 50% detachment (W50)	m s^{-1}	2	7
Spores at Maximum wind for detachment (W_{max}spor)	percent	0.8	14
Maximum wind for detachment (W_{max})	m s^{-1}	3	7
Wetness duration D50 (WD50)	hours	100	7

1: Rupe and others 2008.
2: Marchetti and others 1976.
3: Magarey and others 2005.
4: Kawuki and others 2003.
5: Kitani and others 1960.
6: Pivonia and others 2006.
7: Isaard and others 2007.
8: Caldwell and others 2002.
9: Del Ponte and others 2008.
10: Bourdon and others 1981.
11: Alves 2007.
12: Bonde and others 2007.
13: Kochman and others 1979.
14: Model default.

Puccinia recondite (wheat leaf rust)

Symptoms: Small brown pustules develop on the leaf blades in a random scatter distribution. They may group into patches in serious cases. Infectious spores are transmitted through the soil. Onset of the disease is slow but accelerated in temperatures above 15°C, making it a disease of the mature cereal plant in summer, usually too late to cause significant damage in temperate areas. Losses of 5–20% are normal but may reach 50% in severe cases.

Epidemiology: *Puccinia recondita* can infect with dew periods of three hours or less at temperature about 20°C. At lower temperatures, longer dew periods are required. Most of the severe epidemics occur when uredinia or latent infections survive the winter at some threshold level on the wheat crop or where spring sown wheat is the recipient of exogenous inoculum before heading (Roelfs and others 1992). Disease spread can be very rapid under favorable environmental conditions. A single uredinium can produce about 3,000 spores a day over 20 days.

Variation in severity of rust epidemics in this area depends on differences in crop maturity at the time of infection by primary inoculum, host resistance used, and environmental conditions (Eversmeyer and Kramer 2000).

Geographic distribution: Figure I60 shows the geographic distribution of *Puccinia recondita.*

Figure I60. South American countries in which *Puccinia recondita* is present

Parameters:

Parameter	Unit	Value	Source
Maximum air temperature for infection (T_{max}inf)	°C	30; 20; 30–32	1, 2, 3, 4, 5, 6, 7
Minimum air temperature for infection (T_{min}inf)	°C	2.6; 2; 5; 3	1, 2, 3, 4, 5, 7, 8
Optimum air temperature for infection (T_{opt}inf)	°C	20–25; 20; 25	1, 3, 4, 5, 6, 7
Minimum wetness duration for infection (WDmin)	days	3; 4; 4–6	1, 2, 5, 7
Maximum wetness duration for infection (WDmax)	days	14; 16	1, 2
Maximum air temperature for incubation (T_{max}inc)	°C	32.2; 35	9, 10
Minimum air temperature for incubation (T_{max}inc)	°C	5; 10; 15; 15.6	2, 3, 9, 11
Optimum air temperature for incubation (T_{opt}inc)	°C	20; 26.5; 25; 23.9–26.7	2, 3, 9, 10, 11
Minimum incubation duration (MID)	days	6; 7; 8; 8.3; 10	2, 3, 9, 11, 12
Maximum air temperature for latency (T_{max}lat)	°C	32.2; 35	9, 10
Minimum air temperature for latency (T_{min}lat)	°C	5; 10; 15; 15.6	2, 3, 9, 11
Optimum air temperature for latency (T_{opt}lat)	°C	20; 26.5; 25; 23.9–26.7	2, 3, 9, 10, 11
Minimum latency duration (MLD)	days	6; 7; 8; 8.3; 10	2, 3, 9, 11, 12
Maximum air temperature for infectiousness (T_{max}ness)	°C	30–32; 33; 35	2, 4, 5, 13
Minimum air temperature for infectiousness (T_{min}ness)	°C	10; 20	2, 4, 14
Optimum air temperature for infectiousness (T_{opt}ness)	°C	25	4, 14
Maximum infectiousness duration (MSD)	days	65	11, 15
Maximum air temperature for sporulation (T_{max}spor)	°C	30–32; 33; 35	2, 4, 5, 13
Minimum air temperature for sporulation (T_{min}spor)	°C	10; 20	2, 4, 14
Optimum air temperature for sporulation (T_{opt}spor)	°C	25	4, 14
Minimum rel. humidity for sporulation (RH_{min}spor)	percent	90	16
Rain for 50% detachment (Rain50)	mm day^{-1}	2.5–4.9	17
Maximum catch rain ($Rain_{max}$)	mm day^{-1}	2.5–4.9	17
Minimum wind for detachment (W_{min})	m s^{-1}	1.3; 0.5–1.5	17, 18
Wind for 50% detachment (W50)	m s^{-1}	5	20
Spores at Maximum wind for detachment (W_{max}spor)	percent	0.8	20
Maximum wind for detachment (W_{max})	m s^{-1}	6	20
Wetness duration D50 (WD50)	days	1; 1–2	1, 19

1: Magarey and others 2005.
2: Wójtowicz 2007.
3: Clifford and Harris 1981.
4: Singh and others 1992.
5: NAPPFAST Pest record 2003.
6: Wiese and Ravenscroft 1979.
7: Vallavieille Pope and others 1995.
8: Angus and others 1981.
9: Eversmeyer and Kramer 2000.
10: Roelsf and others 1992.
11: Tomerlin and others 1983.
12: Kovalenko and others 2004.
13: Rapilly 1979.
14: Dick and Johnson 1983.
15: Mehta and Zadocks 1970.
16: Agricultural Development and Advisory Service.
17: Sache 2000.
18: Geagea and others 1997.
19: Stuckey and Zadocks 1989.
20: Model default

Pyricularia oryzae (blast disease)

Symptoms: At the beginning, the symptoms occur with the appearance of gray-green spots on the leaves, with a darker border. As lesions mature they become whitish-greenish with brown-reddish edges, and they assume an oval-elliptic form. When the sporulation starts, the center of the spots turn ash grey. Dark-brown spots also come about on the culm and on the panicle; node damages can lead to breakage of the culm (Castejón-Muñoz 2007).

Epidemiology: *Pyricularia oryzae* is an ascomycete that can infect rice crop by means of airborne conidia, when the environmental conditions are suitable. The pathogen overwinters inside affected rice straw remaining from the previous year. From these straws primary inoculum develops. The production of conidia occurs when air temperature and air relative humidity rise. After the infection process fulfilled, the mycelium develops inside the host tissue and then causes lesions in which conidia are formed. An epidemic breaks out when several cycles are repeated. The factors that could enhance the severity of an epidemic are the number of conidia produced by the lesions, the suitability of meteorological conditions, and the inner resistance of the cultivar. Also agricultural management practices could affect the dynamics of blast disease epidemics.

Geographic distribution: Figure I61 shows the geographic distribution of *Pyricularia oryzae.*

Figure I61. South American countries in which *Pyricularia oryzae* is present

For this pathogen, no literature review was needed since its simulation will be carried out via the UNIMI.BlastDisease component (see also section iii of this document), implementing a specific model for this disease.

Land resources database

All the data sets (climate, crop, soil, vegetation) were created and standardized within a dedicated GIS developed and described for the previous deliverable (D2 – January 30; Ref. 4).

For some areas, the soil information discussed for D2 (derived from Hogenboom and others 2009) was not available. After searching for alternatives and evaluating different options, we identified another soil database (SOTERLAC version 2.0 database; 1:5 million scale) from the World Data Centre for Soils (www.isric.org/content/world-data-centre-soils). The Hogenboom and others (2009) database is more suitable for cropping systems model applications. However, the SOTERLAC database has a more regular cover of the Latin America and Caribbean: 1,660 representative soil profiles, corresponding to an average density of profile observation of 0.09 per 1,000 km^2 (Batjes 2005). Therefore, the SOTERLAC database information will be used to complete the soil database delivered for D2, and the soil properties not available (but needed by the AZS-BioMA model) will be derived using pedotransfer functions.

Figure I62 shows the information available in the SOTERLAC database, and figure I63 shows the regularity in the distribution of Latin American and Caribbean sites for which SOTERLAC profiles are available.

Figure I62. Occurrence, in percentage, of the attributes in the SOTERLAC 2.0

TERRAIN	% filled	**TERRAIN COMPONENT**	%	**SOIL COMPONENT**	%
1 ISO country code	100	11 ISO country code	100	17 ISO country code	100
2 SOTER unit-ID	100	12 SOTER unit-ID	100	18 SOTER unit-ID	100
3 year of data collection	95	13 terrain component number	100	19 terrain component number	100
4 map-ID	60	14 proportion of SOTER unit	100	20 soil component number	100
5 slope gradient	100	15 length of slope	84	21 proportion of SOTER unit	100
6 relief intensity	95	16 local surface form	70	22 profile-ID	88
7 major landform	100			23 position in terrain component	88
8 regional slope	100			24 surface rockiness	83
9 hypsometry	100			25 surface stoniness	83
10 general lithology	100			26 rootable depth	87
PROFILE	%		%		%
27 profile-ID	100	33 lab ID	81	39 classification FAO'88	100
28 profile database ID	62	34 drainage	100	40 classification version	100
29 latitude	82	35 infiltration rate	-	41 phase (FAO)	19
30 longitude	82	36 surface organic matter	-	42 national classification	50
31 elevation	76	37 classification WRB	-	43 Soil Taxonomy	50
32 sampling date	68	38 WRB classification specifier	-		
HORIZON	%		%		%
44 profile-ID	100	61 fine sand	32	81 soluble CO_3^{2-}	-
45 horizon number	100	62 very fine sand	10	82 exchangeable Ca^{2+}	33
46 diagnostic horizon	65	63 total sand	91	83 exchangeable Mg^{2+}	33
47 diagnostic property	38	64 silt	91	84 exchangeable Na^{+}	34
48 horizon designation	97	65 clay	91	85 exchangeable K^{+}	34
49 lower depth	100	66 particle size class	91	86 exchangeable Al3^{+}	32
50 distinctness of transition	24	67 bulk density	36	87 exchangeable acidity	33
51 moist colour	94	68 moisture content at various tensions	-	88 CEC soil	90
52 dry colour	-	69 hydraulic conductivity	-	89 total carbonate equivalent	-
53 grade of structure	22	70 infiltration rate	-	90 gypsum	-
54 size of structure	22	71 pH H_2O	92	91 total organic carbon	89
55 type of structure	92	72 pH KCl	33	92 total nitrogen	73
56 abundance of coarse fragments	87	73 electrical conductivity	-	93 P_2O_5	25
57 size of coarse fragments	-	74 soluble Na^{+}	-	94 phosphate retention	-
58 very coarse sand	10	75 soluble Ca^{2+}	-	95 Fe dithionite	-
59 coarse sand	32	76 soluble Mg^{2+}	-	96 Al dithionite	-
60 medium sand	10	77 soluble K^{+}	-	97 Fe pyrophosphate	-
		78 soluble Cl^{-}	-	98 Al pyrophosphate	-
		79 soluble SO_4^{2-}	-	99 clay mineralogy	-
		80 soluble HCO_3^{-}	-		

Figure I63. Spatial distribution of the soil profiles of SOTERLAC 2.0

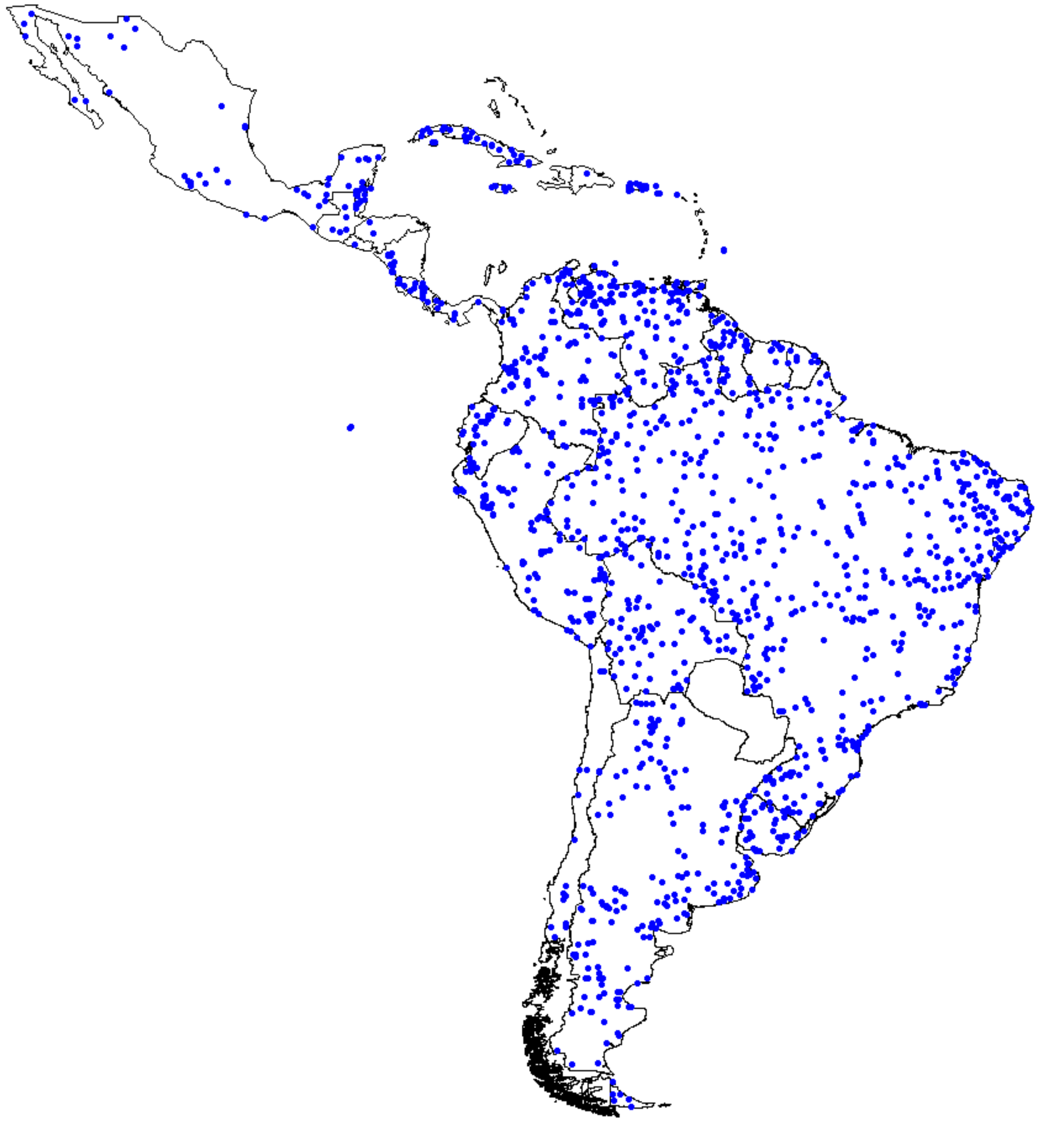

Table I9 lists the main information of layers, profiles, and soils stored in SOTERLAC 2.0. For a comparison with the information in the Hogenboom database, see appendix C of the deliverable D2 (Ref. 4).

Table I9. List of the main information enclosed in SOTERLAC 2.0 related to layers, profiles, and soil components

Name	Label	Description
		Layer
PRID	Profile-ID	Code for the representative profile
HONU	Horizon number	A consecutive number, starting with the surface horizon
DIAH	Diagnostic horizon	Diagnostic horizon - Revised Legend of the FAO-UNESCO Soil Map of the World (FAO 1988)
DIAP	Diagnostic property	Diagnostic property - Revised Legend of the FAO-Unesco Soil Map of the World (FAO 1988)
HODE	Horizon designation	Master horizon with subordinate characteristics (FAO 1990)

HBDE	Lower depth	The average depth of the lower boundary in centimeters
HBDI	Distinctness of transition	Abruptness of horizon boundary to underlying horizon (FAO 1990)
SCMO	Colour - moist soil	The Munsell color of the moist soil
SCDR	Colour - dry soil	The Munsell color of the dry soil
STGR	Grade of structure	Grade of structure (FAO 1990)
STSI	Size of structure elements	Size of structure elements (FAO 1990)
STTY	Type of structure	Type of structure (FAO 1990)
MINA	Abundance of coarse fragments	Classes of volume (%) of rock or mineral fragments (> 2mm) in the soil matrix (FAO 1990)
MINS	Size of coarse fragments	Size of dominant rock or mineral fragments in classes (FAO, 1990)
SDVC	Very coarse sand	Weight (%) of particles 2.0–1.0 mm (very coarse sand) in fine earth fraction
SDCO	Coarse sand	Weight (%) of particles 1.0–0.5 mm (coarse sand) in fine earth fraction
SDME	Medium sand	Weight (%) of particles 0.5–0.25 mm (medium sand) in fine earth fraction
SDFI	Fine sand	Weight (%) of particles 0.25–0.1 mm (fine sand) in fine earth fraction
SDVF	Very fine sand	Weight (%) of particles 0.1–0.05 mm (very sand) in fine earth fraction
SDTO	Total sand	Weight (%) of particles 2.0–0.05 mm (total sand) in fine earth fraction
STPC	Silt	Weight (%) of particles < 0.002 mm (silt) in fine earth fraction
CLPC	Clay	Weight (%) of particles < 0.002 mm (clay) in fine earth fraction
PSCL	Particle size class	Particle size class as derived from the particle size analysis
BULK	Bulk density	The bulk density in kg per cubic dm
MCT1	Soil moisture (field capacity)	Soil moisture (%) at tension 1 (field capacity, –33 KPa)
TEN2	Water tension 2	Water tension 2 (KPa)
MCT2	Soil moisture (tension 2)	Soil moisture (%) at tension 2
TEN3	Water tension 3	Water tension 3 (KPa)
MCT3	Soil moisture (tension 3)	Soil moisture (%) at tension 3
TEN4	Water tension 4	Water tension 4 (KPa)
MCT4	Soil moisture (tension 4)	Soil moisture (%) at tension 4
MCT5	Soil moisture (wilting point)	Soil moisture (%) at tension 5 (wilting point, –1,500KPa)
HYDC	Hydraulic conductivity	The saturated hydraulic conductivity in cm/hour
INFR	Infiltration rate	The basic infiltration rate in cm/hour
PHAQ	pH (H2O)	pH (H2O) in a supernatant suspension of a 1:2.5 soil - water mixture
PHKC	pH (KCl)	pH (KCl) in a supernatant suspension of a 1:2.5 soil - 1M KCl mixture
ELCO	Electrical conductivity	The electrical conductivity of saturation extract (dS/m)
SONA	Soluble Na	The soluble Na+ content of the saturated paste in cmol(c) / liter
SOCA	Soluble Ca	The soluble Ca++ content of the saturated paste in cmol(c) / liter
SOMG	Soluble Mg	The soluble Mg++ content of the saturated paste in cmol(c) / liter
SOLK	Soluble K	The soluble K+ content of the saturated paste in cmol(c) / liter
SOCL	Soluble Cl	The soluble Cl- content of the saturated paste in cmol(c) / liter
SSO4	Soluble SO4	The soluble SO4-- content of the saturated paste in cmol(c) / liter
SCO3	Soluble CO3	The soluble CO3- content of the saturated paste in cmol(c) / liter
HCO3	Soluble HCO3	The soluble HCO3- content of the saturated paste in cmol(c) / liter
EXCA	Exchangeable Ca	The exchangeable Ca in cmol(+) / kg
EXMG	Exchangeable Mg	The exchangeable Mg in cmol(+) / kg
EXNA	Exchangeable Na	The exchangeable Na in cmol(+) / kg
EXCK	Exchangeable K	The exchangeable K in cmol(+) / kg
EXAL	Exchangeable Al	The exchangeable Al in cmol(+) / kg
EXAC	Exchangeable acidity	The exchangeable acidity, as determined in 1N KCl, in cmol(+) / kg
CECS	CEC soil	The cation-exchange capacity of the soil at pH 7.0 in cmol(+) / kg

TCEQ	Total carbonate equivalent	The content of carbonates in g / kg
GYPS	Gypsum	The gypsum content in g / kg
TOTC	Total carbon	The content of total organic carbon in g / kg
TOTN	Total nitrogen	The content of total N in g / kg
P2O5	P2O5	The P2O5 content in mg / kg
PRET	Phosphate retention	The phosphate retention in percent
FEDE	Fe, dithionite extractable	The Fe fraction, in weight (%), extractable in dithionite
FEPE	Fe, pyrophosphate extractable	The Fe fraction, in weight (%), extractable in pyrophosphate at PH 10
ALDE	Al, dithionite extractable	The Al fraction, in weight (%), extractable in dithionite
ALPE	Al, pyrophosphate extractable	The Al fraction, in weight (%), extractable in pyrophosphate at PH 10
CLAY	Clay mineralogy	The dominant type of mineral in the clay fraction
	Profile	
PRID	Profile-ID	Code for the representative profile
PDID	Profile database-ID	ID for the owner, institute or organization that holds (part of) the national soil profile database
LATI	Latitude	Latitude in decimal degrees. Latitudes in the southern hemisphere are negative
LNGI	Longitude	Longitude in decimal degrees. Longitudes in the western hemisphere are negative
ELEV	Elevation	The elevation of the representative profile in meters above sea level
SAYR	Sampling year	The year in which the profile was described and sampled
MNUM	Sampling month	The month in which the profile was described and sampled
LABO	Lab-ID	ID for the soil laboratory that analyzed the samples
DRAI	Drainage	Present drainage class of a soil component represented by this profile
INFR	Infiltration rate	Basic infiltration rate category (BAI 1991)
ORGA	Surface organic matter	Surface organic matter - thickness and degree of decomposition
WRBC	WRB Classification	Classification according to World reference base for soil resources (WRB) - full name
WRBS	WRB Classification - specifier	Classification according to World reference base for soil resources (WRB) - specifier
CLAF	FAO classification	Characterization of the profile - revised legend of the FAO-Unesco Soil Map of the World Legend (FAO 1988)
CLAV	Classification version	The year of publication of the version of the FAO Legend used for the profile's characterization
PHAS	FAO phase	Any potentially limiting factor related to (sub)surface features of the terrain
CLAN	National classification	The original national classification of the profile, if different from the FAO classification
STAX	Soil Taxonomy	Classification according to Soil Taxonomy
	Soil components	
ISOC	ISO country code	ISO-3166 country code (1994)
SUID	SOTER unit-ID	The identification code of a SOTER unit on the map and in the database
TCID	Terrain component number	The sequence number of the terrain component in the terrain (largest comes first)
SCID	Soil component number	The sequence number of the soil component in the terrain component (largest comes first)
PRID	Profile-ID	Code for the representative profile

NRPR	Number of reference profiles	The number of reference profiles that was considered for the selection of the representative profile
POSI	Position	The relative position of the soil component within the terrain component
RKSC	Surface rockiness	The percentage coverage of rock outcrops - classes (FAO 1990)
STSC	Surface stoniness	The percentage cover of coarse fragments (> 0.2 cm), completely or partly at the surface - classes (FAO 1990)
ERTY	Erosion/deposition type	Characterization of the erosion or deposition type according to FAO (1990)
ERAA	Area affected	The area affected by erosion or deposition. Classes according to UNEP-ISRIC (1988)
ERDE	Erosion degree	Degree of erosion (FAO 1990)
SCAP	Sensitivity to capping	The degree in which the soil surface has a tendency to capping and sealing (FAO 1990)
RDEP	Rootable depth	Estimated depth to which root growth is unrestricted by physical or chemical impediments— classes after FAO (1990)
RELA	Relation with other soil components	The relationship between this soil component and adjoining soil components

Annex II. Crop Yield Simulation Results

Wheat, 2020, No Adaptation

Table II1. Percentage impact (no adaptation) of climate change on wheat yields for potential, water limited, abiotic damaged, diseased, and actual production levels; projections for 2020

Country	Climate change scenario	Climate change impact (percentage difference compared to the baseline productivity				
		Potential	Water limited	Abiotic damaged	Diseased	Actual
Argentina	Hadley, A1B, 2020	–13.74	–21.70	–13.74	–22.33	–31.23
Argentina	Hadley, B1, 2020	–15.45	–22.68	–15.45	–33.39	–31.38
Argentina	NCAR, A1B, 2020	–16.40	–23.67	–16.40	–23.70	–30.97
Argentina	NCAR, B1, 2020	–15.99	–23.60	–15.99	–23.61	–31.74
Brazil	Hadley, A1B, 2020	–21.96	–26.05	–21.96	–26.02	–30.78
Brazil	Hadley, B1, 2020	–24.69	–28.24	–24.69	–27.67	–31.34
Brazil	NCAR, A1B, 2020	–30.47	–34.76	–30.47	–32.80	–36.47
Brazil	NCAR, B1, 2020	–24.83	–29.99	–24.83	–27.34	–32.40
Chile	Hadley, A1B, 2020	+0.20	–24.43	+1.99	–12.40	–33.03
Chile	Hadley, B1, 2020	–0.33	–23.49	+2.04	–12.70	–31.62
Chile	NCAR, A1B, 2020	–0.97	–21.44	+1.34	–13.47	–30.02
Chile	NCAR, B1, 2020	–0.85	–21.51	+1.93	–13.43	–29.80
Colombia	Hadley, A1B, 2020	–30.50	–32.80	–30.50	–29.29	–28.61
Colombia	Hadley, B1, 2020	–29.81	–32.14	–29.81	–28.63	–28.14
Colombia	NCAR, A1B, 2020	–29.62	–31.99	–29.62	–27.50	–26.11
Colombia	NCAR, B1, 2020	–25.91	–28.45	–25.91	–26.24	–25.60
Ecuador	Hadley, A1B, 2020	–16.12	–18.03	–16.12	–17.07	–18.57
Ecuador	Hadley, B1, 2020	–15.40	–17.94	–15.40	–16.25	–18.49
Ecuador	NCAR, A1B, 2020	–12.63	–14.82	–12.63	–14.16	–15.91
Ecuador	NCAR, B1, 2020	–10.55	–12.85	–10.55	–12.35	–14.24
Mexico	Hadley, A1B, 2020	–39.99	–36.93	–39.99	–41.25	–37.69
Mexico	Hadley, B1, 2020	–36.59	–33.18	–36.59	–37.83	–33.99
Mexico	NCAR, A1B, 2020	–37.27	–32.04	–37.27	–39.18	–32.40
Mexico	NCAR, B1, 2020	–34.14	–29.74	–34.14	–35.61	–29.77
Peru	Hadley, A1B, 2020	–5.43	–7.29	–7.18	–3.45	–4.56
Peru	Hadley, B1, 2020	–4.89	–7.48	–6.68	–2.84	–4.80
Peru	NCAR, A1B, 2020	–4.11	–5.91	–6.02	–2.00	–3.13
Peru	NCAR, B1, 2020	–3.38	–5.31	–5.08	–1.21	–2.18
Uruguay	Hadley, A1B, 2020	–17.65	–17.05	–17.65	–15.66	–14.55
Uruguay	Hadley, B1, 2020	–22.37	–20.15	–22.37	–19.55	–16.05
Uruguay	NCAR, A1B, 2020	–25.91	–24.53	–25.91	–22.36	–18.58
Uruguay	NCAR, B1, 2020	–23.04	–23.06	–23.04	–19.71	–17.98
Rest of South America	Hadley, A1B, 2020	–13.90	–21.59	–13.93	–22.29	–31.02
Rest of South America	Hadley, B1, 2020	–15.61	–22.61	–15.64	–23.36	–31.18
Rest of South America	NCAR, A1B, 2020	–16.71	–23.77	–16.75	–23.82	–30.94
Rest of South America	NCAR, B1, 2020	–16.09	–23.50	–16.12	–23.54	–31.54
Central America & Caribbean	Hadley, A1B, 2020	–39.89	–36.87	–39.89	–41.20	–37.64
Central America & Caribbean	Hadley, B1, 2020	–36.53	–33.16	–36.53	–37.80	–33.96
Central America & Caribbean	NCAR, A1B, 2020	–37.19	–32.04	–37.19	–39.14	–32.39
Central America & Caribbean	NCAR, B1, 2020	–34.06	–29.72	–34.06	–35.57	–29.75

Maize, 2020, No Adaptation

Table II2. Percentage impact (no adaptation) of climate change on maize yields for potential, water limited, abiotic damaged, diseased, and actual production levels; projections for 2020

Country	Climate change scenario	Climate change impact (percentage difference compared to the baseline productivity				
		Potential	Water limited	Abiotic damaged	Diseased	Actual
Argentina	Hadley, A1B, 2020	–16.07	–16.46	–16.07	–15.60	–15.17
Argentina	Hadley, B1, 2020	–10.75	–11.11	–10.75	–10.37	–10.01
Argentina	NCAR, A1B, 2020	–14.69	–14.82	–14.69	–14.33	–13.70
Argentina	NCAR, B1, 2020	–14.13	–14.35	–14.13	–13.70	–13.15
Brazil	Hadley, A1B, 2020	–27.86	–28.32	–27.86	–27.83	–27.14
Brazil	Hadley, B1, 2020	–20.30	–20.84	–20.30	–20.07	–19.61
Brazil	NCAR, A1B, 2020	–38.09	–38.49	–38.09	–38.94	–37.98
Brazil	NCAR, B1, 2020	–34.05	–34.49	–34.05	–35.04	–34.16
Chile	Hadley, A1B, 2020	–11.23	–10.36	–11.23	–11.43	–10.16
Chile	Hadley, B1, 2020	–8.64	–7.11	–8.64	–8.82	–6.94
Chile	NCAR, A1B, 2020	–11.84	–11.03	–11.84	–12.10	–10.86
Chile	NCAR, B1, 2020	–12.62	–11.87	–12.62	–12.90	–11.72
Colombia	Hadley, A1B, 2020	–19.16	–20.16	–19.16	–16.89	–16.69
Colombia	Hadley, B1, 2020	–18.20	–19.18	–18.20	–16.11	–15.91
Colombia	NCAR, A1B, 2020	–19.85	–20.87	–19.85	–18.54	–18.21
Colombia	NCAR, B1, 2020	–16.70	–17.75	–16.70	–14.54	–14.18
Ecuador	Hadley, A1B, 2020	–37.18	–38.20	–37.18	–37.76	–37.95
Ecuador	Hadley, B1, 2020	–34.82	–36.07	–34.82	–35.33	–35.68
Ecuador	NCAR, A1B, 2020	–34.25	–35.07	–34.25	–34.70	–34.76
Ecuador	NCAR, B1, 2020	–30.62	–31.67	–30.62	–30.65	–31.13
Mexico	Hadley, A1B, 2020	–28.25	–28.83	–28.42	–29.77	–30.09
Mexico	Hadley, B1, 2020	–24.42	–25.12	–24.63	–25.49	–25.86
Mexico	NCAR, A1B, 2020	–24.48	–25.21	–24.76	–25.88	–26.38
Mexico	NCAR, B1, 2020	–22.72	–25.53	–23.02	–24.10	–24.70
Peru	Hadley, A1B, 2020	–13.95	–15.55	–13.95	–13.93	–13.87
Peru	Hadley, B1, 2020	–12.05	–13.67	–12.05	–12.13	–12.26
Peru	NCAR, A1B, 2020	–9.96	–11.92	–9.96	–8.85	–9.03
Peru	NCAR, B1, 2020	–9.17	–11.22	–9.17	–8.22	–8.46
Uruguay	Hadley, A1B, 2020	–13.86	–14.40	–13.86	–13.51	–13.24
Uruguay	Hadley, B1, 2020	–8.68	–9.27	–8.68	–8.45	–8.31
Uruguay	NCAR, A1B, 2020	–12.99	–13.28	–12.99	–12.99	–12.48
Uruguay	NCAR, B1, 2020	–14.06	–14.51	–14.06	–13.74	–13.33
Rest of South America	Hadley, A1B, 2020	–15.65	–16.76	–15.65	–14.95	–14.80
Rest of South America	Hadley, B1, 2020	–12.90	–14.04	–12.90	–12.17	–12.13
Rest of South America	NCAR, A1B, 2020	–13.97	–15.17	–13.97	–13.21	–13.10
Rest of South America	NCAR, B1, 2020	–13.16	–14.43	–13.16	–12.25	–12.17
Central America & Caribbean	Hadley, A1B, 2020	–27.92	–28.51	–28.08	–29.33	–29.63
Central America & Caribbean	Hadley, B1, 2020	–24.19	–24.89	–24.39	–25.16	–25.51
Central America & Caribbean	NCAR, A1B, 2020	–24.30	–25.04	–24.57	–25.62	–26.10
Central America & Caribbean	NCAR, B1, 2020	–22.50	–23.31	–22.79	–23.77	–24.34

Soybean, 2020, No Adaptation

Table II3. Percentage impact (no adaptation) of climate change on soybean yields for potential, water limited, abiotic damaged, diseased, and actual production levels; projections for 2020

Country	Climate change scenario	Climate change impact (percentage difference compared to the baseline productivity				
		Potential	Water limited	Abiotic damaged	Diseased	Actual
Argentina	Hadley, A1B, 2020	–24.42	–15.98	–24.42	–24.41	–15.01
Argentina	Hadley, B1, 2020	–15.63	–6.31	–15.63	–15.63	–5.18
Argentina	NCAR, A1B, 2020	–14.97	–5.28	–14.97	–14.97	–4.13
Argentina	NCAR, B1, 2020	–18.17	–9.07	–18.17	–18.16	–7.99
Brazil	Hadley, A1B, 2020	–39.04	–38.71	–39.04	–39.04	–37.25
Brazil	Hadley, B1, 2020	–31.74	–31.37	–31.74	–31.74	–29.71
Brazil	NCAR, A1B, 2020	–39.86	–39.59	–39.86	–39.86	–38.12
Brazil	NCAR, B1, 2020	–36.29	–36.03	–36.29	–36.29	–34.47
Chile	Hadley, A1B, 2020					
Chile	Hadley, B1, 2020					
Chile	NCAR, A1B, 2020					
Chile	NCAR, B1, 2020					
Colombia	Hadley, A1B, 2020	–24.98	–24.79	–24.98	–29.12	–29.09
Colombia	Hadley, B1, 2020	–23.00	–22.80	–23.00	–26.78	–26.74
Colombia	NCAR, A1B, 2020	–18.44	–18.07	–18.44	–22.07	–21.78
Colombia	NCAR, B1, 2020	–19.20	–19.00	–19.20	–20.50	–20.34
Ecuador	Hadley, A1B, 2020	–48.73	–50.56	–48.73	–48.73	–48.80
Ecuador	Hadley, B1, 2020	–46.22	–48.20	–46.22	–46.22	–46.35
Ecuador	NCAR, A1B, 2020	–44.98	–47.01	–44.98	–44.98	–45.11
Ecuador	NCAR, B1, 2020	–39.63	–41.86	–39.63	–39.73	–39.74
Mexico	Hadley, A1B, 2020					
Mexico	Hadley, B1, 2020					
Mexico	NCAR, A1B, 2020					
Mexico	NCAR, B1, 2020					
Peru	Hadley, A1B, 2020					
Peru	Hadley, B1, 2020					
Peru	NCAR, A1B, 2020					
Peru	NCAR, B1, 2020					
Uruguay	Hadley, A1B, 2020	–10.66	–11.51	–10.66	–10.57	–10.42
Uruguay	Hadley, B1, 2020	–18.06	–18.88	–18.06	–18.00	–17.92
Uruguay	NCAR, A1B, 2020	–15.63	–16.52	–15.63	–15.53	–15.52
Uruguay	NCAR, B1, 2020	–13.93	–14.48	–13.93	–13.82	–13.45
Rest of South America	Hadley, A1B, 2020	–23.99	–15.83	–23.99	–23.98	–14.85
Rest of South America	Hadley, B1, 2020	–15.71	–6.74	–15.71	–15.70	–5.62
Rest of South America	NCAR, A1B, 2020	–15.00	–5.66	–15.00	–14.98	–4.52
Rest of South America	NCAR, B1, 2020	–18.04	–9.25	–18.04	–18.03	–8.18
Central America & Caribbean	Hadley, A1B, 2020	–32.26	–32.70	–32.26	–35.89	–35.88
Central America & Caribbean	Hadley, B1, 2020	–30.08	–30.58	–30.08	–33.47	–33.47
Central America & Caribbean	NCAR, A1B, 2020	–26.60	–26.99	–26.60	–30.02	–29.86
Central America & Caribbean	NCAR, B1, 2020	–25.71	–26.30	–25.71	–27.38	–27.29

Rice, 2020, No Adaptation

Table II4. Percentage impact (no adaptation) of climate change on rice yields for potential, water limited, abiotic damaged, diseased, and actual production levels; projections for 2020

Country	Climate change scenario	Climate change impact (percentage difference compared to the baseline productivity				
		Potential	Water limited	Abiotic damaged	Diseased	Actual
Argentina	Hadley, A1B, 2020	–1.62		–1.28	–0.13	+0.20
Argentina	Hadley, B1, 2020	+0.21		+0.24	+1.47	+1.49
Argentina	NCAR, A1B, 2020	+0.56		+0.85	+1.09	+1.37
Argentina	NCAR, B1, 2020	–0.07		+0.27	+0.53	+0.85
Brazil	Hadley, A1B, 2020	–7.56		–7.32	–4.03	–3.78
Brazil	Hadley, B1, 2020	–5.46		–5.28	–2.58	–2.40
Brazil	NCAR, A1B, 2020	–4.05		–3.76	–1.17	–0.87
Brazil	NCAR, B1, 2020	–4.23		–3.96	–1.48	–1.21
Chile	Hadley, A1B, 2020					
Chile	Hadley, B1, 2020					
Chile	NCAR, A1B, 2020					
Chile	NCAR, B1, 2020					
Colombia	Hadley, A1B, 2020	+8.89		+8.89	+12.32	+12.32
Colombia	Hadley, B1, 2020	+7.39		+7.39	+10.39	+10.39
Colombia	NCAR, A1B, 2020	+9.29		+9.29	+13.50	+13.50
Colombia	NCAR, B1, 2020	+9.59		+9.59	+13.00	+13.00
Ecuador	Hadley, A1B, 2020	–1.12		–1.12	+6.06	+6.06
Ecuador	Hadley, B1, 2020	–2.08		–2.08	+4.93	+4.93
Ecuador	NCAR, A1B, 2020	+1.10		+1.10	+7.29	+7.29
Ecuador	NCAR, B1, 2020	+1.14		+1.14	+7.28	+7.28
Mexico	Hadley, A1B, 2020	–9.16		–9.16	–6.57	–6.57
Mexico	Hadley, B1, 2020	–9.34		–9.34	–6.85	–6.85
Mexico	NCAR, A1B, 2020	–9.23		–9.23	–7.04	–7.04
Mexico	NCAR, B1, 2020	–9.46		–9.46	–7.05	–7.05
Peru	Hadley, A1B, 2020	+2.00		+2.00	+6.98	+6.98
Peru	Hadley, B1, 2020	+2.02		+2.02	+6.05	+6.05
Peru	NCAR, A1B, 2020	+4.31		+4.31	+8.89	+8.89
Peru	NCAR, B1, 2020	+3.33		+3.33	+6.93	+6.93
Uruguay	Hadley, A1B, 2020	+0.19		+2.03	+0.72	+2.54
Uruguay	Hadley, B1, 2020	+0.38		+1.83	+1.17	+2.62
Uruguay	NCAR, A1B, 2020	+2.68		+4.46	+2.77	+4.53
Uruguay	NCAR, B1, 2020	+1.16		+3.04	+1.18	+3.03
Rest of South America	Hadley, A1B, 2020	+1.32		+1.33	+4.32	+4.33
Rest of South America	Hadley, B1, 2020	+1.77		+1.77	+4.53	+4.53
Rest of South America	NCAR, A1B, 2020	+3.92		+3.93	+6.31	+6.32
Rest of South America	NCAR, B1, 2020	+3.37		+3.38	+5.32	+5.33
Central America & Caribbean	Hadley, A1B, 2020	–2.84		–2.84	–1.74	–1.74
Central America & Caribbean	Hadley, B1, 2020	–2.98		–2.98	–1.92	–1.92
Central America & Caribbean	NCAR, A1B, 2020	–2.26		–2.26	–1.26	–1.26
Central America & Caribbean	NCAR, B1, 2020	–2.15		–2.15	–1.21	–1.21

Wheat, 2050, No Adaptation

Table II5. Percentage impact (no adaptation) of climate change on wheat yields for potential, water limited, abiotic damaged, diseased, and actual production levels; projections for 2050

Country	Climate change scenario	Climate change impact (percentage difference compared to the baseline productivity				
		Potential	Water limited	Abiotic damaged	Diseased	Actual
Argentina	Hadley, A1B, 2050	–25.69	–32.84	–25.69	–29.70	–35.70
Argentina	Hadley, B1, 2050	–21.48	–29.40	–21.48	–26.34	–33.46
Argentina	NCAR, A1B, 2050	–26.36	–33.43	–26.36	–29.87	–35.42
Argentina	NCAR, B1, 2050	–16.48	–25.64	–16.48	–22.04	–29.91
Brazil	Hadley, A1B, 2050	–51.50	–54.32	–51.50	–50.48	–50.50
Brazil	Hadley, B1, 2050	–35.01	–38.85	–35.01	–34.98	–37.01
Brazil	NCAR, A1B, 2050	–40.52	–45.05	–40.52	–39.27	–40.88
Brazil	NCAR, B1, 2050	–23.42	–29.66	–23.42	–22.93	–27.33
Chile	Hadley, A1B, 2050	+0.33	–28.96	+5.08	–9.01	–29.16
Chile	Hadley, B1, 2050	+1.20	–27.54	+3.61	–9.49	–31.10
Chile	NCAR, A1B, 2050	–0.16	–23.08	+4.38	–9.54	–23.76
Chile	NCAR, B1, 2050	+2.67	–21.95	+5.63	–8.74	–25.95
Colombia	Hadley, A1B, 2050	–64.97	–68.03	–64.97	–58.32	–56.99
Colombia	Hadley, B1, 2050	–52.76	–56.51	–52.76	–47.16	–46.23
Colombia	NCAR, A1B, 2050	–55.83	–60.19	–55.83	–49.53	–48.06
Colombia	NCAR, B1, 2050	–28.28	–35.17	–28.28	–23.07	–22.02
Ecuador	Hadley, A1B, 2050	–27.32	–33.37	–27.32	–21.29	–22.71
Ecuador	Hadley, B1, 2050	–23.95	–28.97	–23.95	–19.71	–21.33
Ecuador	NCAR, A1B, 2050	–21.03	–27.96	–21.03	–14.86	–16.78
Ecuador	NCAR, B1, 2050	–13.19	–19.23	–13.19	–9.17	–11.01
Mexico	Hadley, A1B, 2050	–66.71	–62.16	–66.71	–68.59	–62.21
Mexico	Hadley, B1, 2050	–55.95	–52.82	–55.95	–56.66	–51.60
Mexico	NCAR, A1B, 2050	–57.67	–52.19	–57.67	–59.46	–50.85
Mexico	NCAR, B1, 2050	–43.02	–39.10	–43.02	–43.74	–36.90
Peru	Hadley, A1B, 2050	–7.08	–15.46	–7.85	–2.16	–2.78
Peru	Hadley, B1, 2050	–5.46	–12.70	–6.76	–1.07	–2.73
Peru	NCAR, A1B, 2050	–4.94	–12.70	–6.07	+0.98	+1.68
Peru	NCAR, B1, 2050	–1.78	–8.36	–3.55	+3.84	+3.68
Uruguay	Hadley, A1B, 2050	–35.51	–34.48	–35.51	–29.96	–24.54
Uruguay	Hadley, B1, 2050	–24.42	–22.92	–24.42	–19.32	–14.17
Uruguay	NCAR, A1B, 2050	–36.14	–35.48	–36.14	–30.15	–24.24
Uruguay	NCAR, B1, 2050	–24.31	–26.49	–24.31	–18.60	–16.59
Rest of South America	Hadley, A1B, 2050	–26.32	–33.34	–26.34	–30.16	–35.95
Rest of South America	Hadley, B1, 2050	–21.69	–29.44	–21.72	–26.52	–33.35
Rest of South America	NCAR, A1B, 2050	–26.49	–33.48	–26.52	–29.91	–35.32
Rest of South America	NCAR, B1, 2050	–16.47	–25.47	–16.50	–21.85	–29.57
Central America & Caribbean	Hadley, A1B, 2050	–66.69	–62.25	–66.69	–68.55	–62.18
Central America & Caribbean	Hadley, B1, 2050	–55.92	–52.87	–55.92	–56.63	–51.57
Central America & Caribbean	NCAR, A1B, 2050	–57.65	–52.31	–57.65	–59.42	–50.83
Central America & Caribbean	NCAR, B1, 2050	–42.87	–39.04	–42.87	–43.66	–36.81

Maize, 2050, No Adaptation

Table II6. Percentage impact (no adaptation) of climate change on maize yields for potential, water limited, abiotic damaged, diseased, and actual production levels; projections for 2050

Country	Climate change scenario	Climate change impact (percentage difference compared to the baseline productivity				
		Potential	Water limited	Abiotic damaged	Diseased	Actual
Argentina	Hadley, A1B, 2050	–31.53	–32.77	–31.53	–30.69	–29.92
Argentina	Hadley, B1, 2050	–22.40	–23.49	–22.40	–21.60	–20.94
Argentina	NCAR, A1B, 2050	–29.43	–30.43	–29.43	–28.68	–27.69
Argentina	NCAR, B1, 2050	–17.92	–19.03	–17.92	–17.20	–16.54
Brazil	Hadley, A1B, 2050	–68.35	–69.06	–68.35	–69.61	–68.21
Brazil	Hadley, B1, 2050	–53.44	–54.33	–53.44	–54.19	–53.02
Brazil	NCAR, A1B, 2050	–59.52	–60.37	–59.52	–60.84	–59.34
Brazil	NCAR, B1, 2050	–40.88	–41.82	–40.88	–41.56	–40.40
Chile	Hadley, A1B, 2050	–19.94	–20.02	–19.94	–20.03	–18.87
Chile	Hadley, B1, 2050	–15.24	–14.83	–15.24	–15.37	–13.84
Chile	NCAR, A1B, 2050	–21.79	–22.15	–21.79	–21.84	–20.98
Chile	NCAR, B1, 2050	–11.62	–11.51	–11.62	–11.84	–10.51
Colombia	Hadley, A1B, 2050	–38.10	–41.30	–38.10	–40.91	–40.89
Colombia	Hadley, B1, 2050	–32.74	–35.32	–32.74	–32.75	–32.62
Colombia	NCAR, A1B, 2050	–33.13	–36.67	–33.13	–34.32	–34.28
Colombia	NCAR, B1, 2050	–21.36	–24.54	–21.36	–18.80	–18.50
Ecuador	Hadley, A1B, 2050	–74.50	–74.81	–74.50	–77.51	–75.49
Ecuador	Hadley, B1, 2050	–63.50	–63.89	–63.50	–67.08	–65.06
Ecuador	NCAR, A1B, 2050	–62.04	–63.39	–62.04	–65.47	–64.19
Ecuador	NCAR, B1, 2050	–42.91	–44.49	–42.91	–44.06	–43.94
Mexico	Hadley, A1B, 2050	–44.55	–46.46	–44.97	–43.46	–44.07
Mexico	Hadley, B1, 2050	–41.66	–43.37	–41.97	–41.63	–42.25
Mexico	NCAR, A1B, 2050	–36.73	–38.91	–37.08	–37.08	–37.66
Mexico	NCAR, B1, 2050	–28.09	–30.31	–28.49	–28.39	–29.12
Peru	Hadley, A1B, 2050	–30.69	–34.32	–30.69	–31.38	–30.44
Peru	Hadley, B1, 2050	–24.34	–27.66	–24.34	–24.85	–24.20
Peru	NCAR, A1B, 2050	–20.39	–25.70	–20.39	–18.31	–18.38
Peru	NCAR, B1, 2050	–11.24	–16.03	–11.24	–9.56	–9.97
Uruguay	Hadley, A1B, 2050	–31.47	–32.73	–31.47	–30.96	–30.19
Uruguay	Hadley, B1, 2050	–20.23	–21.56	–20.23	–16.69	–19.16
Uruguay	NCAR, A1B, 2050	–26.54	–27.75	–26.54	–26.07	–25.20
Uruguay	NCAR, B1, 2050	–15.46	–16.82	–15.46	–14.90	–14.30
Rest of South America	Hadley, A1B, 2050	–33.67	–36.39	–33.67	–34.42	–33.83
Rest of South America	Hadley, B1, 2050	–25.86	–28.34	–25.86	–25.60	–25.15
Rest of South America	NCAR, A1B, 2050	–26.54	–30.02	–26.54	–25.90	–25.72
Rest of South America	NCAR, B1, 2050	–15.71	–18.96	–15.71	–14.27	–14.21
Central America & Caribbean	Hadley, A1B, 2050	–44.23	–46.18	–44.63	–43.30	–43.89
Central America & Caribbean	Hadley, B1, 2050	–41.28	–43.01	–41.58	–41.28	–41.87
Central America & Caribbean	NCAR, A1B, 2050	–36.57	–38.79	–36.91	–36.96	–37.51
Central America & Caribbean	NCAR, B1, 2050	–27.85	–30.10	–28.23	–28.06	–28.76

Soybean, 2050, No Adaptation

Table II7. Percentage impact (no adaptation) of climate change on soybean yields for potential, water limited, abiotic damaged, diseased, and actual production levels; projections for 2050

Country	Climate change scenario	Climate change impact (percentage difference compared to the baseline productivity				
		Potential	Water limited	Abiotic damaged	Diseased	Actual
Argentina	Hadley, A1B, 2050	–44.60	–38.23	–44.60	–44.61	–37.58
Argentina	Hadley, B1, 2050	–30.63	–22.76	–30.63	–30.63	–21.89
Argentina	NCAR, A1B, 2050	–35.07	–27.54	–35.07	–35.07	–26.76
Argentina	NCAR, B1, 2050	–20.35	–11.46	–20.35	–20.34	–10.42
Brazil	Hadley, A1B, 2050	–79.56	–79.42	–79.56	–79.56	–79.05
Brazil	Hadley, B1, 2050	–66.24	–66.06	–66.24	–66.24	–65.37
Brazil	NCAR, A1B, 2050	–66.77	–66.58	–66.77	–66.76	–65.88
Brazil	NCAR, B1, 2050	–45.04	–44.82	–45.04	–45.04	–43.52
Chile	Hadley, A1B, 2050					
Chile	Hadley, B1, 2050					
Chile	NCAR, A1B, 2050					
Chile	NCAR, B1, 2050					
Colombia	Hadley, A1B, 2050	–46.57	–46.37	–46.57	–56.22	–56.23
Colombia	Hadley, B1, 2050	–38.58	–38.40	–38.58	–47.61	–47.62
Colombia	NCAR, A1B, 2050	–28.20	–27.78	–28.20	–35.58	–35.28
Colombia	NCAR, B1, 2050	–21.47	–21.17	–21.47	–26.22	–26.00
Ecuador	Hadley, A1B, 2050	–86.21	–86.56	–86.21	–86.21	–86.25
Ecuador	Hadley, B1, 2050	–76.94	–77.65	–76.94	–76.94	–77.02
Ecuador	NCAR, A1B, 2050	–75.93	–76.68	–75.93	–75.93	–76.02
Ecuador	NCAR, B1, 2050	–56.68	–58.19	–56.68	–56.68	–56.77
Mexico	Hadley, A1B, 2050					
Mexico	Hadley, B1, 2050					
Mexico	NCAR, A1B, 2050					
Mexico	NCAR, B1, 2050					
Peru	Hadley, A1B, 2050					
Peru	Hadley, B1, 2050					
Peru	NCAR, A1B, 2050					
Peru	NCAR, B1, 2050					
Uruguay	Hadley, A1B, 2050	–23.59	–25.83	–23.59	–23.49	–23.37
Uruguay	Hadley, B1, 2050	–37.57	–39.85	–37.57	–37.49	–37.44
Uruguay	NCAR, A1B, 2050	–15.82	–18.15	–15.82	–15.71	–15.37
Uruguay	NCAR, B1, 2050	–29.24	–31.65	–29.24	–29.15	–28.87
Rest of South America	Hadley, A1B, 2050	–43.95	–37.81	–43.95	–43.95	–37.10
Rest of South America	Hadley, B1, 2050	–30.85	–23.34	–30.85	–30.84	–22.42
Rest of South America	NCAR, A1B, 2050	–34.47	–27.22	–34.47	–34.46	–26.37
Rest of South America	NCAR, B1, 2050	–20.63	–12.15	–20.63	–20.62	–11.05
Central America & Caribbean	Hadley, A1B, 2050	–59.07	–59.00	–59.07	–66.86	–66.84
Central America & Caribbean	Hadley, B1, 2050	–50.55	–50.60	–50.55	–57.91	–57.90
Central America & Caribbean	NCAR, A1B, 2050	–43.16	–43.04	–43.16	–49.83	–49.62
Central America & Caribbean	NCAR, B1, 2050	–32.58	–32.82	–32.58	–37.04	–36.89

Rice, 2050, No Adaptation

Table II8. Percentage impact (no adaptation) of climate change on rice yields for potential, water limited, abiotic damaged, diseased, and actual production levels; projections for 2050

Country	Climate change scenario	Climate change impact (percentage difference compared to the baseline productivity				
		Potential	Water limited	Abiotic damaged	Diseased	Actual
Argentina	Hadley, A1B, 2050	+0.25		+0.68	+3.96	+4.38
Argentina	Hadley, B1, 2050	+2.39		+2.81	+4.59	+5.00
Argentina	NCAR, A1B, 2050	+4.81		+5.26	+7.75	+8.19
Argentina	NCAR, B1, 2050	+7.08		+7.47	+8.49	+8.86
Brazil	Hadley, A1B, 2050	–15.24		–14.96	–7.70	–7.40
Brazil	Hadley, B1, 2050	–11.09		–10.80	–5.36	–5.05
Brazil	NCAR, A1B, 2050	–2.33		–2.01	+3.35	+3.69
Brazil	NCAR, B1, 2050	+2.29		+2.60	+6.62	+6.95
Chile	Hadley, A1B, 2050					
Chile	Hadley, B1, 2050					
Chile	NCAR, A1B, 2050					
Chile	NCAR, B1, 2050					
Colombia	Hadley, A1B, 2050	+10.61		+10.61	+21.50	+21.50
Colombia	Hadley, B1, 2050	+10.27		+10.27	+18.12	+18.12
Colombia	NCAR, A1B, 2050	+15.38		+15.38	+26.53	+26.53
Colombia	NCAR, B1, 2050	+17.72		+17.72	+25.33	+25.33
Ecuador	Hadley, A1B, 2050	–1.90		–1.90	+12.75	+12.75
Ecuador	Hadley, B1, 2050	–1.92		–1.92	+10.38	+10.38
Ecuador	NCAR, A1B, 2050	+4.91		+4.91	+19.17	+19.17
Ecuador	NCAR, B1, 2050	+7.23		+7.23	+16.93	+16.93
Mexico	Hadley, A1B, 2050	–15.01		–15.01	–11.57	–11.57
Mexico	Hadley, B1, 2050	–14.79		–14.79	–11.86	–11.86
Mexico	NCAR, A1B, 2050	–7.79		–7.79	–4.47	–4.47
Mexico	NCAR, B1, 2050	–6.06		–6.06	–2.81	–2.81
Peru	Hadley, A1B, 2050	+7.08		+7.08	+18.73	+18.73
Peru	Hadley, B1, 2050	+5.38		+5.38	+14.33	+14.33
Peru	NCAR, A1B, 2050	+10.65		+10.65	+20.64	+20.64
Peru	NCAR, B1, 2050	+9.54		+9.54	+16.58	+16.58
Uruguay	Hadley, A1B, 2050	+5.80		+8.24	+7.32	+9.75
Uruguay	Hadley, B1, 2050	+5.98		+8.33	+7.28	+9.62
Uruguay	NCAR, A1B, 2050	+9.36		+11.88	+10.78	+13.29
Uruguay	NCAR, B1, 2050	+9.09		+11.36	+10.37	+12.64
Rest of South America	Hadley, A1B, 2050	+3.29		+3.30	+8.40	+8.41
Rest of South America	Hadley, B1, 2050	+4.14		+4.15	+7.74	+7.75
Rest of South America	NCAR, A1B, 2050	+8.46		+8.48	+12.75	+12.76
Rest of South America	NCAR, B1, 2050	+10.16		+10.17	+13.64	+13.65
Central America & Caribbean	Hadley, A1B, 2050	–3.89		–3.89	–0.07	–0.07
Central America & Caribbean	Hadley, B1, 2050	–3.91		–3.91	–1.70	–1.70
Central America & Caribbean	NCAR, A1B, 2050	+1.50		+1.50	+5.64	+5.64
Central America & Caribbean	NCAR, B1, 2050	+3.29		+3.29	+6.23	+6.23

Wheat, 2020, With Adaptation

Table II9. Percentage impact (with adaptation) of climate change on wheat yields for potential, water limited, abiotic damaged, diseased, and actual production levels; projections for 2020

Country	Climate change scenario	Climate change impact (percentage difference compared to the baseline productivity				
		Potential	Water limited	Abiotic damaged	Diseased	Actual
Argentina	Hadley, A1B, 2020	–4.62	–12.67	–4.62	–18.62	–25.51
Argentina	Hadley, B1, 2020	–6.46	–13.78	–6.46	–19.85	–25.73
Argentina	NCAR, A1B, 2020	–8.48	–15.90	–8.48	–21.30	–25.97
Argentina	NCAR, B1, 2020	–7.66	–15.39	–7.66	–20.55	–26.39
Brazil	Hadley, A1B, 2020	–12.99	–18.88	–12.99	–13.57	–16.16
Brazil	Hadley, B1, 2020	–11.64	–17.35	–11.64	–12.12	–13.35
Brazil	NCAR, A1B, 2020	–8.56	–15.12	–8.56	–8.46	–11.08
Brazil	NCAR, B1, 2020	–14.02	–19.64	–14.02	–13.20	–15.78
Chile	Hadley, A1B, 2020	+4.34	–21.25	+4.85	–12.45	–32.57
Chile	Hadley, B1, 2020	+3.90	–19.97	+4.74	–12.75	–31.07
Chile	NCAR, A1B, 2020	+3.03	–18.16	+4.22	–13.73	–29.44
Chile	NCAR, B1, 2020	+2.99	–18.01	+4.15	–13.98	–29.43
Colombia	Hadley, A1B, 2020	–17.88	–20.48	–17.88	–17.75	–18.37
Colombia	Hadley, B1, 2020	–16.77	–19.40	–16.77	–17.21	–18.16
Colombia	NCAR, A1B, 2020	–18.74	–21.33	–18.74	–18.27	–17.55
Colombia	NCAR, B1, 2020	–13.74	–16.54	–13.74	–15.84	–16.48
Ecuador	Hadley, A1B, 2020	–10.13	–12.21	–10.13	–11.31	–12.43
Ecuador	Hadley, B1, 2020	–9.27	–11.69	–9.27	–10.45	–11.93
Ecuador	NCAR, A1B, 2020	–6.59	–8.93	–6.59	–8.49	–9.83
Ecuador	NCAR, B1, 2020	–4.53	–6.97	–4.53	–6.82	–8.17
Mexico	Hadley, A1B, 2020	+21.26	–8.93	+21.26	+36.88	+2.47
Mexico	Hadley, B1, 2020	+25.83	–4.31	+25.83	+42.00	+7.81
Mexico	NCAR, A1B, 2020	+22.12	–6.09	+22.12	+35.92	+4.55
Mexico	NCAR, B1, 2020	+17.98	–6.02	+17.98	+30.87	+4.34
Peru	Hadley, A1B, 2020	+1.76	–0.48	+0.40	+3.07	+3.25
Peru	Hadley, B1, 2020	+2.27	–0.83	+0.89	+3.68	+2.92
Peru	NCAR, A1B, 2020	+2.76	+0.88	+1.40	+4.15	+4.94
Peru	NCAR, B1, 2020	+3.50	+1.29	+2.08	+5.08	+5.59
Uruguay	Hadley, A1B, 2020	–7.12	–10.06	–7.12	–0.60	+4.10
Uruguay	Hadley, B1, 2020	–8.71	–10.54	–8.71	–1.68	+4.67
Uruguay	NCAR, A1B, 2020	–6.23	–10.47	–6.23	+1.06	+4.74
Uruguay	NCAR, B1, 2020	–7.03	–7.95	–7.03	+1.22	+7.84
Rest of South America	Hadley, A1B, 2020	–4.81	–12.67	–4.84	–18.27	–24.99
Rest of South America	Hadley, B1, 2020	–6.49	–13.67	–6.52	–19.39	–25.11
Rest of South America	NCAR, A1B, 2020	–8.48	–15.73	–8.50	–20.81	–25.40
Rest of South America	NCAR, B1, 2020	–7.48	–15.06	–7.51	–19.93	–25.65
Central America & Caribbean	Hadley, A1B, 2020	+20.88	–9.10	+20.88	+36.67	+2.34
Central America & Caribbean	Hadley, B1, 2020	+25.42	–4.53	+25.42	+41.78	+7.65
Central America & Caribbean	NCAR, A1B, 2020	+21.73	–6.31	+21.73	+35.72	+4.42
Central America & Caribbean	NCAR, B1, 2020	+17.67	–6.17	+17.67	+30.69	+4.22

Maize, 2020, With Adaptation

Table II10. Percentage impact (with adaptation) of climate change on maize yields for potential, water limited, abiotic damaged, diseased, and actual production levels; projections for 2020

Country	Climate change scenario	Climate change impact (percentage difference compared to the baseline productivity				
		Potential	Water limited	Abiotic damaged	Diseased	Actual
Argentina	Hadley, A1B, 2020	–9.80	–10.12	–9.80	–10.42	–8.95
Argentina	Hadley, B1, 2020	–4.26	–4.57	–4.26	–4.88	–3.61
Argentina	NCAR, A1B, 2020	–7.05	–7.08	–7.05	–7.60	–6.12
Argentina	NCAR, B1, 2020	–7.30	–7.44	–7.30	–7.83	–6.38
Brazil	Hadley, A1B, 2020	–14.91	–14.63	–14.91	–20.85	–19.08
Brazil	Hadley, B1, 2020	–8.09	–7.82	–8.09	–14.46	–12.85
Brazil	NCAR, A1B, 2020	–27.75	–27.57	–27.75	–33.47	–31.36
Brazil	NCAR, B1, 2020	–26.04	–25.88	–26.04	–31.75	–29.66
Chile	Hadley, A1B, 2020	–6.94	–6.89	–6.94	–8.19	–6.32
Chile	Hadley, B1, 2020	–3.77	–2.99	–3.77	–5.02	–2.53
Chile	NCAR, A1B, 2020	–7.83	–7.77	–7.83	–9.15	–7.33
Chile	NCAR, B1, 2020	–8.40	–8.38	–8.40	–9.75	–7.92
Colombia	Hadley, A1B, 2020	–11.43	–12.00	–11.43	–10.38	–10.15
Colombia	Hadley, B1, 2020	–11.29	–11.85	–11.29	–10.40	–10.17
Colombia	NCAR, A1B, 2020	–10.55	–11.14	–10.55	–9.93	–9.66
Colombia	NCAR, B1, 2020	–7.22	–7.85	–7.22	–6.87	–6.60
Ecuador	Hadley, A1B, 2020	–8.46	–9.50	–8.46	–8.28	–8.93
Ecuador	Hadley, B1, 2020	–6.27	–7.07	–6.27	–6.01	–6.51
Ecuador	NCAR, A1B, 2020	–5.67	–6.65	–5.67	–5.40	–6.01
Ecuador	NCAR, B1, 2020	–1.00	–2.72	–1.00	–0.58	–2.02
Mexico	Hadley, A1B, 2020	–17.47	–19.57	–17.67	–19.35	–21.53
Mexico	Hadley, B1, 2020	–14.12	–16.19	–14.46	–16.13	–18.35
Mexico	NCAR, A1B, 2020	–13.99	–16.13	–14.30	–15.76	–18.01
Mexico	NCAR, B1, 2020	–12.51	–14.77	–12.80	–14.45	–16.83
Peru	Hadley, A1B, 2020	–8.64	–9.78	–8.64	–9.15	–8.34
Peru	Hadley, B1, 2020	–6.31	–7.40	–6.31	–7.03	–6.24
Peru	NCAR, A1B, 2020	–4.10	–5.57	–4.10	–3.94	–3.33
Peru	NCAR, B1, 2020	–2.12	–3.65	–2.12	–1.82	–1.31
Uruguay	Hadley, A1B, 2020	–9.14	–9.60	–9.14	–9.59	–8.52
Uruguay	Hadley, B1, 2020	–3.91	–4.48	–3.91	–4.39	–3.58
Uruguay	NCAR, A1B, 2020	–7.50	–7.74	–7.50	–8.07	–6.95
Uruguay	NCAR, B1, 2020	–8.91	–9.33	–8.91	–9.28	–8.17
Rest of South America	Hadley, A1B, 2020	–23.52	–24.39	–23.52	–24.95	–23.72
Rest of South America	Hadley, B1, 2020	–7.51	–8.29	–7.51	–7.62	–6.95
Rest of South America	NCAR, A1B, 2020	–7.41	–8.32	–7.41	–7.44	–6.82
Rest of South America	NCAR, B1, 2020	–6.80	–7.59	–6.80	–7.03	–6.33
Central America & Caribbean	Hadley, A1B, 2020	–17.25	–19.29	–17.45	–19.05	–21.14
Central America & Caribbean	Hadley, B1, 2020	–14.01	–16.02	–14.34	–15.93	–18.07
Central America & Caribbean	NCAR, A1B, 2020	–13.85	–15.94	–14.16	–15.56	–17.72
Central America & Caribbean	NCAR, B1, 2020	–12.31	–14.51	–12.59	–14.19	–16.48

Soybean, 2020, With Adaptation

Table II11. Percentage impact (with adaptation) of climate change on soybean yields for potential, water limited, abiotic damaged, diseased, and actual production levels; projections for 2020

Country	Climate change scenario	Climate change impact (percentage difference compared to the baseline productivity				
		Potential	Water limited	Abiotic damaged	Diseased	Actual
Argentina	Hadley, A1B, 2020	–14.16	–4.57	–14.16	–14.16	–3.50
Argentina	Hadley, B1, 2020	–5.59	+4.91	–5.59	–5.58	+6.12
Argentina	NCAR, A1B, 2020	–4.18	+6.78	–4.18	–4.17	+8.02
Argentina	NCAR, B1, 2020	–7.67	+2.61	–7.67	–7.66	+3.78
Brazil	Hadley, A1B, 2020	–25.94	–25.19	–25.94	–25.94	–23.64
Brazil	Hadley, B1, 2020	–14.84	–14.01	–14.84	–14.85	–12.17
Brazil	NCAR, A1B, 2020	–23.57	–22.79	–23.57	–23.57	–21.14
Brazil	NCAR, B1, 2020	–20.63	–19.90	–20.63	–20.63	–18.18
Chile	Hadley, A1B, 2020					
Chile	Hadley, B1, 2020					
Chile	NCAR, A1B, 2020					
Chile	NCAR, B1, 2020					
Colombia	Hadley, A1B, 2020	–16.57	–18.54	–16.57	–14.41	–14.76
Colombia	Hadley, B1, 2020	–19.99	–21.69	–19.99	–12.83	–12.91
Colombia	NCAR, A1B, 2020	–14.17	–15.62	–14.17	–7.55	–7.15
Colombia	NCAR, B1, 2020	–10.45	–12.21	–10.45	–4.37	–4.27
Ecuador	Hadley, A1B, 2020	–1.42	–4.09	–1.42	–1.42	–1.45
Ecuador	Hadley, B1, 2020	+1.70	–1.00	+1.70	+1.70	+1.73
Ecuador	NCAR, A1B, 2020	+2.33	–0.46	+2.33	+2.33	+2.30
Ecuador	NCAR, B1, 2020	+10.44	+7.33	+10.44	+10.44	+10.36
Mexico	Hadley, A1B, 2020					
Mexico	Hadley, B1, 2020					
Mexico	NCAR, A1B, 2020					
Mexico	NCAR, B1, 2020					
Peru	Hadley, A1B, 2020					
Peru	Hadley, B1, 2020					
Peru	NCAR, A1B, 2020					
Peru	NCAR, B1, 2020					
Uruguay	Hadley, A1B, 2020	+8.68	+8.66	+8.68	+7.80	+9.32
Uruguay	Hadley, B1, 2020	+16.14	+16.03	+16.14	+15.42	+16.88
Uruguay	NCAR, A1B, 2020	+10.47	+10.67	+10.47	+10.25	+11.81
Uruguay	NCAR, B1, 2020	+9.61	+9.53	+9.61	+9.12	+10.44
Rest of South America	Hadley, A1B, 2020	–14.13	–4.90	–14.13	–14.13	–3.84
Rest of South America	Hadley, B1, 2020	–5.58	+4.51	–5.58	–5.57	+5.72
Rest of South America	NCAR, A1B, 2020	–4.29	+6.26	–4.29	–4.28	+7.50
Rest of South America	NCAR, B1, 2020	–7.74	+2.14	–7.74	–7.73	+3.31
Central America & Caribbean	Hadley, A1B, 2020	–11.30	–13.53	–11.30	–9.40	–9.64
Central America & Caribbean	Hadley, B1, 2020	–12.84	–14.91	–12.84	–7.56	–7.62
Central America & Caribbean	NCAR, A1B, 2020	–8.85	–10.78	–8.85	–4.10	–3.88
Central America & Caribbean	NCAR, B1, 2020	–3.62	–5.87	–3.62	+0.97	+0.98

Rice, 2020, With Adaptation

Table II12. Percentage impact (with adaptation) of climate change on rice yields for potential, water limited, abiotic damaged, diseased, and actual production levels; projections for 2020

Country	Climate change scenario	Climate change impact (percentage difference compared to the baseline productivity				
		Potential	Water limited	Abiotic damaged	Diseased	Actual
Argentina	Hadley, A1B, 2020	–1.62		–1.28	–0.13	+0.20
Argentina	Hadley, B1, 2020	+0.21		+0.24	+1.47	+1.49
Argentina	NCAR, A1B, 2020	+0.56		+0.85	+1.09	+1.37
Argentina	NCAR, B1, 2020	–0.07		+0.27	+0.53	+0.85
Brazil	Hadley, A1B, 2020	+3.26		+3.60	+8.50	+8.86
Brazil	Hadley, B1, 2020	+5.62		+5.97	+10.22	+10.58
Brazil	NCAR, A1B, 2020	+6.76		+7.11	+11.32	+11.69
Brazil	NCAR, B1, 2020	+6.50		+6.85	+10.90	+11.26
Chile	Hadley, A1B, 2020					
Chile	Hadley, B1, 2020					
Chile	NCAR, A1B, 2020					
Chile	NCAR, B1, 2020					
Colombia	Hadley, A1B, 2020	+8.89		+8.89	+12.32	+12.32
Colombia	Hadley, B1, 2020	+7.39		+7.39	+10.39	+10.39
Colombia	NCAR, A1B, 2020	+9.29		+9.29	+13.50	+13.50
Colombia	NCAR, B1, 2020	+9.59		+9.59	+13.00	+13.00
Ecuador	Hadley, A1B, 2020	+9.51		+9.51	+19.19	+19.19
Ecuador	Hadley, B1, 2020	+8.57		+8.57	+17.76	+17.76
Ecuador	NCAR, A1B, 2020	+12.09		+12.09	+20.70	+20.70
Ecuador	NCAR, B1, 2020	+11.47		+11.47	+20.21	+20.21
Mexico	Hadley, A1B, 2020	+1.21		+1.21	+4.14	+4.14
Mexico	Hadley, B1, 2020	+1.02		+1.02	+3.97	+3.97
Mexico	NCAR, A1B, 2020	+1.32		+1.32	+3.93	+3.93
Mexico	NCAR, B1, 2020	+1.12		+1.12	+3.90	+3.90
Peru	Hadley, A1B, 2020	+2.00		+2.00	+6.98	+6.98
Peru	Hadley, B1, 2020	+2.02		+2.02	+6.05	+6.05
Peru	NCAR, A1B, 2020	+4.31		+4.31	+8.89	+8.89
Peru	NCAR, B1, 2020	+3.33		+3.33	+6.93	+6.93
Uruguay	Hadley, A1B, 2020	+0.19		+2.03	+0.72	+2.54
Uruguay	Hadley, B1, 2020	+0.38		+1.83	+1.17	+2.62
Uruguay	NCAR, A1B, 2020	+2.68		+4.46	+2.77	+4.53
Uruguay	NCAR, B1, 2020	+1.16		+3.04	+1.18	+3.03
Rest of South America	Hadley, A1B, 2020	+1.32		+1.33	+4.32	+4.33
Rest of South America	Hadley, B1, 2020	+1.77		+1.77	+4.53	+4.53
Rest of South America	NCAR, A1B, 2020	+3.92		+3.93	+6.31	+6.32
Rest of South America	NCAR, B1, 2020	+3.37		+3.38	+5.32	+5.33
Central America & Caribbean	Hadley, A1B, 2020	+3.09		+3.09	+4.97	+4.97
Central America & Caribbean	Hadley, B1, 2020	+2.27		+2.27	+4.11	+4.11
Central America & Caribbean	NCAR, A1B, 2020	+3.00		+3.00	+4.77	+4.77
Central America & Caribbean	NCAR, B1, 2020	+3.19		+3.19	+4.87	+4.87

Wheat, 2050, With Adaptation

Table II13. Percentage impact (with adaptation) of climate change on wheat yields for potential, water limited, abiotic damaged, diseased, and actual production levels; projections for 2050

Country	Climate change scenario	Climate change impact (percentage difference compared to the baseline productivity				
		Potential	Water limited	Abiotic damaged	Diseased	Actual
Argentina	Hadley, A1B, 2050	–16.50	–24.02	–16.50	–24.78	–29.23
Argentina	Hadley, B1, 2050	–12.59	–20.88	–12.59	–22.33	–27.47
Argentina	NCAR, A1B, 2050	–17.72	–25.19	–17.72	–25.80	–29.37
Argentina	NCAR, B1, 2050	–7.84	–17.31	–7.84	–18.90	–24.21
Brazil	Hadley, A1B, 2050	–46.21	–50.45	–46.21	–42.11	–42.30
Brazil	Hadley, B1, 2050	–26.11	–31.62	–26.11	–22.71	–23.71
Brazil	NCAR, A1B, 2050	–7.72	–15.42	–7.72	–4.04	–6.89
Brazil	NCAR, B1, 2050	–28.29	–33.91	–28.29	–23.07	–24.77
Chile	Hadley, A1B, 2050	+5.54	–25.19	+8.38	–8.96	–28.36
Chile	Hadley, B1, 2050	+5.54	–23.91	+6.23	–9.96	–30.41
Chile	NCAR, A1B, 2050	+4.74	–19.21	+7.97	–9.73	–22.69
Chile	NCAR, B1, 2050	+6.65	–18.68	+8.37	–9.41	–25.35
Colombia	Hadley, A1B, 2050	–57.92	–61.41	–57.92	–50.29	–50.13
Colombia	Hadley, B1, 2050	–43.68	–47.98	–43.68	–37.60	–38.03
Colombia	NCAR, A1B, 2050	–48.17	–53.07	–48.17	–41.29	–40.85
Colombia	NCAR, B1, 2050	–18.21	–25.74	–18.21	–14.11	–13.84
Ecuador	Hadley, A1B, 2050	–22.79	–29.06	–22.79	–16.73	–17.25
Ecuador	Hadley, B1, 2050	–19.02	–24.27	–19.02	–14.62	–15.48
Ecuador	NCAR, A1B, 2050	–16.56	–23.65	–16.56	–10.45	–11.34
Ecuador	NCAR, B1, 2050	–7.53	–13.83	–7.53	–3.99	–4.86
Mexico	Hadley, A1B, 2050	–34.70	–46.72	–34.70	–27.37	–39.34
Mexico	Hadley, B1, 2050	–6.25	–28.86	–6.25	+7.04	–17.49
Mexico	NCAR, A1B, 2050	+10.58	–13.93	+10.58	+24.96	–0.63
Mexico	NCAR, B1, 2050	–19.92	–32.04	–19.92	–11.03	–21.34
Peru	Hadley, A1B, 2050	–2.59	–10.44	–3.54	+2.92	+3.98
Peru	Hadley, B1, 2050	–0.81	–7.44	–2.37	+3.94	+4.28
Peru	NCAR, A1B, 2050	+0.20	–7.12	–1.11	+6.50	+9.02
Peru	NCAR, B1, 2050	+5.28	–1.20	+3.99	+10.08	+12.00
Uruguay	Hadley, A1B, 2050	–26.53	–27.49	–26.53	–15.59	–9.74
Uruguay	Hadley, B1, 2050	–12.51	–11.83	–12.51	–2.72	+7.11
Uruguay	NCAR, A1B, 2050	–6.55	–12.70	–6.55	+4.06	+6.68
Uruguay	NCAR, B1, 2050	–20.98	–21.96	–20.98	–9.51	–2.31
Rest of South America	Hadley, A1B, 2050	–17.39	–24.80	–17.41	–25.12	–29.41
Rest of South America	Hadley, B1, 2050	–12.89	–21.04	–12.92	–22.11	–27.11
Rest of South America	NCAR, A1B, 2050	–17.79	–25.19	–17.82	–25.42	–28.93
Rest of South America	NCAR, B1, 2050	–7.57	–16.92	–7.60	–18.16	–23.38
Central America & Caribbean	Hadley, A1B, 2050	–34.93	–46.94	–34.93	–27.45	–39.40
Central America & Caribbean	Hadley, B1, 2050	–6.61	–29.14	–6.61	+6.87	–17.61
Central America & Caribbean	NCAR, A1B, 2050	+10.01	–14.51	+10.01	+24.71	–0.86
Central America & Caribbean	NCAR, B1, 2050	–19.90	–31.95	–19.90	–11.04	–21.30

Maize, 2050, With Adaptation

Table II14. Percentage impact (with adaptation) of climate change on maize yields for potential, water limited, abiotic damaged, diseased, and actual production levels; projections for 2050

Country	Climate change scenario	Climate change impact (percentage difference compared to the baseline productivity				
		Potential	Water limited	Abiotic damaged	Diseased	Actual
Argentina	Hadley, A1B, 2050	–26.89	–27.39	–26.89	–27.02	–25.39
Argentina	Hadley, B1, 2050	–16.95	–17.46	–16.95	–17.16	–15.67
Argentina	NCAR, A1B, 2050	–23.83	–24.21	–23.83	–23.98	–22.36
Argentina	NCAR, B1, 2050	–11.18	–11.76	–11.18	–11.48	–10.08
Brazil	Hadley, A1B, 2050	–64.13	–64.29	–64.13	–67.82	–65.84
Brazil	Hadley, B1, 2050	–41.52	–41.62	–41.52	–45.59	–43.50
Brazil	NCAR, A1B, 2050	–36.36	–36.53	–36.36	–41.59	–39.34
Brazil	NCAR, B1, 2050	–36.36	–36.53	–36.36	–41.59	–39.35
Chile	Hadley, A1B, 2050	–15.77	–15.14	–15.77	–16.88	–14.54
Chile	Hadley, B1, 2050	–11.76	–11.27	–11.76	–12.96	–10.65
Chile	NCAR, A1B, 2050	–16.74	–16.49	–16.74	–18.05	–15.83
Chile	NCAR, B1, 2050	–8.30	–8.51	–8.30	–9.59	–7.76
Colombia	Hadley, A1B, 2050	–35.70	–37.30	–35.70	–39.08	–38.93
Colombia	Hadley, B1, 2050	–27.58	–28.94	–27.58	–29.39	–29.18
Colombia	NCAR, A1B, 2050	–14.13	–15.84	–14.13	–12.62	–12.39
Colombia	NCAR, B1, 2050	–14.13	–15.84	–14.13	–12.62	–12.39
Ecuador	Hadley, A1B, 2050	–54.75	–55.16	–54.75	–59.40	–56.89
Ecuador	Hadley, B1, 2050	–40.80	–41.47	–40.80	–45.12	–43.19
Ecuador	NCAR, A1B, 2050	–14.34	–16.01	–14.34	–14.56	–15.26
Ecuador	NCAR, B1, 2050	–14.34	–16.01	–14.34	–14.55	–15.26
Mexico	Hadley, A1B, 2050	–43.40	–45.00	–43.72	–43.93	–45.19
Mexico	Hadley, B1, 2050	–37.47	–39.53	–37.73	–38.23	–40.06
Mexico	NCAR, A1B, 2050	–20.79	–23.32	–21.10	–22.28	–24.30
Mexico	NCAR, B1, 2050	–20.79	–23.32	–21.10	–22.27	–24.29
Peru	Hadley, A1B, 2050	–26.93	–28.66	–26.93	–29.46	–27.97
Peru	Hadley, B1, 2050	–17.87	–19.85	–17.87	–20.16	–19.22
Peru	NCAR, A1B, 2050	–14.62	–17.89	–14.62	–14.36	–13.88
Peru	NCAR, B1, 2050	–6.59	–8.96	–6.59	–6.84	–5.82
Uruguay	Hadley, A1B, 2050	–28.17	–28.73	–28.17	–28.38	–27.02
Uruguay	Hadley, B1, 2050	–16.07	–16.78	–16.07	–16.33	–15.14
Uruguay	NCAR, A1B, 2050	–22.37	–22.89	–22.37	–22.54	–21.15
Uruguay	NCAR, B1, 2050	–10.64	–11.38	–10.64	–10.89	–9.63
Rest of South America	Hadley, A1B, 2050	–17.38	–18.59	–17.38	–17.94	–17.36
Rest of South America	Hadley, B1, 2050	–20.57	–21.99	–20.57	–21.78	–20.97
Rest of South America	NCAR, A1B, 2050	–10.56	–12.21	–10.56	–10.45	–9.58
Rest of South America	NCAR, B1, 2050	–17.45	–19.32	–17.45	–17.52	–16.80
Central America & Caribbean	Hadley, A1B, 2050	–43.10	–44.69	–43.40	–43.74	–44.95
Central America & Caribbean	Hadley, B1, 2050	–37.09	–39.13	–37.35	–37.91	–39.67
Central America & Caribbean	NCAR, A1B, 2050	–20.56	–23.05	–20.85	–21.96	–23.90
Central America & Caribbean	NCAR, B1, 2050	–20.56	–23.05	–20.85	–21.95	–23.89

Soybean, 2050, With Adaptation

Table II15. Percentage impact (with adaptation) of climate change on soybean yields for potential, water limited, abiotic damaged, diseased, and actual production levels; projections for 2050

Country	Climate change scenario	Climate change impact (percentage difference compared to the baseline productivity				
		Potential	Water limited	Abiotic damaged	Diseased	Actual
Argentina	Hadley, A1B, 2050	–34.00	–28.47	–34.00	–34.02	–25.68
Argentina	Hadley, B1, 2050	–19.33	–12.02	–19.33	–19.33	–9.17
Argentina	NCAR, A1B, 2050	–24.34	–16.43	–24.34	–24.34	–14.66
Argentina	NCAR, B1, 2050	–7.71	+0.33	–7.71	–7.70	+3.76
Brazil	Hadley, A1B, 2050	–73.67	–73.80	–73.67	–73.67	–72.99
Brazil	Hadley, B1, 2050	–55.64	–56.62	–55.64	–55.64	–54.37
Brazil	NCAR, A1B, 2050	–30.57	–32.61	–30.57	–30.57	–28.44
Brazil	NCAR, B1, 2050	–30.57	–32.61	–30.57	–30.57	–28.44
Chile	Hadley, A1B, 2050					
Chile	Hadley, B1, 2050					
Chile	NCAR, A1B, 2050					
Chile	NCAR, B1, 2050					
Colombia	Hadley, A1B, 2050	–38.88	–43.80	–38.88	–44.03	–44.19
Colombia	Hadley, B1, 2050	–29.64	–34.07	–29.64	–33.17	–33.43
Colombia	NCAR, A1B, 2050	–13.80	–20.17	–13.80	–16.24	–15.85
Colombia	NCAR, B1, 2050	–11.32	–16.42	–11.32	–5.39	–5.13
Ecuador	Hadley, A1B, 2050	–65.31	–66.63	–65.31	–65.31	–65.39
Ecuador	Hadley, B1, 2050	–45.69	–49.05	–45.69	–45.69	–45.72
Ecuador	NCAR, A1B, 2050	–10.13	–16.80	–10.13	–10.13	–10.22
Ecuador	NCAR, B1, 2050	–10.13	–16.80	–10.13	–10.13	–10.22
Mexico	Hadley, A1B, 2050					
Mexico	Hadley, B1, 2050					
Mexico	NCAR, A1B, 2050					
Mexico	NCAR, B1, 2050					
Peru	Hadley, A1B, 2050					
Peru	Hadley, B1, 2050					
Peru	NCAR, A1B, 2050					
Peru	NCAR, B1, 2050					
Uruguay	Hadley, A1B, 2050	–12.59	–13.14	–12.59	–12.66	–11.18
Uruguay	Hadley, B1, 2050	+2.68	+0.51	+2.68	+2.48	+3.94
Uruguay	NCAR, A1B, 2050	+9.16	+6.86	+9.16	+8.83	+10.34
Uruguay	NCAR, B1, 2050	+9.16	+6.86	+9.16	+8.83	+10.34
Rest of South America	Hadley, A1B, 2050	–33.98	–28.71	–33.98	–33.99	–25.93
Rest of South America	Hadley, B1, 2050	–19.31	–12.33	–19.31	–19.30	–9.49
Rest of South America	NCAR, A1B, 2050	–24.37	–16.78	–24.37	–24.37	–15.01
Rest of South America	NCAR, B1, 2050	–7.77	–0.11	–7.77	–7.76	+3.30
Central America & Caribbean	Hadley, A1B, 2050	–47.53	–51.22	–47.53	–51.82	–51.92
Central America & Caribbean	Hadley, B1, 2050	–34.72	–38.79	–34.72	–37.60	–37.76
Central America & Caribbean	NCAR, A1B, 2050	–12.09	–18.60	–12.09	–13.56	–13.35
Central America & Caribbean	NCAR, B1, 2050	–11.31	–16.93	–11.31	–7.57	–7.44

Rice, 2050, With Adaptation

Table II16. Percentage impact (with adaptation) of climate change on rice yields for potential, water limited, abiotic damaged, diseased, and actual production levels; projections for 2050

Country	Climate change scenario	Climate change impact (percentage difference compared to the baseline productivity				
		Potential	Water limited	Abiotic damaged	Diseased	Actual
Argentina	Hadley, A1B, 2050	+0.25		+0.68	+3.96	+4.38
Argentina	Hadley, B1, 2050	+2.39		+2.81	+4.59	+5.00
Argentina	NCAR, A1B, 2050	+4.81		+5.26	+7.75	+8.19
Argentina	NCAR, B1, 2050	+7.08		+7.47	+8.49	+8.86
Brazil	Hadley, A1B, 2050	–3.64		–3.32	+5.50	+5.85
Brazil	Hadley, B1, 2050	+0.10		+0.43	+7.62	+7.98
Brazil	NCAR, A1B, 2050	+9.35		+9.71	+17.33	+17.71
Brazil	NCAR, B1, 2050	+13.43		+13.80	+19.75	+20.15
Chile	Hadley, A1B, 2050					
Chile	Hadley, B1, 2050					
Chile	NCAR, A1B, 2050					
Chile	NCAR, B1, 2050					
Colombia	Hadley, A1B, 2050	+10.61		+10.61	+21.50	+21.50
Colombia	Hadley, B1, 2050	+10.27		+10.27	+18.12	+18.12
Colombia	NCAR, A1B, 2050	+15.38		+15.38	+26.53	+26.53
Colombia	NCAR, B1, 2050	+17.72		+17.72	+25.33	+25.33
Ecuador	Hadley, A1B, 2050	+8.37		+8.37	+26.39	+26.39
Ecuador	Hadley, B1, 2050	+8.27		+8.27	+24.31	+24.31
Ecuador	NCAR, A1B, 2050	+15.35		+15.35	+32.81	+32.81
Ecuador	NCAR, B1, 2050	+17.65		+17.65	+30.58	+30.58
Mexico	Hadley, A1B, 2050	–6.08		–6.08	–2.26	–2.26
Mexico	Hadley, B1, 2050	+4.18		+4.18	+7.93	+7.93
Mexico	NCAR, A1B, 2050	+1.81		+1.81	+5.66	+5.66
Mexico	NCAR, B1, 2050	+4.18		+4.18	+7.93	+7.93
Peru	Hadley, A1B, 2050	+7.08		+7.08	+18.73	+18.73
Peru	Hadley, B1, 2050	+5.38		+5.38	+14.33	+14.33
Peru	NCAR, A1B, 2050	+10.65		+10.65	+20.64	+20.64
Peru	NCAR, B1, 2050	+9.54		+9.54	+16.58	+16.58
Uruguay	Hadley, A1B, 2050	+5.80		+8.24	+7.32	+9.75
Uruguay	Hadley, B1, 2050	+5.98		+8.33	+7.28	+9.62
Uruguay	NCAR, A1B, 2050	+9.36		+11.88	+10.78	+13.29
Uruguay	NCAR, B1, 2050	+9.09		+11.36	+10.37	+12.64
Rest of South America	Hadley, A1B, 2050	+3.29		+3.30	+8.40	+8.41
Rest of South America	Hadley, B1, 2050	+4.14		+4.15	+7.74	+7.75
Rest of South America	NCAR, A1B, 2050	+8.46		+8.48	+12.75	+12.76
Rest of South America	NCAR, B1, 2050	+10.16		+10.17	+13.64	+13.65
Central America & Caribbean	Hadley, A1B, 2050	+0.24		+0.24	+4.68	+4.68
Central America & Caribbean	Hadley, B1, 2050	+0.61		+0.61	+3.53	+3.53
Central America & Caribbean	NCAR, A1B, 2050	+6.05		+6.05	+10.90	+10.90
Central America & Caribbean	NCAR, B1, 2050	+8.40		+8.40	+12.13	+12.13

Table II17. Application of coupled AZS-ENVISAGE platform: change in agricultural value added from climate‑induced damages in the four focus crops (%)

	NCARA1B		NCARB1		HADA1B		HADB1	
Countries/regions	**2020**	**2050**	**2020**	**2050**	**2020**	**2050**	**2020**	**2050**
Argentina	–7.0	–28.7	–9.7	–15.3	–13.7	–32.3	–8.6	–21.5
Brazil	–8.6	–10.3	–7.9	–11.8	–8.5	–15.3	–6.1	–14.2
Chile	–2.2	–1.1	–2.3	–0.9	–2.8	–1.3	–2.5	–1.4
Colombia	–1.9	–2.4	–1.5	–2.0	–1.9	–4.9	–2.2	–3.8
Ecuador	–0.5	–0.9	–0.3	–1.0	–0.4	–2.4	–0.3	–1.7
Peru	0.2	–0.3	0.4	0.0	0.1	–0.9	0.0	–0.4
Mexico	–1.2	–3.5	–1.1	–3.8	–1.7	–10.4	–1.2	–8.4
Uruguay	1.0	2.5	0.5	3.1	0.0	–4.5	1.3	1.2
Central America & Caribbean	–0.3	0.5	0.0	0.2	–0.6	–4.6	–0.5	–3.0
Rest of South America	2.2	1.0	1.5	2.5	2.0	4.9	2.0	3.5
Latin America & Caribbean	–3.5	–8.0	–3.4	–7.0	–4.2	–12.1	–3.0	–9.9